Novel Developments in Perimetry, Ocular Coherence Tomography and Vision Restoration Therapies

A thesis submitted to the University of Manchester

for the degree of Doctor of Philosophy

in the Faculty of Biology, Medicine and Health

2017

Emmanouil Tsamis

School of Health Sciences – Division of Pharmacy and Optometry

Table of Contents

Figures and Tables

List of Abbreviations

AE	Adverse Event
ALT	Argon Laser Trabeculoplasty
AMD	Age-related Macular Degeneration
ARVO	Association of Research in Vision and Ophthalmology
asb	apostilb
BCVA	Best Corrected Visual Acuity
COAG	Chronic Open Angle Glaucoma
CSMO	Clinically Significant Macular Oedema
CVS	Core Vitreous Segmentation
dB	decibel
DM	Direction of Motion
DMC	Damato Multifixation Campimetry
DR	Diabetic Retinopathy
DVL	Deep Vascular Layer
DVP	Deep Vascular Plexus
ETDRS	Early Treatment Diabetic Retinopathy Study
FA	Fluorescein Angiography
FAZ	Foveal Avascular Zone
FD-OCT	Fourier-Domain Ocular Coherence Tomography
FDT	Frequency Doubling Technology
FLORA	Functional Low-Vision Rated Assessment
FN	False Negative
FOS	Frequency-of-Seeing
FP	False Positive
FT	Full Threshold
GA	Geographic Atrophy
GSS 2	Glaucoma Staging System 2
GUI	Graphics User Interface
GVA	Grating Visual Acuity
HFA	Humphrey Field Analyzer
HRQoL	Health-Related Quality of Life
HRT	Heidelberg Retina Tomograph

ICGA	IndoCyanine Green Angiography
ILM	Internal Limiting Membrane
INL	Inner Nuclear Layer
IPL	Inner Plexiform Layer
IPS	Imaging and Perimetry Society
IQR	Inter-Quartile Range
IVB	Intravitreal Bevacizumab
JOAG	Juvenile Open Angle Glaucoma
MD	Mean Deviation
MDT	Motion Displacement Test
MREH	Manchester Royal Eye Hospital
MRF	Melbourne Rapid Fields
NHS	National Health Services
NICE	National Institute for Health and Clinical Excellence
NPDR	Non Proliferative Diabetic Retinopathy
NPV	Negative Predictive Value
NV	Neovascularization
NVD	NeoVascularization of the Disc
NVE	NeoVascularization Elsewhere
OAG	Open Angle Glaucoma
OCT	Ocular Coherence Tomography
OCTA	Ocular Coherence Tomography Angiography
OCTARA	Ocular Coherence Tomography Angiography Ratio Analysis
OHT	Ocular Hypertension
ON	Optic Nerve
ONH	Optic Nerve Head
ONL	Outer Nuclear Layer
OVS	Outer Vitreous Segmentation
PACG	Primary Angle Closure Glaucoma
PDR	Proliferative Diabetic Retinopathy
POAG	Primary Open Angle Glaucoma
PPV	Pars Plana Vitrectomy
PPV	Positive Predictive Value

PSD	Pattern Standard Deviation
PXF	Pseudoexfoliation
RD	Retinal Detachment
RGB	Red-Green-Blue
RGCs	Retinal Ganglion Cells
RNFL	Retinal Nerve Fibre Layer
ROC	Receiver Operating Characteristic
RP	Retinitis Pigmentosa
SAE	Serious Adverse Event
SAP	Standard Automated Perimetry
SD-OCT	Spectral-Domain Ocular Coherence Tomography
SDT	Signal Detection Theory
SITA	Swedish Interactive Thresholding Algorithm
SL	Square Localisation
SLT	Selective Laser Trabeculoplasty
SSADA	Split Spectrum Amplitude Decorrelation Angiography
SS-OCT	Swept-Source Ocular Coherence Tomography
SS-OCTA	Swept-Source Ocular Coherence Tomography Angiography
SUS	System Usability Scale
SVL	Superficial Vascular Layer
SVP	Superficial Vascular Plexus
SWAP	Short-Wavelength Automated Perimetry
TD-OCT	Time-Domain Ocular Coherence Tomography
TN	True Negative
TP	True Positive
UK	United Kingdom
UKEGS	UK and Eire Glaucoma Society
UWF-FA	Ultra-Wide Field Fluorescein Angiography
VA	Visual Acuity
VEGF	Vascular Endothelial Growth Factor
VF	Visual Field
VH	Vitreous Haemorrhage
VPU	Vision Processing Unit

VRS	Vitreo-Retinal Segmentation
XLRS	X-Linked RetinoSchisis
ZATA	Zippy Adaptive Threshold Algorithm
ZEST	Zippy Estimate by Sequential

Thesis Abstract

This thesis presents the outcomes of research work whose focus lies on the development and investigation of new approaches in 3 technologies: perimetry, ocular coherence tomography and retinal implants for the purposes of vision restoration. The thesis is separated in 3 sections:

Section 1 consists of a series of studies related to perimetry and glaucoma. The initial investigation of the rate of VF deterioration in patients with different stages of glaucomatous loss showed the relatively low proportion of patients with rapid progression highlighting the effectiveness of current treatment plans. However, the large proportion of patients with advanced field loss presented for the first time emphasised the need for earlier detection of the disease. The following studies focused on the development and evaluation of a new computer-based visual field (VF) self-administered test for enhanced case-finding of eyes with glaucomatous VF defects. Online VF self-tests were identified and undergone usability evaluation to identify design and testing features that are more attractive to users; such a feature, for example, was the presentation of multiple stimuli. The results of that study were implemented into the design of the new test: a multiple stimulus supra-threshold (i.e. 10dB above age-matched normal threshold) algorithm to test a 20 location subset of the 24-2 pattern with a multisampling (i.e. 3 seen or missed, maximum 5 trials) technique. The performance evaluation of the new test reported specificity at 97% and sensitivity at 85-90%, depending on the stage of loss. Section 2 introduces the new technology of non-invasive angiography by means of ocular coherence tomography. Five studies utilising ocular coherence tomography angiography (OCTA) report and discuss the newly acquired knowledge of the eye's vasculature in pathologies, such as diabetic retinopathy or age-related macular degeneration. OCTA proved to be a quick and non-invasive mean for angiographic analysis, although drawbacks, such as artefacts or limitations in image acquisition and processing, make it harder to introduce OCTA as a replacement of fundus fluorescein angiography (i.e. the clinical standard for the visualisation of the eye's vasculature). At the end of the section, the potentials of this new technology and future research pathways are thoroughly discussed.

The last section describes a clinical trial that evaluates the safety and efficacy of the Argus II retinal implant in patients with advanced non-exudative age-related macular degeneration. The presented results emphasise the structural alterations that the implantation caused and the inability of the functional testing to detect any benefits of the Argus II system to the implanted eyes. The section concludes with a critical review of the study's protocol, highlighting its strengths and weaknesses.

Executive Summary

Given the special nature of this doctorate work, an executive summary has been included to provide further details to the readers on how the undertaken work fits together and to clarify the author's contribution to each study.

The reported work spans across a period of approximately 4 years; from January 2014 to October 2017. During this period research time was split between two research labs: Prof David Henson's team with an expertise in visual fields (VF) and active collaborations with glaucoma consultants and Prof Paulo Stanga's Manchester Vision Regeneration (MVR) Lab which undertakes research in pathologies of the posterior pole (ie. vitreoretinal diseases); all research was conducted at Manchester Royal Eye Hospital (MREH) premises.

Research work at the doctorate level during collaboration with Prof Henson was an extension and further development of the work undertaken at the Masters level in 2012. Initially, the VF database of MREH was utilised to investigate rates of VF progression in patients with a sole diagnosis of glaucoma. The results showed that patients progress at a relatively slow rate under routine clinical management; however, the proportion of those presenting with advanced disease for the first time is relatively high. This outcome highlighted the issue of detection in glaucoma. The following research steps focused on the development of a portable computer-based VF self-test that could potentially tackle the above-mentioned issue.

Particular focus was given to the usability of the new test. One of the undertaken studies investigated online VF self-tests that were available in 2014, where perimetry experts and lay participants were asked to test themselves and identify usability features that they preferred. Those features were implemented in the design of the new self-test whose performance was evaluated by means of VF defect simulation; a technique that was developed by the author. This research process, or in other words this series of studies, is presented in Section 1 of this thesis. All research ideas and design, data collection, analysis and interpretation belong to the author, with the kind guidance of his supervisors.

Sections 2 and 3 involve the work that was undertaken under the supervision of Prof Stanga. The second section, in particular, brings together research studies with the recently introduced technology of Ocular Coherence Tomography Angiography (OCTA). The MVR Lab was in close collaboration with Topcon (Topcon Corp., Tokyo, Japan) that provided its OCTA devices for qualitative evaluation of their performance. This provided a great opportunity for the author not only to expertise in a different means of a pioneering imaging technology (i.e. the OCT) but also to expand his knowledge outside the world of glaucoma and into the vitreoretinal diseases. In all studies, but one, the author's contribution was restricted to the design of the study protocols, data collection and statistical analysis. Research questions were set by the clinicians of the team as well as a significant contribution to the interpretation of the data; given the author's initial lack of expertise on retinal pathologies. The study involving the measurement of the foveal avascular zone and its association with the stage of diabetic

retinopathy was an idea of the author with the kind help of Dr Francesco Stringa and Prof Paulo Stanga for the interpretation. This second section of the doctorate work offered the opportunity to the author to explore the benefits and drawbacks of the OCTA technology (thoroughly reported through the second section of this thesis), develop critical review over novel hardware and software and suggest potential improvements to future versions of the technology.

One of the most important collaborations of the MVR Lab was with Second Sight (Second Sight Medical Products Inc., Sylmar, California, USA) and the clinical trial for the evaluation of the Argus II Epiretinal Implant in patients with advanced non-exudative age-related macular degeneration; MREH being the first and only centre worldwide. This collaboration provided another great opportunity for the author considering his role in this study. Although the study protocols were provided by Second Sight, the author had significant contribution into the collection of all structural and functional data, the analysis and interpretation, as well as the reporting and decision-making for the adoption of different tests and techniques that would suit the needs of this clinical trial. Section 3 presents the results of the first 12 months of the study and includes a thorough discussion on the study outcomes, highlights flaws of the study design and suggests directions for future research on the field.

Declaration

No portion of the work referred to in the thesis has been submitted in support of an application for another degree or qualification of this or any other university or other institute of learning

Copyright Statement

Acknowledgments

I would like to thank my supervisory team, Ms Cecilia Fenerty, Prof Tariq Aslam and Prof David Henson. All three of them have helped me through this journey in many different ways. But most importantly I am grateful to them for trusting me to fully lead on this project, allowing for ‘freedom of movement’ which helped me explore, do mistakes and learn from them, while always being there to advise and get me back on course.

Prof Paulo E Stanga and the MVR Lab team had a significant role during the PhD years. I would like to thank Prof Stanga for letting me into his team and providing me with the opportunity to be part of pioneering research, expand my horizon beyond glaucoma and to the exciting world of ‘retina’, meet people across the world and exchange ideas. Special thanks to Ms Danielle Marrochia for her invaluable help as a colleague and a friend. Also thanks to MVR Lab fellows and collaborators: Francesco Stringa, Soon Ch’ng, Francesco Romano, Assad Jalil, Alessandro Papayannis, Kasia Chwiejczak and Niall Doherty.

Last I would like to say a big thank you to friends and family, who accompanied me through this journey, coped with me through the hard times and helped me get out of them and for the times they provided an escape from my books. This work would have never been completed without them.

This PhD thesis effectively marks the last PhD supervised by Prof Henson; now a retired academic who explores his incredible skills in woodturning! There will never be enough words to thank him for all the guidance and mentorship not only in professional but also personal aspects. It is a great

honour to be his last PhD student; a title that I will always carry with pride and hope that my developing career will always make him proud.

This PhD thesis is dedicated to my father and my sister, the strongest people that I know…

Preface – The Author

Emmanouil (Manos) Tsamis is a PhD student at the University of Manchester specialising in perimetry (visual fields), imaging and other diagnostic tests for glaucoma. His current work focuses on the development of a novel computer-based visual field self-administered test for glaucoma screening purposes.

Manos is also collaborating with Prof Paulo E Stanga and the Manchester Vision Regeneration Lab for the design of clinical trials and the structural and functional examination of patients taking part in them. Among others, he is heavily involved in the “ARGUS II Epiretinal prosthesis in Advanced AMD” study and the NiGHT study, a unique approach of gene therapy in choroideremia.

In 2012, he was awarded the MSc Investigative Ophthalmology and Vision Sciences while his first degree is in Optics – Optometry, National Technological Institute of Athens, Greece.

Section 1

Development and Evaluation of a Computer-Based Visual Field Self-Test for Glaucoma Screening Purposes

1.1 Glaucoma – 'The Silent Thief of Sight'

Visual perception is considered to be the most significant and important sense for humans. The eyes gather approximately 80% of the total information that is transmitted to the brain from various sense organs. Hence, adequate visual function is highly associated with good quality of life. Glaucoma is one of the top three ocular disorders worldwide that can lead to severe visual impairment.[1-3] The term of glaucoma describes a group of optic neuropathies whose clinical characteristics are the progressive loss of retinal ganglion cells (RGCs). It is associated with changes in the structure of the optic nerve head (ONH) and the retinal nerve fibre layer (RNFL) and specific functional defects to the visual field (VF).[4] It is often, but not always, associated with high intraocular pressure (IOP).[5, 6] It is usually slowly progressive and in its early stages asymptomatic. Unfortunately, the structural and functional damage caused by glaucoma is irreversible. Once detected it requires life-long management with medication and/or surgical intervention to decelerate, or even stop, further progression of the disease. If left untreated it can lead to visual impairment and blindness.[7-12]

The prevalence of glaucoma increases with advancing age, affecting 1.5% over 40 years and 4% over 75 years of age.[13] Important risk factors include race and family history of glaucoma; see Figure 1.1 for a detailed list of risk factors associated with open-angle glaucoma.[14] After taking into consideration these risk factors, the National Health Services (NHS) in the UK established schemes that offer free annual eye tests for first degree

relatives of glaucomatous patients over the age of 40 and for patients more than 60 years of age.[15]

Category	Factor	Prevalence	Incidence	Progression	Response to Treatment
State of the individual	Age	+	+	?	Surgery response worse in younger patients
	Sex	0	0	0	Females less likely to receive treatment
	Ethnicity	Black +, Indian +, Hispanic +	Black +	?	?
	Family history	+		0	
Ocular anatomy and physiology	Increased IOP	+	+	+	
	Increased diurnal IOP variation	+	+	+	
	Exfoliation syndrome	+	+	+	
	Pigment dispersion	+			
	Myopia	+	0	0	
	Decreased corneal thickness		+		Improved response
	Increased disc diameter	+			
	Disc crescent	+		+	
Signs of damage	Increased CDR	+	+		
	Disc hemorrhage			+	
	Decreased choroidal thickness	+			
Systemic disease	Hypertension	?	0		
	Diabetes	?	?		
	Thyroid	+	?		
	Cardiovascular disease	0			
	Migraine	+			
	Sleep Apnea	+			
	Raynaud's		0		
Nonglaucoma medications	Corticosteroids	+	0		
	Cholesterol lowering	−			
	Calcium channel blockers	0		−	
Personal behaviors	Exercise	Decreases IOP			
	Smoking	0	0	0	
	BMI	0			
	Alcohol	0	0		
	Caffeine	0			
	Fat intake	?			
	Increased venous pressure	?			
	Acceptance of therapy				
	Persistence with therapy				Improved response

Rows are grouped using the categories described in the text. The columns report each factor's impact on each of 4 aspects of the disease: increased risk (+), decreased risk (−), no change in risk (0), unclear effect (?).

Figure 1.1: *List of risk factors associated with open-angle glaucoma, Boland and Quigley (2007)[14]*

1.1.1 Pathophysiology of Glaucoma

The progressive loss of RGCs and gradual degeneration of the optic nerve (ON) are the main characteristics of glaucomatous optic disc neuropathies. Multiple elements are believed to have an important role in glaucoma's

pathophysiology. According to various theories, factors like elevated IOP and vascular dysregulation contribute to the glaucomatous atrophy of one of the RGCs' basic compartments, the axons, at the lamina cribrosa.[16] These two elements can result in the alteration of the ON microcirculation and cause changes in the laminar glial and the connective tissue at the level of the lamina.[17] The "cupping of the optic disc" is a characteristic change in the ONH and an indication of where RGC axons have been lost (see figure 1.2). Death of RGCs in glaucomatous human eyes occurs by apoptosis, a programmed cell death process that takes place without any inflammation.[18]

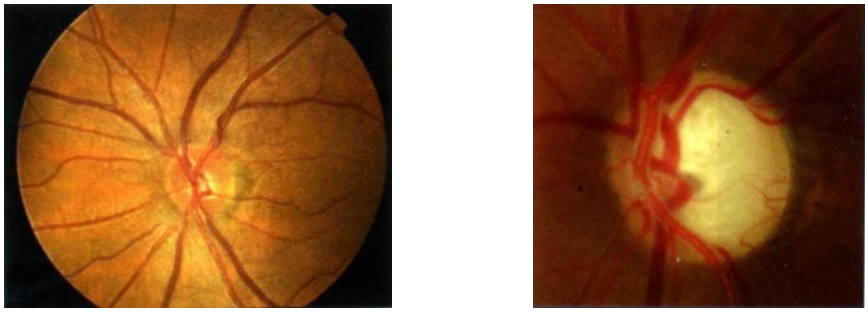

Figure 1.2: *Colour photographs of a normal eye (left image) and a glaucomatous eye with cup enlargement (right image), Spry and Harper (2010)*[19]

High IOP seems to have a role in RGC apoptosis; however, it is still unclear how important that factor is. There is good clinical evidence showing that an IOP reduction often helps to decelerate the progression of degenerative structural changes. However not all glaucoma patients present with high IOP. Various studies have showed that only one-third to half of the glaucomatous

study population presented with elevated IOP at the early stages of the disease.[20, 21] On average, 30-40% of patients with glaucomatous VF defects have normal values of IOP when diagnosed.[22] Thus, an elevated level of IOP is now believed to be a major risk factor for glaucoma, rather than the cause of the disease.

The finding that therapeutic control of IOP in many cases is not sufficient and also that glaucomatous changes have been observed in individuals with normal IOP suggest a critical role of other factors in the induction and progression of degenerative changes. Circumstantial evidences point towards an association between vascular insufficiency and glaucoma. A positive association of glaucoma has been observed with dysregulations of cerebral and peripheral vasculature, such as migraine and peripheral vascular abnormalities respectively.[23-26] For the proper understanding of this association between glaucoma and vascular deficiency, we need to comprehend the differences in the autoregulatory mechanism between a healthy and a glaucomatous eye.

The high metabolic demands of the vital parts in a healthy eye are met by the constant blood flow in the retina and the ONH. For the maintenance of a constant rate of blood flow an efficient autoregulatory mechanism operates over a wide range of day-to-day fluctuations in ocular perfusion pressure that is dependent on both the systemic blood pressure and IOP.[27] These autoregulatory mechanisms are not as vigorous in aging individuals as in youth. Therefore, deficient autoregulatory mechanisms leading to ischemia may contribute to the development of glaucomatous neuronal damage with increasing age. Glaucoma patients have been shown to have a chronically

reduced ONH and retinal blood flow, especially in people being diagnosed with low systemic blood pressure leading to reduced ocular perfusion pressure.[28-30] Thus, reduced diastolic perfusion pressure is now recognised as another significant risk factor for glaucoma.[31] The progressive decline in cerebral and ocular perfusion that has been observed with increasing age supports the definition of glaucoma as an age-related disease.[32, 33]

1.1.2 Classification and Types of Glaucoma

There is, actually, no simple mutually exclusive classification system for glaucoma; that in part reflects the lack of understanding of the pathophysiologic processes. Types of glaucoma can be classified in many ways. For instance, classification can be based on aetiology (primary and secondary), occurrence type (chronic and acute) and the outcome of gonioscopy (open- and close- angle) and IOP measurement (normal and hyper- tension).[34] Primary glaucoma, either open-angle (POAG) or close-angle (PACG), accounts for over 90% of the total glaucomatous cases observed worldwide.[35]

The time of onset may also be used to specify the type of a glaucomatous condition. Glaucoma cases of late onset are the most common and the average age of detection is approximately 65 years of age.[34] Those of early onset include congenital or developmental glaucoma cases with the most representative condition being juvenile open-angle glaucoma (JOAG); a rare,

often inherited condition that affects 1 in 10,000 infants and develops after the 3rd year of life.[36] Lastly, glaucoma can be classified as genetic or acquired.[34] Congenital or infantile glaucoma is evident either at birth or within the first few years of life.

There are three broad types of glaucoma: POAG, PACG and secondary glaucoma. American Academy of Ophthalmology defines POAG as “a progressive, chronic optic neuropathy in adults in which IOP and other currently unknown factors contribute to damage and in which, in the absence of other identifiable causes, there is a characteristic acquired atrophy of the ON and loss of RGCs and their axons. This condition is associated with an anterior chamber angle that is open by gonioscopic appearance” therefore allowing aqueous to access the trabecular meshwork. POAG is the most common type of glaucoma in Europe accounting for more than 80% of primary glaucoma cases.[37]

As mentioned above, the closure of the anterior chamber caused by multiple mechanisms is associated with PACG. Pupil block is an important factor for the pathogenesis of the majority of PACG patients. The pressure in the posterior chamber is higher than the anterior chamber causing the bowing of the iris, therefore blocking the trabecular meshwork and the outflow of the aqueous humor. As a result, IOP is elevated which can potentially lead to the damaging of the RGC fibres.[38-40]

Secondary glaucoma includes conditions such as pigmentary glaucoma, pseudoexfoliative glaucoma and uveitic glaucoma. Pigmentary glaucoma is associated with pigment dispersion syndrome which is an iris and ciliary

body disorder. The mechanical pigment liberation from iris pigmented epithelium causes the clogging of the angle and the reduction of the aqueous outflow. Glaucoma secondary to pseudoexfoliation syndrome (PXF) is called pseudoexfoliative glaucoma and is caused by the accumulation of fibillogranular material that reduces the outflow of the aqueous humor.

Cases with blunt trauma to the globe can lead to raised IOP and traumatic open-angle glaucoma. There are various mechanisms that act on this type of secondary glaucoma; from angle scarring and physical damage to the obstruction of the aqueous outflow by debris. Uveitic glaucoma is associated with various uveitic conditions in the anterior or intermediate part of the eye. As expected, there is reduction in the aqueous outflow either by trabecular changes or trabecular obstructions. Other secondary types of the pathology are neovascular glaucoma, which is associated with irregular vessel growth, and aphakic glaucoma which develops in aphakic patients, mostly after cataract surgery. [19]

1.1.3 Epidemiology of Glaucoma

Glaucoma affects more than 60 million people worldwide with an estimated 8.4 million people being blind due to the disease (table 1.1). Women are affected more than men representing 59% of all glaucomatous cases, while the Asians are the largest group affected, comprising 47% of the total population with all types of glaucoma and 87% of PACG. The prevalence of

glaucoma is projected to increase due to population growth and longer life expectancy; it is estimated that, by 2020, 76 million people will be affected by the disease while 11.2 million will be severely visually impaired.[35, 41]

World region	Total glaucoma	Total population >40	Ratio glaucoma to population >40
China	15,782,196	593,278,000	2.66%
Europe	12,064,740	541,993,000	2.23%
India	11,944,896	468,426,000	2.55%
Africa	6,458,023	149,408,000	4.32%
Latin America	5,677,158	169,215,000	3.35%
SE Asia	4,257,620	178,899,000	2.38%
Japan	2,662,446	72,007,000	3.70%
Middle East	1,618,718	110,094,000	1.47%
World	60,465,796	2,283,320,000	2.65%

Table 1.1: *Number of people worldwide with glaucoma in 2010, Quigley et al (2006)*[35]

Glaucoma is the second leading cause of blindness globally, after cataract. 2010 estimates reported that 4.5 million people were blind due to POAG and

3.9 million were blind due to PACG; the risk of blindness being greater for PACG than POAG.[37]

It is estimated that in the UK about 2% of people over 40 years of age have POAG and this number rises to approximately 10% in people over 75 years of age. There are approximately 480,000 people affected by POAG in England and around 10% of total UK blind registrations are due to glaucomatous optic neuropathy. The number of people affected by glaucoma is expected to rise with changes in UK population demographics.[42]

1.1.4 The Structure – Function Relationship in Glaucoma

It seems reasonable to assume a relationship between the amount of RGC loss and degree of visual dysfunction. The classic teaching is that for the assessment of a glaucoma patient a clinician should look for an agreement between structural changes at the ONH and functional changes to the VF. When this is identified, glaucoma can be confidently diagnosed. If there is a mismatch then other diagnoses should be considered. Although the site of primary damage is still in debate, loss of a group of nerve fibres and death of the corresponding RGCs will typically produce defined scotoma that should match the topography of the dysfunctional retinal nerve fibres. However, clinical cases have shown that it does not always work this way in early cases and clinicians can find that the match between the structural

appearance and the functional loss is not always as good as might have been expected.[43]

Early research work reported that structural loss occurs before functional changes in vision can be detected.[44-46] However, the frequently quoted notion, that at least 25% of RGCs are lost before any functional loss is evident, has been challenged by many later reports. Studies by Harwerth et al. used primates with experimentally induced glaucoma to demonstrate that there is a linear relationship between structure and function when both are plotted on a log scale[47] and that the relationship strengthened significantly when retinal eccentricity was taken into account.[48] However, this study, along with other studies, used primates where glaucomatous damage ranged from mild to very severe. A study of longitudinal VF change in glaucoma found a poor relationship between perimetry and optic disc change and concluded that function and structure provide largely independent measures of progression.[49] Nonetheless, while there may be a significant association between these two parameters when looking at a wide range of field loss, when we look at patients with early damage it is clear that the relationship between the two measures is less obvious.[50] The ideal diagnostic test would show a significant relationship between psychophysical threshold and RGC density in early glaucoma or, more impressively, in normal subjects.[51]

The different test strategies employed for perimetry and imaging provide an inherent problem in combining and comparing structure and function. As VFs are normally reported on a logarithmic scale and the nerve fibre layer on a linear scale, the relationship between the two is unlikely to be linear. A small change in sensitivity thresholds represents a much greater change than the

associated nerve fibre layer changes measured in microns on a linear scale. Typically, in early stages of glaucoma, structural loss appears greater than functional loss, while in advanced cases it seems as if functional loss still progresses when further structural loss is no longer apparent. However, more sensitive techniques for the assessment of early functional loss and better measurement of individual RGCs might produce different results with the two running in parallel. What is more, RGC dysfunction prior to actual death of the cell may play an important role in cases where functional loss appears to occur first.[43]

The sensitivity of diagnostic tests to early glaucomatous damage depends on relative variation of results in healthy controls and initial structural and functional status. A study from Gonzalez-Hernandez et al. (2009) examined the structure-function relationship of glaucoma in 228 controls and 1007 glaucoma suspects and glaucoma patients of different severity.[52] They observed that when the analysis is performed independently for the initial and advanced stages of glaucoma no curvilinear relationship is demonstrated. Furthermore, scatter plots between mean RNFL thickness and mean VF sensitivity showed the inter-individual morphological variability in early stages of the disease, thus reducing the strength of the association between structural and functional loss (figures 1.3 and 1.4). They concluded that the determination of the degree of functional damage based on structural data is not possible; patients with very mild or no functional damage demonstrate morphological values which are close to normal. Therefore, it is better to detect glaucoma by looking for changes over time,

assessing both structure and function of a glaucomatous patient or a glaucoma suspect.

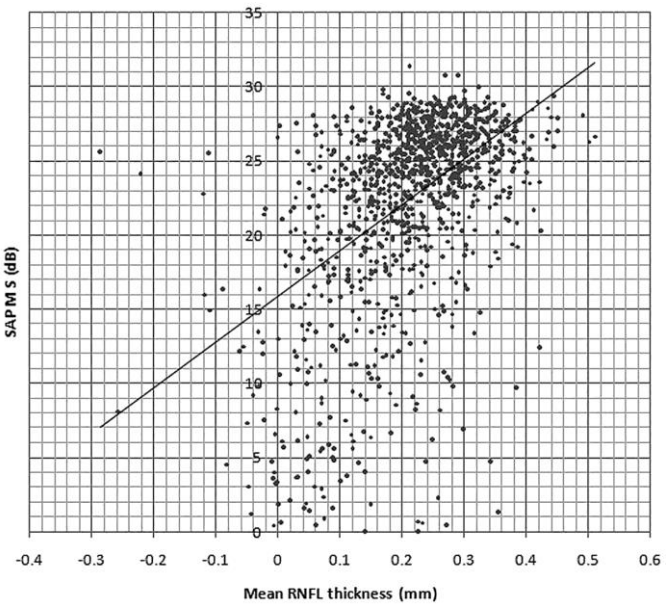

Figure 1.3: *Scatter plot of the whole sample between mean sensitivity (MS) – standard automated perimetry (SAP) and mean retinal nerve fibre layer (RNFL) thickness – Heidelberg Retinal Tomograph, Gonzalez-Hernandez et al. (2009)*[52]

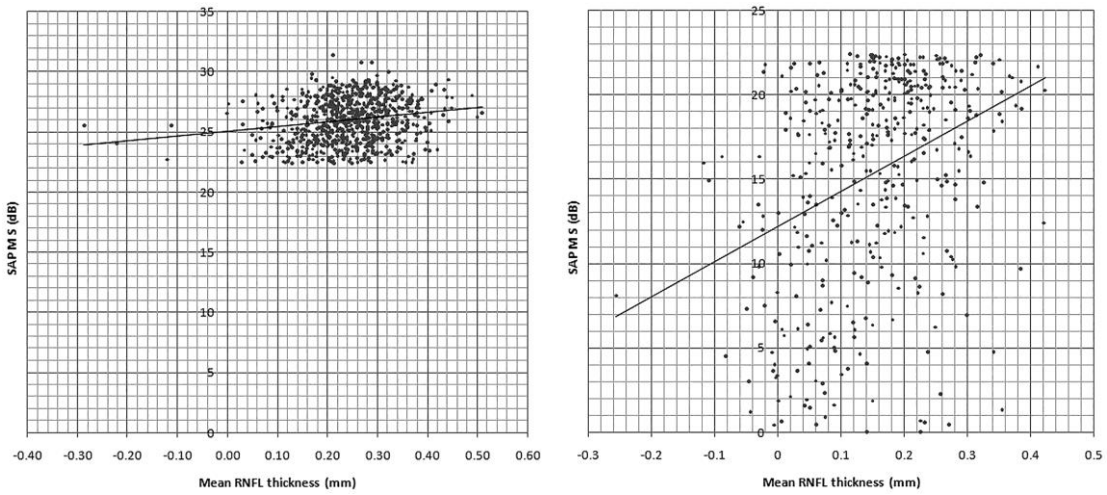

Figure 1.4: *Scatter plots of mean sensitivity (MS) vs retinal nerve fibre layer (RNFL) thickness in cases with MS higher (left) and lower (right) than 22.42 dB – breakpoint identified by piecewise linear regression. The high variability in structural measurements among individuals at early glaucoma stages is obvious, Gonzalez-Hernandez et al. (2009)*[52]

1.1.5 Diagnosis and Monitoring of Glaucoma

The diagnosis of glaucoma is based upon the identification of typical structural changes at the ONH with corresponding functional evidence of damage to the VF. The assessment of more than one parameter is essential for the early diagnosis of the disease. Those with isolated early structural changes or early VF loss are classified as glaucoma suspects, and they are followed-up at specific time intervals to monitor their status before being discarded (i.e. disease-free) or diagnosed (i.e. disease onset). The National Institute for Health and Clinical Excellence (NICE) in the UK has published

guidelines for the screening and monitoring of glaucoma. In these guidelines, NICE recommends the assessment of the ON structure, the VF function and the IOP along with central corneal thickness measurement and the appearance of the anterior chamber angle for the correct diagnosis of glaucoma and recognition of eyes at risk of developing the disease.[42]

Direct ophthalmoscopy offers a magnified view of the optic disc, but the view is not stereoscopic with limited ability to see changes in the depth of tissues at the ONH. The NICE recommendation for the assessment of the ONH is to use stereoscopic slit lamp biomicroscopy. The examination should include the dilation of patient's pupil for the accuracy of the assessment as ocular co-pathology may be missed. NICE accepts that stereophotography accompanied with bio-microscopic slit lamp examination is not always practical. However, it recommends the obtaining of an optic disc image at diagnosis for baseline reference. The variability in inter-observer agreement of the optic disc assessment has driven research and clinical practice towards more objective assessment techniques such as the confocal scanning laser ophthalmoscopy (Heidelberg Retina Tomograph; HRT) and Ocular Coherence Tomography (OCT).

The use of RNFL measurements for the diagnosis of glaucoma has increased considerably, since the development of OCT imaging techniques. Originally called optical coherence interferometry, OCT was firstly introduced in 1991[53]. A large number of studies reporting the diagnostic accuracy of TD- OCT have shown higher specificities, approximately 90%, than sensitivities, typically ranging from 70% to 90%.[54-58] A few more studies comparing time- and spectral-domain OCT (TD- and SD-OCT, respectively)

have reported similar or slightly better diagnostic accuracy with the latter.[59-63]

The confocal scanning laser ophthalmoscopy, developed by Heidelberg Engineering (Heidelberg, Germany), uses a diode laser beam that scans the ONH and provides measurements of ONH topography. It then generates a number of stereometric parameters, such as rim area, cup area, cup-to-disc ratio etc. The device has good glaucoma discriminatory ability, which is comparable to optic disc assessment by glaucoma experts.[64, 65] The latest version of this technology, the HRT III, offers a large normative database and advanced analytical tools, such as the Moorfields Regression Analysis[66] and the Glaucoma Probability Score[67], which improve the diagnostic accuracy of the instrument[68]. Nonetheless, the severity of VF loss has a significant influence on the diagnostic performance of all imaging instruments (both HRT III and OCT), with more severe stages being associated with higher sensitivity.[69]

The evaluation of the functional status in a suspected eye is essential for the diagnosis of glaucoma. The clinical method for the assessment of a patient's VF is called perimetry. NICE recommends the most widely used technique for VF testing, the Standard Automated Perimetry (SAP), with central thresholding test. Perimetry is invaluable to glaucoma management as it is the only method to reflect functional changes. An agreement between functional and structural changes/loss gives more confidence to glaucoma diagnosis, whereas a mismatch might indicate other ocular disorders. As functional changes are at the epicentre of this study, more details on the evaluation of VFs are given in section 1.1.7.

Goldmann applanation tonometry (slit lamp mounted) is considered to be the reference standard in IOP measurement. As mentioned previously, high IOP has been identified as an important risk factor for developing glaucoma but cannot be used to accurately discriminate between normal subjects and patients with glaucoma or quantify the disease severity. The normal upper limit of IOP is taken to be 21 mmHg.[70] However, numerous studies have reported on the positive relationship between age and IOP value and also the higher prevalence of increased IOP in black populations in comparison to whites. There are also diurnal changes in IOP, where IOP normally peaks early in the morning with a trough in the afternoon. These changes have been reported to be more evident in open-angle glaucoma (OAG) patients than normal-tension glaucoma patients and normal subjects.[71] Another shortcoming of IOP measurement alone for glaucoma detection is the influence of central corneal thickness and the anterior chamber configuration on IOP values. Therefore, NICE recommends supplementary tests to measure the central corneal thickness and assess the configuration and depth of peripheral anterior chamber.

Precise knowledge of the state of the anterior chamber angle is essential for the diagnosis of angle closure glaucoma. The process of gonioscopy involves the use of a goniolens (or gonioscope) in cooperation with a slit lamp to gain a view of the anatomical angle formed between the eye's cornea and iris. This iridocorneal angle defines the type of the disease (open- or closed- angle glaucoma) and its management. Recent developments in OCT have also allowed the use of this technique for the assessment of the anterior chamber angle. Central corneal thickness has

been identified as a risk factor for converting from ocular hypertension (OHT) to OAG.[5] The measurement of corneal thickness, also called corneal pachymetry, has been proven to be an indicator of glaucoma development when combined with standard measurements of IOP. The process of corneal pachymetry involves ultrasonic and optical methods with contact and non-contact techniques. NICE guidelines recommend the measurement of central corneal thickness by both contact and non-contact methods, although it recognizes that contact measurement techniques may be associated with potential corneal injury or transmission of infection.[42]

Glaucoma is a lifelong condition with variable clinical features. Thus, follow-up is required to evaluate rates of progression, long-term risk of impairment and suitability of current management. The maintenance and availability of reliable records is necessary for the coherent continuity of the health care. NICE recommends the assessment of four parameters in a single visit: 1) the IOP levels, 2) the structural appearance of the ONH, 2) the visual function and 4) the configuration of the anterior chamber depth.[42] The process of examination is the same as that for diagnosis, apart from the parameter of iridocorneal angle where, given that gonioscopy's accurate results have been recorded on diagnosis, Van Herrick's test is preferred for follow-up assessment due to its time-effective advantage. If a change in the ONH status is observed, a new image should be obtained for the patient's records for future assessments and comparisons. Central corneal thickness measurement is repeated only in cases where a change is suspected, e.g. following laser refractive surgery or at onset or progression of corneal pathology .[42]

1.1.6 Management and Treatment in Glaucoma

Treatment for glaucoma seeks to control the disease with no evidence of progression or progression at a rate which will preserve adequate visual function for the rest of the patient's life. It is focused on the only factor that can be modified, the IOP. In some cases, no treatment may be needed due to the static state of the disease while in others a more aggressive approach is required to confront a rapidly progressive condition. The main aim when treating glaucomatous patients is the lowering of IOP levels to a clinically pre-determined 'target pressure'. This target IOP is established on the basis of current IOP level, severity of disease at diagnosis and rate of disease progression and is subject to modification during follow-up. Other factors, such as age and life expectancy are also taken into account.[72]

IOP can be lowered either by medication or surgery. Medication is the first line treatment for most cases. There are five main classes of drug available: prostaglandin analogues, beta-blockers, sympathomimetics, miotics and carbonic anhydrase inhibitors. They achieve lowering of the IOP in the affected eye either by reducing the production of the intraocular fluid (aqueous humour) or by increasing the rate of outflow. The positive effect of different IOP reduction medications was reviewed by a meta-analysis of trials conducted by Vass et al. (2007).[73] Numerous studies and clinical trials have provided evidence showing the positive benefits of decreased IOP upon rates of progression and a delay in conversion from OHT to POAG.[8, 74-76] However, there is still a significant proportion of cases who despite achieving target levels in IOP continue to progress. Inversely, there are patient

subgroups that show no progression without any treatment. These findings indicate the presence of other factors that might contribute to the progression of the disease; further details on the theories behind potential mechanisms in the disease have been discussed earlier in section 1.1.1. An on-going placebo-controlled randomized clinical trial that is undertaken in the UK further investigates the effect of medical treatment on glaucoma.[77]

When drug delivery is not enough and target IOP has not been achieved, the option of surgery can be offered. Surgical treatments can be classified as penetrating and non-penetrating, all of which aim to lower IOP. NICE recommends trabeculectomy as a penetrating surgical procedure and deep sclerectomy and viscocanalostomy as non-penetrating. There are also laser techniques available for treating glaucomatous eyes, such as argon or selective laser trabeculoplasty (ALT; SLT). These two techniques are quite similar and involve the trabecular meshwork. The theory behind this treatment is that ALT and SLT are thought to activate trabecular cells, thus improving outflow through the trabecular meshwork.

1.1.7 Evaluation of Function

The assessment of the functional status of a glaucomatous eye is essential for the diagnosis and management of the disease. This section will provide an in-depth view on the clinical methods used to assess visual function.

The VF is defined as a three-dimensional space from which light can enter the eye and stimulate a visual response. The normal eye's VF extends approximately 60° nasally, 100° temporally, 60° superiorly and 70° inferiorly.[78] According to the Imaging and Perimetry Society (IPS), "the measurement of visual functions of the eye at [various] locations in the VF area" is called perimetry. A perimeter is an instrument designed to measure the VF by examining the differential light sensitivity.[79] The differential light sensitivity varies across the VF with the peak sensitivity occurring at the fixation point in photopic conditions, decreasing rapidly in the 10° around fixation and then more gradually towards the periphery.[80] RGC fibres transmit the visual signal through the sclera at the ONH, typically 10-15° nasally to fixation. At this location, there are no photoreceptors, creating a normal absolute scotoma, the "blind spot". Any damage to the visual pathway, such as glaucoma and optic neuritis, will affect the VF. Currently, the standard method of VF evaluation is SAP and can be undertaken with a range of perimeters including the Humphrey Field Analyzer (HFA), Octopus and Henson perimeters.

1.1.8 History of Perimetry

Albrecht von Graefe, in 1856, was probably the first person to report a quantitative VF analysis by examining his patient's VFs with the movement of a small stimulus along a flat surface; this examination procedure is termed campimetry.[81] The first perimeter with a complete bowl and control of the

background luminance was described in 1872.[82] The first multiple-stimuli technique for VF examination was introduced by Harrington and Flocks.[83] They designed an automated tangent screen on which several supra-threshold stimuli could be presented at different locations of the field of vision, while the patient had to report how many stimuli had been detected. Landmarks for the development of static supra-threshold perimetry were the development of the Friedmann Visual Field Analyzer and computer driven Henson Central Field Analyzer 2000.

The Swiss ophthalmologist Hans Goldmann introduced his bowl perimeter in 1945; this instrument set a new standard for perimetry by controlling many of the parameters known to affect the VF (figure 1.5). A decade later, Armaly and Drance, created a form of quantitative static perimetry on the Goldmann perimeter. A below-threshold stimulus was presented in the VF and its intensity was increased in constant steps, until it was reported as seen by the patient. It soon became obvious that this technique had advantages over kinetic examinations, although manual static perimetry was a demanding task for the examiner and patient. In the 1970s, Heijl and Krakau in Sweden, as well as Spahr and Fankhouser in Switzerland, contributed to the development of improved instrumentation.[84-86] Spahr et al. introduced the Octopus Perimeter (Interzeag, Switzerland), the first computerised static perimeter which became commercially available in 1978. Two years later, Humphrey Systems (Dublin, CA.) presented the HFA (Carl Zeiss Meditec Inc., Dublin, CA), which has, through its popularity, set a standard for SAP.

Figure 1.5: *Goldmann's bowl perimeter (left); modern perimetric devices – the Humphrey Field Analyzer (HFA; Carl Zeiss Meditec, Inc., Dublin, CA) (right)*

During the last three decades SAP has gradually replaced kinetic techniques for the investigation of the fields of vision. Research concentrated on the development of threshold algorithms that produce reliable estimates of the sensitivity, while keeping the time of the investigation as low as possible. The various algorithms/strategies that are currently available are explained in detail in section 1.1.12.

1.1.9 Classification of Perimetry

Perimetry can be broadly classified into two types: Kinetic and Static. In kinetic perimetry the intensity of the stimulus is kept constant while it is moved, usually from a non-seeing area to a seeing area, across the VF. The patient is expected to respond and report when the stimulus is first noticed; this location is then recorded on a VF chart. By moving the stimulus across the VF, areas of VF defect will be detected when the stimulus appears to vanish. The speed of the stimulus should be standardised, typically 2-4 degrees per second.

In static perimetry the stimuli are fixed at predetermined locations but their intensity varied to give measures of sensitivity. Most modern perimeters incorporate a series of different static tests that test different regions of the VF. Static perimetry can also be sub-classified into two techniques of investigation: threshold and supra-threshold. In threshold perimetry, an estimate of the patient's differential light sensitivity is obtained at each test location and compared with those from a normal population of the same age (age-corrected) as the observer. The stimulus intensities, locations and timing of presentations are controlled by a computer, according to a threshold algorithm. In supra-threshold perimetry the stimuli are presented at intensity calculated to be above the threshold of a normal observer. Further details are given later in this section; supra-threshold approach being a crucial part of the reported PhD project.

1.1.10 Psychophysics of Perimetry

In order to understand the term of threshold, we need to look further into the psychophysical background of perimetry. The idea of a “threshold” originated in the late 19th century when Fechner worked on the relationship between stimulus intensity and likelihood of perception.[87] According to his “high-threshold” theory, there is a threshold below which a stimulus is not perceived, and above which it is perceived. Psychophysical data demonstrate a continuous zone of stimulus intensities between “definite perception” and “definite non-perception”. The high-threshold theory explained this transition as an outcome of random fluctuations of the “true” threshold.

In static perimetry, sensitivity is expressed on a logarithmic, instrument-specific ratio scale of “stimulus attenuation”, in decibel (dB) units (equation 1).

$$S = 10 \times log_{10} \frac{\Delta L_{Max}}{\Delta L_{Stim}} \qquad (1)$$

The scale shows the relationship between the luminance increment of the stimulus (ΔL_{Stim}) to the maximum luminance increment (ΔL_{Max}) that the instrument is capable of producing. Thus, the most powerful stimulus is referred to as 0 dB, while a stimulus of 40 dB has been attenuated by 4 log units, which accounts for 1/10000 of the maximum luminance increment. Due

to the dependence of the scale on the maximum luminance increment, sensitivity estimates from different instruments cannot readily be compared.

Sensitivity and response variability at a specific retinal location are well described by the frequency-of-seeing (FOS) curve. A FOS curve shows the probability of a positive response for a number of different stimulus intensities. These curves are generally S-shaped and their general form is given by equation 2.

$$p_+ = fp + (1 - fp - fn) \times f(I) \qquad (2)$$

For yes-no tasks, such as static perimetry, the threshold is usually defined as the stimulus intensity at the 50th percentile on the FOS curve (figure 1.6). The slope of the curve defines the physiological response variability, or, in other words, the width of the transition zone between “always perceived” and “never perceived”. False-positive and false-negative rates give information on how likely it is that the observer responds even though no stimulus was shown (false-positive) and fails to respond in intense supra-threshold stimuli (false negative).[88]

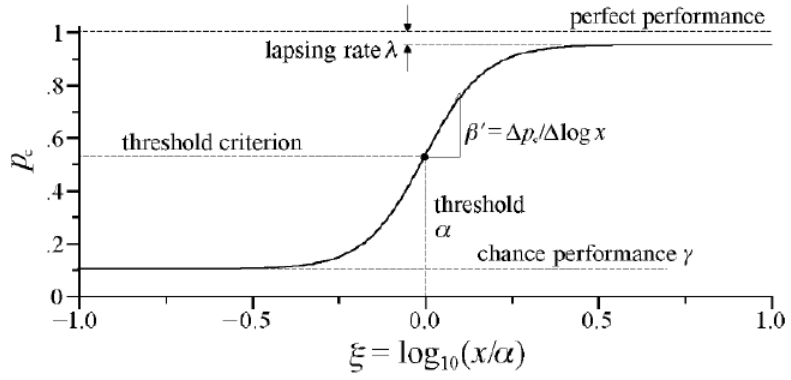

Figure 1.6: *Example of a frequency-of-seeing curve. The curve never reaches perfect performance (False Negative rate) and never reaches zero value (False Positive rate)*

The influence of response behaviour on FOS curves is described by signal detection theory (SDT) by Green and Swets in 1966.[89] SDT proposes that the observer's detection system is noisy; thus, there is a baseline neural activity even in the absence of a visual signal – stimulus. The presence of a stimulus will increase the level of activity.

FOS data have been generated from normal, suspect and OAG eyes by several research groups.[90-92] They have established that variability increases as the sensitivity reduces.[93] In 2000, Henson et al. compared the relationship between sensitivity and response variability in the VF of normal eyes, eyes and those with optic neuritis, glaucoma and OHT.[94] FOS data showed that the relationship between these two parameters was similar between the four groups, with the authors concluding that the results provided further evidence to support the hypothesis that response variability is dependent on functional RGC density. According to this hypothesis, the

relationship would be similar in glaucoma and optic neuritis despite the different patterns of VF defects and the different mechanism of nerve fibre damage.[95]

1.1.11 Current Perimetric Specifications

Stimulus and Background

During VF examination individuals are asked to respond to a series of stimuli presented in different locations within their VF. The most commonly used measure of VF testing in glaucoma is the white-on-white perimetry, where achromatic light spots are displayed on a white background. The HFA perimeter uses a background level of 31.5 apostilb [asb; equal to ~ 10 candelas per square metre (cd/m^2)] therefore producing photopic conditions in which cones are primarily tested. Stimulus intensity varies from 10,000 asb to 0.1 asb in the HFA, allowing the machine to measure thresholds over a 50 dB range.

Other alternative stimuli/backgrounds have also been developed. Blue-on-yellow perimetry (also called short-wavelength automated perimetry; SWAP) targets specific visual pathways that are thought to be selectively damaged in early glaucoma. Studies have shown that the use of blue stimuli on a yellow background is superior to white-on-white perimetry for assessing functional damage in early glaucoma. However, SWAP has some limitations that prevent a wide adoption of this technique. Media opacities are thought to

influence threshold estimations while SWAP demonstrates, in general, higher test-retest variability.

Frequency-doubling technology (FDT) is another variation of perimetry. The FDT technology is based on the frequency-doubling effect which occurs when a low-spatial-frequency grating is flickered at a high temporal rate and results in the grating's appearing to have twice its original spatial frequency. It is believed that the frequency-doubling concept targets a small subset of RGCs (approximately 2% of the total population) that are again thought to be selectively damaged in early glaucoma. FDT perimetry uses frequency-doubling stimuli and contrast thresholds are measured for detection of the FDT stimulus.[96]

Alternative forms and developments of modern perimetry, such as the ones mentioned above, aim to improve detection of glaucoma by selectively testing specific RGCs. For example, high-pass resolution perimetry (or ring perimetry) is presumed to selectively test the parvocellular system.[97] The stimuli used in this variation of modern perimetry are rings of variable size with dark borders and bright centres. These rings are projected at different locations on the screen and create an average stimulus luminance equal to the background luminance. The results of this test are believed to correspond to the density of RGCs and, concerning glaucoma, ring perimetry is comparable to standard perimetry in terms of diagnostic performance.[98]

In the early 1980s, Prof Fitzke investigated motion displacement thresholds in glaucomatous and normal population and developed the first Motion Displacement Test (MDT) at the Institute of Ophthalmology, London. He

found evidence of elevated motion displacement threshold in defective areas of the VF. MDT's most recent development, the Moorfields MDT (research product of collaboration between Moorfields' Glaucoma Research Unit and Institute of Ophthalmology, UCL) incorporates 31 line stimuli which are scaled in size by estimate of RGC density. Moorfields MDT is a Windows-based software that fits a 15-inch laptop screen at a test distance of 30 cm. The test task is to look at a central spot and press the computer mouse each time a line on the screen is seen to move. The aim of the Moorfields MDT test development is to offer an affordable, portable and sensitive method of case-finding in the community.

Stimuli Distributions

There are numerous stimuli distribution patterns each of which is selected according to the needs of the VF examination; for example, whether emphasis should be given at the inferior or superior field, if the test is for screening or monitoring purposes etc. The most common stimulus distributions are the central 30-2, 24-2 and 10-2 distributions (figures 1.7 and 1.8). The 30-2 pattern examines the central 30 degrees of VF. It includes 76 stimulus places located on a square matrix of 6 degrees, displaced from the horizontal and vertical midlines by 3 degrees. The 24-2 distribution is simply a subset of the 30-2 pattern with 54 locations falling within the central 24 degrees along with two points at 27 degrees in the nasal field. While the 30-2 pattern provides the most information for the central VF, the 24-2 test has a shorter test time and smaller variability. The appearance of lens rim artefacts

at the peripheral points of the 30-2 test, and hence low discriminatory power, is another reason that the 24-2 programme is routinely used in most ophthalmic clinics.[99]

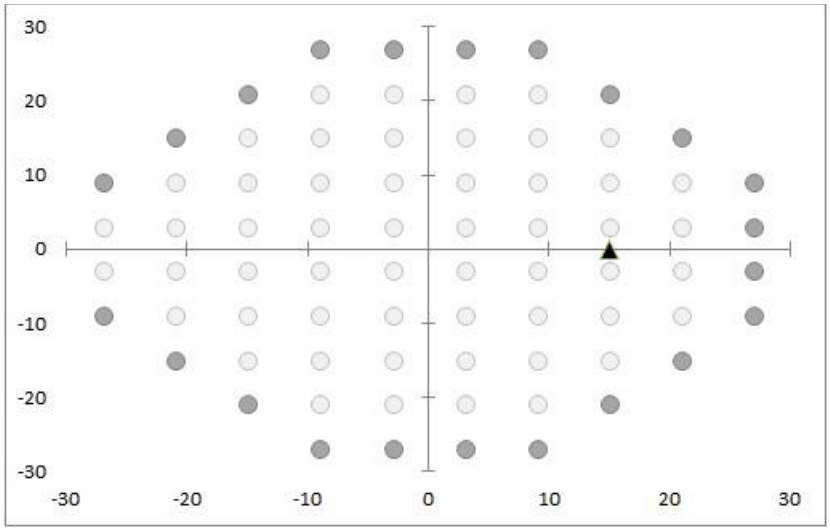

Figure 1.7: *Light grey dots represent the 54 locations of the 24-2 stimulus distribution, while dark grey dots represent the extra locations included in the 30-2 distribution. Filled triangle shows the typical location of the blind spot, which is normally 1-2 degrees below the horizontal line (example of a right eye)*

When higher spatial resolution is needed (e.g. patients with small central fields), the 10-2 programme can be used to assess the residual visual function. The 10-2 pattern examines 68 locations within the central 10 degrees on a 2 degrees square matrix. Although the 10-2 test is routinely used for patients with advanced glaucoma, it is known that the macula (i.e. central field) is affected even in early glaucoma. Based on this theory,

Traynis et al. hypothesised that some patients might fail a 10-2 test while presenting normal 24-2 results.[100] They found that this was the case for 16% of the glaucomatous eyes they tested, therefore emphasising the poor detection of central loss with the 6 degree square matrix and suggesting that the 24-2 test is not optimal for detecting early damage of the macula.

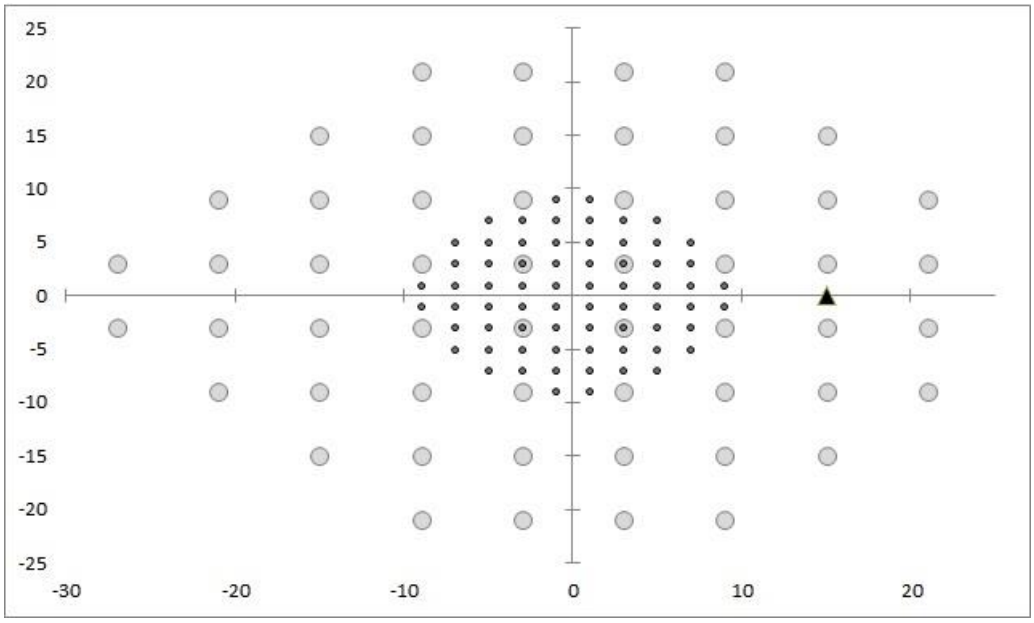

Figure 1.8: *A comparison between the locations of 24-2 and 10-2 distributions, with the latter being more dense in the central 10 degrees of the visual field*

Early work has shown that the informational value of each test location in the VF is likely to vary. Henson et al. analysed data obtained with a Friedman Visual Field Analyzer and showed that stimuli at locations greater than 20 degrees of eccentricity along with those around the blind spot give the least information.[101, 102] This evidence stimulated further work from Wang and

Henson to evaluate the diagnostic performance of VF testing for early glaucomatous loss with subsets of the 24-2 test pattern (figure 1.9).[103] They found that 11 locations (including 2 in the blind spot) did not contribute anything to the performance of the 24-2 test. They also presented optimized distributions with 10, 20 and 30 locations that retained good diagnostic performance.

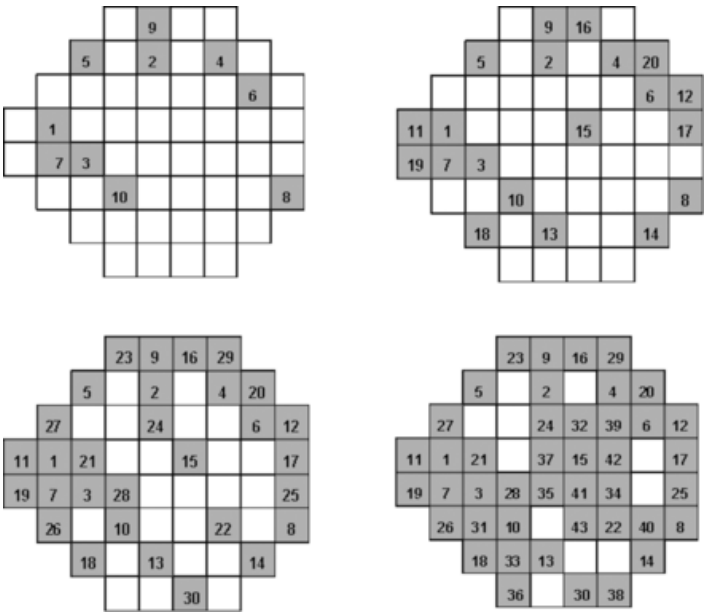

Figure 1.9: *Optimal subsets of the 24-2 distributions with 10 (top left), 20 (top right) and 30 (bottom left) locations. 43 locations (bottom right) contribute significantly to the performance of the 24-2 test, Wang and Henson (2013)*[103]

Stimulus Size and Duration

A human's ability to visually detect targets on a uniform background has been described by several laws in the past. One such law is Ricco's law, which describes the relationship between a target area and target contrast required for detection (equation 3). Ricco's law is based on the fact that the light energy required to lead to the target being detected is summed over the area and is thus proportional to this area. Ricco's area is the area of complete summation; in other words, the largest target/stimulus size required for which the multiplication of area and intensity is constant at threshold. This region is variable based on the amount of background luminance[104] and retinal eccentricity[105].

$$Contrast \times Area = k \qquad (3)$$

As a result, stimulus size has a significant role in perimetry. Stimulus sizes were standardised by Goldmann in 1945 (Table 1.2), who based them on an estimated relationship between size and intensity, so that each step gives an approximately 5dB intensity change. In a HFA the size of standard stimulus is Goldmann III, approximately 0.5 degrees. Taking Ricco's law into account, however, it is evident that the conventional stimulus size is smaller than Ricco's area for retinal eccentricities over approximately 15°. Thus, thresholds for Goldman III stimuli in SAP are determined by complete spatial summation for those retinal regions only. Within 15° of the fovea, thresholds for SAP are determined by probability summation as stimuli are larger than Ricco's area. Previous research has shown that there is no observable

change in Ricco's area as a function of age.[106] However, there is a significant enlargement of the region in early glaucomatous cases suggesting that perimetric stimuli should be capable of adjusting their size as well as their contrast, therefore boosting the "glaucoma signal" within measurement noise.[107]

Goldmann size	I	II	III	IV	V
Area (mm^2)	1/4	1	4	16	64

Table 1.2: *Goldmann stimulus sizes*

The effect of stimulus size in perimetry has been investigated by various studies. Wall et al., in 1997, studied the influence of stimulus size on the slope of psychometric function in normal and glaucomatous eyes.[108] They concluded that the larger Goldmann V stimulus produced significantly steeper FOS curves than sizes III and I. In a more recent study, which tested a large number of patients with size III, V and with a method that varies stimulus size for a fixed contrast (namely size threshold perimetry), it was reported that the number of abnormal locations is the same for all different parameters.[109] The study also highlighted the increased variability for size III and concluded that the adoption of a single stimulus size is not of great importance and new developments in visual perimetric stimulis should focus on other properties, such as lower variability, reduced illumination etc.

The human visual system responds through the absorption of light photons over both space and time. In the temporal domain, summation relates the duration of a stimulus to the threshold contrast achieved (i.e. Bloch's law). When summation is complete, stimulus duration and contrast are inversely related at threshold (equation 4).

$$Stimulus\ Duration\ \times Contrast = k \qquad (4)$$

After taking Bloch's law into account, we can assume that stimuli presented for longer durations are more likely to be seen as a result of temporal summation of information. However, Pennebaker et al. studied the effect of various stimulus duration times and concluded that between a range of 0.1 – 0.5 seconds the stimulus presentation time had little effect on threshold fluctuation in healthy individuals.[110] Most static perimeters take into account Bloch's law, which simply states that up to a certain presentation time the detection of a stimulus increased with increasing presentation time. More specifically, for photopic conditions, the critical duration is below 100 ms. In an attempt to provide a common framework for VF measurement, the IPS standardised most of the perimetric parameters, including the stimulus duration.[79] The typical presentation time is 200 milliseconds; an interval longer than the critical duration of Bloch's law, but shorter than the latency of a refixation saccade (~250 milliseconds) which would displace the retinal stimulus. A recent PhD work, by Padraig Mulholland, investigating temporal summation reported a significantly lower critical duration (~30 milliseconds)

compared to results from previous studies.[111] Such difference lies in the use of different analysis techniques and the assumptions they make concerning the degree of partial summation exhibited. Mulholland also reported on variations in summation in both the spatial and temporal domain in glaucoma, suggesting that stimuli modulating in area, duration and luminance may improve the sensitivity of SAP.

1.1.12 Visual Field Testing Algorithms and Strategies

Threshold methods

There are numerous algorithms for deriving threshold estimates. Threshold algorithms may be adaptive or non-adaptive. In adaptive threshold algorithms, the stimulus intensity used on any trial depends on the observer's responses to previous presentations whereas in non-adaptive methods, the intensities are pre-determined and independent of the subject's response; the most common example being the "method of constant stimuli".[112] Early in perimetry's history adaptive methods were considered more effective than non-adaptive, despite the uncertainty about the initial threshold value.[113-115] The reason for this favoured view towards adaptive techniques was the acknowledgment that stimulus intensities closer to the true threshold value are generally more informative than those far from it and test times would be shorter.

One of the first adaptive threshold algorithms to be used in perimetry is known as the Full Threshold (FT) algorithm. In the FT algorithm the stimulus

is first presented either at a value that is derived from neighbouring threshold estimates or, when these are not available, on the basis of normal values. The stimulus intensity is then decreased (or increased) according to the patient's response (or non-response) at fixed increments (i.e. 4 dB) until the stimulus is not seen (or seen). The step size is then reduced from 4 to 2 dB and the direction reversed until the stimulus is seen (or not seen). The threshold estimate is taken as the attenuation (dB) of the last stimulus seen at that location. This process is called a "staircase algorithm", due to the specific increments in the algorithm. The FT algorithm was developed by Bebie et al. in 1976.[116] Their algorithm used the mean sensitivity of the observer's age group as a starting level of stimulus intensity and was terminated once a response reversal occurred at a stepsize of 2 dB. The threshold value is taken as lying between the presentations that mark the second reversal; see example in figure 1.10. The method "4…2…1", as they called it, derived from simulations that took into account the response variability in normal eyes and was quickly accepted as one of the optimal strategies. However, the FT algorithm requires approx. 5 presentations per test location and hence is exhausting, when combined with the 24-2 test pattern, for most patients (test times often exceeding 10 minutes per eye).

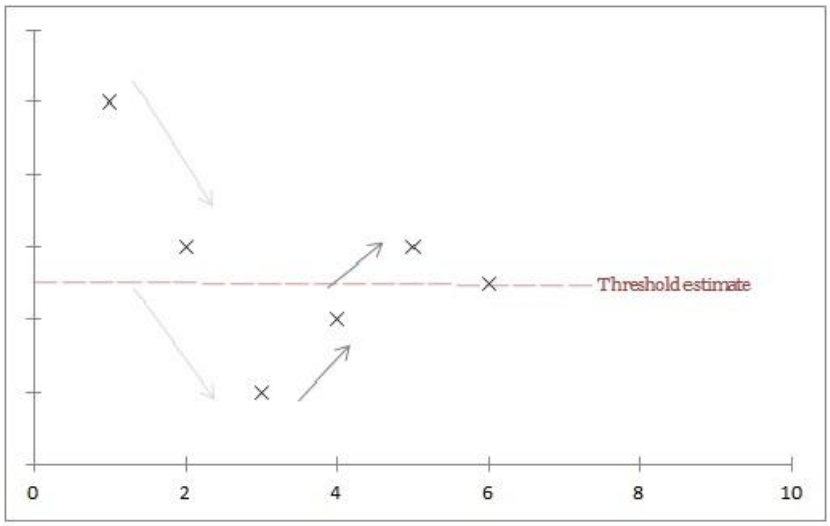

Figure 1.10: *An example of the "4…2…1" staircase algorithm. Light grey down arrows indicate a reduction in stimulus intensity of 4 dB, followed by an increase of 2 dB increments (dark grey arrows) after first reversal. A correction of 1 dB follows the second reversal for the final result.*

The Fastpac algorithm was developed for the HFA to reduce the test times of the FT algorithm. The Fastpac algorithm uses steps of 3 dB with a single reversal. Although it is faster than the FT method in normal eyes and in patients with mild VF loss, it underestimates the severity of VF defects[117] and has greater variability. Also, the speed advantage is reduced in cases with advanced field loss.[118]

In pursuit of shorter test times that would increase the accuracy of VF testing, perimetric experts and researchers explored the benefits of other adaptive procedures, which make use of both previous knowledge about the shape of the psychometric function and the observer's previous responses to guide further testing. The advantages of such an approach were discussed in

the ‘60s by numerous authors, but it was Andrew Watson and Dennis Pelli in 1983 who introduced a Bayesian adaptive psychometric method.[119] QUEST, as they named it, is an efficient method of measuring threshold based on three steps: 1) specification of prior knowledge of threshold, including an initial probability density function (pdf; details are discussed further below), 2) a method for choosing the stimulus intensity of any trial and 3) a method for choosing the final threshold estimate. Watson and Pelli introduced a Bayesian framework to calculate a current pdf which takes into account prior knowledge of the psychometric function and data from previous tests. This pdf is then applied on steps 2 and 3.

The determination of the maximum likelihood threshold for each test location requires an initial pdf, which states for each possible threshold the probability that any patient will have a threshold at that location (see Figure 1.11). The first stimulus is then presented according to that initial pdf (e.g. the median or mean of the pdf). The observer’s response to that stimulus is used to modify the pdf for the next presentation. This process is repeated until the specified terminating criteria have been met; for example when the standard deviation of the pdf falls below a fixed value.

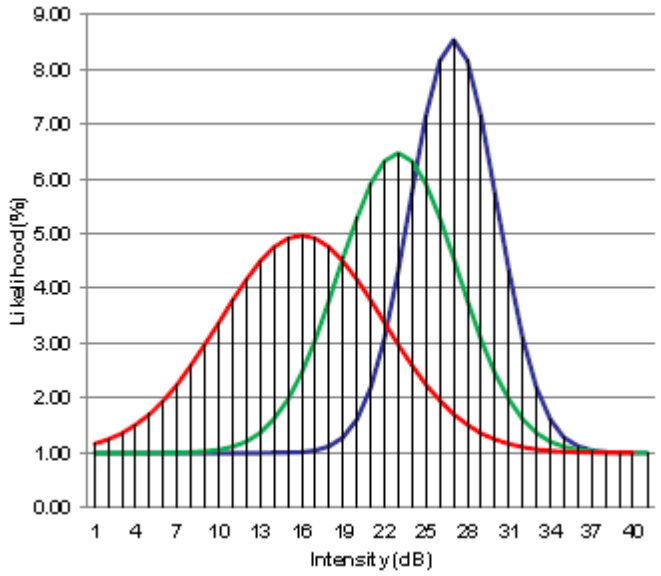

Figure 1.11: *Group of PDFs, one for each threshold level. Broader PDFs in low thresholds indicate higher test-retest variability*

King-Smith et al evaluated various modifications on the QUEST threshold method, particularly on the technique for choosing the intensity of the next presentation but also on steps 1 and 3.[120] They concluded that their Zippy Estimate by Sequential Testing algorithm (ZEST; a QUEST variant) which sets the intensity to the mean of the current pdf provided greater precision than the original QUEST method or other simulated variations.

Visual Field Testing Strategies

Following on from King-Smith's work several perimeters introduced algorithms that adopted some of the maximum likelihood principles. The Swedish Interactive Thresholding Algorithm (SITA) was the first to adopt the more efficient Bayesian methods to derive threshold estimates of similar

precision to the FT and Fastpac algorithms but with substantially fewer presentations.[121] The SITA strategy was initially developed for the HFA perimeter and estimates threshold sensitivity at each point based on observer's responses to stimuli at that location, as well as responses from nearby points. Thus, an assumption is made about the underlying psychometric function, placing the stimulus intensity at the next location as close as possible to the nearby threshold. FT strategy is still followed for the first 4 points tested, one in each quadrant of the VF. At least one reversal from decreasing to increasing intensity is obtained for each location. Test times in normal eyes are halved from FT tests, with similar or better reproducibility.[122, 123] SITA includes variable inter-stimulus intervals, new methods for detecting false positives and follows the "4-2" staircase algorithm for stimulus intensities. There are two version of the SITA strategy: SITA Standard and SITA Fast; the latter having looser terminating criteria, shorter test times and greater test-retest variability in areas of low sensitivity.

Another widely used strategy is the Zippy Adaptive Threshold Algorithm (ZATA), which is used in the Henson perimeters. The Henson ZATA test uses a modified ZEST algorithm. It differs from SITA by using the pdfs for deciding test level. It also uses prior VF test thresholds, when available, for setting starting test intensities and the use of terminating criteria that change through the test according to the patients' responses. Quite recently, the ZEST strategy was also adapted for the FDT and was implemented in the new Humphrey Matrix perimeter. Turpin et al, in 2002, developed a new test procedure for FDT perimetry that adopts ZEST principles for threshold estimations.[124, 125]

Multisampling Supra-Threshold Techniques

Many clinical applications call for quick, simple, yet reliable VF tests that can be performed by patients without the need of training. Conventional supra-threshold tests are easier to perform as they reduce the number of stimulus presentations and therefore test duration. However, supra-threshold perimetry is thought to be less able to detect mild VF defects than threshold testing. The conventional criterion for defining a VF location as defective is when no stimulus is seen twice out of 2 presentations. This criterion may reduce false positive errors, but also reduces the ability of the test to identify correctly those who have the condition of interest (or in other words the sensitivity of the test) by a small, yet significant, amount.[126]

Paul Artes et al attempted to tackle the issues of sensitivity and variability in supra-threshold perimetry by developing an optimal multisampling technique.[126] The criterion for the classification of a location as normal or defective was 3 seen or missed presentations (3/5), respectively; meaning that between 3 and 5 stimuli were required to be presented at each location. They evaluated their newly developed technique along a range of defects and in comparison with conventional supra-threshold (1/2) and FT strategies. They demonstrated that multisampling could be a powerful alternative to other strategies as it shows similar sensitivity to that of the FT, which is considered the gold-standard, without sacrificing specificity (i.e. the ability of the test to identify correctly those without the disease).

Multiple-Stimulus Perimetry

Most of the current clinical VF tests use single-stimulus techniques to obtain threshold measurements. These techniques are demanding for patients; it is not unusual for individuals to report difficulties in maintaining their attention during testing. Wall et al. provided evidence showing that brief lapses of attention might be associated with overall reduced sensitivity and increase response variability.[108]

In the ‘50s, Harrington and Flocks introduced multiple stimulus perimetry as a screening test.[83] During this type of testing up to 4 stimuli are presented at each exposure. The patient verbally reports the number of seen stimuli, along with their location if this number is smaller than the actual number of presented stimuli. Verbal feedback has been shown to be a parameter that can contribute to the maintenance of patient’s attention and reduction of variability. Recently, Miranda and Henson measured the perimetric sensitivity and the response variability of both single- and multiple-stimulus perimetry in glaucoma and demonstrated that a multiple-stimulus technique could reduce variability by more than 1 dB on average while increasing threshold sensitivity by almost 2 dB.[127] Their work showed that changes in both the ways that stimuli are presented and patients respond could improve routine clinical perimetry.

Parameters influencing Perimetry

Variability in VF testing can be subdivided into short- and long-term (intra- and inter-test respectively). Variability during testing can be represented, as previously shown, by the slope of the FOS curve. It is observed to be higher in defective locations with a standard deviation of approximately 7 dB.[128] Inter-test variability has been examined in glaucoma patients tested with both conventional (30-2, HFA) and FDT perimetry.[129] Both techniques showed larger re-test variability in areas with reduced sensitivity compared with normal locations.

Two factors that influence perimetric outcomes are the stimulus characteristics and the observer. Stimulus size has been associated with variability, with smaller stimulus sizes (Goldmann I and II) demonstrating larger variability compared with larger sizes (Goldmann III, IV, V).[130] In a study conducted by Henson et al, a statistical analysis between variability and numerous factors showed that significant fluctuations in threshold measurement are related to sensitivity (with reduced sensitivity demonstrating larger variability), diagnosis and false-negative rate, whereas no association was established between variability and factors, such as age, eccentricity, fixation losses and false positive rate.[94]

The observer's variables that affect the slope of the FOS curve include perimetric experience (learning effects), fatigue, and loss of attention. More specifically, patients tend to perform better in follow-up tests as they gain test experience.[90, 131] The learning effect is usually greatest between the first and second test. Therefore, a patient's first VF result should be interpreted

with caution. Patient fatigue may result in decreased retinal sensitivity.[132] It has been the limiting factor for attempts to increase the accuracy of testing by extending the time of the examination. The fatigue effect on VF testing has been confirmed in both normal and glaucoma groups, with the latter demonstrating a larger increment of variability.

Visual Field Loss in Glaucoma

Glaucomatous VF defects can be diffuse, as with cataract cases or patients with corneal opacification, or localised.[133] VF loss associated with glaucoma is also, especially in its early stages, usually asymmetric about the horizontal meridian and typically correlates with the arrangement of the RGC axons within the RNFL.

A typical glaucomatous defect is the nasal step, where an area in the nasal VF has reduced sensitivity on one side of the horizontal meridian and normal sensitivity on the other. Another characteristic feature of glaucomatous functional loss, and a sign of a moderate stage of the disease, is the classic arcuate scotoma; a comma-shaped defect arching over the central VF. Other typical types of VF defects in glaucoma are: a paracentral defect 10°-20° from the blind spot, generalised constriction (tunnel vision) and, of course, complete VF loss at the end stages of the disease (figure 1.12).[134]

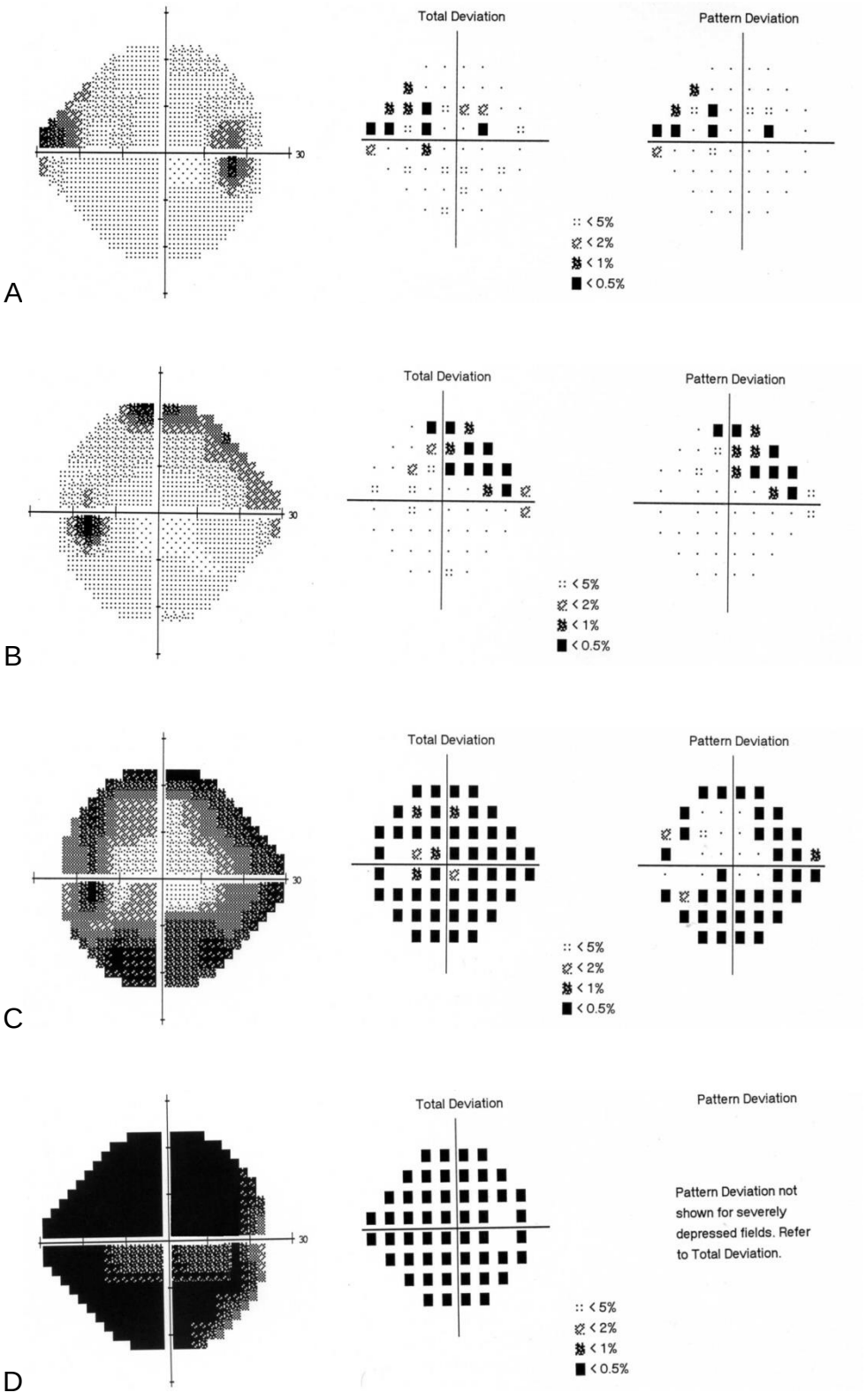

Figure 1.12: *Examples of typical glaucomatous defects: A) nasal step, B) arcuate scotoma, C) generalised constriction (tunnel vision) and D) full loss of visual field.*

1.1.13 Assessment of Clinical Tests

There are numerous clinical tests applied for the confirmation or rejection of the presence of a disease or to help the diagnostic process. Ideally such tests correctly identify all those who are disease-free and all those who have the condition of interest. However, most clinical tests fall short of this ideal.[135] The terms: true positive, false positive, true negative and false negative are fundamental measures of tests efficacy:

- True positive: The test is positive and the patient indeed has the disease
- False positive: The test is positive but the patient does not have the disease
- True negative: The test is negative and the patient indeed is disease-free
- False negative: The test is negative but the patient has the disease

Sensitivity/Specificity and Other Diagnostic Characteristics

Test performance is measured by an unbiased comparison of the test result against a reference (also called gold-standard or criterion standard). Sensitivity and specificity are two key terms when evaluating the performance of a diagnostic tool, such as perimetry. Sensitivity describes the ability of the test to identify correctly those who have the disease (i.e. the true positive rate). Specificity describes the ability of the test to identify those who

do not have the disease; or, in other words, the true negative rate (see Table 1.3). The ideal test would have a 100% specificity and sensitivity. However, in the real world, and for certain purposes, the test's ability to identify true positives might need to be sacrificed for a higher specificity; or vice versa.[136]

For each test one or a series of cut-off criteria might be used to define when a result is normal or defective. For example, for a screening test, any value above or below a certain cut-off level might trigger further investigation. No matter what is the chosen cut-off value, there will be a number of false positive and false negative results. The choice of a particular cut-off point depends on the tests objectives: confirm the disease, refute the presence of the disease or to screen the population. If the objective is to rule out the disease, the test with the fewest false-negatives should be chosen. Such a test will present high sensitivity, where nearly all diseased patients will have a positive test result. On the other hand, when the objective is to confirm a diagnosis, a test with high specificity should be chosen, which will present the fewest false-positives.[137]

Other useful terms that characterise a clinical test are the positive and negative predictive value (PPV and NPV respectively). PPV shows the likelihood that a patient has the disease given that the test result is positive, while NPV reports how likely it is that a patient does not have the disease given a negative test result (see Table 1.3). Unlike sensitivity and specificity, the PPV and NPV are dependent on the prevalence of the disease in the sampled population. For example, consider a population of 1000 people, divided equally into diseased and disease-free where the screening test has a sensitivity and specificity of 95%. Screening this population would result in

475 true positives and 475 true negatives with 25 patients failing the test when in fact are disease-free and 25 patients testing negative when they are diseased. Therefore, the PPV of this test is also 95%. However, if there are 950 disease-free people in the population, the number of false positives increases to ~48 and the PPV falls to approximately 50%.

	Gold - Standard		
	Disease Present D^+	Disease Absent D^-	
Positive Test T^+	True Positive (TP)	False Positive (FP)	Positive Predictive Value (PPV) $\frac{TP}{TP + FP}$
Negative Test T^-	False Negative (FN)	True Negative (TN)	Negative Predictive Value (NPV) $\frac{TN}{TN + FN}$
	Sensitivity $\frac{TP}{TP + FN}$	Specificity $\frac{TN}{TN + FP}$	

Table 1.3: *Calculating sensitivity, specificity, positive and negative predictive values of a diagnostic test*

Screening is defined, by the UK National Screening Committee, as “the systematic application of a test, or inquiry, to identify individuals at sufficient risk of a specific disorder to warrant further investigation or direct preventive action”.[138] The preference of a highly sensitive or specific screening test depends on the nature of the disease and its treatment capabilities. For example, screening to prevent transmission of a preventable disease (such as HIV in blood donors) requires optimal sensitivity. However, when the cut-off value is chosen for maximal sensitivity, the compromise is a loss of specificity. In this situation, there is a danger of diagnostic facilities being overloaded with patients labelled positive by a screening test who do not actually have the condition of interest. Reversely, a highly specific test is preferred on occasions where the costs or risks of further examination are significant, e.g. surgical biopsy. Optimal specificity is also sought when screening for diseases with low prevalence in the population tested in order to improve the level of correctness of the test result. Nonetheless, a cut-off point with the right sensitivity/specificity balance should be chosen after assessing for possible costs and benefits, including the assessment of cost-effectiveness and the potential for harm.

Receiver Operator Characteristic Curves

An important tool for the evaluation of diagnostic performance is the Receiver Operating Characteristic (ROC) curve, a graphical plot which demonstrates the performance as the cut-off criteria is varied (figure 1.13). It is created by plotting the fraction of true positives out of the total number of

positives (i.e. the true positive rate or sensitivity) against the false positive rate (or 1 – specificity), which is the fraction of false positives out of the total number of negatives, at various cut-offs. ROC analysis provides the means to select the optimal cut-off criteria. The upper left corner of the ROC space represents the best possible result, 100% sensitivity and 100% specificity. The area under the ROC curve is another useful summary statistic that gives a criterion free measure of test performance. An area of 1 represents a perfect test, while an area of 0.5 signifies a test which is no better than tossing a coin.[139]

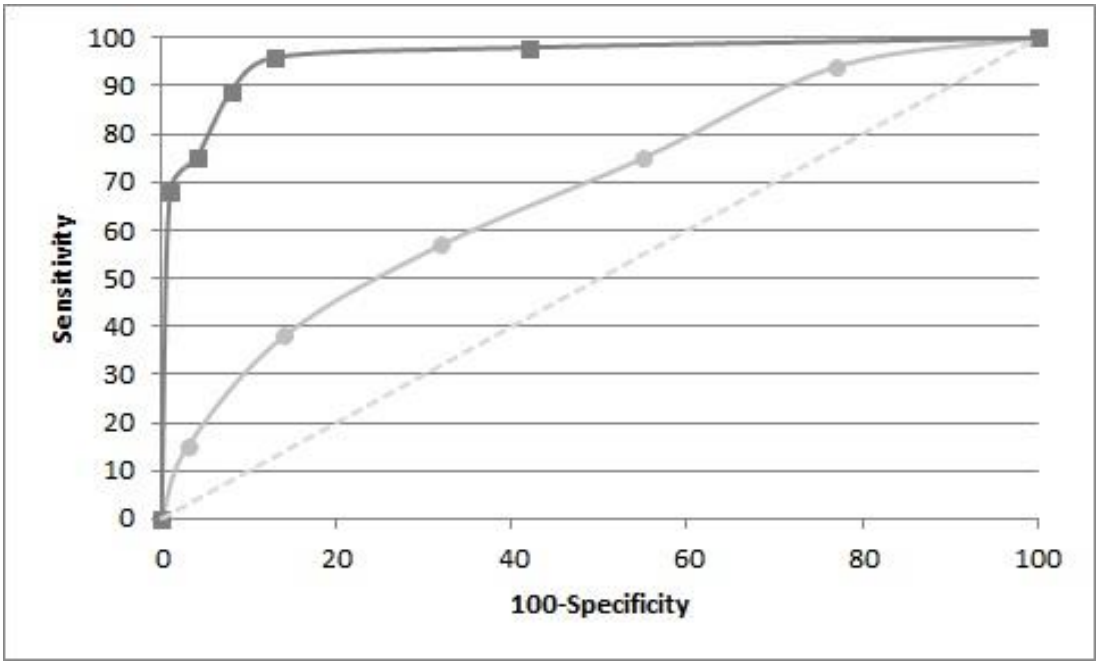

Figure 1.13: *Two Receiver Operating Characteristic (ROC) curves demonstrating the diagnostic performance of two tests at different cut-off points. The test represented with the dark grey curve performs better than the one represented with the light grey curve. The dotted line on the graph represents the line of zero discrimination with an area-under-the-curve of 0.5.*

1.1.14 The Issue of Detection in Glaucoma

In a recent UK study, that used a large database to estimate the rates of VF loss in glaucomatous patients, Saunders et al. reported that more than 90% of patients, expected to reach statutory blindness, had at least one eye with moderate VF defects at first presentation.[140] Advanced VF loss being present at the time of initial diagnosis has been identified as a major risk factor for future visual impairment.[141, 142]

A systematic review on the prevalence of OAG has been undertaken by Rudnicka et al.[143] Rudnicka's review included 46 published observational studies reporting on the relationship between OAG prevalence and age. Most of these population studies referred to the current poor detection rates where approximately half of the participating glaucoma cases were previously undiagnosed. In the latest UK study (North London, Reidy et al., 1998) patients were examined with the 76-point screening test of the HFA. The research team defined significant field loss as: 1) an absolute defect (missed at 0dB, that is the maximum instrument intensity) within the central 10 degrees of VF or 2) 2 (or more) absolute defects adjacent to each other or 3) 3 (or more) absolute defects in one quadrant. The percentage of previously undetected cases in this North London study was 75%.[144]

In a review by King et al. (2011) the percentage of patients first presenting with advanced loss in at least one eye was reported to be between 10 and 39%, with the chronologically latest study giving the highest percentage.[145] An important parameter accounting for the poor detection rate of the disease is its asymptomatic nature in the early stages. Patients are rarely aware of

any symptoms until the field defects start encroaching on the central field and affects visual acuity. The detection of cases with early loss relies mainly on whether patients seek routine optometric care. Opportunistic case detection by optometrists is responsible for over 90% of glaucoma referrals within the UK. Those not routinely seeking optometric care are more likely to first present with advanced VF loss.[146, 147] Previous studies have also shown that one of the strongest risk factors for late presentation is no previous family history of glaucoma, meaning that persons who lack previous glaucoma experience from their families are less likely to visit their optometrist for an eye examination.[141, 142]

Glaucoma screening

Delayed detection and access to early treatment are main risk factors for severe visual impairment. Reasons for delayed access to treatment may be related to patient in terms of attendance to testing, system delay leading to delayed referral, or process delay in terms of missed detection.[148] The public health importance of glaucoma and the reported poor detection rates of the disease would seem to provide strong support for the introduction of a national screening programme.

The WHO has set criteria, described by Wilson and Jungner in 1968, for reviewing the viability, effectiveness and appropriateness of a screening programme.[149] Before adopting a screening test evidence is required that the benefits of screening (e.g. reduced visual impairment) outweigh any harms (e.g. costs, anxiety etc.).

There are very limited data on the annual cost of sight impairment. The health costs of severe glaucomatous visual loss have been estimated as £935 per year (updated to 2014 prices).[150] The Royal National Institute for the Blind has reported that the cost of sight impairment is £12,457 per person per year; a figure that includes indirect costs, such as productivity losses, costs due to lower employment and premature mortality.[151] Previous studies, however, have shown that screening the UK population based on age alone was unlikely to be cost effective due to the low prevalence in all age groups (i.e. screening at age 40 or 65 or 75). Yet, they suggested that a screening programme targeted to higher risk groups, such as individuals with family history in glaucoma, ethnic groups or ocular risk factors, might be worthwhile.[152-154]

1.1.15 The Potential Of Visual Field Self-Testing – Study Aim

A potentially cost-effective approach to screening for glaucoma would be to promote methods for self-testing. There is a general trend towards self-monitoring of health status that is expected to increase in the near future. From heart rate and blood pressure management to the assessment of glucose or alcohol levels in blood, more and more patients use self-administered devices to check their health status. It is true that systematic reviews and individual studies do not fully agree and cannot yet confidently determine the specific positive impact on healthcare services and costs.[155-158] However, it is widely accepted that it is worthwhile investigating this research field to understand the process by which home telemonitoring

works in terms of improving outcomes, identify optimal strategies and the duration of follow-up for which it confers benefits. Nonetheless, it has been acknowledged that self-monitoring has the potential to reduce the pressure placed on secondary care services, but this may lead to increase in services elsewhere in the system.[156]

The field of ophthalmological examination has previously proven to be a potential target for self-testing, where numerous self-administered visual tests have been developed.The overarching aim of the research work reported in this section was the design and development of a new computer-based VF self-test for glaucoma screening purposes. Such a test could potentially tackle the issue of poor detection in glaucoma and prove to be a cost-effective way for the glaucoma screening of high-risk population groups. The following chapters provide, in details, the course of the research process that led to the development of VF testing software, which is appropriately designed to be self-administered. At the beginning, the VF database from the Manchester Royal Eye Hospital (MREH) was utilised to primarily investigate rates of glaucomatous VF progression, but also to highlight the issue of late presentation. Then, VF tests that are currently available online were identified and evaluated to derive useful design features that would make the new test user-friendly. A detailed description of the final design of the new test is also provided before reporting on the outcomes of the test's diagnostic performance. To conclude, the results and findings of this investigational process are debated at the end of the section, while discussing the research's potential future impact.

1.2 The Relationship between Rates of Visual Field Loss and Glaucomatous Stage of Loss

Contributions

During the year of my postgraduate studies (MSc Investigative Ophthalmology and Vision Sciences; academic year 2011-2012), and for the purposes of my dissertation, I examined the rates of VF loss in 200 eyes with advanced defects.

The research study presented in this chapter is effectively a step further to the study design and data analysis of that previous work. There is no overlap between the results reported in the MSc dissertation and the research outcomes shown here, as a different approach of analysis was adopted. For example, patients were included from all glaucomatous stages, their medical records were thoroughly examined to ensure no other co-morbidities existed while different statistical approaches were tested and utilised for the interpretation of the results.

Presentations / Publications

The outcome of this research has been presented (fully or partially) in a number of local (i.e MREH, University of Manchester, Manchester Optometry Meeting) and national (UKEGS) meetings.

Manuscripts related to this work have been submitted and peer-reviewed in a number of journals, such as the Investigative Ophthalmology and Vision Sciences, Eye and OPO; however, without success in being accepted. Reviewers' invaluable feedback and comments have been taken into account to finalise the presentation of the study in this chapter.

1.2.1 ABSTRACT

Purpose: Reported median rates of glaucomatous VF loss, measured with the global index Mean Deviation (MD), vary. Most previous reports have used populations not ideally suited to examining the relationship between rate and severity of VF loss. This study focuses on that relationship using data specifically selected to address this question.

Methods: From a database of 10,646 eyes 100 eyes in each of the first six Glaucoma Staging System (GSS2) stages, and 81 in the most severe stage were selected. Least squares regression of MD was utilised to estimate rates of VF progression and a modified hyperbolic secant model to fit to the resulting rates of progression.

Results: All 681 selected eyes fulfilled the only inclusion criterion; that being a diagnosis or suspicion of open-angle glaucoma and no other diagnosed eye pathology. Median rate of VF change increased from -0.14dB/year for early loss (stages 1-2) to -0.30dB/year for advanced loss (stages 4-5). The negative skew of progression rate distributions increased with the extent of VF loss. The number of localised absolute defects (0dB), where further progression cannot occur, attenuated rates of loss measured with MD. 82% of cases with advanced loss (GSS2 stages 4-5) first presented with advanced loss.

Conclusion: Median rate of VF loss increased with the extent of loss. However, caution must be exercised when interpreting rates in advanced loss, as floor effects may cause a slowing of the rate of change of MD unrelated to a true slowing of the disease process.

1.2.2 INTRODUCTION

Chronic open angle glaucoma (COAG) usually develops slowly and is asymptomatic until it reaches an advanced stage. In the UK the majority of COAG cases (~90%) are initially detected by community optometrists who opportunistically screen patients attending for other purposes (e.g. refractive errors, contact lenses).[159] Once referred, patients' management requires the assessment of visual function (visual field), structure (ONH, RNFL and peripapillary region) and IOP at regular intervals to detect any progression or risk of progression.

A high proportion of patients with treated glaucoma show progressive loss when monitored over a long period of time.[8] However, published average rates of loss vary substantially, ranging from -0.05dB/year to -0.62dB/year.[11, 160-164] Factors such as age,[11, 160, 165-167] peak IOP,[11, 160, 168] type of COAG (hypertensive glaucoma, normal-tension glaucoma, exfoliative etc.),[11, 160] length of follow-up, central corneal thickness,[160] type of loss,[169] and type of study[166, 170] are sample characteristics known to influence rates of loss.

A potentially important parameter that could also affect rates of loss is the baseline stage of loss. If the rate changes with the baseline stage and the stage distribution varies between studies this could account for some of the reported differences. Four studies have reported on the relationship between rate and extent of loss. De Moraes and Chauhan both reported that there was no significant relationship between baseline MD and rate of loss. [160, 166] While Boodhna et al. reported an increased rate for advanced VF loss when

samples are broken down into 3 VF severity groups but that the overall effect is small relative to other factors such as age.[165]

Most of the reports on VF progression rates come from studies with populations that are not ideally suited to examining the relationship between rate of loss and extent of VF loss. Populations were often heavily biased towards cases of early loss,[140, 166] and included eyes with comorbidities that can influence the rate of loss (e.g. age-related macular degeneration (AMD), diabetes) which are common in cases of advanced loss. Understanding the relationship between the extent of loss and rate of loss is important for the setting of follow-up times. It can also aid the clinician when discussing the risk of future visual impairment and in the planning of future management.

This retrospective study examines the relationship between rate of loss, measured with the global index MD, in a balanced sample of eyes with a clinical diagnosis of glaucoma and no comorbidity likely to affect the VF. Specifically, this research project tested the hypothesis that progression rates increase with more advanced glaucoma stages. The study also reports on the suitability of the global indices MD for the measurement of the rate of loss and the stage of loss when patients first present.

1.2.3 METHODS

Data extraction and inclusion criteria

MREH is a teaching hospital offering secondary and tertiary care to referred suspect and/or diagnosed glaucoma patients. Over 150,000 VF tests of the 24-2 pattern acquired with the SITA were successfully extracted from a network of 8 HFAs into a Microsoft Excel® Database (Microsoft Office Professional Plus 2010, Microsoft, Redmond, Washington, United States). From this database, 10,646 eyes with at least 3 years of follow-up and 4 tests in the last 4 years were extracted for further analysis. Short follow-up periods were used to reduce the impact of changes in management and to provide clinically relevant data for management decisions. While long sequences, often collected over many years, give more reliable statistical measures of rate they often cover periods in which there are changes to management and do not reflect the needs of clinicians who often have to make management decisions on the basis of short sequences.

The extent of field loss (median MD and pattern standard deviation (PSD) of last 3 records) was classified with the GSS2 which places eyes into one of seven stages: from ‘normal’ through ‘borderline’ and then onto 5 levels of glaucomatous loss.[171] Eyes were randomly extracted from the subset of 10,646 eyes to produce a test sample of 100 eyes (1 eye per patient) in each of the seven GSS2 stages. Each included eye was subjected to a 2-part record review by the author to ensure that the eye had a clinical diagnosis of glaucoma, or suspect glaucoma, with no other comorbidity (e.g. cataract,

diabetic retinopathy (DR), AMD) likely to affect the VF. Initially, correspondence letters from the consultants were reviewed via the digital platform of Medisec. Eyes with multiple diagnoses reported in those letters were excluded and another randomly chosen eye would be chosen as a replacement to ensure that the sample size was 100 eyes. Those eyes would go through another thorough review of their medical records to confirm the absence of another eye pathology. The number of excluded eyes with comorbidity was also recorded to understand how frequently glaucomatous eyes have accompanying pathologies. The final sample was composed of 681 eyes as only 81 eyes with the most advanced loss (stage 5) fulfilled all the inclusion criteria.

Data analysis

Analysis was based upon the global index MD, which is the weighted average difference between the sensitivity of an eye at 54 test locations and those from a normal age-matched eye. A least squares regression analysis of MD values over time was used to derive progression rates expressed in dB/year.

The subjective nature of a VF test introduces some variability to the results and sometimes patients will produce a result that is clearly out of line with those seen both before and after. Retaining these outliers in a regression analysis can have a large impact upon the calculated rate of loss, especially if they appear at the beginning or end of the series. Their removal leads to a more accurate measure of the rate of loss. Peirce’s criterion is a simple way

for the detection of outliers used extensively in the 19th century. [172] It only depends on characteristics of the observation data (rather than the actual observations), therefore offering high repeatability and independence of other processes. This feature makes Peirce's criteria for outlier identification more appropriate for small data sets and the identification of two or more abnormal observations. Outliers were subjected to a further criterion of being more than 2dB from the estimated value after performing least squares linear regression with suspect test point removed (Figure 1.14). This second stage was introduced to guard against cases where small deviations are excluded solely on the basis of Peirce's criteria. The above-mentioned method for the detection of outliers is, of course, not flawless; its major drawback being the fact that Peirce's criterion does not take into account the distribution of the extreme order statistics from a normal distribution. However, this method was selected over others for its simplicity and effectiveness in small samples.

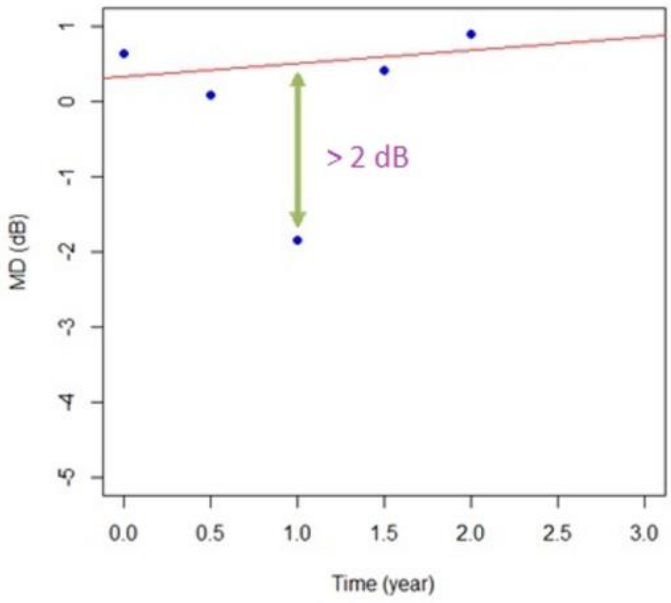

Figure 1.14: *An example of outlier removal with Peirce's criterion in least square regression analysis. A suspect point (middle blue dot in the series) would be removed if deviated more than 2 dB (green arrow) from the estimated value derived from a regression analysis with the point removed.*

For the purposes of establishing the relationship between presenting stage of loss and progression, cases in stages 1 and 2 were considered early VF loss, while those in stages 4 and 5 were regarded as advanced loss.

Fitting in the distribution of VF progression rates

Distributions were fitted with a modified hyperbolic secant, a model that has been described and used in the past to describe the distributions of glaucomatous rates of VF loss.[120, 173] In brief, this model includes 3

modifiable parameters: *t* which is equivalent to the mode and *B* and *C* which describe the positive and negative width of the distribution.

A bootstrap procedure (n=1000) was used on the data within each stage before fitting the modified hyperbolic secant. The medians of the three parameters for each GSS2 stage were entered into a regression analysis to determine if these parameters are significantly altered with disease stage. For stages 4 and 5 only all cases were re-classified based on their VF status at baseline. The aforementioned fitting method was performed again in order to identify any potentially significant differences in the model's parameters that the classification method could be blamed for. Lastly, the mean number of locations with absolute defects (0 dB) was calculated for each stage in order to establish the potential impact of these locations on the rate of loss.

All statistical analyses were undertaken in Microsoft Excel® and MATLAB (The MathWorks, Inc., Natick, Massachusetts, United States) while distribution histograms and appropriate graphs were generated with R (R Foundation for Statistical Computing, Vienna, Austria). The study was approved by the local ethical committee and followed the tenants of the Declaration of Helsinki. Following the advice of the ethical committee and the processes of a clinical audit all patient-identifiable data were removed right after exporting the data and prior to their analysis and interpretation and were given a study ID number. A separate piece of paper, or 'code sheet' was then kept safely at a Central Manchester Foundation Trust's computer as a key.

1.2.4 RESULTS

Comorbidity with conditions that can affect MD was common, especially in cases with advanced loss. Two hundred and sixty one eyes within the database were classified in stage 5. Only 81 met the inclusion criteria of no comorbidity likely to affect the VF. All 681 glaucomatous eyes were included in the analyses. Their demographic characteristics are given in Table 1.4. The average patients' age was 72.0 years. The average number of VF tests per series was 6.0; (after the removal of outliers). The mean follow-up period was 3.7 years. Eighty-two percent of eyes with final loss classified as advanced had advanced loss at first presentation.

Rates of loss for each GSS2 stage are shown in Table 1.5. Higher rates were found in those eyes with advanced VF defects. However, the increase is small going from -0.14dB/year for early loss to -0.30dB/year for advanced loss. Approximately 2% of the total number of eyes (i.e. suspects and diagnosed) had a rapid rate of loss (i.e. >2 dB/year). All of the cases with rapid rates of loss had defects that fell within GSS2 stages 3-5. Figure 1.15 gives the distribution of rates of loss for eyes with early and advanced loss.

GSS2 Stage		Eye records reviewed	Number of included eyes	Male/Female ratio	Age (years)	Mean (SD) number of field tests	Mean (SD) number of follow-up years	Chronic open angle glaucoma	Angle closure glaucoma	Suspect glaucoma	Presenting late with Advanced Glaucoma
Normal		131	100	1.12	67.1	5.9 (±1.0)	3.7 (±0.5)	35%	1%	64%	
Borderline		128	100	0.88	71.5	6.0 (±1.3)	3.6 (±0.5)	52%	4%	44%	
Early	**1**	168	100	1.08	73.2	6.3 (±1.3)	3.7 (±0.6)	72%	4%	24%	
	2	208	100	0.96	73.1	6.0 (±1.5)	3.7 (±0.5)	84%	9%	7%	
3		198	100	0.66	73.8	6.1 (±1.4)	3.8 (±0.6)	91%	4%	5%	
Advanced	**4**	215	100	0.85	73.7	6.0 (±1.3)	3.8 (±0.6)	94%	6%	0%	72%
	5	261	81	0.84	72.1	5.8 (±1.3)	3.7 (±0.5)	84%	6%	0%	95%

Table 1.4*: The demographics of the patients included in this study. The eyes involved in this study were classified in 7 different stages according to the median of the last 3 visual field test results.*

GSS2 Stage		Median (IQR) MD (dB)	Mean (±SD) rate of loss (dB/year)		Median (IQR) rate of loss (dB/year)		Max / min rate of loss (dB/year)	Percentage with rate of loss >2 dB/year	Mean (±SD) number of locations with absolute (0dB) loss	Eyes that outlier was removed (eyes "flagged" by Peirces' criterion)
Normal		0.2 (3.9)	0.05 (±0.40)		0.02 (0.43)		-1.20 / 1.10	0%	0.7 (±1.2)	9 (30)
Borderline		-1.5 (3.4)	0.04 (±0.43)		-0.02 (0.45)		-1.10 / 2.13	0%	0.8 (±0.9)	21 (51)
Early	**1**	-2.9 (2.6)	-0.12 (±0.39)	-0.14 (±0.50)	-0.14 (0.46)	-0.14 (0.56)	-0.94 / 1.04	0%	1.0 (±1.0)	14 (43)
	2	-4.6 (6.0)	-0.16 (±0.59)		-0.13 (0.65)		-1.57 / 1.85	0%	1.5 (±1.7)	21 (41)
3		-7.3 (5.9)	-0.41 (±0.82)		-0.28 (1.00)		-3.63 / 1.59	2%	2.9 (±2.6)	21 (35)
Advanced	**4**	-13.00 (10.3)	-0.46 (±0.89)	-0.52 (±0.87)	-0.25 (0.84)	-0.30 (0.74)	-3.36 / 2.13	7%	9.2 (±6.7)	24 (39)
	5	-19.9 (11.8)	-0.58 (±0.85)		-0.35 (0.59)		-4.43 / 0.95	6%	17.9 (±8.0)	23 (32)

Table 1.5: *The results of the linear regression analysis performed on the series of visual field tests from 681 eyes, classified according to GSS2.*[171]

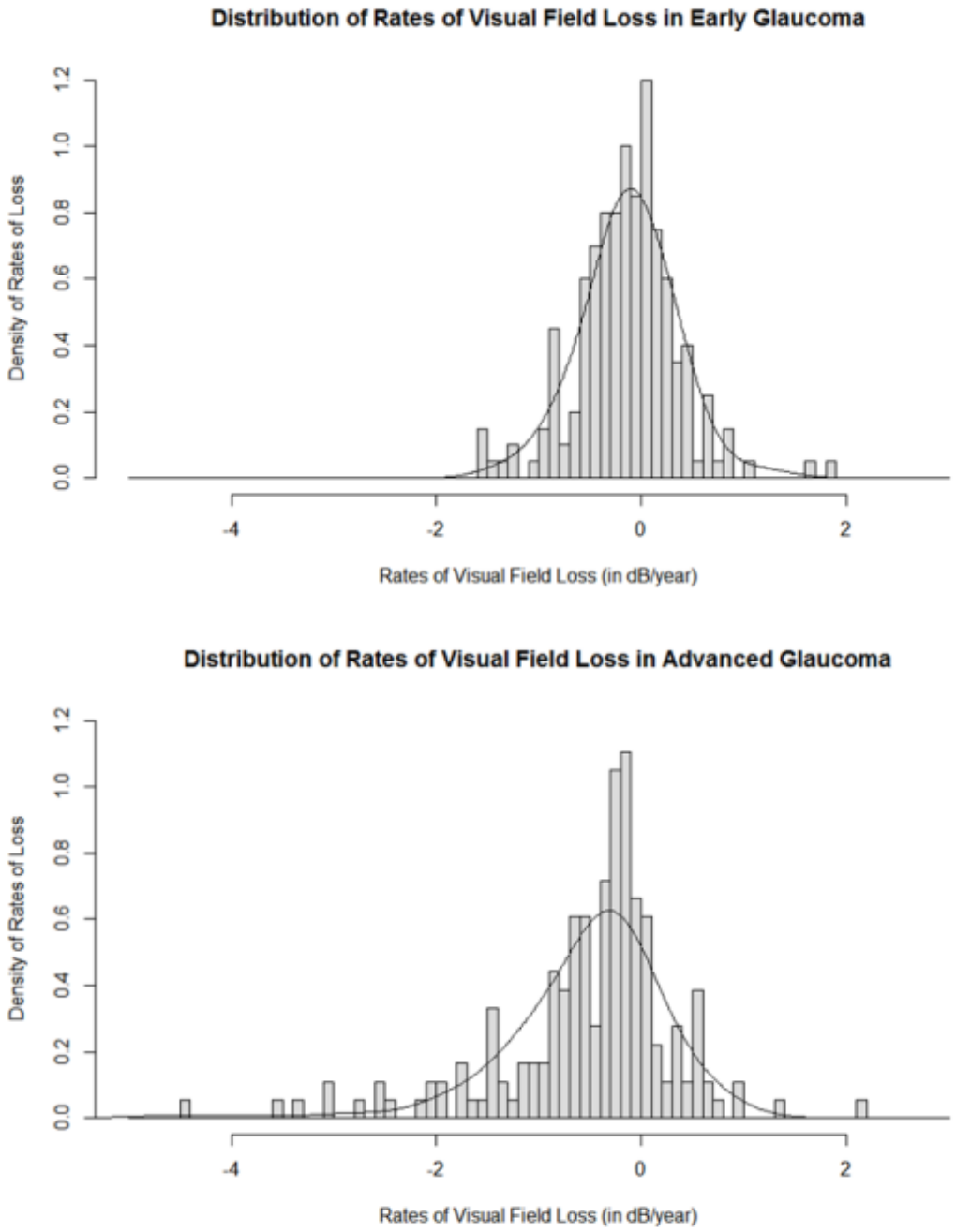

Figure 1.15: *Distribution plot of rates of visual field loss in early (GSS2 Stages 1-2) and advanced (Stages 4-5) glaucoma. Black line is the best fitting modified hyperbolic secant.*

Regression analysis for the three parameters showed significant change for two of those parameters, the negative width of the distribution *C* and the mode *t* (p-value <0.01), while the *B* parameter (positive width of the distribution) did not reach statistical significance (p-value 0.48).

Figure 1.16 shows the medians of the three parameters for each GSS2 stage along with the upper and lower confidence limits (i.e. 97.5% and 2.5% respectively). In order to highlight the relative changes in parameters *B* and *C*, we plotted the ratio of these two parameters (i.e. *B* over *C*) across the different GSS2 stages. This ratio is approximately 1 for Normal, Borderline and early glaucomatous stages indicating that the two parameters are fairly similar and therefore the distribution at these stages quite symmetric. For moderate and advanced glaucomatous stages the *B/C* ratio showed an increase with increasing stage.

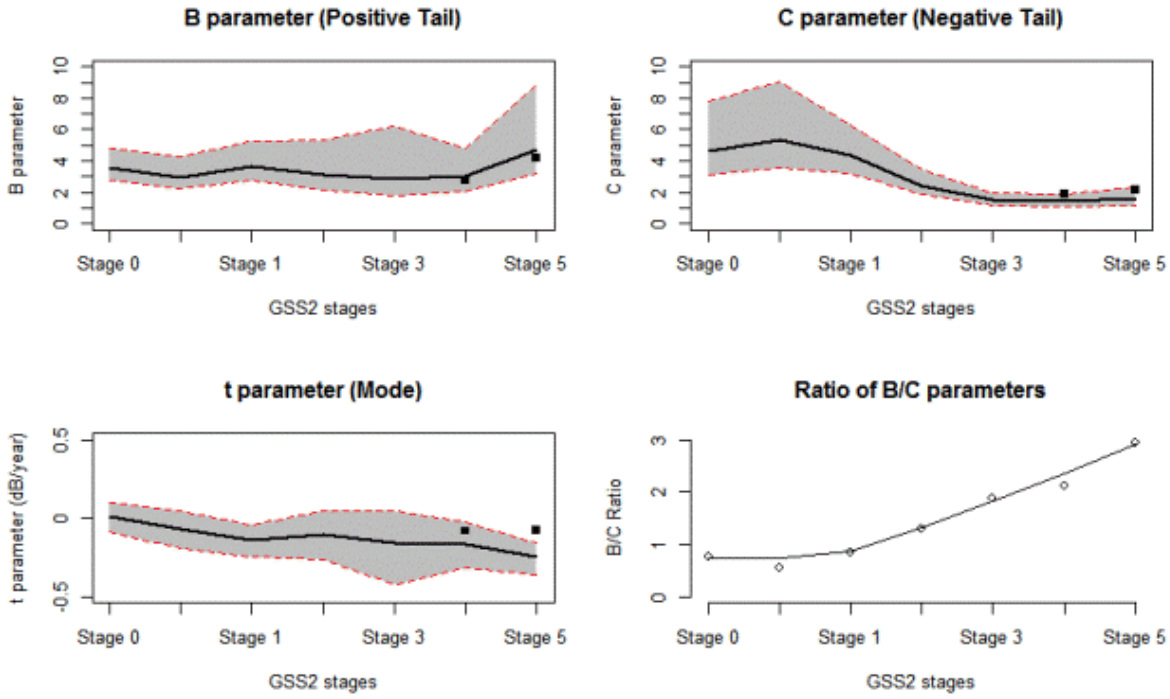

Figure 1.16: *Median (and upper/lower confidence limits) of the three parameters of the best fitting modified hyperbolic secant for each GSS2 stage. Filled square dots indicate the median of each parameter after re-classification of GSS2 stages 4 and 5 (advanced glaucoma) according to baseline loss. Bottom right plot shows the ratio of B/C parameters across all GSS2 stages*

1.2.5 DISCUSSION

In this retrospective study, glaucomatous eyes with a range of VF defects were randomly selected from a large database of records collected during routine management of patients attending a UK NHS eye hospital. The median rate of change was greater in patients with more advanced loss.

However, a rate of -0.30dB/year corresponds to moving from an already advanced defect (MD=-15dB) to the visual impairment threshold (-22dB in the USA)[168] in approximately 23 years. Considering the mean age of patients in stages 4&5 is ~72 years it is clear that most treated eyes with advanced loss will not reach the impairment threshold within the patients' normal life span. Studies on the relationship between health-related quality of life (HRQoL) and VF loss have shown little effect on HRQoL until the best eye of a patient has advanced loss (glaucoma level 5, MD≤25dB)[174] although patients are unlikely to meet the standard required for driving (an important milestone) with lesser degrees of loss.[175]

A potentially more important statistic when discussing long term outcomes for patients with diagnosed glaucoma is the probability of becoming visually impaired. While the nature of the data set does not allow us to make such predictions the percentage of eyes with rates of over 2dB/year (a rate defined as rapid by Chauhan et al 2008) can be established.[176] Only 6.6% of eyes with advanced loss (~1 in 15 people) had rates of over 2dB/year. Moreover, there are no cases in this sample of such high rates in eyes with early glaucoma.

The fitting of the modified hyperbolic secant model in the different GSS2 groups showed a significant decline in 2 model parameters (the mode and the width of the negative tail). The increasing width of the negative tail showed an unexpected reduction from stage 4 to 5 with a similar reduction in the width of the positive tail. The calculation of MD includes locations with absolute defects (i.e. 0dB), where progression is no longer possible. An increase in the number of absolute defects will therefore reduce both the

positive and negative rates of change. For stage 5 the number of absolute defects was almost twice as high as stage 4 (mean number of locations with absolute defect: 9.2 and 17.9 for stages 4 and 5 respectively). Replacing absolute values for the positive and negative tails with the ratio of the values overcomes this floor effect and shows a continuous increase with extent of loss (figure 1.16).

There is good clinical evidence showing that a reduction of IOP often helps to decelerate the progression of glaucomatous loss.[8, 177-181] Although an analysis of IOP values and treatment strategies for individuals was not included in the current study, it is assumed that a more aggressive approach, such as surgery, was followed for cases of advanced glaucoma; the UK guidelines for glaucoma suggest surgery as a primary treatment for patients who present with advanced visual loss.[42] Therefore, aggressive treatment strategies, particularly in those with advanced loss at first presentation, are likely to have had an effect upon the rates of loss. Indeed, this has been reported by Baril et al. who examined the rates of VF loss in a group of patients undergone trabeculectomy and a matched patient group who were medically treated.[180] The reported rates between the two cohorts were similar.

In this study eyes were classified according to the disease stage at the end of the VF series. Such an approach can potentially lower the likelihood of underestimating rates of MD change in advanced stages, due to the increased number of locations with absolute defects (a ‘floor’ effect) which is found here to be almost 6 times higher in the most advanced stage compared to moderate glaucoma (i.e. Stage 5 and 3 respectively). A

potential limitation of classifying eyes according to their end stage is the increasing likelihood of rapid progressors falling in the advanced stages; an eye with a fast rate of loss will rapidly progress through the glaucomatous stages before reaching the advanced stages which are broader than the earlier stages. In order to reduce this effect the analysis of VF series was performed over a 4-year period; a timeline which is more representative of the current/recent clinical management of each study eye, making changes in a patient's glaucoma stage over this short period unlikely. This approach appears to have been effective; if those patients classified as stage 4 or 5 (n = 100 & 81, respectively) were reclassified based on their VF status at baseline, the majority (n = 72 & 67, or 75% & 87%) remained in the same glaucoma stage. Furthermore, modified hyperbolic fits to these reclassified data returned parameters very close to those in our original analysis (Figure 1.16: filled square symbols). These can be considered strong evidence that the choice to classify glaucoma stage at the end of the VF series does not explain the study's principal finding that those with more severe glaucoma stages show more rapid VF progression. On the other hand, the finding of a larger number of improvers with early loss is likely to have been influenced by learning effect. Patients tend to get better at VF tests after their first test and the early loss sample had more cases where the first data point came from the patient's first field test.

There are quite a few comparable studies recording VF loss rates in clinical populations. A USA study reported a decreasing trend of rates of loss according to baseline MD.[182] Mean rates were found to be at -0.5dB/year for mild cases shifting to -0.4dB/year and -0.3dB/year for cases with moderate

and severe loss respectively. Results are likely to have been influenced by both centre specific treatment protocols and variations in the distributions of risk factors. It is also quite likely that rates were underestimated in the group with severe loss due to the 'floor' effect explained above. Chauhan et al. reported that the rate of VF loss was not dependent upon baseline MD but was dependent upon age with older eyes showing a significantly faster rate than younger ones.[166] In this study there was no significant difference in the mean age of patients within stages 1-5 (see Table 1.4). More recently, Heijl et al. reported VF loss rates in routine clinical glaucoma care in Sweden.[183] The authors found that, for a patient population with median MD at study start being -10dB, the median rate of loss was -0.62dB/year. The rates in Sweden are likely to have been influenced by the high proportion of the more aggressive PXF glaucoma seen in Scandinavian countries although this is unlikely to account for all of the difference.[6, 184]

The study reported here excluded eyes with co-morbidities that can affect the VF and included approximately equal numbers of eyes for each stage of loss. Earlier studies were often heavily biased towards cases with early loss and included relatively few cases of advanced loss. A balanced distribution is more appropriate for establishing changes in the rate of loss with the stage of loss.

This report also highlights that the majority (82%) of eyes with advanced loss first presented with advanced loss, i.e. that they do not represent failures of management but of detection. Several studies have reported similar findings highlighting that one of the greatest risk factors for visual impairment from glaucoma is late presentation.[142, 175, 185] This study also demonstrates a

further risk factor in late presenters; not only do they typically have more advanced field loss, but they are more likely to show rapid progression (Figure 1.15 & Table 1.5).

There are, however, a number of limitations in this study. First of all, data derived from one centre only (i.e. MREH), although some similarities not only in the demographics but also in the reported rates of progression can be found among this study and others. The greater variability in those with greater loss can also have an impact on the reported progression rates. The method of analysis partially accounted for that by implementing an outlier detection technique to identify and remove inconsistent VF tests in a patient's series. It is unknown, however, if that technique alone is adequate enough to counterbalance this limitation.

In conclusion, this report, along with Boodhna et al. which reports from 4 NHS clinics, highlights the effectiveness of current glaucoma management that can be achieved in routine NHS care.[165] Relatively few eyes have progression rates likely to lead to the visual impairment threshold; however, the proportion of those progressing rapidly is higher in the more advanced stages of the disease. It also highlights that the majority of eyes at risk of reaching the impairment threshold first present with advanced loss emphasizing the importance of early detection and the adoption of screening tests for glaucoma. Finally, this study finds that the risk of future impairment is very low in eyes with early glaucomatous loss.

1.2.6 CONCLUSIONS

This study report provides evidence that rates of VF deterioration, an indication of disease progression, are relatively slow in patients with COAG. While slow glaucomatous rates have been reported in a number of studies, this study is different in its design in 3 main points: 1) the cohort in this research is carefully reviewed and chosen to include sole glaucoma cases, 2) the VF series in this analysis represent a relatively short period of time (i.e. 4 years) where the impact of changes in treatment during a patient's management course is relatively small and 3) the sample is balanced across different disease stages, ranging from normal to advanced glaucoma.

The study outcomes also highlight the somewhat higher risk of faster VF deterioration for patients with advanced VF defects. The rate of VF deterioration, however, may be underestimated in cases with advanced glaucoma due to the estimation process of the MD value, where a large number of locations have reached their minimum value and further progression cannot occur. As a final point, the study underlines the low probability for future impairment in eyes with early glaucoma and suggests that VF screening of high-risk groups may be potentially cost-effective.

1.3 Usability Evaluation of 5 Self-Administered Visual Field Tests Distributed via the Internet

Contributions

The outcomes of the previous study led to the idea of developing a self-administered VF test that could be undertaken with a personal computer, laptop or tablet; the targeted outcome from the development and introduction of such a test being more widespread testing within the community and a reduction in the number of late presenters.

This chapter describes the first step of the design and development process - an evaluation of currently available online VF tests. VF self-tests that are currently available online were evaluated for their user-friendliness (usability) with a scope to adopt some of the features that patients prefer to the new test; or inversely avoid features that patients dislike.

My involvement included the study design, data collection/analysis and dissemination of the study outcomes.

Presentations / Publications

The outcome of this research has been presented as a poster in the UK and Eire Glaucoma Society (UKEGS) meeting in Leicester 2015. Also the study design has been presented at MREH research meetings for adoption of the methodology in future research.

1.3.1 ABSTRACT

Purpose: To identify the best features used in current on-line VF self-tests. Where a feature choice is available submit this to a usability trial the results from which can be used to develop a new VF test.

Methods: Five online tests designed to detect VF defects were identified; Damato's Multifixation Campimeter, Peristat, NovaVision Online VF Screening Test, EyesCream and VuScope. Their usability was evaluated by using a modified version of the System Usability Scale (SUS) questionnaire. Extra questions, prompting participants (10 perimetric experts and 18 subjects with no previous experience – Group 1) to highlight favourable design and testing characteristics, were also included. The quantitative and qualitative analysis generated 5 pairs of design/test features (e.g. response with a mouse click or a key stroke) which were evaluated by 28 participants (Group 2) with mixed perimetric experience.

Results: All questionnaires from Group 1 were included in the analysis. The NovaVision test presented the highest SUS score for both cohorts, with a median score of 90/100 (IQR – 26.25) and 82.5/100 (IQR – 12.5) for experts and lay participants respectively. The expert cohort showed higher variability among their scoring and frugality with only 1 test passing the reported threshold of 68, compared to the 3 tests for the lay cohort. Qualitative analysis marked as areas of high importance the presence of adequate and simple instructions and the simplicity of the testing method. Group 2 highlighted the multiple stimuli approach as the best testing method while it showed no preference on a constantly moving fixation target. Preference to

respond via mouse click or keyboard stroke showed no difference. Also, the presence or absence of feedback did not seem to make any difference for the participants in comparison to its frequency.

Conclusions: User-friendliness of health self-tests is rarely taken into account. Usability evaluation of currently available devices and software can assist developers of new systems identify design and testing features that will make their products more appealing to the patients thereby increasing take-up and test completion rates.

1.3.2 INTRODUCTION

Tracking health indicators, such as weight, heart rate or blood pressure, and keeping notes on one's health, have been shown to be tools for improving health outcomes.[186, 187] Recent advancements in technology, for example sleep and activity trackers, and the exploitation of devices, such as smartphones, laptops and tablets, have allowed various health measures to get "closer to patient's home" for reasons such as disease self-detection or self-monitoring. Through research and development, such devices and health applications have achieved high repeatability and fair accuracy when compared to gold-standard techniques.

Numerous self-administered ophthalmic tests have been developed; the most common type of test being visual acuity.[188, 189] Snellen charts are available either online or in paper-form and, provided with adequate instructions, they can be used to measure visual acuity in a quick and reliable manner. Colour testing is another type of ophthalmic examination that has a large number of self-administered versions. Most of these tests follow the Ishihara test principles but are limited by the performance characteristics of display monitors. Other types of ophthalmic self-tests, available either online or in paper-form (or both), are the Amsler Grid for AMD testing, VF tests for conditions such as glaucoma and contrast sensitivity tests.[190, 191]

Displays in modern personal computers and tablets allow for good levels of luminance control and presentation timing and therefore could be used to

record and present the results of a VF self-test.[192, 193] A number of computer-based self-tests have been produced and distributed via the Internet. Despite the fact that there is a range of VF self-tests available online, there are no publications reporting on their take-up rate. Take-up rates of self-tests are highly dependent upon their usability and marketing.

Usability testing is considered important for the identification of problematic design issues and test shortcomings;[194] features that could make a patient give up on a self-test before it is completed. This chapter describes the initial stages of the development of the new computer-based VF self-test (i.e. the epicentre of this Section) which involved an extensive, iterative period of testing and re-designs to ensure that the test will not only serve its clinical purpose but it will also be user-friendly. In this study, usability has been addressed, firstly through assessment of currently available online VF self-tests and then through a series of trials based on patient preferences to aspects such as: test strategy and how to record patient responses.

1.3.3 METHODS

The online visual field tests under evaluation

For the identification of VF self-tests that are currently freely available online the Google Inc.'s web search engine was utilised and the keywords "free online VF test" were used to generate a list of search results. This web

search occurred in January 2014. From this list the first 5 relevant entries were selected for usability evaluation in this study. These entries are:

1. Damato's Multifixation Campimeter
2. NovaVision Online VF Screening Test
3. VuScope
4. Peristat VF Test
5. EyesCream – Free VF Analyzer; this can be downloaded and executed whether the computer is online or not. Note that this is the oldest of the above-mentioned tests while this project seemed abandoned.

A brief summary of the various test characteristics of the reviewed on-line VF tests is given in table 1.6.

	Publications	Application type	Stimulus Parameters	Fixation Point Parameters	Background / Stimulus Colour	Degrees of field tested	Number of Presentations
Multifixation Campimeter	Yes[195, 196]	Online	Single, Circle-shaped, Fixed size	Multifixation, Circle-shaped, Number or Smiley Face	White / Black and Grey	24°	42*
Vutest® - VuScope	No	Online	Multiple, Circle-shaped, Fixed size	Multifixation, Cross-shaped, White-coloured	Dark Grey† / White	Short-Cycle: 25°, Long-Cycle: 33°	Short-Cycle: 53, Long-Cycle: 77
EyesCream	No	Windows Program	Single, Cross-shaped, Increasing size	Fixed Point, Circle-shaped, Continuous fluctuation in size and colour (blue-green)	Black / White	N/A	N/A
PeriStat	Yes[197]	Online	Single, Circle-	Fixed Point, Circle-	Black / White	N/A	>110

			shaped, Fixed size	shaped, White-coloured	or Dark Grey		
NovaVision	No	Online	Single, Circle-shaped, Fixed size	Fixed Point, Circle-shaped, Green-coloured (Yellow Triangle for False Positive Trials)	Dark Grey / White	N/A	80

Table 1.6: *Testing and display characteristics of the 5 selected visual field self-tests performed with a personal computer or laptop.*

Damato's Multifixation Campimeter

Professor Bertil Damato and Mr Carl Groenewald from St Paul's Eye Unit, Royal Liverpool University Hospital developed an online version of Damato's previous work, the Multifixation Campimeter.[195, 196] In brief, the user clicks on the fixation point with their pointing device (i.e. mouse) to briefly present a black spot/stimulus somewhere in their screen. If they saw the stimulus they need to move the cursor (arrow) towards the area that the stimulus appeared; then a new fixation point appears and the process is repeated. If they fail to respond correctly to the stimulus a bell rings and an arrow points towards the area of the missed stimulus.

There are three different versions of the test: Basic, Standard and Advanced. The difference between the first and the last two is that there is an extra process involving the fixation point to ensure correct fixation. More specifically, a number between 1 and 4 appears at the fixation point. The user needs to click on the number for the black spot to flash and the number to disappear. As soon as the user moves their pointing device towards the stimulus location, 4 numbers around a square emerge; the user now needs to click on the number they saw on their screen prior to the stimulus presentation. Standard and Advanced versions have a simpler process with regards to the fixation point where a smiley face appears and the user is asked to just click on it for the stimulus to flash. In addition the Advanced test has three different test levels: light grey, dark grey and black; whereas the Standard version only presents black stimuli. The developers claim that the Advanced type is a more sensitive version of the test and it is designed to detect mild abnormalities of the VF.

All three versions share a similar menu with 5 tabs: Preparation, Practise the Test, Do the Test, Results and Analysis. The ‘Preparation’ tab is the same for all versions and includes instructions about cleaning the monitor, wearing glasses or not during the test, covering one eye and positioning the user’s head. The ‘Practise the Test’ tab provides further instructions about the actual process of the test, such as the need for the user to click the fixation target to initiate a presentation and moving the cursor towards the area of the screen that the stimulus flashed. Instructions are provided in two forms: written and in the form of an animation. The user is also able to practice the test prior to any data collection.

When the user clicks on the ‘Do the Test’ tab the correct testing distance is set with the aid of a special display. Two spots (one blue-coloured on the left and one red-coloured on the right) appear. Depending on the eye tested, one of the spots is constant while the other flashes continuously. The user is instructed to cover the eye not being tested and to look at the constant presented spot while moving forwards or backwards until the flashing target disappears, i.e. falls into their normal blind spot. When the right eye is tested the blue target is constant while the target on the right (red) flashes; and vice-versa for the left eye. When the correct testing distance has been established the patient triggers the start of the test.

After the completion of the test, the user can see the results in a graphical form on the ‘Results’ tab. The graph presents all the locations tested and shows whether they have been seen or missed (figure 1.17). It also shows if the normal blind spot has been detected successfully or not. The ‘Analysis’ tab provides general instructions for the user to self-interpret their results. It

gives examples of normal and abnormal results and further instructions if any points have been missed. These instructions include the repetition of the test to check repeatability and advice on further action.

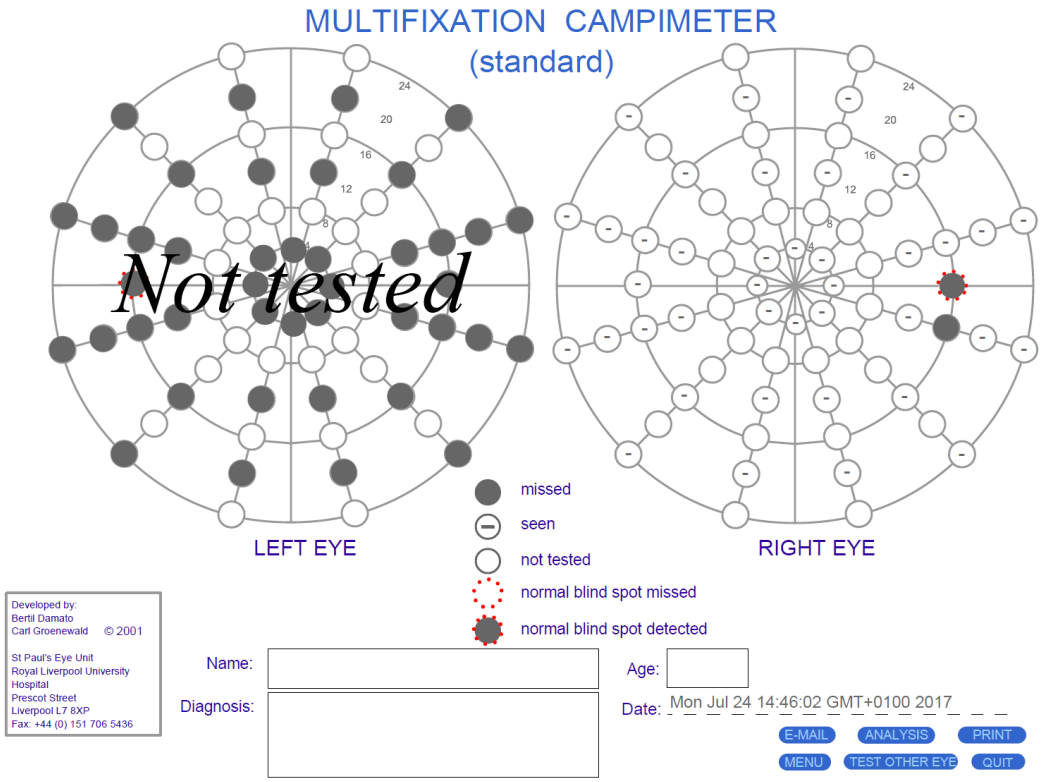

Figure 1.17: *Test results in Damato's Multifixation Campimeter. In this example, the right eye has been evaluated and tested locations (seen and not seen) are highlighted. The results can be printed and further notes/comments can be added.*

The test stimuli follow a radial pattern with 42 locations (including the normal blind spot) covering the central 24 degrees of the VF. The background is white and the stimuli are black spots (apart from some stimuli in the

Advanced version). Each one of these locations is tested once in the Basic and Standard versions of the test. In the Advanced version each location may be tested up to three times, depending on the user's responses. In the advanced version the stimuli are initially light grey. If not seen a darker shade of grade is presented at the same location. If not seen again the spot turns black reaching its maximum contrast from the white background. The location of the stimuli follows a fixed pseudo-random order which is the same for recurrent tests, therefore making the next location of a stimulus quite predictable after performing the test a few times.

Vutest® - VuScope

Vutest® was developed by optometrists, vision scientists and programmers at EyeLab (UK) Ltd., in 1991. It is designed to analyse the user's ability to see comfortably and use their eyes correctly whilst using a computer. Thus, it is not a test closely related to glaucoma but rather a general vision screening system. Vutest® has a package of vision tests that include visual acuity and colour testing, reaction time examination, VFs and drivers' visual assessment. The following paragraphs will focus on VuScope, the VF testing section of Vutest®.

The initial screen of the test provides general instruction on the set up before the user performs the test. More specifically, it states that the distance from the computer screen should be 1.5 times the display width of the monitor. It also asks the user to make sure that there are no reflections on the display and to wear any reading glasses. VuScope offers two different types of test:

the short cycle, which checks the central 25 degrees of the VF and the long cycle, which extends the examined VF area up to 33 degrees.

The test uses a multi-stimulus technique with a moving fixation point. The fixation point is a big white cross and the user is instructed to click on it for the stimulus (or stimuli) to be presented; the background is dark grey. The first step of the test sets the contrast level. By clicking the cross/fixation point four white spots flash, one in each quadrant of the screen. The user is asked if they saw all 4 spots or not. Depending on their answer the background intensity changes; luminance is increased (i.e. a decrease in stimulus contrast) for a positive answer otherwise the background gets dimmer. This calibration process is repeated until the first reversal in the user's responses. During the test the fixation point moves to a new location before each stimulus presentation and when the user clicks on the fixation point up to 4 white spots/stimuli flash (figure 1.18). After the presentation of the spots, the user is asked how many dots they saw. If they reply with fewer spots than presented, then the test shows the locations that the stimuli flashed and asks the user to click on the areas that they saw the spots. If their reply is correct, the fixation point moves to a new location where the process is repeated until all locations have been tested.

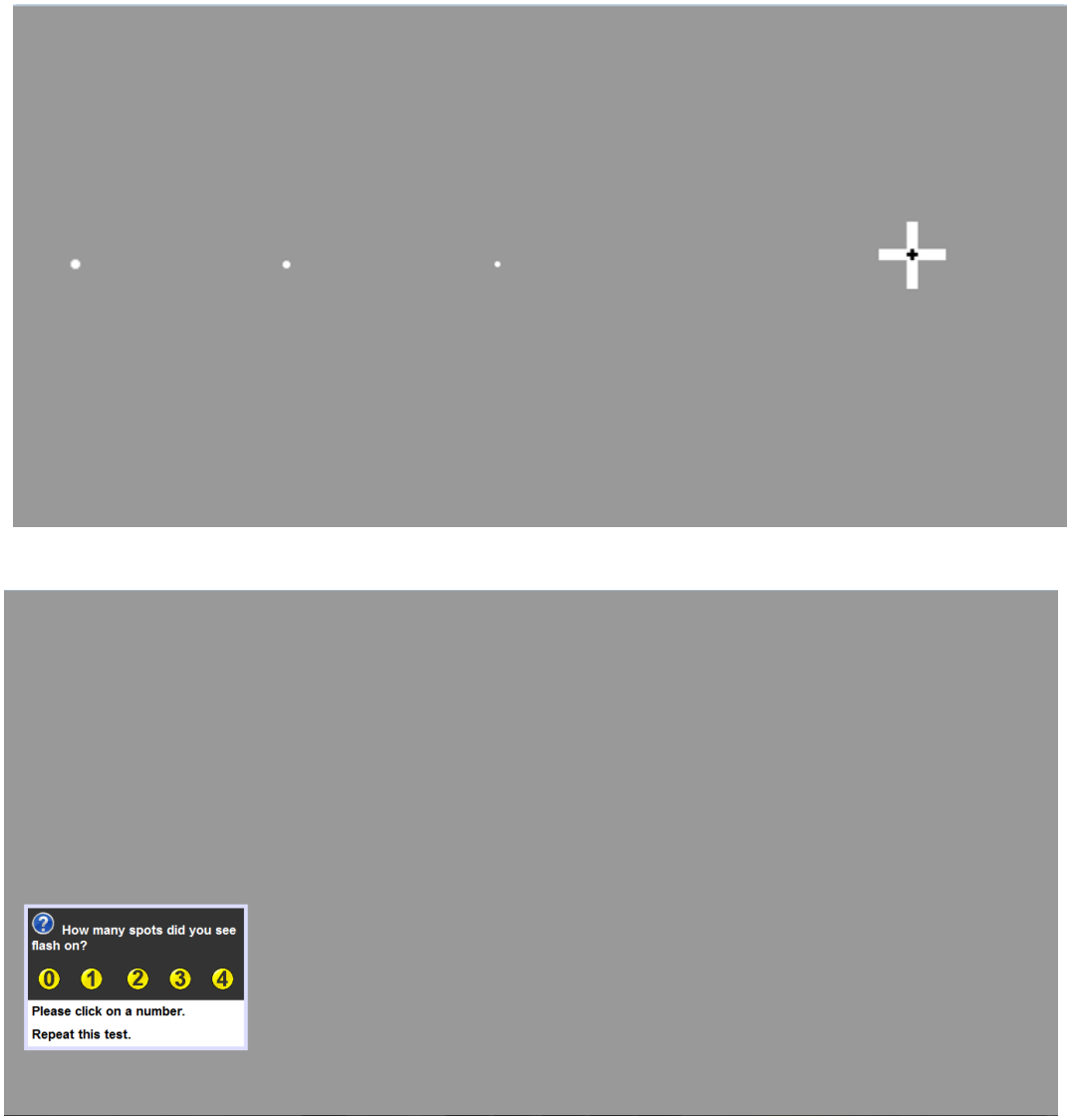

Figure 1.18: *Screenshots of the VuScope and its multi-stimulus technique. Up to 4 stimuli are presented before the user is asked how many of them were seen.*

When the test is completed the screen displays the locations that the targets were seen or missed. There is also general advice stating that if more than 3 spots have been missed, the user should repeat the test and if the defect(s) are confirmed then they should consult their eye care practitioner.

Fifty three locations are tested in the short cycle and 77 in the long cycle; both tests include locations in the normal blind spot. The short cycle uses 15 patterns of stimuli while the long cycle uses 27. Both cycles test each location once. Although the multi-stimulus approach of VuScope benefits from short testing times, the choice of locations in some patterns makes it hard for the user to distinguish the exact number of spots presented. For example, 2 or more stimuli flashing momentarily in the same quadrant can cause confusion on the exact number seen.

EyesCream

EyesCream is a VF self-test that is downloadable from the Internet. On its website, the developer gives instruction on how to download the program. Instructions are given both in written form and with videos. The initial screen gives written instructions with figures detailing how to set the correct distance from the screen (<half width of a large TV screen), the use of response keys (spacebar or left mouse button) during the test and keys for pausing and aborting the test (figure 1.19).

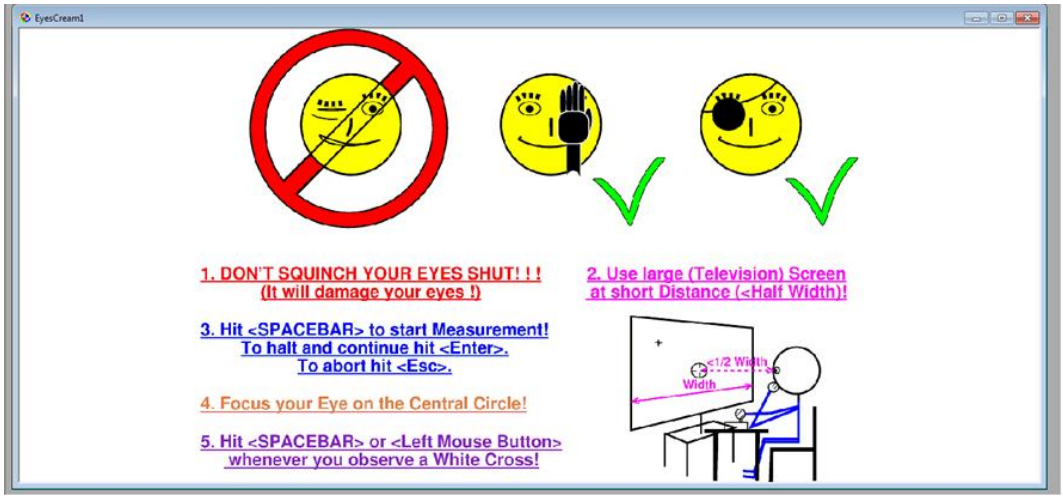

Figure 1.19: *Initial screen of EyesCream giving instructions on how to perform the test.*

The background is black during the test and the fixation point is a circle which increases and decreases its size while changing its colour between green and blue. The stimulus is a white cross which increases its size until the user responds. When all locations have been tested the screen draws two colour maps representing the prompt response time and the sensitivity. There are no instructions given concerning the interpretation of these results (figure 1.20).

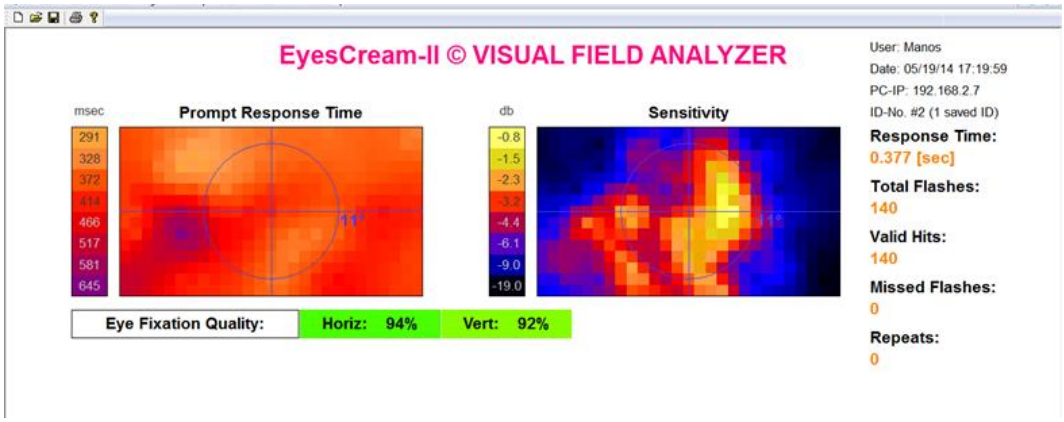

Figure 1.20: *An example of the results screen of EyesCream with colour maps of the response time and the sensitivity.*

EyesCream is clearly designed for use by perimetric experts as it provides the opportunity to modify a number of VF testing features. In the configuration tab one can adjust settings for parameters controlling the acquisition, the data analysis and the graphics. The minimum and maximum size of the stimulus and the fixation cross can also be adjusted accordingly, along with the brightness and the level of size increments. More complicated settings include dynamic enhancement of the stimulus (size and duration) in a linear or quadratic form. The above could prove to be very useful for someone with perimetric expertise; however, an average user/patient would probably find these settings very confusing.

<u>Peristat</u>

The Peristat online VF self-test has been developed by Dr Tsontcho Ianchulev (San Francisco, CA) and is the only test giving measures of

diagnostic performance. In a cohort of 58 eyes with mixed VF defect severity (10=no defect, 28=mild defects; MD>-5.00, 20=moderate & severe; MD<-5.00) the sensitivity and specificity were reported to be ~80% and ~95% respectively.[197] However, no independent publication exists. On Peristat's website the user must register to gain free access to the provided VF test. Once a username and a password have been set the user can start a VF test.

The initial screen of the test provides written instructions about the testing process. The background colour is black and there is a white fixation point constantly placed in the centre of the screen. There is also a green circle which flashes constantly during the test and is placed on the area where the normal blind spot should fall. The user is instructed to move their head forwards or backwards until the circle disappears and they should not be able to see it at all times during the test. The stimuli present at random locations either with their maximum intensity (i.e. white colour) or with a dark grey colour (Figure 1.21). Users respond by pressing the 'spacebar' key on their keyboard or clicking their left mouse button. The exact algorithm and number of stimulus presentations is unknown. On a normal eye test the number of presentations is more than 110, including catch trials (false positives and fixation losses).

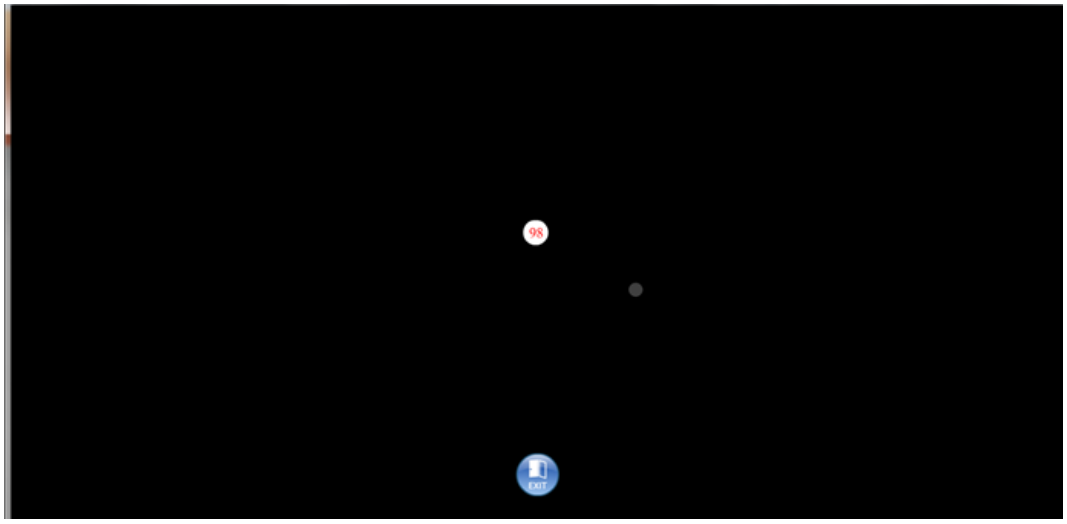

Figure 1.21: *Visual field testing with Peristat. The white circle acts as a fixation point and shows the total number of stimulus presentations. The grey circle is the stimulus which is presented at random locations.*

When the test is completed the user is informed about the reliability of their test. If the reliability indices of the test are low the user is advised to repeat the test. Reliable results are reviewed by a consultant ophthalmologist who gives feedback (via email) within 24 hours. Feedback is normal or defective along with advice to repeat the test on a regular basis and undertake a full eye examination annually. The email/report does not provide a VF chart or further information on the outcomes of the test.

<u>NovaVision Online Visual Field Screening Test</u>

The purpose of this test is to check for potential neurological loss of vision after a stroke or brain injury. It follows similar principles with the other aforementioned VF tests (e.g. single stimulus presentation, fixation target in

the middle of the screen, dimmed room lights etc). The test is binocular performed with both eyes open.

The instructions focus both on the 'environment setup' (figure 1.22), that is the preparation of the device (e.g. maximise window) and the patient (e.g. set the correct distance), along with patient instructions. The patient has three main tasks to perform: 1) keep their eyes on the fixation at all times, 2) press the space bar when the fixation point changes and 3) press the space bar when they see a stimulus. At this point, the patient has the option either to practice the test with approximately 10 stimuli and 3 fixation trials or take the test. A unique feature of this test is that it offers the option to enlarge the letter fonts for patient with poor acuity. Audio instructions are also available.

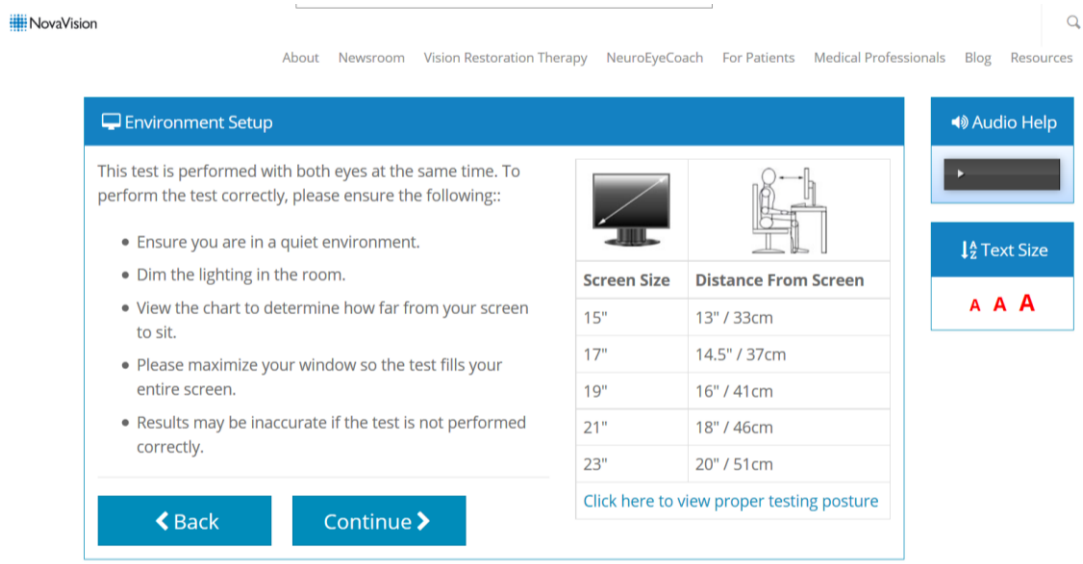

Figure 1.22: *Instructions provided by the NovaVision Online Visual Field Screening Test for the setup prior to testing. The instructions focus extensively on the testing distance, while the options for bigger letter fonts and audio help are available.*

The test is performed in a new window which the user is advised to maximise prior to commencing the test. The background colour is dark grey and the stimulus a white spot. There is no calibration process. Every presentation (or fixation target change) is accompanied by a bleep. At the end of the test an overview of the results is given (figure 1.23); also sent to the patient via email. The results are presented in a colour coded grid, (white-seen, black-missed). Information about the number of presentations seen, response time, fixation accuracy and false positive response rate is also provided.

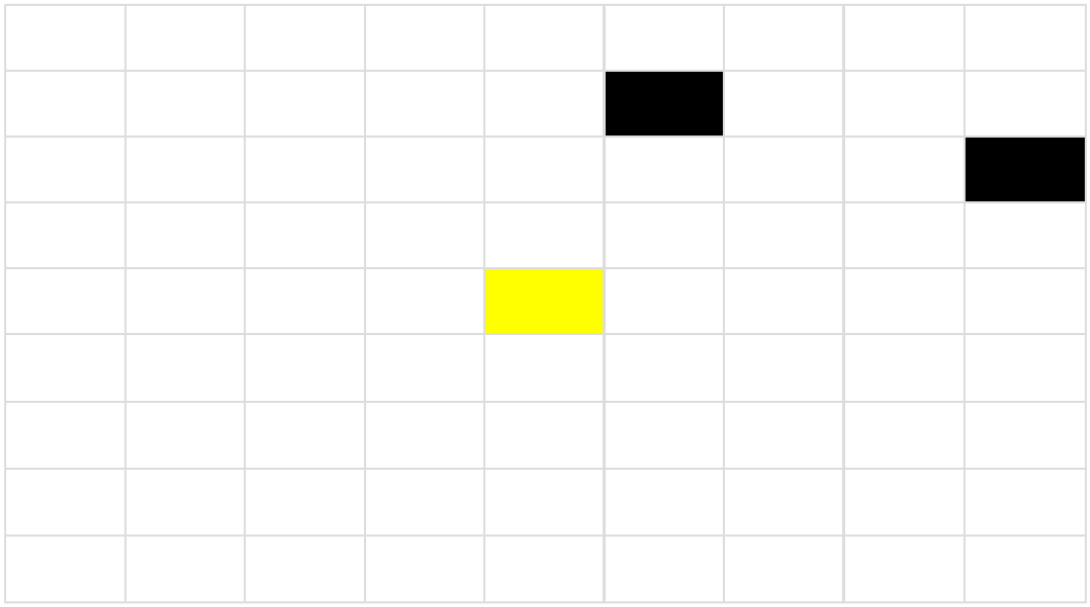

Overview

The graph shows your responses during the test. In every square, one light stimulus was presented. White squares on the graph show the areas where you responded to the light stimulus; black squares indicate the areas where you did not respond. The yellow square in the center represents the position of the fixation point.

Results

- **Stimulus Detection** - You correctly responded to 79 light stimuli out of 80 shown. This is a percentage of 99 %
- **Response Time** - Your average response time to the light stimuli was **0.59 seconds**.
- **Fixation Accuracy** - You correctly responded to 9 fixation changes out of 9. This is a percentage of 100 %. A high percentage is an indicator of good test reliability.
- **False Positive Responses** - Your false positive response percentage was **0 %**. The program registers a “false positive” every time you press the space bar while no light stimulus was shown. A high percentage is an indicator of low test reliability.

Figure 1.23: *Overview results of the NovaVision Online Visual Field screening test, provided after the end of the test and also in .pdf form via email.*

Usability evaluation

The usability of these tests was evaluated by recruiting 10 perimetric experts (i.e. glaucoma consultants, optometrists with perimetric experience, perimetric researchers) and 18 computer-literate volunteers with minimal (if any) VF experience, namely Group 1. Participants of Group 1 provided their feedback by undertaking each test (random order) and completing a modified questionnaire of the “quick and dirty” SUS. The SUS was introduced by John Brooke in 1996 and since then has become an industry standard for measuring usability.[198] It is a simple, ten-item Likert scale (ranging from point 1: strong disagreement to point 5: strong agreement) and provides a practical solution for the measurement of perceived usability in a quantitative way. Positive and negative items are alternated in the scale to reduce continuity effects. The final score is on a scale of 0 – 100. We chose to use this Likert-style format for its simplicity, its reliability, even in small sample sizes, and its independence on the product/service’s nature; SUS allows for the evaluation of a wide range of products, including hardware and software, websites and applications. The reason for implementing SUS in our usability assessment methods was not to evaluate the usability of the 5 different VF self-tests per se, but to identify a system that appeals to the users and could act as a model for the design of the new test. The questionnaire also provided space for participants to write any comments or thoughts after completion of each test. After completion of all 5 tests each subject was asked to name up to 3 positive or negative features that they liked, or disliked respectively, in any of these tests. A sample of this questionnaire is given in Appendix I.

The quantitative analysis of these questionnaires returned a usability score for each investigated online VF test, while qualitative data were used to identify design and testing features that make a computer-based VF test more appealing to its users. Demographic data from the participants were collected. Mean age, male/female ratio, mean number of previous VF tests was calculated (Table 1.7). The usability score for the tests performed first, second, third and so forth were collected to create 5 new cohorts and repeated-measures one-way ANOVA was performed to check whether order of testing had a significant impact in usability scoring.

	Perimetric Experts	**Lay Volunteers**
Sample size	10	18
Mean age (±st. deviation) years	47.5 (±13.86)	51 (±14.46)
Female/Male ratio	1:1	1:1.25
Median (IQR) number of visual field tests previously undertaken	N/A	0 (1)

Table 1.7: *Demographic characteristics of participants in the usability evaluation of the 5 online tests.*

The qualitative analysis of the questionnaire stratified the participants' responses into 6 key fields of interest: 1) the design of the software and

navigation through it, 2) its delivery method (i.e. downloadable, available offline etc.), 3) the presence and quality of introduction and testing instructions, 4) the opportunity to trial the test before actual testing commences, 5) the method of testing and 6) the presentation of test results.

Testing features regularly commented on were put together in pairs for further testing. Five pairs of features were generated: 1) response with a mouse click vs a key stroke, 2) change of fixation target at various locations across the monitor after each presentation vs after a group of presentations, 3) single vs multiple stimuli presentation, 4) audio feedback (bleep sound) vs no feedback during testing and 5) constant feedback vs feedback at random stages of the test.

Twenty-eight new volunteers with mixed perimetric experience (ranging from no previous VF tests to regular annual testing) and a mean age of 54 (±21.25) years were recruited (Group 2), Each volunteer evaluated the 5 pairs of testing features identified by the qualitative analysis of the questionnaires. In each trial, participants performed 2 tests in which a single feature (e.g. single vs multiple stimuli) has been changed. They were then asked which they preferred using a Likert-scale ranging from point 1: Definitely Feature A through point 3: No difference to point 5: Definitely Feature B. Their responses were recorded and analysed to establish preferred features.

1.3.4 RESULTS

All participants from Group 1 completed the assessment of all 5 VF tests that are available online. The mean age of lay participants was 51 (±14.46) years and all of them were considered computer literate after stating that they own and use a computer and feel comfortable with the use of the Internet. All data were considered valid and were included in the analysis. The order of testing did not prove to be a factor affecting the usability scores (p=0.87).
NovaVision Online VF Screening Test scored the highest usability score in both cohorts (i.e. perimetric experts and lay participants) with a median score of 90 (IQR – 26.25) and 82.5 (IQR – 12.5), respectively. Figure 1.24 shows the SUS score boxplot for all 5 tests from both cohorts. It is worth noting the broad scoring of perimetric experts (i.e. long boxes), mainly due to the experts' tendency to provide absolute responses at the two ends of the SUS scoring spectrum; meaning they would, most of the times, totally agree or totally disagree with a statement. Lay participants were more lenient with their scoring: 3 tests scored above the suggested cut-off of 68%,[194, 198] the average SUS score of 500 products, compared to the experts cohort where only one test passed that threshold.

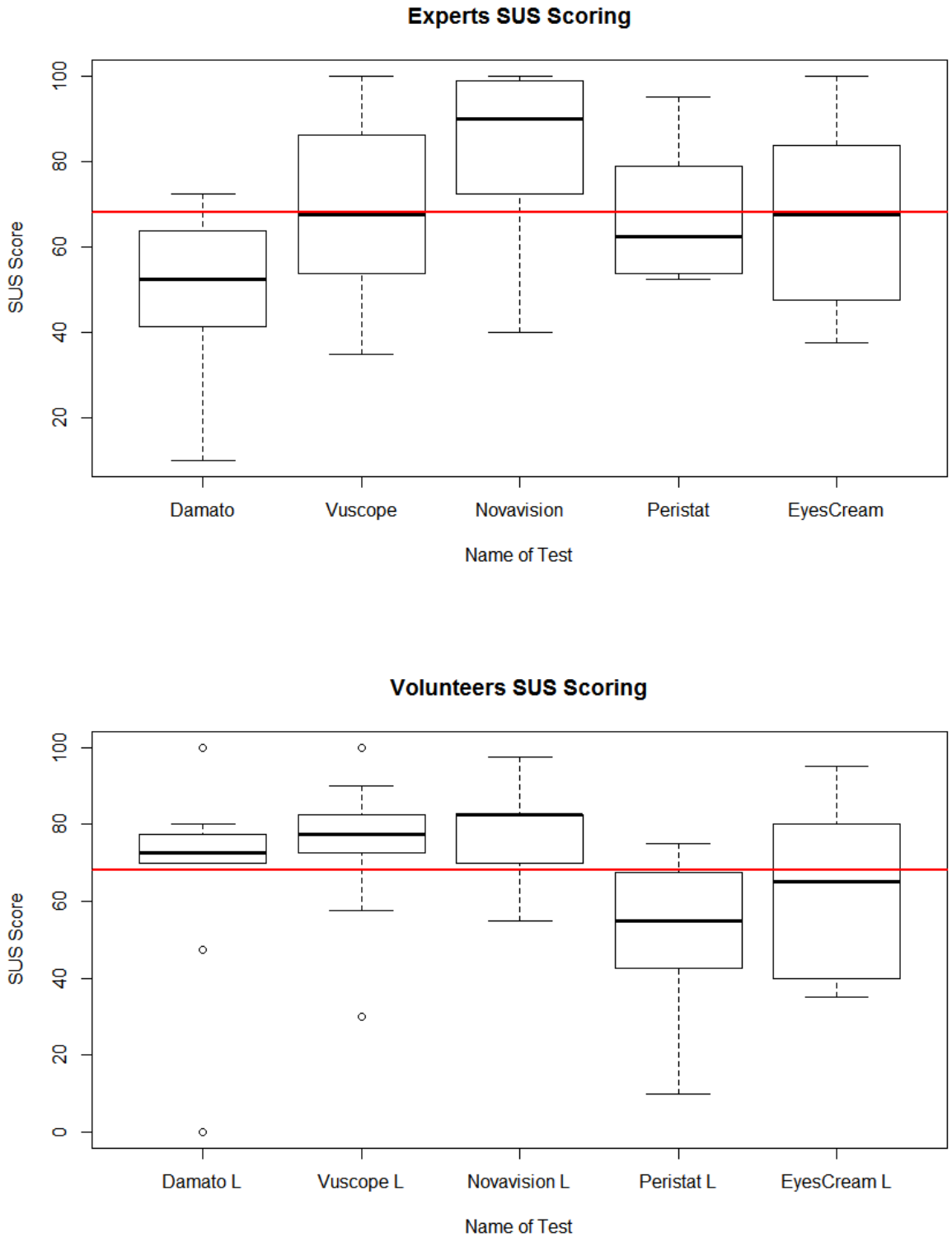

Figure 1.24: *Boxplots showing SUS scores for the 5 visual field tests; upper for experts, lower for lay volunteers. Red line shows the average SUS score of 500 products at 68%.*[199]

The qualitative analysis of the participants' comments with regards to design and testing features revealed that test parameters, such as the method of testing and the presence and quality of instructions, are highly important for the user's experience (figure 1.25). The prospect of practising the test before actual testing and the visual presentation of the test results are also appreciated by the users.

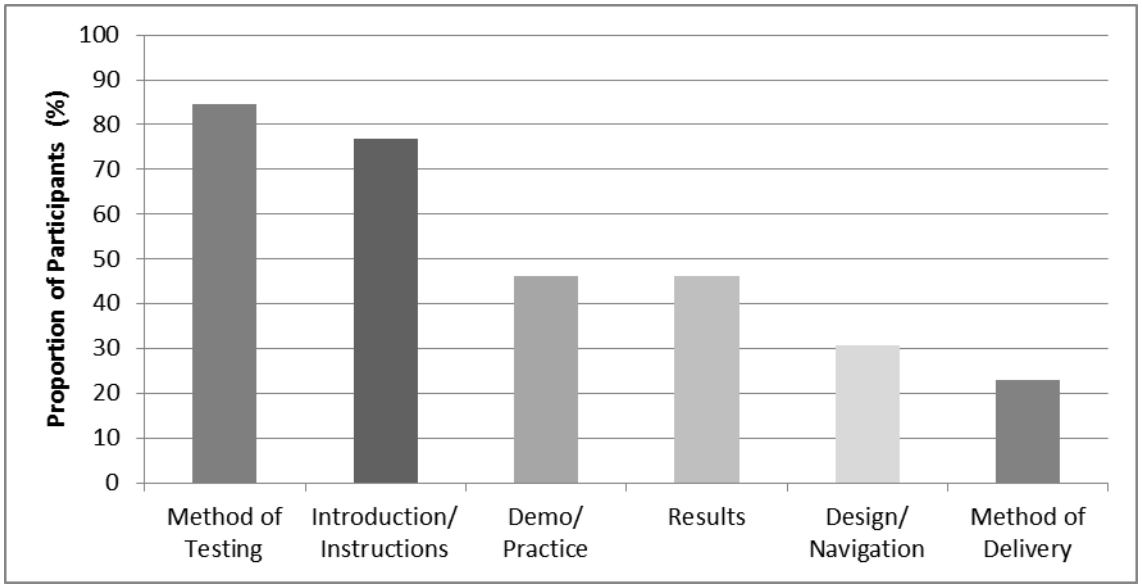

Figure 1.25: *Design and testing areas highlighted as important for users' experience*

Users' (group 2) preferences are shown in Figure 1.26, with multiple stimuli presentation showing a remarkable preference over single stimulus while there was no preference between mouse and keyboard as a mean of response. Participants showed no particular preference in the absence or

presence of feedback. Should some sort of feedback exist though, volunteers seemed to appreciate a lower frequency rather than constant presence of a text or sound message.

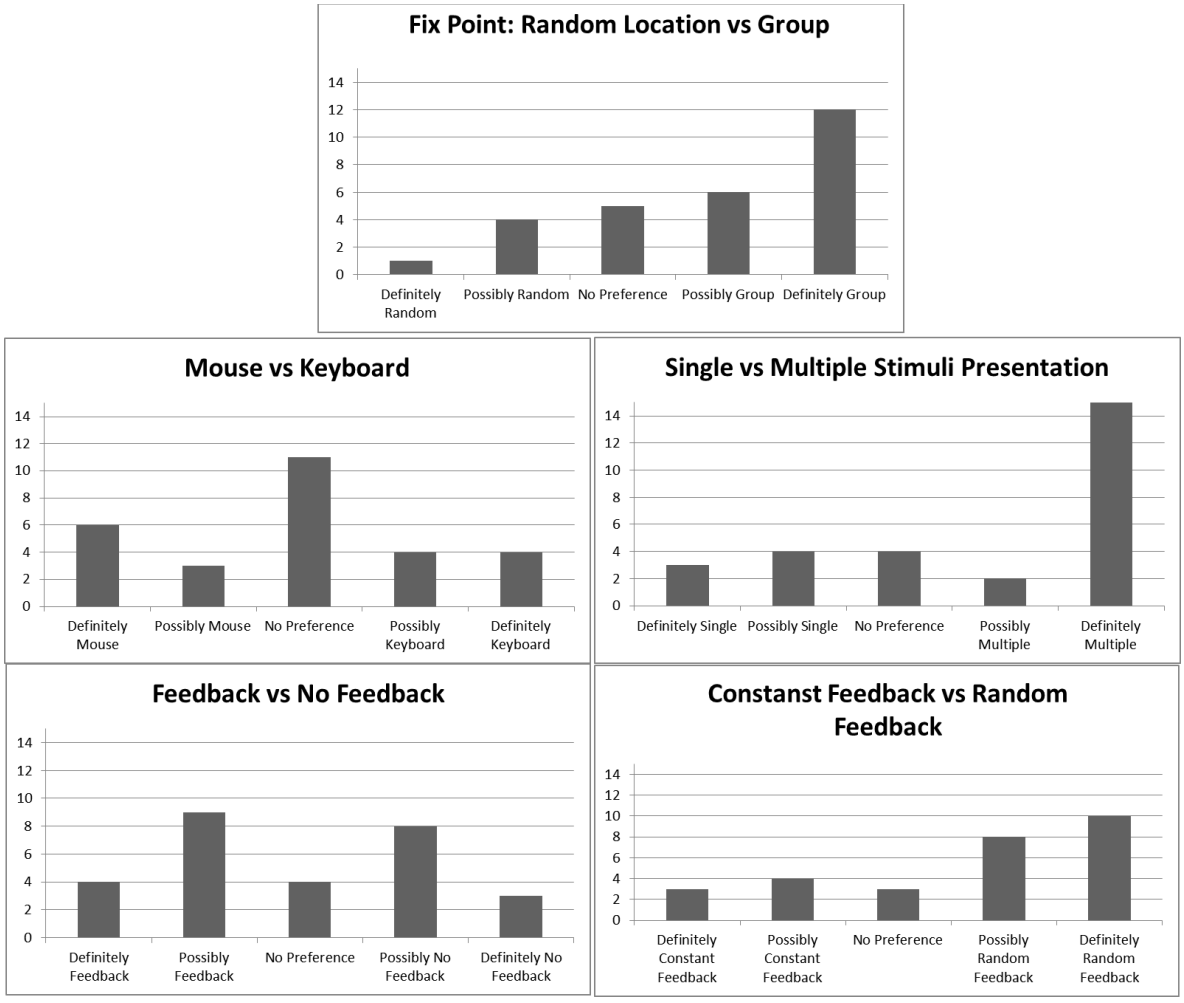

Figure 1.26: *Column charts showing the users' preference in 5 different comparison tests of design features*

1.3.5 DISCUSSION

A product with high usability is characterised by a number of attributes, such as learnability, efficiency or accessibility to name a few.[200] The International Organization for Standardization (ISO 9241-11) endorses these by stating that assessment of usability needs to report on the user's ability to complete the task requested (i.e. effectiveness), the resources required to complete the task (i.e. efficiency), and satisfaction.[201] Usability testing is an essential process during the development of a system that allows designers to create prototypes, test them and through an iterative process improve them.

Despite the increasing number of self-administered VF tests available online, there are no reports from research assessing their usability. The primary aim of this study was to identify design and test features that are preferred by users. These would then be implemented in a new VF self-test. Five online self-administered tests were taken by a cohort of users who commented on the design and the test features that they liked or disliked. Their responses revealed that users pay particular attention to the method of testing: how long the test will last, how they interact with the system during testing and what feedback they get. Another important factor that was highlighted from the users was the instructions and preparation prior to starting the test. Comprehensive and fairly short instructions along with the presence of a practice session received positive comments from the participants and were recommended as essential features for our new test.

The NovaVision Online VF Screening Test received the highest SUS score from both experts and naïve users. The NovaVision test is characterised by simple, clear instructions in bullet points, a demonstration of the test and the option to try it before actual testing commences. It is worth mentioning though that NovaVision is performed with both eyes open, compared to the monocular testing approach of the other tests. This might have affected the usability scoring. Differences in the scoring between the two cohorts were noted in terms of variability and total score. Perimetric experts tended to be more variable and generally scored the 5 tests lower than the non-expert participants. A potential reason for this variability may be that experts' are prone to provide more extreme responses (strongly agree or strongly disagree) with the evaluated statements.

Participants were also asked to suggest up to 3 positive and negative features from the 5 tests that they performed and provide any further feedback or thoughts they might have. The responses to this simple question provided a pool of test and design features that users found attractive, unpleasant or even annoying. Features that were mentioned in the majority of the responses were paired with their counterparts (e.g. response to a stimulus via mouse or keyboard) and were then subjected to a trial on a new cohort of volunteers to assess feature they preferred. It is worth mentioning at this point that 4 out of the 5 online VF self-tests that were assessed during the initial stages have a single-stimulus testing approach. Previous research has provided strong evidence that patients prefer multiple stimuli presentations to single stimulus presentations.[202] It was therefore tempting to put these two features to the test. The results totally justified this decision

as 17 out of 24 participants (excluding 4 participants that showed no preference) stated that they preferred multiple stimuli presentations. The feeling of interaction with the system seems to be appreciated by the users while, from a clinical point of view, it has been recorded that the maintenance of attention is higher with the multiple stimuli testing approach.

Recent research has highlighted the importance of vision testing instruments in a portable, low-cost form.[193, 203] Portable devices, such as laptops and tablets, have been shown to be very useful in testing contrast sensitivity and visual acuity. They can be used for the detection of disease and monitoring where access to traditional testing procedures is limited.[204, 205] The usability assessment of self-administered health tests, such as the ones evaluated in this study, is crucial to ensure the acceptability and user-friendliness of these systems as this is critical to their take-up rates. Increased take-up rates of self-administered VF tests can lead not only to more frequent testing but also promote wider dissemination and earlier diagnosis.

1.3.6 CONCLUSIONS

The initial stages of the development of the new VF self-test included the overview of perimetric tests that are currently available online and the evaluation of their user-friendliness. The purpose of this study was to identify design and testing features that either appeal to the users or discourage

them from completing the test. To the author's surprise, and best of his knowledge, there is no previous research on usability testing of any VF test. The closest qualitative investigation of VF testing is provided by the study of Glen et al. , where they report that interviewed patients did not enjoy the VF test, albeit recognising the importance of regular monitoring for preserving their vision.[206]

A literature review for usability tools returned a number of similar techniques. The SUS questionnaire, slightly modified accordingly to serve the study's evaluated subjects, proved to be a reliable method; simple, quick, easy for analysis and outcome interpretation. The study's questionnaire also included open questions asking participants to highlight positive and negative design features.

The two different cohorts, comprised of experts and lay participants, offered a different perspective during this study whose outcomes were adopted in the following stages of the software development by implementing favourable testing and design characteristics and further evaluating them.

Participants in this study paid particular attention to the format and clarity of instructions and highlighted this attribute, along with the opportunity of a test practice session, as the most important aspects in the design of a new VF test. One of the most favourite self-test characteristics seemed to be the multiple stimuli testing approach. In contrast, constant movement of the fixation point across the screen before each presentation seemed to annoy the majority of the participants while another unfavourable feature was repetitive feedback after every presentation; mainly in the form of a bleep

sound. The method of responding to a stimulus and whether this is by striking the keyboard or clicking the mouse showed no particular preference to one technique or the other.

The above usability features and outcomes of this study were taken into account in the final stages of the design of the new VF test. The product of this process is presented in details in the next chapter; in brief, the newly developed VF test featured a multiple stimuli presentation, a fixation target that was moving in 5 different locations (i.e. center and left, down, right, up respectively), while the response was open to the user's preference, meaning that both key strokes and mouse clicks were accepted. With regards to instructions, these were concise and were kept to the minimum.

1.4 Proposal for a New Computer-Based Visual Field Self-Test for Glaucoma Screening Purposes

1.4.1 Features of the new test

The software design process largely focused on the review of currently available online VF tests but also included:

- Compatibility with all the popular operating systems; namely Microsoft products, Apple Inc.' iOS and Android.
- Relatively fast test; less than 2-3 minutes per eye.
- Good diagnostic performance for screening purposes, especially for mild cases of glaucoma; with specificity higher than 80% to ensure low numbers of false positives.
- Easy and understandable test, with clear instructions; and other usability features that will make the test attractive and increase its take-up rate.

In order to address the issue of compatibility, Java programming language was chosen for coding the aforementioned software as it presents unique advantages. Java is:

1. Platform-independent; it can move easily from one computer to another, regardless their operating system.
2. Object-oriented; a specific programming approach that allows for re-usable code and modular/segmented programs.
3. Easily distributed; due to its networking capabilities.

4. Robust and secure; Java compilers and runtime environments put a lot of emphasis on early checking of errors.

Java 1.8.0 (and subsequent update versions) were downloaded and utilised for coding using the software development platform NetBeans (NetBeans IDE, version 8.0.2, Oracle Corp., CL, USA). A great help during the process of learning this fairly easy programming language was David J. Eck's e-book 'Introduction to Programming Using Java', version 6.0.[207] Online video tutorials and various outcomes from internet searches also proved to be very helpful in resolving minor programming issues.

High diagnostic performance in a relatively short testing time was an essential element of the new test. To achieve the above recent perimetric developments were implemented in the new test. In terms of testing pattern the new test uses 20 optimal test locations, as those derive by Wang et al.'s recent study (Figure 1.27; also shown previously at Figure 1.9).[208] More specifically, the researchers investigated the diagnostic performance of various subsets of the 24-2 testing pattern (24-2) and concluded that smaller numbers of the 24-2 could achieve relatively high sensitivity and specificity at a significantly reduced testing times. Based on this work, the new test utilises 20 optimal locations of the 24-2 pattern, a subset from which one or more locations would be missed by cases with mild to moderate glaucomatous VF defects (GSS2 stages 2 and 3). Table 1.8 provides further details of the utilised distribution along with reported diagnostic performance by Wang et al.

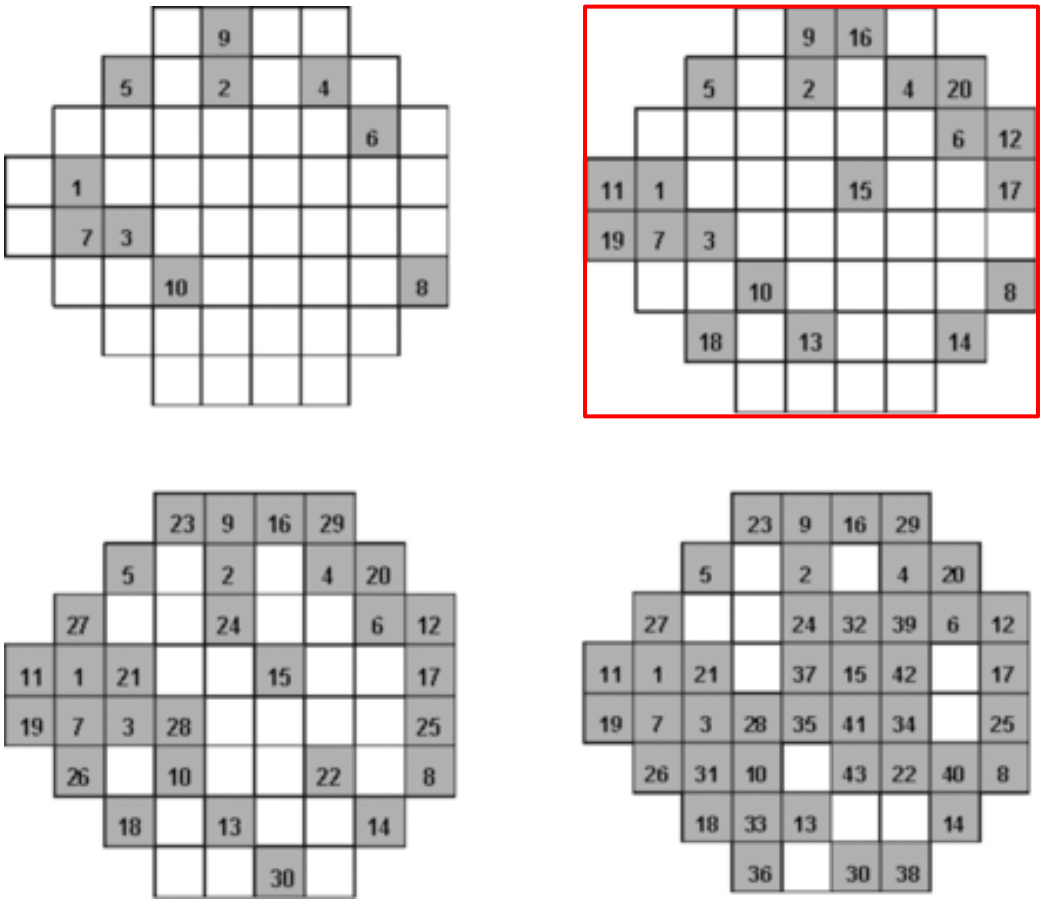

Figure 1.27: *Optimized distributions of 24-2 subsets according to Wang et al.'s study.[208] The distribution with the 20 optimal locations utilised by the new visual field test is highlighted in the red box.*

Total Number of Test Locations	20
Test Locations at Superior Nasal Quadrant	5

Test Locations at Superior Temporal Quadrant	7
Test Locations at Inferior Nasal Quadrant	6
Test Locations at Inferior Temporal Quadrant	2
Test Locations at Central 10°	1
Reported Sensitivity/Specificity %[208]	91.0 / 86.2

Table 1.8: *Distribution characteristics of the test locations implemented in the new test*

In 2003 Artes et al. introduced the multisampling supra-threshold approach as a powerful alternative to other test algorithms.[209] Of the various forms available the 3 seen or 3 missed version was adopted as a compromise between speed and diagnostic accuracy. Each location is tested between 3 to 5 times (3/5) depending on the patients' responses. The number of presentations compared to conventional supra-threshold perimetry (criterion 1/2; defective location if both presentations are missed) may be higher but such an approach offers better sensitivity while producing similar specificity.

Other stimuli features utilised within the new VF self-test include:

- Size equivalent to a Goldmann size III target
- Presentation time at 200ms
- Intensity at 10dB above the normative threshold

- Testing distance at 40 centimetres

Utilising both the 20-location testing pattern and the multisampling supra-threshold technique the new test would present between 60-100 stimuli, including a small number of false-positive trials. Assuming 1.5 seconds per presentation (according to previous literature on SITA Standard)[122, 210, 211] the total testing time was estimated between 1.5 - 2.5 minutes depending on the presence and nature of any VF defect. The diagnostic performance of the new test was expected to be adequate enough so there would be relatively few false-positives (i.e. specificity over 80%; essential for a screening method) but also cases with mild glaucomatous VF defects would also be detected (i.e. high sensitivity for GSS2 stages 1 and 2).

The outcomes of the usability evaluation of other online VF tests contributed significantly to the new design. In terms of testing features that would be appreciated by the users the new software implemented a multi-stimulus approach. Such an approach has shown to present reduced variability and potentially shorter testing times while accuracy remains the same; a potential reason being the better maintenance of attention with multiple stimulus testing.[202] The new software would present a total of 26 rounds of stimuli. Each round would present a set of up to 4 stimuli with no more than one stimulus in each quadrant and minimum inter-stimulus distance of 6 degrees. The stimuli locations at the 26 sets were pre-determined, however each set would be randomly selected for presentation (see Table 1.9 for more detailed information).

Total Number of Stimulus Sets	26
Number of Sets at Fixation #1 (Screen Center)	3
Number of Sets at Fixation #2 (Screen Left Center)	3
Number of Sets at Fixation #3 (Screen Bottom Center)	9
Number of Sets at Fixation #4 (Screen Right Center)	6
Number of Sets at Fixation #5 (Screen Top Center)	5
Number of Sets with 4 Stimuli	3
Number of Sets with 3 Stimuli	7
Number of Sets with 2 Stimuli	11
Number of Sets with 1 Stimulus	5

Table 1.9: *Characteristics of the sets of stimuli implemented in the design of the new visual field test. These sets were designed accordingly in respect to the requirements for 1 stimulus presentation per quadrant and a minimum of 6 degrees between 2 presented stimuli*

After each presentation the patient reports the number seen. In case the reported number was lower (but more than 0) than the number of tested locations, the software would display the previously tested locations again at maximum intensity (i.e. white coloured). At that point, the user selects the exact locations they previously saw. Figures 1.28 and 1.29 show screenshots from the displays described above. If the reported number was higher, a message would appear informing the user of their false response

and asking them to increase the level of their concentration (Figure 1.30). In terms of the testing algorithm, the result is ignored and the pattern repeated at a later stage of the test. In cases that users replied with the correct number of presented locations, or if they saw none, the software would move along to the next presentation round accordingly.

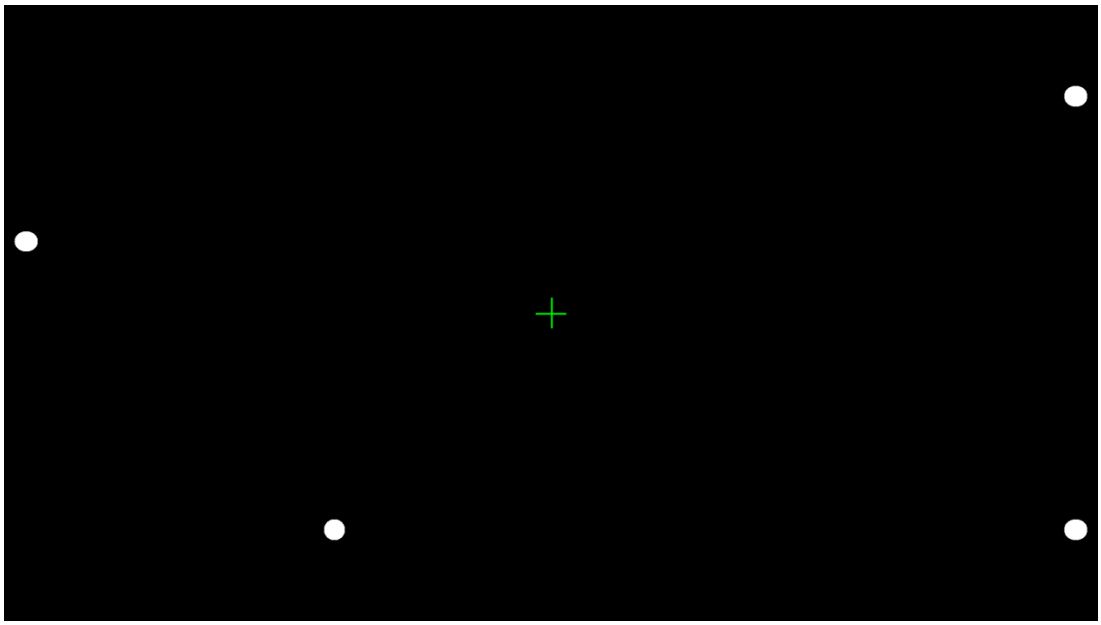

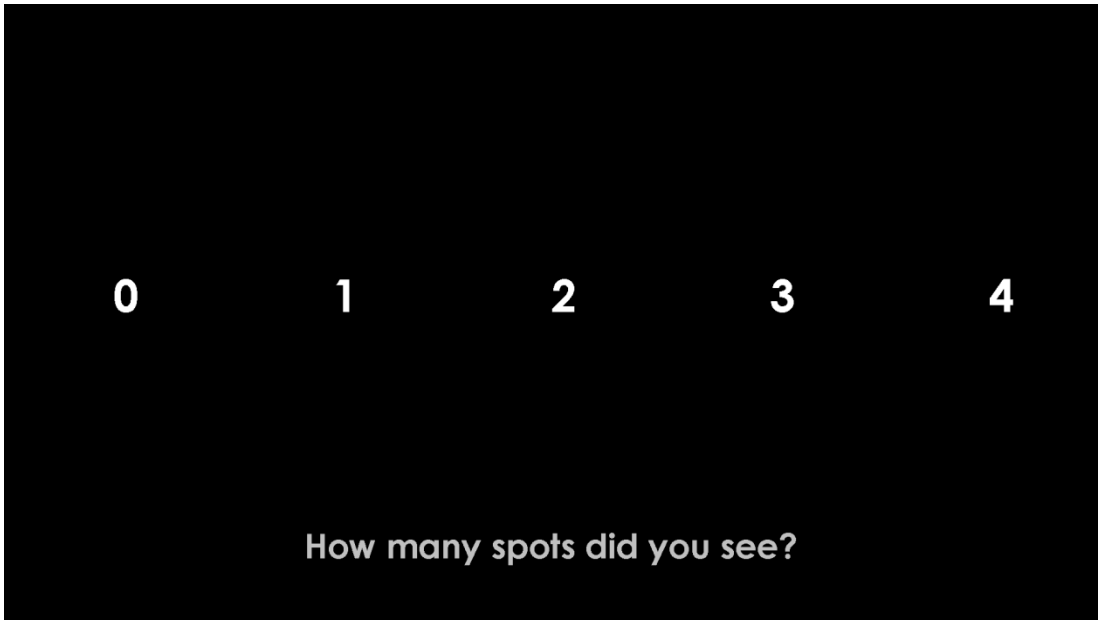

Figure 1.28: *Screenshots of the test display presenting up to 4 stimuli (upper part) and then prompting the user to respond by selecting the appropriate number (lower part). Note: in this example stimuli presentation has been set to maximum intensity for illustrational purposes.*

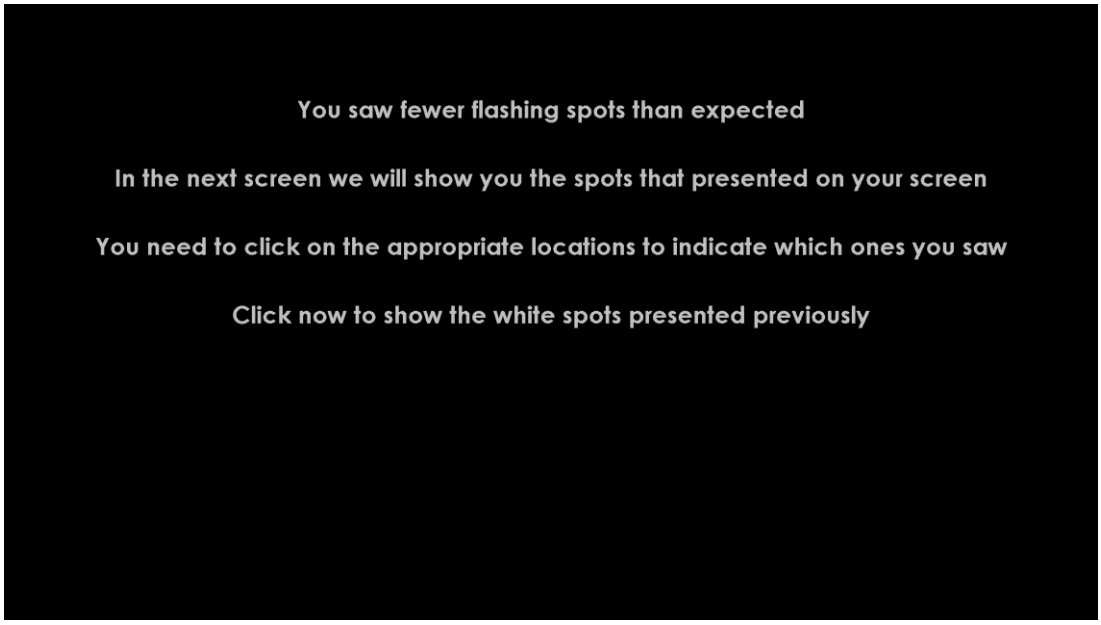

Figure 1.29: *Screenshot of a displayed message will inform the user that their reported number of stimuli was lower than the actual tested number of locations.*

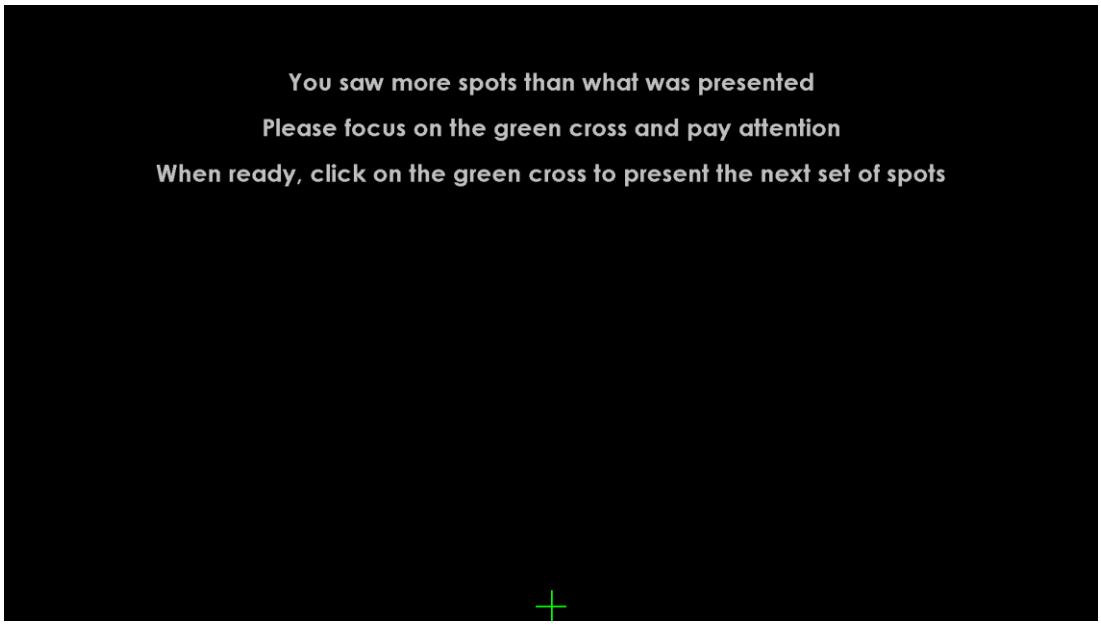

Figure 1.30: *Screenshot of the displayed message in cases where a higher number of stimuli was reported*

The 26 presented sets of stimuli ensure that each of the 20 test locations is presented 3 times. If a location is missed (once or twice) the software switches to single-stimulus presentation until the 3/5 criterion (i.e. 3 seen or 3 missed; pass or fail respectively) is met for all test locations.

To test a sufficient area of the VF the fixation target (green cross) needed to move to one of 5 different locations: first centrally, then left, down, right and up. The user would need to click on the green cross for the software to present the next pattern (figure 1.31). This design approach was adopted to ensure that the patient is looking at the fixation target before the stimuli presentation commences. Changing the location of the fixation target provides the user with the feeling that the test is indeed progressing and heading towards its end. In respect to the outcomes of the usability study the software would examine all available stimuli sets for the current fixation position before proceeding to the next fixation location.

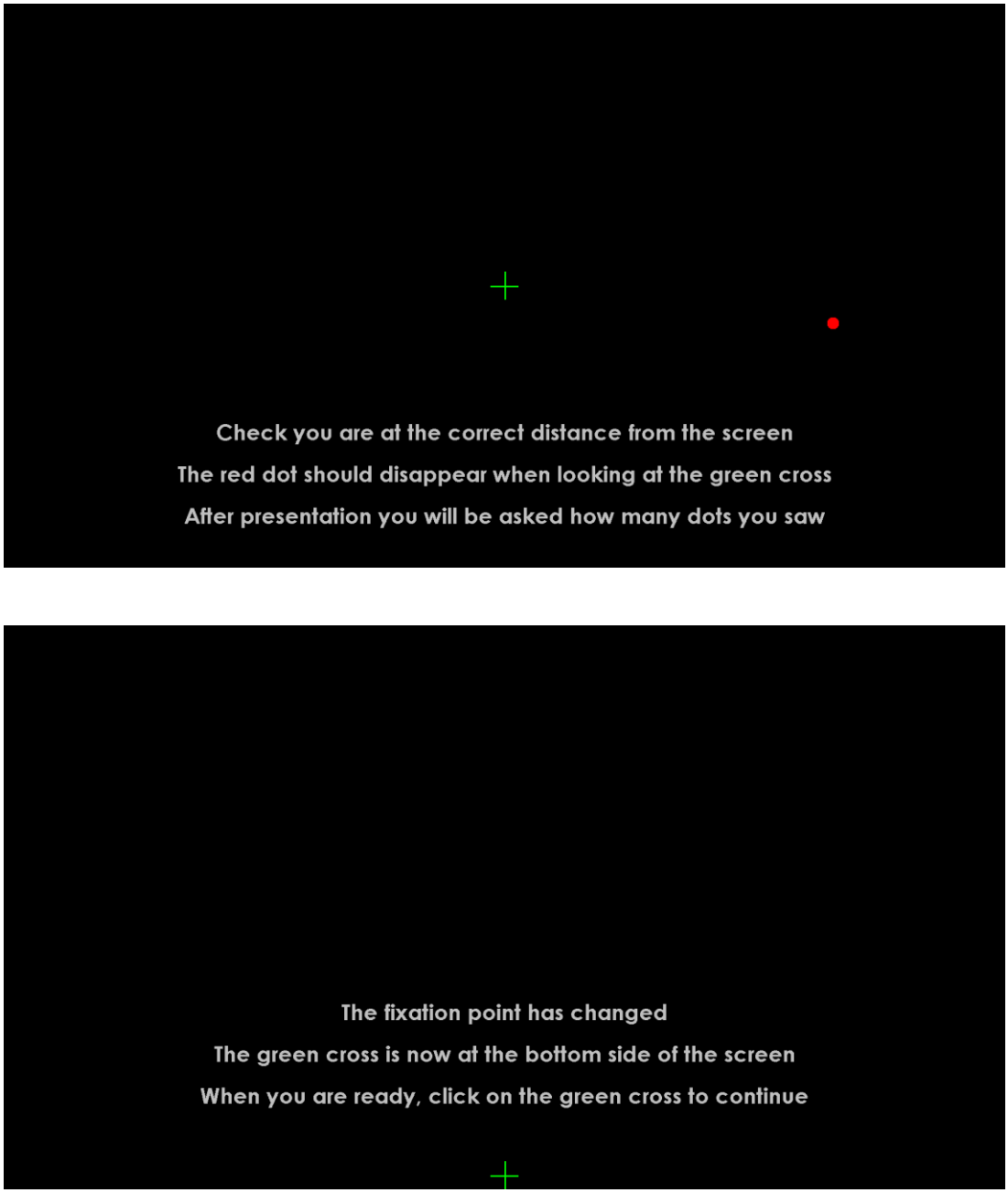

Figure 1.31: *Screenshots of the test displays. Upper part: Displayed message and fixation target at the beginning of the test. Lower part: Displayed message after fixation target has changed location. There are 4 similar displays for all the fixation locations*

Particular attention during the development of the software was given upon the test instruction format and the preparation prior to testing. Instructions aimed to prepare/position the patients appropriately and help them understand how they would perform the test. Guidelines were limited to 4 different displays with clear, concise information. A short animated video (figure 1.32) of approximately 1.5 minutes was also available to guide patients through appropriate positioning and testing method. The animated video was constructed by Benedykt Cien, a college student collaborating in this project and in particular for the graphical design of the instructional video. Although very basic, this animation proved to be very helpful for the education of the patients prior to testing. Patients were also given the opportunity to practise the test prior to actual evaluation. On practice mode, the test would run 5 rounds of presentations during which one location change of the fixation target would occur. In this format the users were given the chance to familiarise with both the response method of the test (i.e. report the number of stimuli they saw) and the fact that the fixation target would move to different locations on the display.

Figure 1.32: *Screenshot of the animated video with instructions for patients on preparation prior testing and how to perform the test*

There is a notion that maintaining the appropriate distance during testing is essential to ensure reliable results. This characteristic is probably one of the weakest aspects of VF evaluation via self-testing with a display monitor (laptop or desktop) or a tablet. The absence of a solid structure, such as a chin-rest at a fixed distance, could potentially allow changes at the testing distance, hence affecting test outcomes. However, Vingrys et al. have recently evaluated the performance of a tablet as a tangent perimeter and the effect of factors, such as blur, miosis, testing distance and ambient light levels.[212] Although their sample size is relatively small (5 participants only) they concluded that testing at 3 different distances (i.e. 25, 33 and 75 centimetres) did not have an effect on their test's average threshold although clearly it alters the eccentricity of the stimuli..

The newly developed software of this study confirms the right positioning of the user in a dual manner. At first, a display appears prior to the test with a fixation target in the centre and a flashing target located at 15 degrees

temporally and 2 degrees inferiorly from the central target. The user is instructed to look at the target in the centre and move backwards or forwards and approximately 40cm from the screen until the flashing light disappears into the blind spot (Figure 1.33). During testing, a red small target (this can be seen in the previous figures) is constantly presented at the blind spot location and the users are advised to ensure that they “cannot see the red circle” when they look at the fixation target before initiating a presentation.

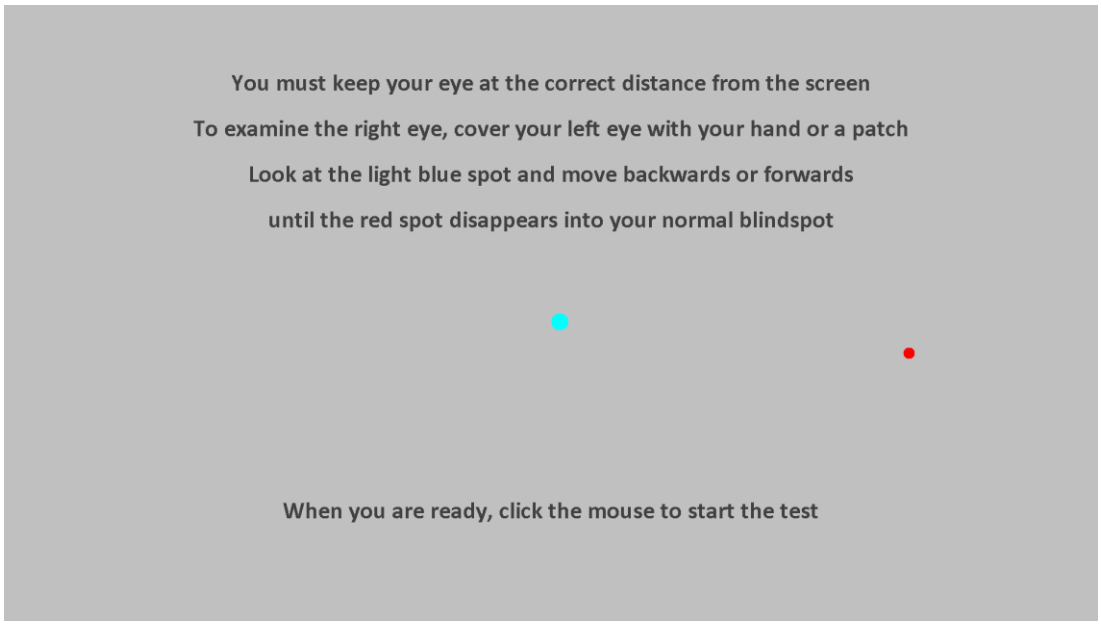

Figure 1.33: *Screenshot of the display before the test where users can set themselves at the correct distance*

1.4.2 Equipment

An Ultrabook Dell XPS 12 was used during this study running in the Microsoft® Windows 8 Pro operating system. One of its key features is the touch-screen capability of this hybrid’s display, making it easy to operate the device both as a laptop and a tablet. Participants in the study evaluating the

diagnostic performance of the proposed test were free to perform the test either by using a mouse or touching the screen. While this specific device may be on the expensive side of the portable devices' price spectrum, it is unlikely that the computing capabilities of cheaper laptops or tablets would affect the performance of the new software. Table 1.10 provides further details on the specification of the device.

Processor	Intel Core i7 3517U; clocking 1.9GHz
RAM	8GB
Graphics Card	None; Intel HD 4000 graphics on the Core i7 processor
Display Size	12.5″ 11″ Horizontal 6″ Vertical
Display Resolution	1920 x 1080
Operating System	Microsoft® Windows 8

Table 1.10: Specification characteristics of the Ultrabook Dell XPS 12 used in this project for developing the software and evaluating the new visual field test

1.4.3 Display characteristics

The luminance of the display was measured at various locations and through the value range of the red-green-blue (RGB) colour model. In brief, the RGB model is an additive colour model that combines red, green and blue light in

various combinations to reproduce a broad array of colours. In PC monitors and programming the RGB values range from 0 to 255, with R-G-B = 0-0-0 representing colour black and 255-255-255 representing colour white. The reasons for measuring the luminance of the Ultrabook's monitor were mainly twofold: first, to identify the differences of luminance levels across the monitor and second to estimate which value of the RGB model would produce a stimulus approximately 10dB above normal threshold. The measured luminance levels could potentially be used to calibrate the screen and produce a display of uniform luminance. However, such a calibration process never took place as the main hypothesis of the project is that the proposed VF test could perform adequately at any PC, laptop or tablet without the need for monitor optimisation. It is worth discussing here that luminance levels vary from one screen to another; and that could potentially be a limitation of this concept. However, most modern screens can produce similar luminance levels while screens from the same products, such as iPad tablets, have shown repeatable measurements across different screens. One last thing to take into account is that a VF test is, by definition, an evaluation of differential contrast sensitivity. Considering the latter, a monitor that fails to produce very bright luminance does not necessarily mean that cannot reproduce stimuli of a specific, albeit small, range of contrasts.

The 20 test locations of the proposed VF test use 38 different spots on the monitor depending on the position of the fixation target. The luminance across the range of the RGB values for all 38 spots was determined in increments of 10; that is from 0 (0-0-0) to 250 (250-250-250) and then 255. In addition, the screen was separated into a 3x4 arrangement, which is 12

different parts. Their central points were also photometrical measured at minimum and maximum luminance only. Figure 1.34 shows the pixel coordinates on the monitor where luminance measurements were taken.

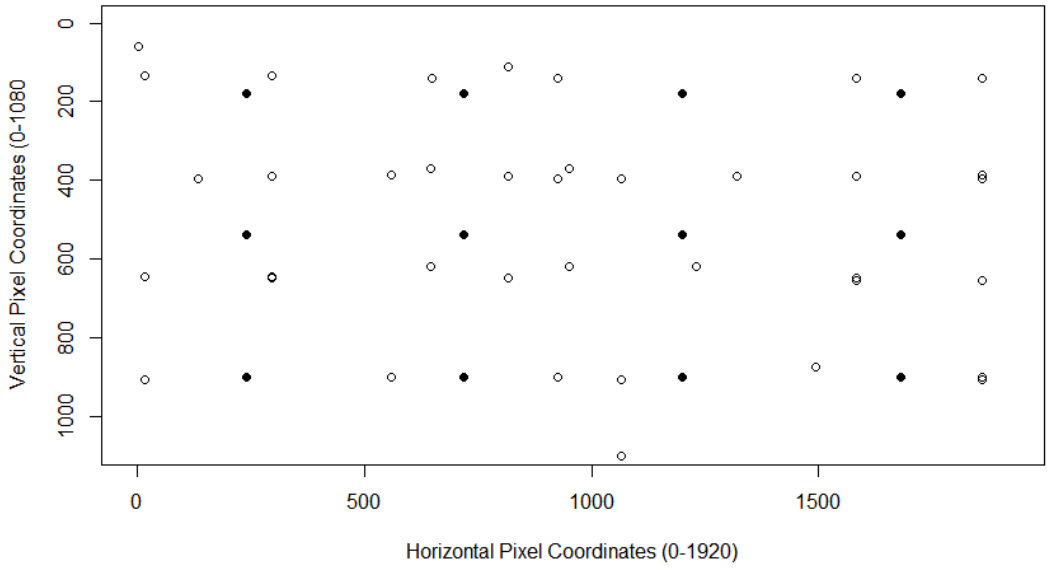

Figure 1.34: *Scatter plot representing the 50 locations on the monitor where luminance measurements were taken. Filled circles indicate the 12 central spots of the 3x4 array with measured minimum and maximum luminance. Open circles indicate the 38 monitor spots where the test locations of the new visual field test are presented. For these locations luminance measurements were taken across the whole range of the RGB model in increments of 10.*

The median minimum luminance of the monitor was 0.38cd/m^2 (IQR–0.04) while median maximum luminance was 295cd/m^2 (IQR–31.75). As expected, the luminance level was not consistent across the monitor with higher variations occurring at brighter levels. Figure 1.35 shows the distribution of luminance levels at different RGB values at the 50 test locations.

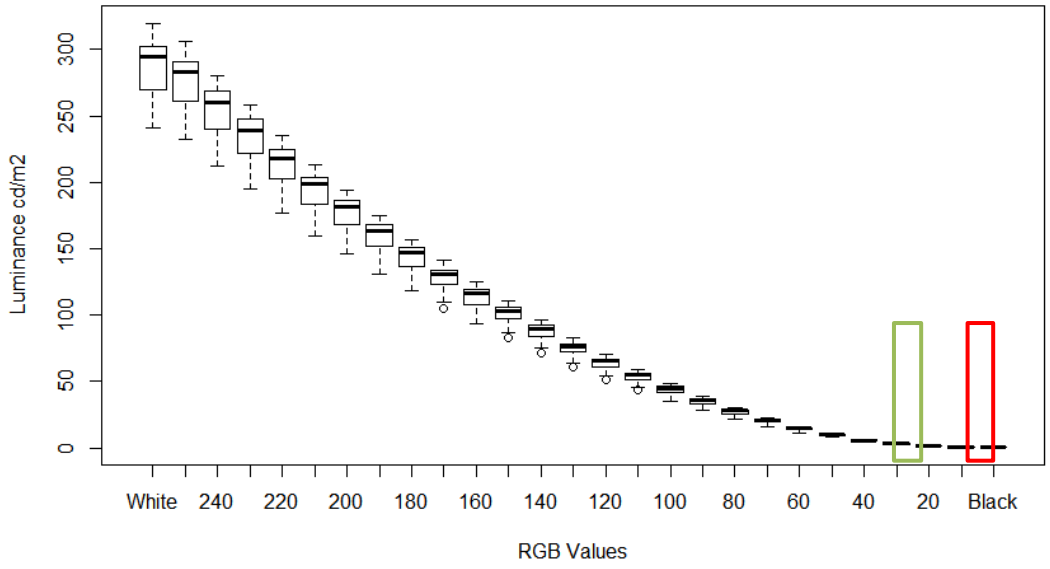

Figure 1.35: *Boxplot of the luminance distributions across the range of RGB values measured at 50 different stimulus locations. Red rectangle shows the approximate range of RGB values that produce contrast at normative threshold levels. Green rectangle shows a similar RGB range for stimuli at 10dB above threshold.*

As mentioned in section 1.1.11, the HFA has a background luminance of 10cd/m^2; this is approximately 25 times brighter than the background luminance of the measured equipment. In order to generate stimuli of similar

contrast, the required luminance for stimulus presentation in the Ultrabook was estimated. Previously published tables on the stimulus luminance of the HFA across its dB scale show that stimuli of 20dB and 22dB (approximately 10dB brighter than the normative thresholds) account for 31.8cd/m^2 (i.e. 100 asb) and 20.1cd/m^2 respectively. By interpolating the acquired luminance measurements across the whole range of RGB values (i.e. 0,1,2,3… etc) and using equation 1, it was possible to estimate the appropriate RGB values to generate the required stimuli. Hence, RGB values of 5 and below would generate stimuli at normative thresholds (i.e. 28 to 32 dB – red rectangle in figure 22) while those between 23 and 30 would be appropriate for an approximately 10dB supra-threshold stimulus; highlighted with a green rectangle in the previous figure. It is worth mentioning that luminance variations across the monitor at this testing level (e.g. RGB value – 25) are still relatively low and insignificant, with ~0.5cd/m^2 of difference between the brightest and the dimmest spot on the monitor accounting for ~1.5dB difference. Therefore, the RGB value of 25 was used to present stimuli at test locations.

Previous studies have taken extensive measurements of physical characteristics (such as luminance, contrast etc.) of the displays from modern portable devices and, effectively, investigate their suitability for vision testing at home. Probably the most complete study has been presented by Tahir et al. who evaluated the screens of 3 tablets: an iPad 3, a Google Nexus 10 and a Galaxy Tab 2.[203] The authors paid particular attention in 4 tasks: they 1) calculated the gamma function of a central point, 2) measured luminance and contrast at central and peripheral locations to establish the

uniformity of luminance, 3) estimated the stability of the screens at various warm-up times and 4) investigated the effect of nearby light sources on contrast of a presented target. They conclude that generally all 3 devices have adequate spatial resolution for vision testing. The achieved contrast ranges, while not as broad as traditional charts for very low levels of contrast, would succeed in testing at normal contrast sensitivity ranges. What is more important, changes in the luminance levels at the peripheral points of the screen did not account for clinically significant changes in the contrast. Last, they acknowledge that reflections on the screen do have an effect upon the target contrast; however, this effect is minimal and insignificant when the tablet screens were not tilted and positioned perpendicular to the floor. The latter was also reported by Vingrys et al. although they do state that ambient illumination having no effect on their test's reported threshold is probably an indication that its performance is on the Weber slope.[212]

During the set-up of the equipment for the performance evaluation of this project's developed test, luminance and contrast measurements were acquired for investigational purposes only. There was no intention to optimise the screen and achieve luminance uniformity as the hypothesis of this project is that un-calibrated commercially available screens are adequate enough to accommodate a simple and fast VF test for glaucoma screening purposes. The nature of the data collected during luminance measurements and more specifically the low variations in luminance at dimmer levels support the idea that the contrast difference between central and peripheral locations of the screen is likely to be clinically insignificant.

1.4.4 Conclusions

The outcomes of the usability evaluation study were brought together with recent advancements in perimetry to propose a new VF self-test that would be fast, user-friendly, sensitive to mild glaucomatous cases and highly specific for the avoidance of a large number of false-positive referrals. The product of this design process resulted in a VF test with these characteristics:

- Testing Pattern: 20 locations – subset of the 24-2 pattern
- Testing Algorithm: Supra-threshold stimuli at ~10dB above normative threshold with a multi-sampling approach – passing criterion 3/5
- Stimulus size: Goldmann III
- Presentation time: 200ms
- 5 fixation target positions: centre, left, right, up and down
- Multiple stimulus presentation for faster testing times and higher usability
- Simple, concise and clear instructions with the opportunity to practise the test prior the actual examination

Luminance levels across the screen of the laptop were taken to derive the appropriate value of the RGB model in order to achieve the required contrasts. After the investigation this was set at the value of 25 (i.e. Red-Green-Blue = 25-25-25) which produces approximate contrasts equivalent to the HFA's 20-22dB. Further analysis of the luminance data

showed small variations across the monitor at the dimmer levels; therefore supporting the notion and recent research evidence that modern monitors are acceptable for home-testing

1.5 Evaluating the Performance of Visual Field Tests via Simulation of Visual Field Loss: A Methodology Report

Contributions

During the first year of the PhD I was significantly involved in the development of a method for simulating VF defects. The idea belongs to the primary supervisor Prof David Henson who previously worked on the initial stages of this concept with a number of MSc (Investigative Ophthalmology and Vision Sciences) students. This study presented an opportunity for me to acquire some basic programme coding skills with Java, which I utilised to adopt the concept and modify it accordingly in order to serve the purposes of a study evaluating the diagnostic performance of a new self-administered VF test.

Presentations / Publications

The outcome of this research has been presented as a poster at the UKEGS Meeting 2015 in Leicester. Parts of this work have also been presented in oral presentations at the ARVO meeting 2016 in Seattle, US, the IPS meeting 2016 in Udine, Italy, and a number of presentations at MREH and the University of Manchester.

A manuscript related to this work has been submitted, peer-reviewed and returned from the Translational Vision Science and Technology Journal and

the Journal of Glaucoma. The feedback of the previous peer-review processes has been taken into account for this chapter.

1.5.1 ABSTRACT

Purpose: To describe a VF defect simulation technique for evaluating the performance of VF tests along with an example of its use for a new self-test.

Methods: The reported method simulates VF defects, via a modification to the perimeter program, in subjects with no known VF loss. In the example provided 30 early/moderate glaucomatous VF defects (24-2 SITA-Standard) were used in the simulations. Participants were recruited from patients and accompanying persons in the outpatient waiting rooms of MREH. Participants without any VF loss were tested 4 times, once without any simulated defect and with 3 randomly selected simulated defects of different severity.

Results: 153 subjects were recruited in <3 months and successful data were obtained from 151. Diagnostic performance was established for 3 different stages of loss.

Conclusions: The diagnostic performance of VF tests has historically been based upon trials involving patients with known VF loss. This method has a number of shortcomings including difficulty in recruiting cases with early loss, differences in the disease and control samples, poor reproducibility and poor characterisation of defects. The new method overcomes many of these problems through the use of simulated VF defects. It captures the intra- and inter-variability seen in patients with glaucoma, eases recruitment, is rapid and cost-effective and provides diagnostic measures to precisely defined stages of VF loss.

1.5.2 INTRODUCTION

Visual field tests are used extensively for the detection and management of COAG. They provide a measure of the functional losses and can detect change well before the occurrence of symptoms and any impact upon a patient's quality of life.[213]

Even though existing VF tests perform well there is always scope for improvement. New algorithms have been introduced to reduce test times[214, 215] and new test protocols are being developed for the testing of children[216, 217] and for self-testing.[218]

The benefits, or otherwise, of a new VF test are normally established with a clinical trial in which there is both a sample of control patients, with no known VF loss, and a sample of diseased/high risk patients with abnormal/suspect clinical findings. This approach has a number of limitations:

1. The sensitivity is highly dependent upon the case mix in the diseased/high risk sample (e.g. if the sample has a high proportion of advanced cases then the sensitivity is likely to be high);
2. There is a lack of a gold standard measure of VF loss. The trials are comparison studies of two perimetric tests rather than a study of diagnostic performance;
3. The dependency of sensitivity on case mix (1) means that it is difficult to compare diagnostic performance across studies.

4. It is difficult to match patient demographics between the two sample populations;
5. There are often differences in prior perimetric experience between the two samples (i.e. cases in the diseased/high risk sample are likely to have more perimetric experience than those in the control sample);
6. The trials are time consuming and expensive.

An alternative approach, that overcomes many of the shortcomings of a clinical trial using both control and diseased populations, is to undertake a clinical trial using only a control population that is tested with and without computer simulated VF defects. Specificity is derived from testing without any simulated defect and sensitivity from testing with simulated defects.

To simulate glaucomatous VF defects the intensity of presentations within an area of loss needs to be attenuated by an amount that corresponds to that loss. For example, to simulate a 9dB loss at a location in the superior field the perimeters' software needs to reduce the intensity of presentations at that location by 9dB every time that location is presented. The complex relationship between response variability and sensitivity in glaucoma, in which variability increases with loss of sensitivity, also needs to be accounted for by adding the appropriate amount of variability to locations with simulated loss.

A database of glaucomatous VF defects can be used to provide a test sample that covers a defined range of defects for simulation. For example, early VF defects falling within the Borderline and stage 1 classification of the

Brusini's GSS2 could be used to evaluate the performance of a test to early loss.[7]

The use of computer simulated VF defects to evaluate diagnostic performance has the following benefits:

1. The perimetric defects are precisely defined. You are measuring true performance rather than undertaking a comparative trial;
2. It is possible to replicate the findings and undertake accurate comparisons between different tests/instruments as the samples are precisely defined (1) and reproducible.
3. The sensitivity and specificity measures are based on the same sample of subjects, i.e. they are perfectly matched with respect to demographics and prior perimetric experience;
4. The sample size is reduced. If each subject is tested, for example, 4 times (once without a simulated defect and with 3 different simulated defects) then the sample is reduced to 25% of that for a conventional clinical trial;
5. There is a large pool of potential subjects;
6. Response errors, losses of attention and fatigue/learning effects will be accurately captured in both arms.

This chapter details a method to simulate glaucomatous VF defects via modification of the perimeters software along with an example of its use on a new VF self-test.

1.5.3 METHODS

Generating a pool of glaucomatous defects

The first step in undertaking a performance trial using simulated defects is to generate a pool of glaucomatous VF defects. In this study random cases were selected from a database of 24-2 SITA-Standard HFA records; inclusion criteria being: reliable results (fixation losses <20%, false positives <33% and false negatives <33%) and stable early or moderate VF defects with a rate of progression between 0.5 and -0.5 dB/year over a 4 year period. The median thresholds for each test location were used to calculate the simulated defect (figure 1.36) with reduced noise. We created a pool of 30 early/moderate defects (10 from each Brusini GSS2 stages 1-3; cases presented in Appendix I).[171] The selection of early cases was to provide a realistic screening challenge to the new software under evaluation. Larger pools with different distributions could equally well be used.

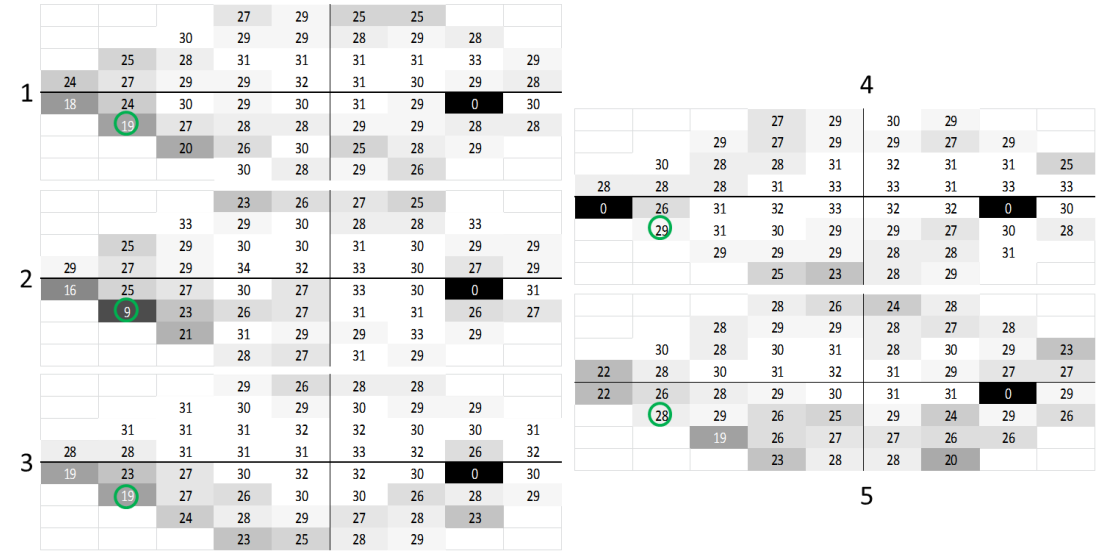

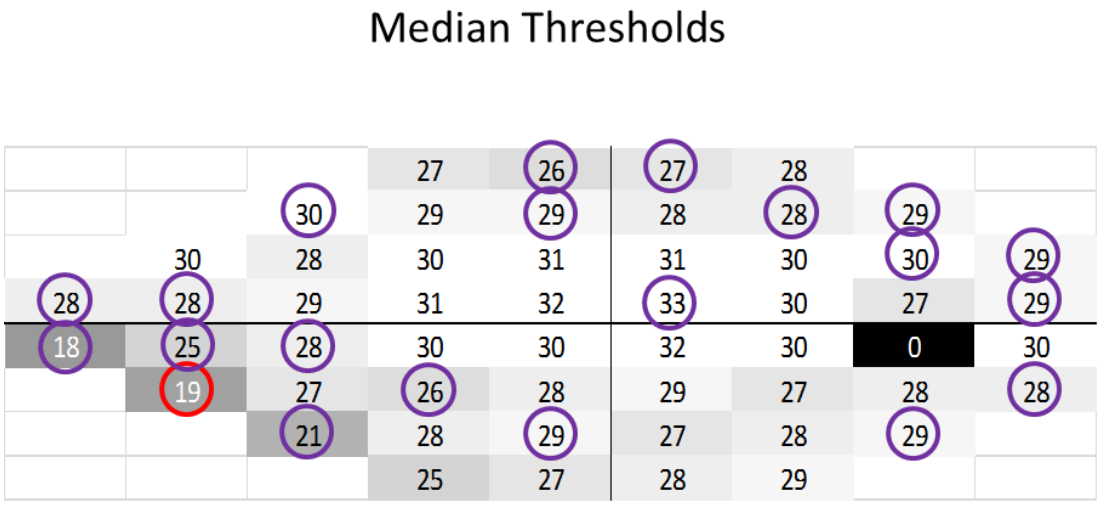

Figure 1.36: *The median (red circle) of the sensitivity thresholds from a series of visual field tests (green circles) was calculated to establish the 'true' threshold. The 20 tested locations, subset of the 24-2 pattern, are highlighted with purple circles.*

Subject selection

One hundred and fifty three subjects were tested. Some were patients with no documented VF loss while the majority were accompanying persons

waiting in the glaucoma outpatient clinics at MREH. The study was approved by the local ethical committee and followed the tenants of the Declaration of Helsinki. All subjects provided written informed consent. All the data for the self-test evaluation was collected by a single researcher.

Test sequence

One eye from each recruited subject was tested once without a simulated VF defect. If the result was a test failure (a single location missed 3 times) the subject was excluded from the study and referred to the glaucoma clinic for further examination. Those that passed the no-defect test were tested a further 3 times with a randomly selected defect from each of the 3 GSS2 stages.

Software modification

Figure 1.37 gives a flow diagram of the steps needed to simulate a glaucomatous VF defect. There is an extra stage to the conventional test that attenuates the stimulus in certain regions by an amount that matches the level of loss (defect) found in a specific case of glaucoma. In addition to altering the intensity of a stimulus falling within the area of a defect the well-established relationship between threshold sensitivity and response variability[94, 95, 219] was used to add variability to the level of loss. Using the example provided in the introduction, the simulation of a 9dB loss will include an additional (beyond that seen at a location with normal sensitivity)

variability element to ensure that the total variability matches that defined by the work of Henson et al., see Figure 1.38.[10] Part of the Java code which includes the 'core' of the simulation process is provided in the Appendix I.

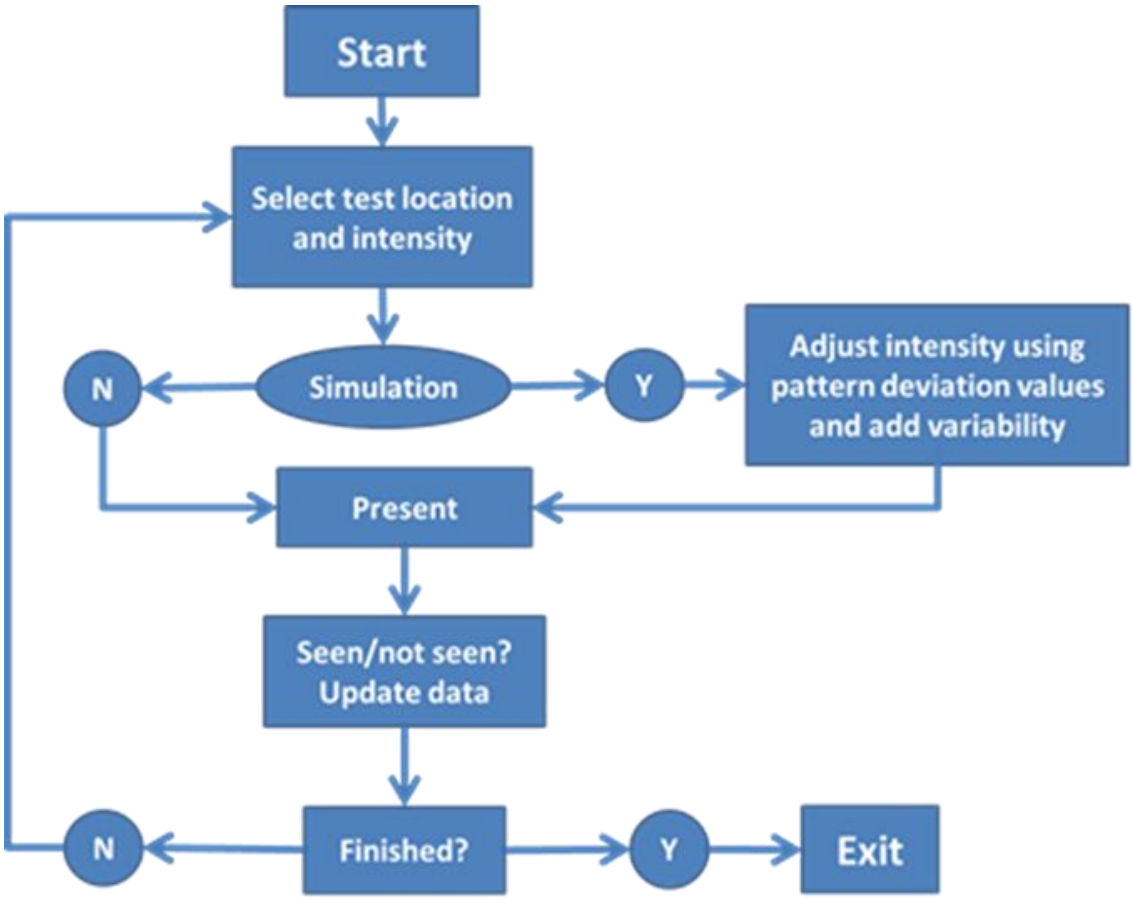

Figure 1.37: *Flow diagram of the software used to simulate glaucomatous loss in subjects with normal visual fields.*

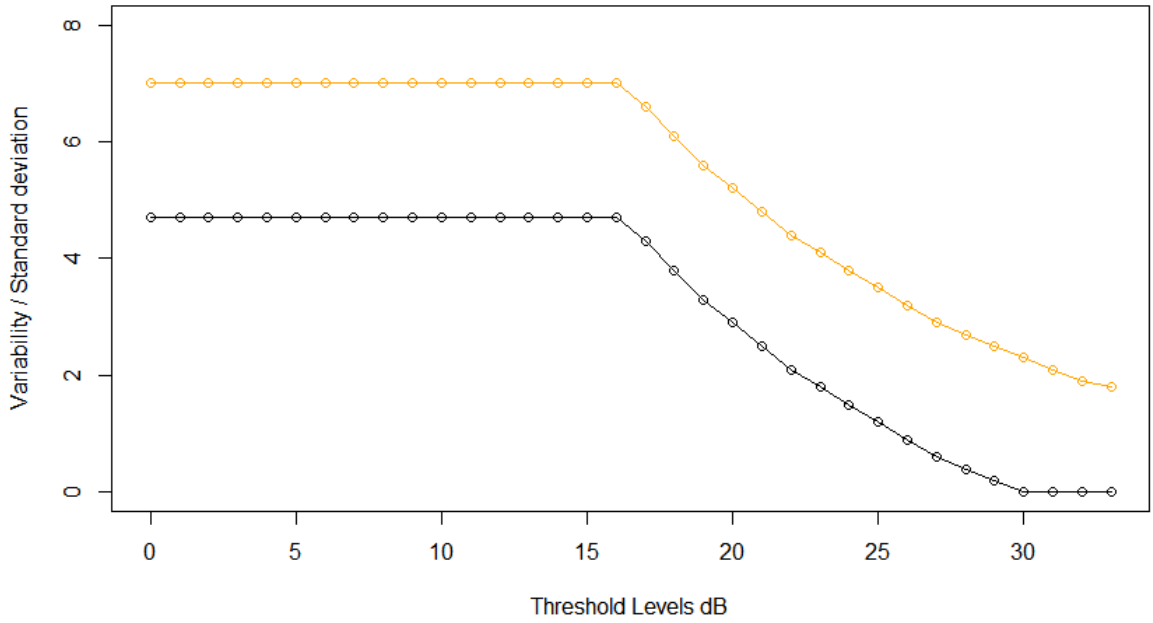

Figure 1.38: *Orange line gives the variability versus threshold derived by Henson et al [94] (modified for threshold levels below 12 dB). The black line gives the additional variability (beyond the one observed in eyes with normal sensitivity) versus threshold used in the simulation.*

1.5.4 RESULTS

Mean age of the subjects was 57.5 (±11.1) years and the male/female ratio was 1.15. In total 420 simulations were performed; 140 for each GSS2 stage 1-3. One hundred and thirty participants completed all 4 tests, 10 completed 3 while 11 were tested twice: once without and subsequently with simulated VF defects. The recruitment period lasted 2.3 months. Table 1.11 gives the sensitivity/specificity of the test for each stage of loss using 5 different cut-off

criteria. The specificity is derived from the number of trials that a positive/negative result was produced when no defects were simulated. The sensitivity is derived from the number of trials a positive/negative result was obtained when a defect was simulated.

Cut-Off	Specificity	Sensitivity		
	No Defect (n=151)	Stage 1 (n=140)	Stage 2 (n=140)	Stage 3 (n=140)
1 abnormal location	97%	82%	89%	100%
2 abnormal locations	97%	51%	80%	100%
3 abnormal locations	98%	27%	62%	100%
4 abnormal locations	98%	13%	56%	100%
5 (or more) abnormal locations	98%	9%	43%	91%

Table 1.11 - *Diagnostic values (sensitivity and specificity) of the evaluated perimetric algorithm for different cut-off values*

1.5.5 DISCUSSION

This chapter describes a new simulation methodology for deriving performance measurements of a VF test. The method attenuates the intensity of presentations according to the patterns of loss seen in real patients. It also introduces variability in the level of attenuation to match the response variability in glaucoma patients. It is effectively then a report on the use of this methodology in evaluating the performance of a new VF self-test.

Subjects were selected from those in the outpatient waiting rooms of MREH and included patients and accompanying persons. When approached the vast majority were keen to be involved and 87% of those who met the inclusion criteria completed 4 tests and provided good results. While the rapid nature of the evaluated self-test (~2 and 3.5mins without and with simulated defects respectively) clearly helped recruitment the method is suitable for all test algorithms and is likely to provide significant reductions in data collection times and costs.

The speed of data collection was aided by each subject providing up to 4 sets of data; no induced loss and 3 levels of induced loss, i.e. reducing the recruitment to 25% of that for a conventional trial. Using the same subjects in both arms of the study has the additional benefit of a perfect demographic match between the two arms. The performance characteristics of patients are also perfectly matched between the two arms. Any influence of fatigue/training on performance was minimised by randomising the order of the 3 induced defects.

The pool of subjects suitable for this method of evaluation is much greater than that for a clinical trial involving patients with established loss. Patients with early loss (GSS2 stages 1-3) are relatively rare within hospital clinics and researchers often need to review large numbers of case records to find a sufficient sample for a clinical trial. This is particularly true for very early cases (GSS2 stage 1) and yet these cases are the ones that best discriminate between test algorithms. The example used in this study included 140 trials where 10 different cases with GSS2 stage 1 defects were induced.

Large samples are important when deriving performance measures as there is considerable inter-subject variability. While some patients produce excellent VF results with good test-retest performance others are not so good. Changes in attention, error rates (FP and FN) and fixation stability can affect performance and vary from one patient to the next. When samples are small inter-subject variability is under sampled with an increased risk of result bias. While the suggested methodology matches response errors, losses of attention and fatigue/learning effects in all cohorts (i.e. normal and GSS2 Stages 1-3 VFs) and introduces appropriate response variability, it is not clear whether it fully reproduces the response behaviour from patients with true defects who may for example show increased fatigue effects.[84] Previous studies have reported on characteristics of the response variability in patients with VF defects on various threshold levels.[123, 220] For the purposes of this study, we selected the variability vs threshold curve presented by Henson et al., that was derived from measures of the psychometric function rather than test-retest performance.[94] For thresholds

below 12dB variability was held constant at the 12dB level to account for the fact that Henson et al.' s curve below 12dB is a projection beyond measured values. The ideal sensitivity of the evaluated VF test at Stage 3 cases, which are characterised by advanced defective locations, can lead to the assumption that potential errors of the projected variability barely affected the reported measures of performance.

Establishing the true extent of functional loss in an early case of glaucoma is often difficult. Repeated measures often show changes that can influence performance measures. The adoption of a technique such as the aforementioned one can utilise simulated defects whose extent of loss is precisely defined and exactly the same for all subjects. Results give a true measure of performance for any given loss that is not corrupted by temporal changes in loss. In this study a pool of ground-truth defects was generated where the estimations are based on HFA's SITA Standard 24-2 VF measurements. SITA is an adaptive sampling method which uses models of responses from glaucomatous and normal retinal locations to efficiently reduce test times. Using SITA VFs to estimate the ground-truth may optimise possible novel VF tests to meet the SITA assumptions instead of approximating the "true" VF loss which might have been missed or biased by SITA. However, SITA Standard 24-2 is the gold-standard in most clinics and has undergone numerous clinical validations and thus was considered appropriate for this study.

Simulation gives a true measure of performance rather than a comparison measure and provides a gold standard for evaluation. Trials based on patients with established loss have no such gold standard and are in effect

comparison studies. When the new test detects a defect not seen with the established test this is invariably viewed as a test failure when it may well be the result of a false negative from the comparison measure.

Defect simulation is particularly valuable when developing VF tests for children. The a priori reason behind the development of children specific tests is that the existing tests are not suitable which makes an evaluation based on a comparison with existing tests almost impossible. Performance measures of paediatric VF tests are thus often based on small samples due to the problems associated with obtaining reliable measures on established perimeters.[204, 217]

Defect simulation can also be useful in the training of eye care professionals, such as optometrists, orthoptists and technicians. Simulated VF defects can provide examples that aid the understanding of variability, the impact of cut off criteria, progression and the performance of current test procedures.

The recent introduction of the Open Perimeter Interface, which has been adopted by the Octopus 900 and the Heidelberg Edge Perimeter, enables users to install their own perimetric software.[221] The diagnostic performance of new tests using simulated defects can thus be quickly evaluated on these platforms.[222] It is likely that other perimeter manufacturers will follow this route in the future. Obtaining measures of performance from existing software, e.g. SITA, will require the cooperation of manufacturers either in providing source code or a method to read in attenuation values.

Simulations have been previously used in the development of perimetric algorithms. These invariably take the form of a simulated patient and provide the rapid measures of performance needed when establishing the impact of adjustments to the many variables involved in a VF test. These simulations use FOS data to define how a patient would respond and frequently introduce defined levels of false positive/negative responses. The results of these simulations rarely match those from clinical trials. There are many factors that influence how a patient will respond that are not sufficiently well understood to allow accurate simulation. For example, the effects of learning and fatigue, prior experience, the environment, the test instructions, the presence/absence of the perimetrist are all known to influence how a patient responds but are ill defined.[84, 223-226]

In contrast, the technique of simulating glaucomatous VF defects with the participation of healthy human subjects, overcomes many of the problems associated with patient simulations to provide a valid measure of clinical performance that is not tainted by the lack of a gold standard or demographic and learning differences between patients in the two arms. Results are likely to be more repeatable and can thus be comparable across time and location.

1.5.6 CONCLUSIONS

This chapter reports on a novel approach in simulating VF defects and involves an example of performance evaluation for a new testing algorithm, described extensively in Chapter 1.4. It focuses on describing the simulation method and discussing its potential utilisation. The results of the clinical trial undergone for the evaluation of the test's performance are only superficially presented here. Further details of the design of the clinical trial and the test's performance are given in Chapter 1.6.

The assets of this technique rely mostly on the introduced variability, based on previous literature, and the participation of healthy human subjects, therefore including the human error and factors such as fatigue, quality of instructions, learning experience and more. This study also showed the significantly reduced recruitment time (and potentially research costs) that VF simulations can offer therefore encouraging more clinical trials.

1.6 Development and Performance Evaluation of a Self-Administered/Assisted Visual Field Screening Tool for Glaucoma

Contributions

As previously mentioned I was deeply involved in the design and development of the VF test whose diagnostic performance was evaluated and the outcomes are extensively presented in this chapter. For the purposes of this study an appropriate Graphics User Interface (GUI) was developed to accommodate the testing. The aforementioned GUI was also built with Java.

The performance evaluation of the software was performed at MREH where patients and carers from the eye clinics were recruited in this study. My contribution involved data collection and analysis, although great help for recruitment was provided by the clinicians of the MREH.

Presentations / Publications

This research has been presented orally in conferences and meetings, such as the ARVO 2016 meeting in Seattle WA, USA and the IPS meeting 2016 in Udine, Italy and also smaller meetings at MREH (e.g. Manchester Optometry Meeting) or the University of Manchester.

1.6.1 ABSTRACT

Purpose: The risk of future visual impairment from chronic open angle glaucoma increases with late presentation. Due to the asymptomatic nature during the early stages of this disease early detection only occurs through screening, normally carried out by optometrists. Those not seeking optometric care are more likely to present late and are at greater risk of future visual impairment. New approaches to glaucoma screening are needed; one such approach is the development and distribution of a self-administered VF test that can run on a wide range of personal computers. Early work led to the development of such a test whose diagnostic performance is evaluated in this chapter.

Methods: The right eye of 140 normal patients (no VF loss) was tested 4 times; once without a simulated defect and with 3 different simulated glaucoma defects; as described previously. During analysis estimates of sensitivity, specificity and positive and negative predictive value were calculated at different cut-off criteria. Testing times and number of presentations were also noted. Patients followed the written instructions on the screen including a demonstration trial. The number of cases which required extra help and demonstration by the researcher (i.e. the author) was also recorded.

Results: All patients completed the self-administered tests with little, if any, help from the researcher. The sensitivity and specificity of the new test on detecting glaucomatous Stage 1 defects were 93.5 and 97.1% respectively with 1 missed location as cut-off criteria. For stages 2 and 3 the sensitivities

were 97.8 and 99.2% with specificities of 97.1%. Median testing time was ~155 seconds per test (i.e. ~2.5 minutes – IQR 41.5 seconds).

Conclusions: The newly developed self-administered screening test was well received by patients and was shown to have high discriminatory power at relatively short testing times.

1.6.2 INTRODUCTION

Despite its prevalence and its risk for causing irreversible blindness, glaucomatous optic neuropathy has remarkably low detection rates. Studies have shown that approximately half of those affected with this pathology are unaware of it; with detection rates ranging from 10% to as high as 75%.[143-145, 227] The asymptomatic nature of OAG, the most prevalent of all glaucomatous types, at its early stages could be blamed for the high percentage of patients presenting late with advanced glaucomatous VF defects.[37]

Considering the above information, population screening for OAG sounds essential. However, a review from the US Preventive Service Task Force found insufficient evidence to assess the balance of benefits and harms for OAG population screening while Burr et al. in a similar review found population screening not to be cost-effective.[154, 228, 229] They did recommend though the screening of high-risk groups, such as those with family history or those of African descent, and they highlighted that detection of glaucoma can improve by refining the current practices or introducing a technology-based first assessment; the latter being the most cost-effective option.

There is increasing evidence showing that current technology in PC monitors, laptops and tablets is adequate enough to offer high spatial resolution and good dynamic range of luminance.[193, 203, 212, 218] Hence, these devices can be considered good candidates as reliable vision

testing tools, mainly due to their portability and their low cost. The usefulness of such portable devices has been reported in several studies and in assessments, such as visual acuity and contrast and macular sensitivity.[188-191, 230] In the last 5 years a number of devices and software have been developed for the assessment of the VF away from a clinical setting that could also potentially be performed without the supervision of a trained eye care professional. These include head mounted displays and computer- or tablet-based devices.[218, 230-232] Some of these devices were reviewed for their user-friendliness in a previous chapter; although only few have reported diagnostic measurements.

The online version of Damato Multifixation Campimetry (DMC) has been available since the early 2000's (according to the website), however it was only recently that its diagnostic performance for detecting glaucomatous defects was determined. Olsen et al. investigated the sensitivity and specificity of all three versions of DMC (see previous chapter for details) and concluded that the most promising test algorithm was two successive tests from DMC's Standard version. While this algorithm achieved specificity of 98.1% (high specificity being a requirement for a screening test) the reported sensitivity was 71.4% for moderate glaucomatous VF defects (classified by the GSS2 classification system) and only 11.8% for mild cases.[195]

Another online perimetric system is Peristat, which has also been included in the usability evaluation of the initial stages of this research. Peristat's diagnostic performance was measured in a pilot study which reported that for moderate and severe glaucomatous defects sensitivity ranges between 84-86% and specificity is approximately 94-97%, when compared to HFA

results.[197] A more extensive study by Lowry et al. included mild glaucoma cases and introduced three masked graders to subjectively evaluate correlations between Peristat and HFA. Their report presented sensitivity and specificity similar to the previous pilot study diagnostic performance for moderate and advanced glaucoma cases. However, for mild defects the sensitivity drops to 54-59% (depending on cut-off criteria).[233]

A tablet perimeter application developed for the iPad platform, named Melbourne Rapid Fields (MRF), is the most recent evaluated perimetric portable system. In brief, MRF tests 66 locations in a radial pattern in the central 30° of field for potential sensitivity loss. The application attempts threshold estimation in 7 discrete steps over a range of 0-30dB with a three-presentation protocol and a modified ZEST procedure. Kong et al. reported on the correlation between outcomes from the MRF and the HFA and provided evidence of high concordance between the two systems, which decreases for mild VF defects.[218] Nonetheless, their study is another strong piece of evidence that portable and out-of-clinic perimetry with tablets, PCs or laptops may provide adequate assessment of the VF.

This chapter will describe the outcomes of the in-house (i.e. MREH) performance evaluation of the new VF self-test described in earlier chapters. The diagnostic performance of the VF test was established on a control population with and without simulated glaucomatous defects in order to derive the new software's sensitivity and specificity respectively

1.6.3 METHODS

Study population and sample size

. The technique of simulating defects has been extensively described in Chapter 1.5. The database of VF defects used for the simulation process comprised of mild and moderate OAG cases; GSS2 stages 1-3, with 10 cases per stage.

Sample size calculations were based on previously described methods of sampling for diagnostic tests.[234] The targeted specificity and sensitivity were set at 97±3% and 92±4% respectively. The appropriate calculations revealed a sample size of 124 eyes per GSS2 stage (i.e. stage 0-normal, stages 1&2-early, stage 3-moderate) to achieve the target specificity and 176 eyes per GSS2 stage for the target sensitivity. The final sample size target was set at 140 normal eyes, and subsequently 140 simulations per stage; therefore, achieving a slightly less than 3% margin of error for the specificity estimates and slightly bigger error margin than the targeted 4% for the sensitivity estimates.

Participants were recruited from the glaucoma outpatient clinics at MREH. Some were patients with no documented VF loss while the majority were accompanying persons. For those with no previous VF records the results of the new test under evaluation (without simulated defect) were used as inclusion criteria. If the participant passed the test the eye would be considered normal and the tests with simulated defects would follow. If the

participant failed the test a 24-2 SITA-Standard with the HFA would be suggested to the patient to derive whether the result was a true or false positive. The study was approved by the local ethical committee and followed the tenants of the Declaration of Helsinki. All subjects provided written informed consent.

Data collection and analysis

Each testing session would create and save a file with important information about the test. This file included:

- Testing time
- Information for every tested location, such as number of missed and seen presentations, number of presentations (i.e. 3-5), location status: normal or defective.
- Total number of presentations

Data were collected and analysed to generate ROC curves for each stage of loss and derive sensitivity and specificity with different cut-off criteria along with positive and negative predictive values. Average testing time and average number of presentations were also estimated. The number of participants unable to complete the test and those who needed extensive help to understand and perform the test were noted.

1.6.4 RESULTS

One-hundred and seventy-two individuals were approached and invited to participate in this study. The total number of recruited participants was 153; all of them volunteers from the outpatient clinics of MREH. Sixty-eight of those (44%) were attending their clinic appointments while the rest were relatives/carers. All of them were approached while waiting at the MREH's clinics. The 68 patients were previously identified by the author or other clinicians after a review of their VF records ensuring that no VF loss was present. One hundred and thirty participants completed all 4 tests, 10 completed 3, while 11 were tested twice: once without and subsequently with simulated VF defects; hence, totalling for 151 normal cases and 140 simulated cases for GSS2 stages 1-3. Recruitment lasted less than 2.5 months.

Two participants failed the new VF test during the no simulations phase. As there were no previous VF records to establish the status of their VF, and subsequently confirm whether the test results were true or false positives, the subjects were invited to undergo additional perimetric testing. One of the two excluded subjects agreed. SITA-Standard examination with the 24-2 testing pattern revealed a superior VF defect that the subject was not aware of which resulted in a referral to the glaucoma clinic.

The ROC curves for GSS2 stages 1 and 2 are given in Figure 1.39. Sensitivity was found to be ~82% and ~89% for the two stages respectively with specificity at 97% with an optimal cut-off point of 1 missed location.

Stage 3 defects resulted in very high sensitivity and specificity estimates and were not therefore subjected to an ROC plot. Details of the diagnostic measured of all disease severities are given in Table 1.12.

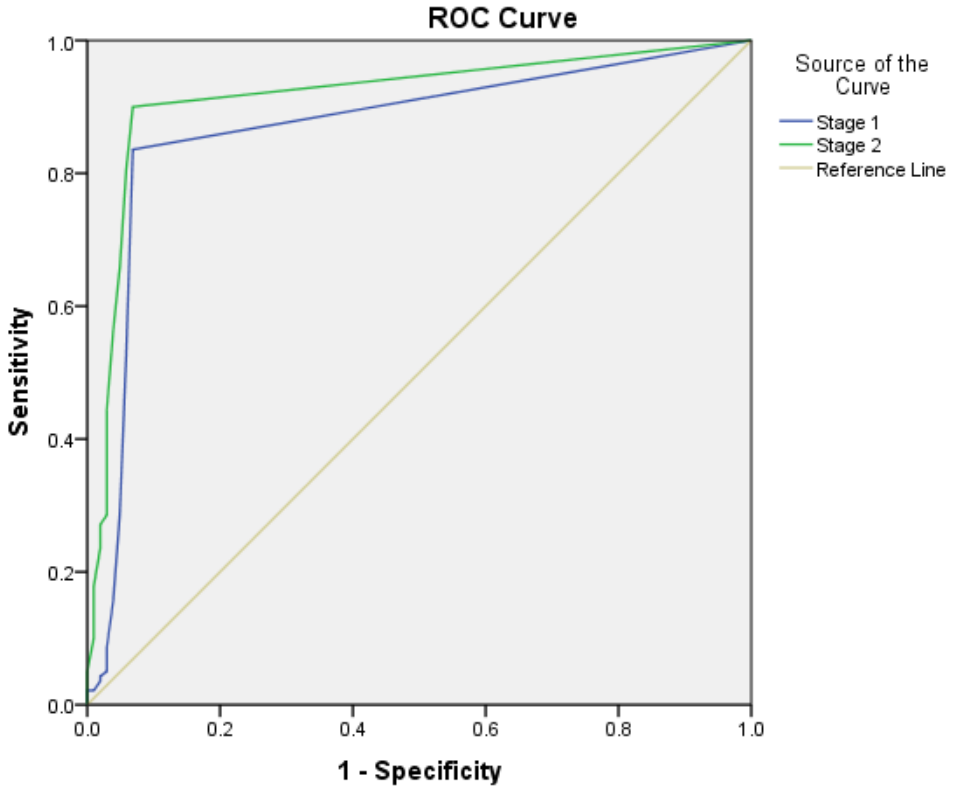

Figure 1.39: *ROC curves of the evaluated visual field test for GSS2 stages 1 (blue line) and 2 (green line). Optimal diagnostic performance was reported for a cut-off point of 1 location missed 3 times.*

	GSS2 Stage 1	GSS2 Stage 2	GSS2 Stage 3	All Stages
Sensitivity	0.82	0.89	1	0.91
Specificity	0.97	0.97	0.97	0.97

Area-Under-Curve (St. Error)	0.87 (0.26)	0.92 (0.20)	N/A	
Positive Predictive Value (PPV)	0.96	0.97	0.97	0.99
Negative Predictive Value (NPV)	0.88	0.91	1.00	0.81
Likelihood Ratio (LR)	30.7	33.7	37.75	34.3

Table 1.12: *Diagnostic measures of the evaluated visual field test for mild (stages 1 and 2) and moderate (stage 3) OAG cases. The cut-off criterion was set at 1 missed location.*

The number of cases, stratified according to the number of missed locations and GSS2 stage is given in Figure 1.40. In total 41 simulated cases passed the test (indicating false negatives), 26 of which derived from GSS2 Stage 1. Further investigation of the simulated cases that were not detected showed that case#1 and case#3 from Stage 1 and Stage 2 pools respectively failed detection most of the time. More specifically, the Stage 1 simulated case was detected 3 times only out of 14 while the Stage 2 case was missed 13 out of 14 times. Both of them were characterised by shallow defects, as shown in Figure 1.41 with sensitivity thresholds on a greyscale map for both examples.

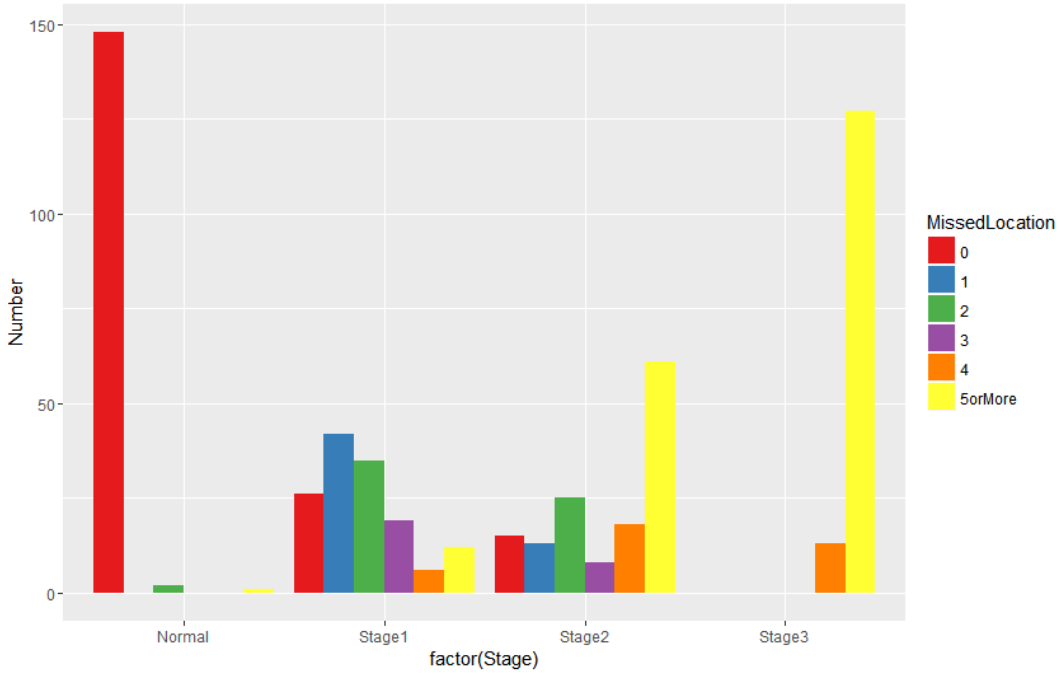

Figure 1.40: *Distribution of number of cases according to the number of missed test locations and stratified by visual field severity.*

			x	23	22	x		
		24	x	25	x	24	23	
	x	x	x	x	x	x	25	22
24	25	x	x	x	30	x	x	27
22	26	28	x	x	x	x	x	x
	x	x	29	x	x	x	x	28
		26	x	29	x	x	27	
			x	x	x	x		

			x	29	26	x		
		24	x	28	x	28	25	
	x	x	x	x	x	x	28	29
27	28	x	x	x	29	x	x	27
27	27	28	x	x	x	x	x	x
	x	x	28	x	x	x	x	25
		24	x	26	x	x	24	
			x	x	x	x		

Figure 1.41: *Sensitivity thresholds and greyscale representation of the 2 simulated cases (upper: Stage 1, lower: Stage 2) that the visual field test failed to detect most of the time*

The boxplot in Figure 1.42 shows the distribution of the number of total presentations for cases with and without simulated defects. The average number among the 3 different stages was found to be similar, with 63 presentations for Stage 1 and 63.7 and 64.0 for Stages 2 and 3 respectively. The reported inter-quartile range in Stage 3 is shown to be smaller than Stage 2 indicating better consistent around the median. The reason behind this is possibly the higher number of test locations with advanced defects in the last simulated stage. Therefore the termination criterion of the multisampling technique would be fulfilled faster than in cases comprised of locations with shallower defects; or in simple words more test locations would be missed 3 times out of 3 presentations in Stage 3 cases.

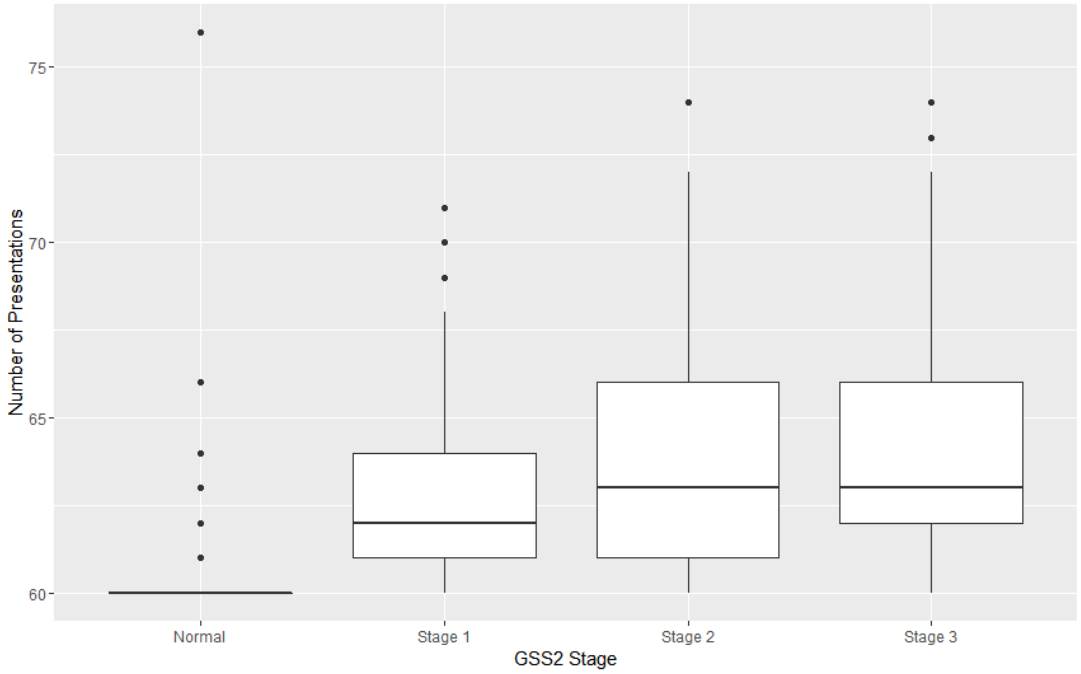

Figure 1.42: *Boxplot of distributions for the total number of presentations across the 4 different groups.*

Test times were ~2.5 mins for non-simulated trials with an extra minute for cases with simulated defects. Figure 1.43 shows a boxplot of the distribution of testing times in seconds across the different groups. It is not a surprise that testing times for Stage 3 present smaller variations around the median of 186 seconds, in a similar way that total number of presentations was previously described. It is worth mentioning that testing time was evaluated with an internal timer that was set up in Java along with the VF test. The timer would start at first presentation and was programmed to stop after the test window closes; the latter required one last action (i.e. key stroke or mouse click) from the user to acknowledge that the test was finished. There were cases where participants did not immediately perform this last action

and would rather engage in conversation about their testing experience. As a result there are outliers in the dataset of time records that do not represent actual true test times. For this reason, statistical measures, e.g. the median and the inter-quartile range, were considered to be more appropriate than mean values as measures of test times. Table 1.13 provides descriptive statistical measures of test times across the 4 groups, while table 1.14 shows the number of cases for every recorded missed location and total number of presentations, separated in each GSS2 group.

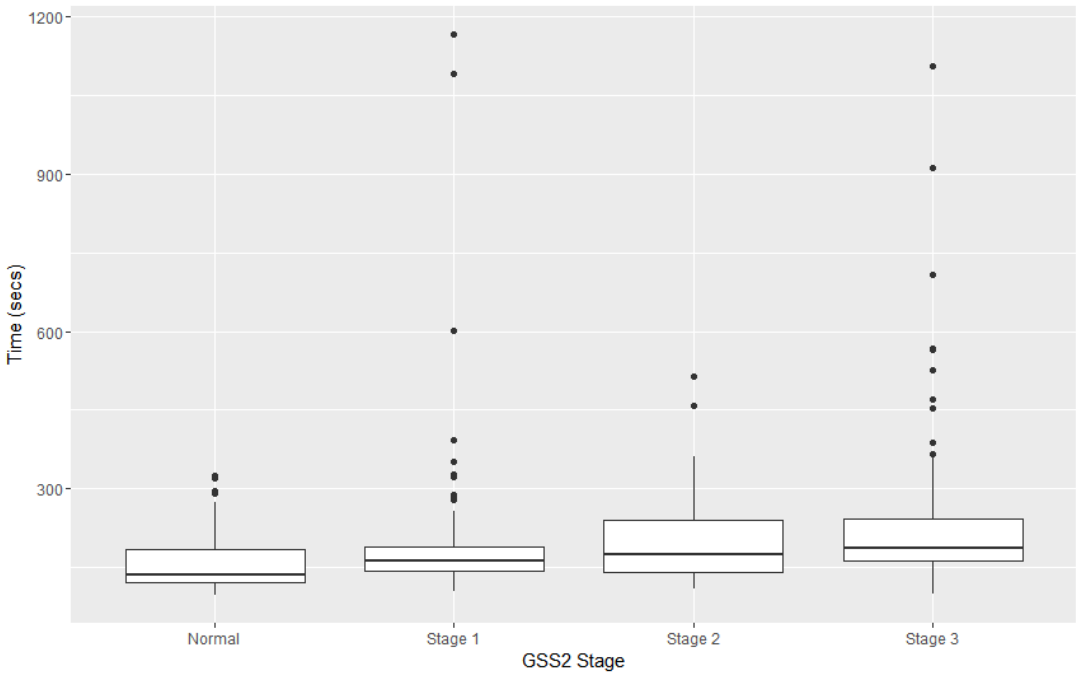

Figure 1.43: *Boxplot representation of the testing time distributions across the 4 groups*

	Mean	SD	Median	IQR
Normal	156.6	52.3	135.5	61.5
Stage 1	194.4	143.1	161.0	47.0
Stage 2	196.6	74.7	173.5	99.5
Stage 3	229.2	134.6	186.0	80.0

Table 1.13: *Descriptive statistics of timing tests across all GSS2 groups. All values are in seconds.*

	Total number of missed locations per test																	
	0	**1**	**2**	**3**	**4**	**5**	**6**	**7**	**8**	**9**	**10**	**11**	**12**	**13**	**14**	**15**	**16**	**17**
Normal	147	1	2	0	0	1	0	0	0	0	0	0	0	0	0	0	0	0
Stage 1	26	42	35	19	6	4	1	1	1	0	1	1	0	0	1	2	0	0
Stage 2	15	13	25	8	18	16	1	5	9	11	9	2	1	1	1	2	2	1
Stage 3	0	0	0	0	13	28	18	16	27	14	7	5	9	1	1	1	0	0

	Total number of presentations per test															
	60	**61**	**62**	**63**	**64**	**65**	**66**	**67**	**68**	**69**	**70**	**71**	**72**	**73**	**74**	**76**
Normal	123	5	6	2	2	0	1	0	0	0	0	0	0	0	0	1
Stage 1	21	22	27	21	16	11	9	3	4	1	3	2	0	0	0	0
Stage 2	30	14	22	12	15	7	9	9	8	6	5	0	2	0	1	0
Stage 3	13	13	25	25	16	13	9	8	6	5	2	2	1	1	1	0

Table 1.14: *Detailed information of the distribution of tests according to missed locations (upper table) and the total number of presentations (lower table)*

1.6.5 DISCUSSION

A number of studies have shown that recent technological advancements in the spatial resolution of monitors in portable devices, such as laptops and tablets, is adequate for certain visual tests.[193, 203, 230] Considering the high picture quality, the portability and affordability, such devices could potentially be used for the assessment of the VF. They may still have a number of shortcomings compared to traditional VF testing devices (e.g. a smaller dynamic range of stimulus intensity) but recently developed perimetric techniques and special software design features could overcome some of these limitations. In previous chapters, a number of online VF tests have been described and the approach of other researchers/designers on how to overcome those deficiencies has been presented.

In this project a new approach for computer-based VF self-assessment has been proposed with a design objective of increasing uptake and reducing the number of late presenters. The new VF self-test utilises perimetric techniques that provide high diagnostic performance with short test times. The new test takes into account the outcomes of usability trials and implements design features that are favoured by users.

An in-hospital diagnostic assessment for the aforementioned VF test took place at MREH. Using a defect simulation technique, the study asked participants to perform the new test between 2 to 4 times to derive diagnostic measures. The reported sensitivity and specificity was found to be at 82% and 97% respectively for cases with mild VF defects (i.e. GSS2 Stage 1)

while for Stage 2 the sensitivity increased to 89%. All simulated cases of moderate Stage 3 VF defects were detected successfully. Overall sensitivity was estimated at 91% for the detection of all simulated glaucomatous defects.

High specificity (low false positive rate) is a prerequisite for a successful screening test as a large number of cases falsely labelled as abnormal would increase the burden of the already overcrowded eye care facilities.[235] The investigated test design mistakenly returned a positive result for only 4 cases out of a total of 151 tested volunteers. The supra-threshold testing approach at ~10dB (variations of 1.5dB across the monitor were reported in a previous chapter) is most likely responsible for this; the presented stimuli were fairly easy to see with a non-pathologic eye. Particular attention should be given to one case that returned a false positive result with 5 missed locations. Review of the participant's previous VF records showed no signs of VF loss. It is believed that this particular user struggled to understand and perform the test, possibly for the first few rounds of presentations. It is quite possible that should the user have been given the chance to run the test again with no simulated defects they might have returned a negative result; hence increasing specificity even further. Therefore repeating the test is likely to decrease further false-positive numbers.

The reported sensitivity measures for the evaluated test were higher than those described in studies of other online VF tests. Lowry et al. evaluated the Peristat system and reported sensitivity between 54% and 59%, depending on cut-off criteria.[233] Their sample size included 63 participants with glaucoma; 35 were considered to have mild glaucomatous defects.

Excluding those 35 mild cases the sensitivity increased between 70% and 85% according to their cut-off points. The evaluation of the online Damato Multifixation Campimeter by Olsen et al. offers possibly the best direct comparison, as the authors also stratify their sample according to the GSS2 classification system.[195] Sensitivity for the most promising testing algorithm (i.e. the Standard version) was found to be as low as 12% for Stage 1 eyes rising to 71% for Stage 2 defects; however their sample is relatively small with 17 and 14 eyes for the two groups respectively. While detection of moderate Stage 3 defects proved to be an easy task for the new VF self-test the fairly low number of false negatives for both mild glaucomatous Stages 1&2 is undoubtedly a noteworthy outcome. The combination of a multisampling technique, as presented by Artes et al.,[126] with the optimal subset of the 24-2 pattern, described by Wang et al.,[103] could account for the high discriminatory power of the new test.

A potentially better measure of performance is the likelihood ratio, which can highlight its potential utility. The likelihood ratio is basically the ratio of two probabilities: the one that the test result is correct to the probability that the result is incorrect. The main advantage of this performance measure is its low dependency (if any) upon the disease prevalence. The value of the likelihood ratio for the new VF self-test was found to be ~31 for mild Stage 1 cases and ~34 overall; with values further away from 1 indicating an increasing utility of the test as it increases the probability of a diagnosis. A comparison of reported likelihood ratios between other self-administered VF tests and the proposed design showed a significant advantage of the latter in cases with early glaucomatous defects. Evaluation of the Peristat system

showed likelihood ratios ranging from 5.7 to 11.8, depending on inclusion criteria.[233] For the group of participants that also included mild cases the likelihood ratio was found to be 8.4. Olsen et al.'s study on Damato Multifixation Campimeter does not directly report on likelihood ratios but these are easy to estimate from the reported sensitivities and specificities across the different GSS2 stages.[195] So for Stage 1 cases DMC's likelihood ratio is 6.2 while this value increases to 34 when all evaluated cases (i.e. across the GSS2 spectrum) are included. Table 1.15 provides a list of likelihood ratios for glaucoma detection related to the most common clinical assessments of structure and function estimated according to previous studies.[236-240] It is worth noting here that the accuracy of a likelihood ratio fully depends upon the quality of a study.

	LR^+
SLP[237]	5.0
OCT (Average RNFL)[236-240]	9.8 – 15.0
OCT (Inferior RNFL)[213, 236-238, 240]	10.4 – 15.2
OCT (Average GCIPL)[239]	13
OCT (C/D Ratio)[236]	16.2
SWAP[237]	5.4
FDT[237]	7.6
HFA (PSD)[236]	16.4
Octopus (MD)[236]	16.0

Table 1.15: *List of positive likelihood ratios (LR^+) for other diagnostic tests according to previous studies. SLP: Scanning Laser Polarimetry, RNFL: Retinal Nerve Fibre Layer, GCIPL: Ganglion Cell Inner Plexiform Layer, C/D: Cup/Disc, SWAP: Short-Wavelength Automated Perimetry, FDT: Frequency-Doubling Technology, HFA (PSD): Humphrey Field Analyzer (Pattern Standard Deviation), MD: Mean Deviation*

It is likely that the performance measures reported in this study were influenced by several factors. The test was conducted within a hospital consulting room where the testing environment was well-controlled rather than at home, e.g. room light dimmed, reflection free screen. A perimetric expert (i.e. the author) was always present; although input was kept to the minimum, see below. Research has shown that ambient light can have an

impact upon target luminance and consequently on a test's performance.[212] It is unknown from studies that involve the evaluation of home-monitoring tests whether users fully complied with the test environment instructions; compliance was simply measured by whether participants performed the test or not at the required time intervals.[241]

Another factor to the performance measures is the use of a single, well characterised laptop computer. It is unknown what levels of luminance the test would produce on different devices and how this would impact on performance. If, for example, the contrast of the presented stimuli was lowered to what extent would this impact upon specificity. Studies evaluating target luminance levels on different devices have concluded that there are indeed differences in luminance values across devices but contrast ranges are quite similar. In one particular study, that from Tahir et al., the authors acknowledge that a test designed for screening purposes would not necessary require contrast-improvement techniques, although they do recommend their screen calibration protocol to be incorporated in screening tools.[203] The monitor utilised in this study was not modified to produce uniform luminance as the study tested the hypothesis that test performance would be adequate for screening purposes even with an uncalibrated screen. Indeed, the proposed VF test does not intend to measure contrast thresholds but has rather been designed as a simple fast screening tool suitable for use in high-risk groups.

The simulation technique used to evaluate the test performance might also have had an impact; more specifically, the pool of simulated defects, which comprised of 10 cases per GSS2 stage. Although one might consider this

database small it covers a wide range of typical glaucomatous defects, from nasal steps to arcuate defects and paracentral scotomas of various depths. Two cases (one per each mild GSS2 stage) with shallow defects failed to be detected most of the time.

It is noteworthy that the new VF self-test achieved relatively short testing times. When test configuration was set for assessing normal eyes, the median duration was slightly more than ~2 minutes. As expected, testing time increased when simulating defects with median duration for moderate Stage 3 cases being ~3 minutes. Olsen et al.'s research on the evaluation of online Damato Multifixation Campimeter as a glaucoma detection tool is the only study that could readily be used for direct comparison with the outcomes of this study.[195] The authors report on testing duration of approximately half a minute shorter that those presented in this chapter; that is for the Standard version of the test which not only presented the shortest times against the other versions but is also recommended for its performance. The different design approaches of the two tests undoubtedly had an impact upon test times. Online Damato Multifixation Campimeter tests a higher number of locations compared to the proposed VF self-test, however it only tests them once rather than 3 times. Nonetheless, test times of between 2-3 minutes are acceptable to most patients and are unlikely to be influenced by losses of attention which have been reported to occur with SAP after about 3 minutes.[242]

One of the main strengths of the proposed test design is the implementation of features identified in the previously described usability trial. The advantage of the application of favoured features such as the instruction format, method

of testing, feedback techniques etc., was demonstrated by the response of this study's participants and the fact that all of them completed the test successfully at least once. It is worth noting that the presence of the researcher (i.e. the author) in the examination room during the study was limited to informing the participants about the study and to receive their consent for participation. The cases that required further explanation on the method of testing were minimal; in fact only 8 cases were prompted to go through the written instructions again[1]. The opportunity given to the users to have a practice session prior to actual testing is likely to have had an impact on completion rates. The experience of the cohort on VF testing prior to recruitment was mixed. The majority of recruited participants were MREH patients and had experience of VF tests. However, many were volunteers/carers of patients with no prior perimetric experience. Nonetheless, multiple stimuli presentation and changes in the position of the fixation target were test features that were new to nearly all participants.

[1] Data not shown. This statement derives from personal records

1.7 Research Impact and Potential

Current Research

This section describes a series of studies, the product of which was the development of a new VF self-test for enhanced case-finding of patients with glaucomatous VF defects. The series starts with the identification of a clinical need and the development of a research question through the preliminary search for existing information to the design and evaluation of a new resource with the view of meeting the above-mentioned clinical need. Indeed, the first chapter of the section retrospectively investigates data from a large VF database to establish rates of glaucomatous VF progression in patient cohorts of different levels of VF loss. The reported outcome was that patients' VFs progress relatively slow; and that a significantly number with advanced disease present late. Hence, the issue for cases with advanced glaucoma does not rely entirely on clinical management but rather on late detection.

The results of that study effectively set the research question: what can be done to reduce the number of undetected cases. A review of current literature showed that population screening for glaucoma may not be cost-effective; however, focusing resources on high-risk groups (such as relatives of diagnosed patients, communities with members of African descent etc.) and especially with a technology-based assessment could help to reduce the cost for screening. In addition, research on the capability of

modern portable devices, such as laptops and tablets, to assess visual function has shown that it is possible to program such devices to return robust and efficient VF results.

The design of a new computer-based VF self-test for glaucoma screening purposes that could potentially reduce the high numbers of undetected cases became the focus of this research process. Initially, VF self-tests that were available online went through a usability evaluation with the participation of both perimetric experts and volunteers with mixed perimetric experience to identify favourable test and design features. It was crucial that the proposed test would be fast and easy to perform and would not produce high numbers of false-positives (an essential requirement for a screening test) while it would efficiently detect most cases with mild VF defects.

The evaluation of the aforementioned test proposal was performed by means of VF defect simulation; a technique, by-product of the research process, that proved to be efficient and cost-effective as it considerably reduced recruitment times. Undertaken in a well-controlled testing environment, the performance evaluation study revealed remarkable measures of sensitivity and specificity, especially for the detection of mild VF losses. In addition, test times were relatively short while the new test itself was deemed to be user-friendly- high completion rates

The research process mainly focused on two aspects: 1) the consideration of high usability during the design of the test and 2) the simulation technique used for the evaluation of the new test's capability to detect glaucomatous VF loss. To the best of the author's knowledge, none of the currently

available VF self-tests, and possibly most of the ophthalmological examination techniques whether these are performed at a clinical setting or from home, have taken into account patients' preference during their design. Especially for systems designed to be self-administered it is important to identify favourable testing and design features and adopt them to ensure users would, first of all, be encouraged to perform and complete the test. The research procedure described prioritised usability throughout the design process and the evaluation study provided encouraging, albeit uncertain, evidence that this approach is appreciated.

The benefits of simulating VF defects for performance evaluation of newly developed test designs have been described thoroughly both in this section (Chapter 1.5) and in literature. The main advantage of the methodology proposed in this thesis is the process of introducing variability to the simulated defect. Patients' threshold variability is dependent upon sensitivity as has been established in many published studies. The proposed methodology utilised a software algorithm to match the known relationship between variability and sensitivity in eyes with simulated loss. In addition, real normal eyes/patients were recruited, instead of simulated patients, to account for factors, such as fatigue, learning ability or response errors.

The overall outcome of the presented research is a new VF test designed for modern portable devices (i.e. PCs, laptops, tablets) that could be utilised for glaucoma screening purposes. The affordability, portability and, most importantly, the capability of these devices to assess visual function outside clinical settings could potentially reduce clinical costs and satisfy unmet

clinical needs, as strong evidence from this (and other published) research suggests.

Future Research

Research invariably raises more questions than it answers. Further research is needed to establish if the test performs equally well in other devices and on different screens. What impact does an uncontrolled testing environment have on its performance? How many people would agree to perform this test from home and what is their compliance? Can this test be modified to encourage home-monitoring and what would be the benefits?

A community-based evaluation of the proposed test could potentially provide an answer for most of those research questions. Recently diagnosed patients could be invited to take the new self-test home and use it to screen relatives (high risk group). Those failing the test would be invited to visit a designated clinician, whether that would be at the Eye Hospital or a community optometrist, for further examination. Other aspects that could potentially be investigated are take-up rates from the invited participants, test completion rates from those performing the test, further usability evaluation of the test and others.

However, there are a number of issues arising upon designing a community clinical trial like the one described above. First of all, the developed software would need to adapt to the different devices that participants possess, while maintaining core testing parameters. For example, physical characteristics of

a monitor, such as screen dimensions, need to be taken into account in order to estimate appropriate testing distance (i.e. the smaller the screen the closer the distance) and modify stimuli sizes accordingly. Another important issue is the transfer of patient data from home to the hospital while ensuring patient confidentiality. While various attempts were made to resolve those issues, it was soon very clear that advanced programming skills, time and other resources (i.e. financial, ethical approval for data transfer etc.) were required to prepare and conduct such a clinical trial; aspects that could not be satisfied during this postgraduate program's timeline.

There is undoubtedly room for improvement in the test design. For example, changes in the testing pattern may yield even better performance measures. There is increased evidence highlighting the importance of evaluating the VF in the central 10°. The current testing pattern includes only 1 location in that region. It would therefore be tempting to modify the testing pattern to include more central points; even by compromising some of the peripheral locations.

Another aspect of the test design that could be modified is the reverting to single-stimulus presentations towards the end of the test. That would occur in cases were all the sets of stimuli have been tested and termination criteria (i.e. 3 seen or 3 missed) have not been met. In cases where more than 2 locations required further testing, single-stimulus presentations significantly increased testing durations. The testing algorithm could be modified to create sets of stimuli (from the remaining locations) and continue with the multiple-stimuli testing approach.

The software also has the potential to be modified for assessment of contrast thresholds for the test locations. However, this would require better control of luminance levels from the utilised monitor. Tablet devices, such as Apple's iPad, Samsung's Galaxy Tab and others, could be exploited and their displays could be calibrated accordingly to serve as tangent perimeters, as studies have shown and has previously been described. Indeed, Kong et al. have recently shown that the Melbourne Rapid Fields application for iPads has strong correlation to the HFA results and a test-retest reliability that is comparable to conventional perimetry.[218]

The feasibility of home-monitoring has been recently shown by the AREDS2-HOME study research group.[241] The investigators separated participants in two cohorts: the 'device arm' which involved a home telemonitoring device plus the standard care visits versus standard care alone. They concluded that detection rates were significantly higher for the home device strategy compared to the prescheduled office visits. In glaucoma, studies have shown that a higher number of VF tests than the one currently provided by standard care is needed to estimate field progression in a reliable manner. Chauhan et al. have suggested six VF tests in a period of two years; a recommendation that official guidelines quickly adopted.[176] Crabb et al. proposed a modified approach where testing is clustered at baseline and at the end of the two-year period.[243] Increased frequency of testing is the crucial point that both approaches make but despite the strong evidence of the benefits current management limits the frequency to approximately 3 times in the first 2 years post diagnosis, with some cases reporting that 10 years were needed to achieve the recommended number of

6 VF tests. Anderson et al. used computer simulations to show that home-monitoring, despite its imperfect compliance and variability, improves detection of rapid progression in glaucoma.[244]

It is therefore apparent that future research will focus on the exploitation of portable devices in an attempt to bring testing out of clinical settings and into patients' homes. Such an approach will not only benefit unmet clinical needs (disease detection, diagnosis or management) but also reduce clinical costs.

Section 2

Novel Developments in Ocular Coherence Tomography:

Introducing Ocular Coherence Tomography Angiography

2.1 Ocular Coherence Tomography Angiography: the most recent Advancement of Retinal Imaging – a Technology Review

Medicine has long been benefited by the establishment of tomographic imaging techniques like ultrasound imaging, X-ray computer tomography or magnetic resonance imaging. In ophthalmology, the introduction of OCT by Huang et al. in the early 1990s had a significant clinical impact as it offered cross-sectional imaging of internal structures of the eye in a non-invasive way.[53] With continuous advancements in its technology and accessibility in extensive clinical databases, OCT has now an important role in the diagnosis and management of a variety of ocular pathologies, like retinal disorders (such as AMD, DR, macular holes etc), neurodegenerative diseases (e.g. glaucoma) and uveitis or tumours.[245]

The principle of OCT imaging is similar to ultrasonography, except that OCT measures light rather than acoustic waves reflected from tissue boundaries. Its operation is based on a technique known as Michelson low coherence interferometry; this is merely the measurements of echo delay and intensity of backscattered light from tissue microstructures.[246] The interference is measured by a photodetector (shown in the schematic example of Figure 2.1) and processed into a signal. The result is two- or three-dimensional cross-sectional tomographic images of optical reflectivity.

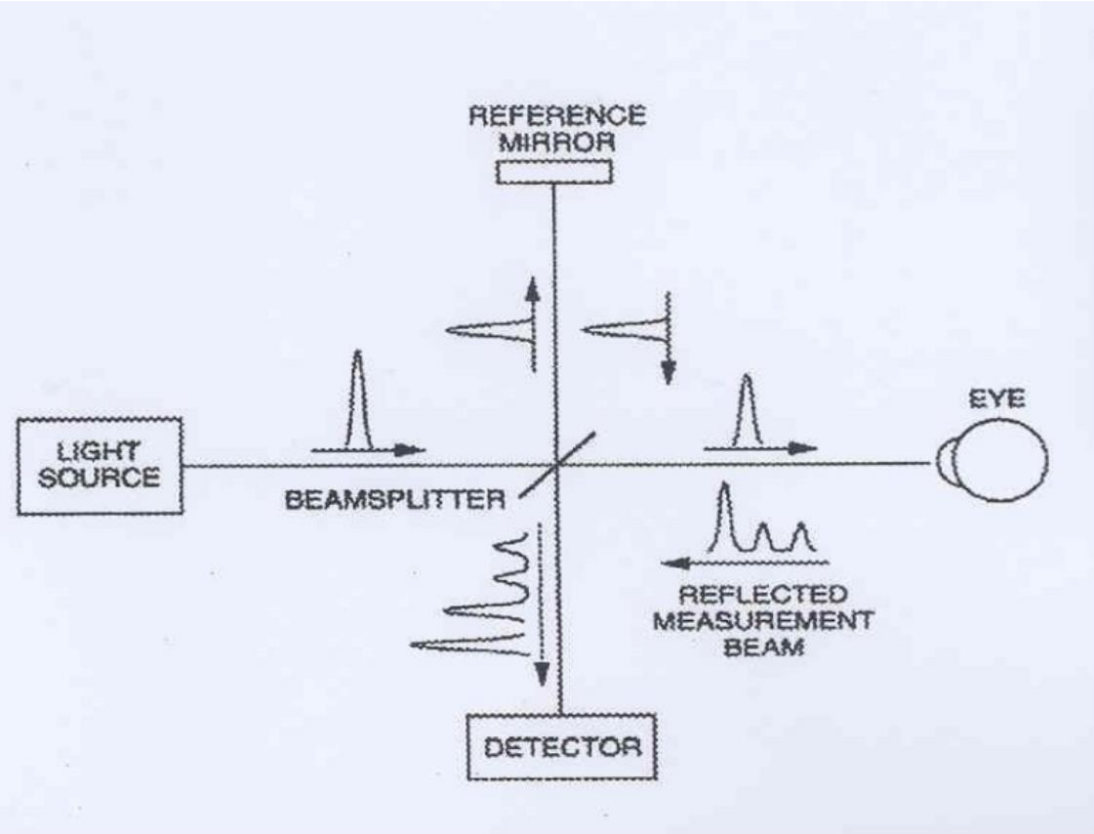

Figure 2.1: *Schematic of the basic principal technique of OCT*

TD-OCT is the oldest type of OCT technology and it is limited by the need for the reference mirror to move in order to match the delays from the various layers of the sample. The fastest TD-OCT scanners can measure 17,000 A-scans per second. These one-dimensional measurements are then combined to create the cross-sectional view of the retina at a given location (also known as a B-scan).[247]

While TD-OCT impressed ophthalmologists and retina specialists it was soon left in the shade as another type of OCT technology was introduced. That is the Fourier-Domain OCT (FD-OCT); where the reference mirror is kept

stationary and the spectral pattern of the interference between the sample and reference reflections is measured. The final product, that is the spectral interferogram, is then Fourier transformed to provide an axial scan. The greatest advantages of FD-OCT over TD-OCT are the short acquisition times due to the absence of moving parts and the simultaneous detection of reflections from all layers of the sample. The generated axial scan is much more efficient, achieving both greater speed (50 to 100-fold compared to TD-OCT), higher signal-to-noise ratio, higher resolution (1 to 3μm axial resolution compared to TD-OCT's 10μm) and 3D representation capabilities.

FD-OCT can be categorised in two ways: the SD-OCT and the Swept-Source (SS-OCT). The difference between the two methods is dual: on the light source and the detector. In SD-OCT a broad-spectrum light source and a spectrometer in the detection arm are utilised.[246, 248-251] SS-OCT, on the contrary, uses a tunable laser which sequentially 'sweeps' through the spectrum while the signal is collected by a single-element photodetector. It can achieve scan speeds twice as fast as SD-OCT (100,000 A-scans per second for SS-OCT) and visualisation of deeper lying structures, thanks to the longer adopted wavelength (1,040nm vs 840nm). As a result, SS-OCT allows visualisation of the choroidal layers (and in some cases the suprachoroidal-sclera boundary) that were previously hardly distinguishable. Utilisation of a longer wavelength also allows for visualisation of the retina in cases with lens opacities.[250, 252]

Recent advancements and novel approaches have increased the capabilities of OCT to include the field of blood flow assessment. Ocular circulation has an important role in the diagnosis and study of eye pathologies, such as

AMD, DR and glaucoma.[253-255] Both fluorescein angiography (FA) and indocyanine green angiography (ICGA; mainly for the choroidal vasculature) are the lead diagnostic methods for retinal diseases.[256] Both of them, however, are invasive assessment methods as they require the intravenous injection of a dye to enhance the contrast of ocular vessels. Although intravenous administration of sodium fluorescein (for FA) and indocyanine green (for ICGA) are considered safe procedures they still hold a percentage of risk. Mild adverse events, such as nausea and vomiting can present in between 1% to 10% of FA cases and 0.15% of ICGA procedures. Although extremely rare, anaphylaxis (a severe adverse event) can also occur.[257-260]

OCT angiography (OCTA) is a novel, non-invasive, three-dimensional imaging technique which can provide detailed assessment of the retinal and choroidal vasculature. The main principle behind this technique is the detection of moving particles, such as the red blood cells, by means of variations in the OCT signal in a series of B-scans.[261, 262] In order to understand this, imagine two OCT signals, one derived from retinal structural tissue and the other from the moving erythrocytes in a blood vessel. If repeated scans from the same location are acquired, the signal from the structural tissue remains the same, while the signal from the flowing blood changes over time. Under this concept, an angiographic contrast can be generated and, therefore, making it possible to visualise the microvasculature (example in figure 2.2). It is noteworthy that any moving particle may generate a motion contrast signal; although movement in the retinal tissue derives predominantly from red blood cells.

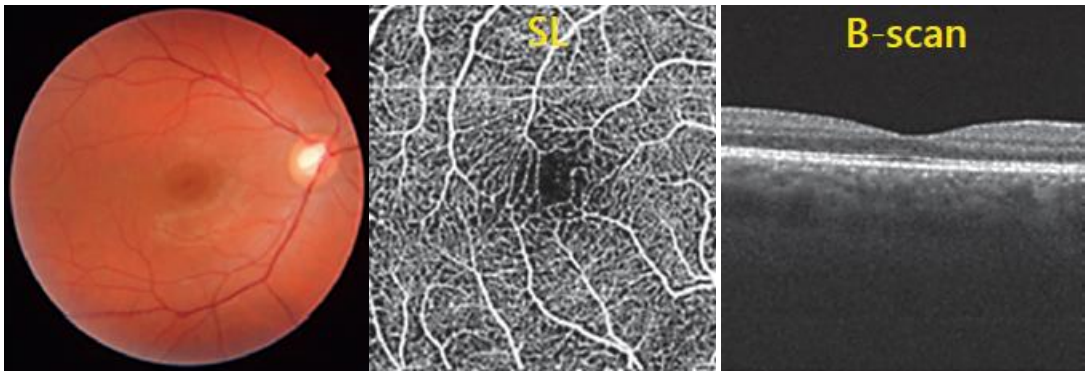

Figure 2.2: *Repeated B-scans (such as the image on the right) on the same location can detect differences in the signal due to moving particles. As a result an OCT-based angiogram (image in the centre; from the superficial layer [SL]) of a healthy eye (fundus image on the left) can be generated. Images courtesy of MVR Lab Imaging Database*

Research labs and relevant companies have developed a vast number of algorithms to analyse and visualise OCT-based angiographic data: optical microangiography, split-spectrum amplitude decorrelation angiography (SSADA), OCTA ratio analysis (OCTARA), speckle- and phase-variance and correlation mapping to name a few.[263-267] It is worth noting that SSADA, which uses multiple spectrums from a single B-scans, was developed by J Huang, who introduced OCT in the 1990s, while OCTARA, an algorithm developed by Topcon (Topcon Corp., Tokyo, Japan), is SS-OCT-specific and utilises intensity ratio calculations.[264, 268]

There are at least 4 sources of artefacts in OCTA images: 1) eye properties and potential pathologies, 2) eye movements; an example of motion artefact

is given in Figure 2.3, 3) data processing and 4) the algorithm used to generate the motion contrast signal.[246, 269] Due to the concept of OCTA (i.e. repeated scans on the same location) imaging is very sensitive to axial and transverse motion that can be caused by microsaccades, cardiac pulsations or even breathing. The implementation of motion-tracking technology can successfully compensate for those artefacts, while various post-processing image registration techniques are utilised by the commercially available systems.[270] The adoption of faster scanning methods, such as SS-OCT, could also minimise the effect of increased scan times and motion artefacts.[268]

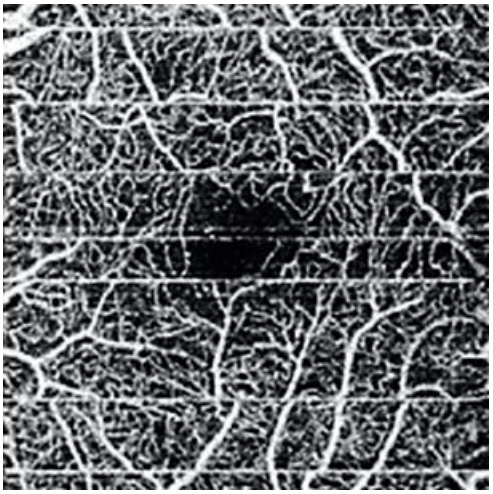

Figure 2.3: *Example of an OCTA image with motion artefacts. Note the white lines and misaligned vasculature. Image courtesy of MVR Lab Imaging Database*

Another major effect that appears quite often on OCTA images is a projection artefact. These artefacts are usually observed in structures that are located below the vasculature.[269] When an OCT beam reaches a blood vessel the light can be absorbed, reflected, refracted or even pass through the vessel. In cases where the light passes through the vessels it will inevitably encounter other parts of retinal tissue below the vessel. If the underlying tissue is hyper-reflective (e.g. the retinal pigment epithelium), the light will be back-scattered therefore generating a ghost image of blood flow. In addition, detection of blood vessels surrounded or under hypo-reflective structures (e.g. floaters, macular holes) is more difficult. For these reasons, such artefacts can limit OCTA's ability to visualise true blood vessels accordingly or may incorrectly present a blood vessel when there is actually none. These artefacts have impacted on aspects such as detection and management of choroidal NV and have become an extra hurdle for the establishment of quantitative metrics. A variety of models and techniques have been proposed to minimise projection artefacts on generated OCTA images; however none of them has been widely adopted.[267, 271, 272]

Since its commercial introduction the clinical role of OCTA has rapidly evolved as more research highlights its strengths and drawbacks over conventional imaging methods of FA and ICGA. Its major advantage is the visualisation of the retinal vasculature on the z plane (i.e. across different retinal layers). FA (and ICGA similarly) generate bi-dimensional images where the fluorescence signals from the superficial and deep layers overlap.[273, 274] A notable strength of FA is that fluorescein dye could leak out of abnormal vessels therefore suggesting the disease status. By

definition, OCTA would not visualise any leakage as there is no motion of blood cells[2]. However, the FA's strength on dye leakage is also its limitation as it can obscure other relevant details surrounding or below the leakage due to the increased background signal.[275, 276]

Today OCTA has an important role in routine ophthalmic care and especially in retinal clinics. Recent research evidence highlights the benefits of OCTA application in complications of retinal vascular diseases or macular abnormalities. In diseases such as DR, AMD and retinal vein occlusion monthly monitoring and constant treatment assessment is essential. However, FA or ICGA are not practical at this frequency. OCTA offers a non-inferior alternative that can uniquely assess real time changes in perfusion or neovascularisation (NV) during treatment (e.g. anti-vascular endothelial growth factor (anti-VEGF)).[277, 278] Published and on-going studies are evaluating the benefits (or otherwise) in other eye pathologies, such as glaucoma, uveitis etc.[271, 279-285]

In early 2014 the MVR Lab at MREH acquired a prototype device with OCTA capabilities (Topcon's Atlantis; Swept-Source Deep Range OCT, Topcon, Tokyo, Japan) for evaluation of its acquisition and image processing algorithms; and subsequently its diagnostic capabilities. A few months later (and approximately a year before its commercial release) Topcon's Triton (Topcon Corp., Japan) joined MVR Lab's research imaging department for a similar evaluation. The following chapters present a series of studies which

[2] For the same reasons (i.e. failure to detect blood cell motion), sclerosed or clotted microaneurysms are also not detected by OCTA but stained by FA or ICGA dye agents.

explored the potential of OCTA and described the benefits (or limitations) this new technology could offer to standard clinical care.

2.2 Pushing the Boundaries of OCTA: a Study on Vitreous and Ultra-Wide Field OCTA Imaging

Contributions

The hypothesis of this study was conceived by Prof Stanga and other clinicians from his team (i.e. clinical research fellows) after the introduction of the newly acquired equipment in their DR and vitreoretinal clinics. For the needs of this study, I was in constant communication with the company Topcon Inc., receiving initially essential training related to the new equipment and later reporting on the study outcomes and advising for further enhancements of ImageNet, the relevant image processing software. During this iterative process, I significantly contributed in developing the vitreous segmentation algorithm described in this chapter; vitreous segmentation later being implemented in the ImageNet's updated version. Other contributions include the data collection and analysis for this study, particularly leading the design of statistical process, the construction of presentations and relevant study reports to the company and other related parties.

This first study described in this Section was effectively the first opportunity to understand and evaluate the novel technology of OCTA. While retinal scans over the macula and the optic disc seemed an easy task for the devices available to the MVR Lab, I intended to explore the capabilities of both the image acquisition and analysis in extreme areas such as the far peripheral retina, the vitreous and the choroid. This report depicts the

knowledge gained and presents the benefits, and otherwise, of OCTA in a clinical setting. At the time this research was conducted segmentation algorithms were fairly poor mainly due to the lack of clinical data; offering, however, a great opportunity to explore and develop new segmentation algorithms, like those reported here.

Presentations / Publications

The outcomes of this study attracted the interest of research meetings and conferences as they were among the first utilising SS-OCT in clinical eye care. Thus, oral presentations and posters were presented in conventions, such as ARVO (2016; Seattle, WA, USA), Euretina 2016 (Copenhagen, Denmark) and others as well as meetings sponsored by Topcon Corp.

Draft manuscripts were submitted in Retina and Investigative Ophthalmology and Vision Sciences journals without being accepted for publication. This chapter is taking into account reviewer's feedback and extensively discusses the results of this research.

2.2.1 INTRODUCTION

Diabetic retinopathy is an ocular microvascular complication of diabetes-mellitus which occurs in approximately 35% of patients with this condition.[286, 287] Proliferative DR (PDR) is one of the major causes of severe visual impairment affecting approximately 7% of patients with DR.[288] Diagnosis, management and follow-up of DR are currently based on imaging provided by FA and OCT, which has facilitated the study of DR and has been quickly and widely adopted in both research and clinical practice. [289, 290]

FA is, as we know already, the clinical standard for evaluating retinal vascular changes in DR.[291] FA can highlight microvascular abnormalities such as ischaemia and NV, both signs of early and/or advanced DR. Peripheral retinal non-perfusion, which represents intra-retinal capillary occlusion or rarefaction, can be observed as a hypo-fluorescent area delimited by the still perfused retinal vessels, while new (weak) vessels can be identified by leakage of dye into the surrounding retinal tissue.[292, 293] Moreover, peripheral and mid-peripheral vascular changes are likely to be related with DR progression.[294]

It has been hypothesized that DR microvascular alterations initially develop in the peripheral retina where they may indicate increased DR severity in 9% to 15% of eyes.[288] Therefore, the concomitant display of peripheral microvascular alterations and areas of capillary non perfusion can help to understand the connection between these lesions and DR evolution. The recent advent of ultra-wide-field imaging systems with the capability of

performing FA (UWF-FA) have expanded the field of view into the peripheral retina (figure 2.4) with the advantage of simultaneous imaging of the four quadrants (where vessels are in the same angiographic phase) and highly contrasted images, eliminating the need of composite images composed of individual sequential images obtained along the angiogram.[295]

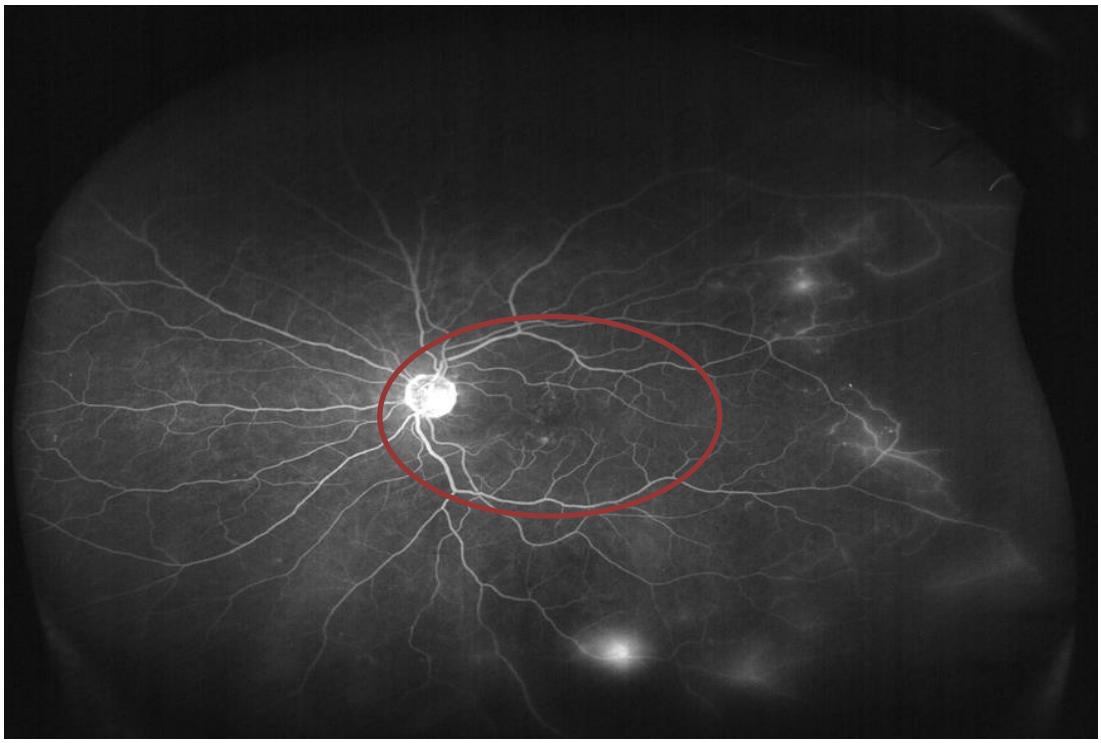

Figure 2.4: *Ultra-Wide field image during fluorescein angiography; captured by Optos California. Retinal areas outside the red circle are considered parts of the peripheral retina. Image courtesy of MVR Lab Imaging Database*

Recent studies have utilized SD-OCT to assess the vitreoretinal morphologic features of PDR, that is NV of the disc (NVD) or NV elsewhere (NVE), which appear as hyper-reflective epiretinal structures on the optic disc or other

parts of the retina encroaching into the vitreous cavity.[296, 297] The presence of vitreous hyper-reflective dots, epiretinal membrane, inner retinal tissue contracture, vitreous invasion and vitreous protrusion have all been identified as distinct signs of disease activity.[297] However, one of OCT's limitations is its restricted scanning area. Most current commercially available devices have a maximum scanning size of 8x8mm which is not sufficient to capture the entirely mid- and extreme peripheral retina (henceforth peripheral retina), where non-perfused areas seem to be primarily located.[298]

Reports have shown that SS-OCT can illustrate vitreoretinal features, such as vitreoschisis, posterior precortical vitreous pockets and adhesions in the vitreous, with remarkably good quality.[299-304] It is therefore tempting to investigate the application of the recently introduced angiographic capabilities of OCT in the clinical care of DR and more specifically those of swept-source technology. Indeed, recent evidence has shown that newly developed OCTA imaging techniques can be used to visualize pathologic vascular changes of DR such as microaneurysms, retinal non-perfusion and NVD.[305, 306] However, despite strong evidence to support the efficacy of OCTA in imaging vascular changes (associated with DR) in the cortical vitreous over the central retina,[305-307] there have been few attempts to acquire OCT angiograms from mid- and extreme periphery; the reason being the bulk-shaped retinal tissue and the relatively short depth range which has a significant impact on the sensitivity of most OCTA devices.

This study reports on the outcomes of an investigation where a SS-OCT device was utilised to image the peripheral retina in order to identify potential vascular changes. The hypothesis was dual: the significant advantages of

swept-source technology would allow imaging of clinically adequate quality from 1) the peripheral retina and 2) across a range that includes not only the various retinal layers (to detect possible vascular changes) but also the cortical vitreous (to identify signs of NVE).

2.2.2 METHODS

Vitreoretinal segmentation

One of the most important variables in the analysis and interpretation of OCTA images is the technique by which the various layers of the tissue are divided and how the segmented layers are brought together to define the 'superficial' or the 'deep' retina. An example of OCT-based angiograms from different layers as presented by Topcon's Triton is given in Figure 2.5. Segmentation methods are unfortunately not standardised among different studies and devices; despite notable attempts to develop a universal segmentation scheme.[308] Even the same segmentation method can be susceptible to errors from normal anatomical variations, much less in pathological changes.

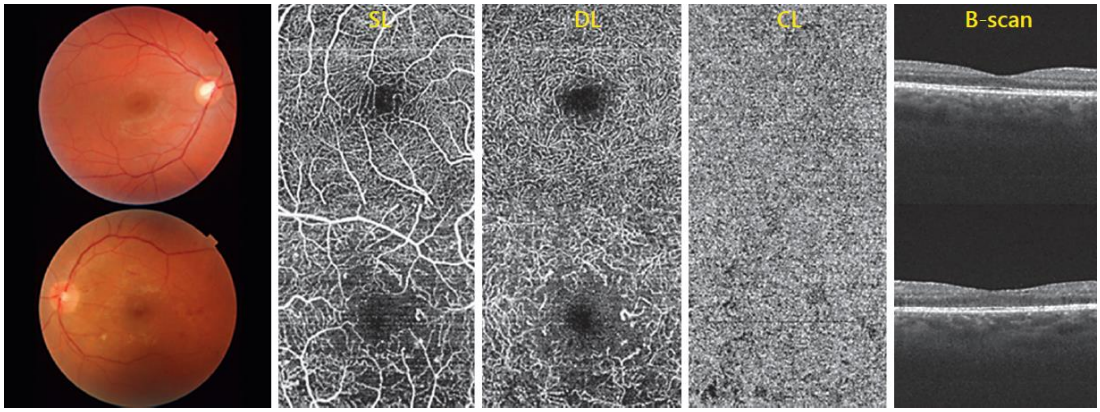

Figure 2.5: *From left to right: fundus photographs, OCTA images from the superficial (SL) and deep layer (DL) and the choriocapillaris (CL), OCT B-scans. Top row: healthy eye; bottom row: nonproliferative diabetic retinopathy with microvascular alterations and enlarged foveal avascular zone.*

Study data were acquired using Topcon's Triton SS-OCT DRI and Topcon's prototype Atlantis DRI SS-OCT-1. The in-built automated segmentation technique (ImageNet 6) was used for the differentiation of the retinal layers. Thus, the superficial neurovascular layer (i.e. the superficial retina) is defined from the internal limiting membrane to the boundary between the inner plexiform layer and inner nuclear layer (IPL/INL); while the deep retina, is demarcated from the IPL/INL to the junction of inner and outer photoreceptors' segment (i.e. the ellipsoid zone). Figure 2.6 shows an SS-OCT B-scan from a healthy eye that allows clear visualization of the retinal layers and the choroid.

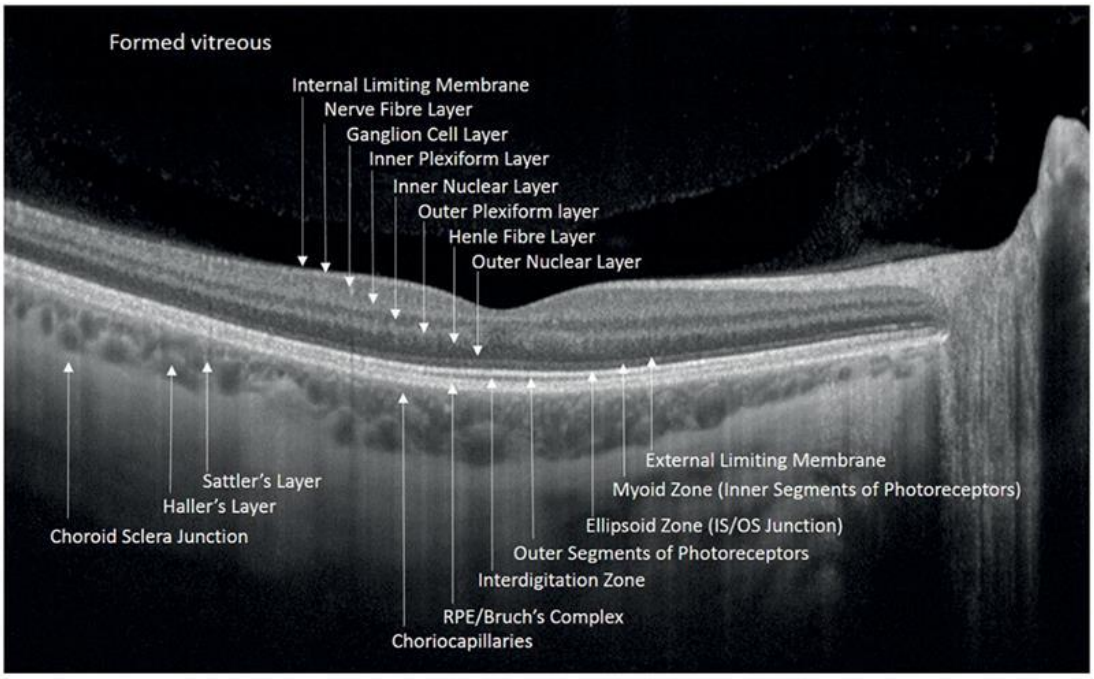

Figure 2.6: *Swept-source OCT B-scan with clear visualization of all the retinal layers down to the choroidoscleral boundary. Image courtesy of Mr Tim Cole, Topcon Inc.*

For the improved visualization of NVs from the superficial retina into the vitreous cavity and the optimal assessment of potential vascular features a manual vitreoretinal and vitreous segmentation technique was developed, evaluated and established to allow standardization across this study. Therefore, the cortical vitreous was segmented manually after modifying the reference planes and manipulating the depth of the boundaries at various levels.

Various types of vitreoretinal segmentation protocols were assessed using the analysis software from both aforementioned SS-OCT devices. Three different types of segmentation protocols were deemed to be the most

effective. The main difference between the segmentation schemes relied on the positioning of the lower boundary between the retinal layers of the superficial plexus and the upper boundary in the vitreous cavity. The segmentation protocols that were specific for the cortical vitreous were:

1. Vitreo-Retinal Segmentation (VRS): the lower limit of the assessed segment is set up posterior to the internal limiting membrane (ILM) so as to include the outer retinal layer and the upper limit ~300μm above and in the cortical vitreous; an example of macular VRS on a B-scan is shown in Figure 2.7
2. Outer Vitreous Segmentation (OVS): the lower limit is placed anterior to the ILM while the upper limit includes the cortical vitreous cavity
3. Core Vitreous Segmentation (CVS): both lower and upper limits fall in the cortical vitreous

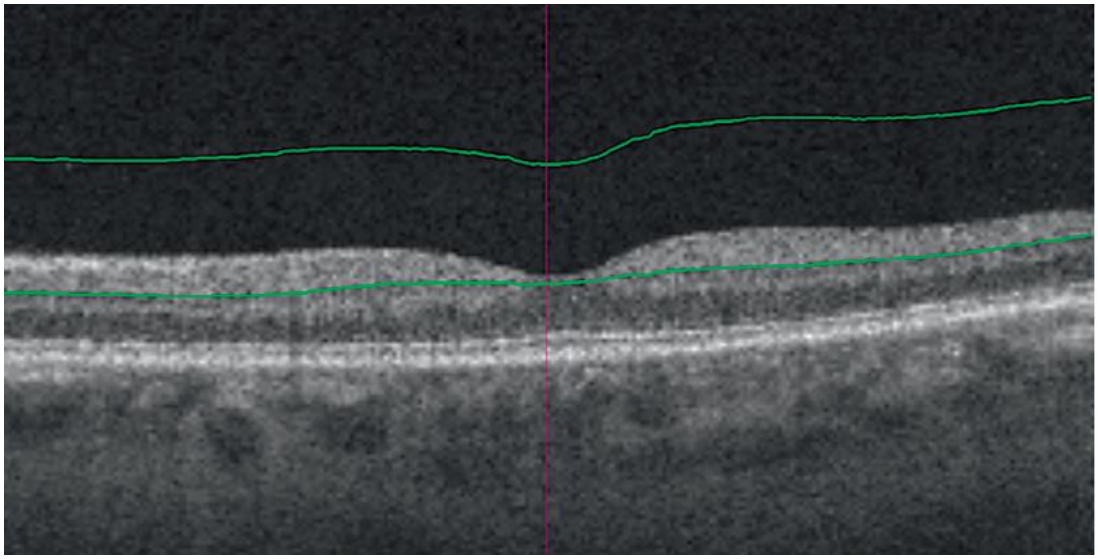

Figure 2.7: *Example of macular vitreoretinal segmentation (VRS). The lower segmentation reference line (green) has been positioned at the inner plexiform layer / inner nuclear layer boundary. The upper segmentation reference line is positioned 300*μm above and inside the vitreous cavity. *Image courtesy of MVR Lab Imaging Database*

The Atlantis device incorporates an extra image processing feature that improved the quality of angiograms and simplified the segmentation analysis; that was the 'flattening' of the B-scan at the level of the ILM. This feature was used in all OCTA images acquired with the Atlantis. Examples of the 3 aforementioned protocols for both the Atlantis and Triton are given in Figures 2.8 and 2.9 below.

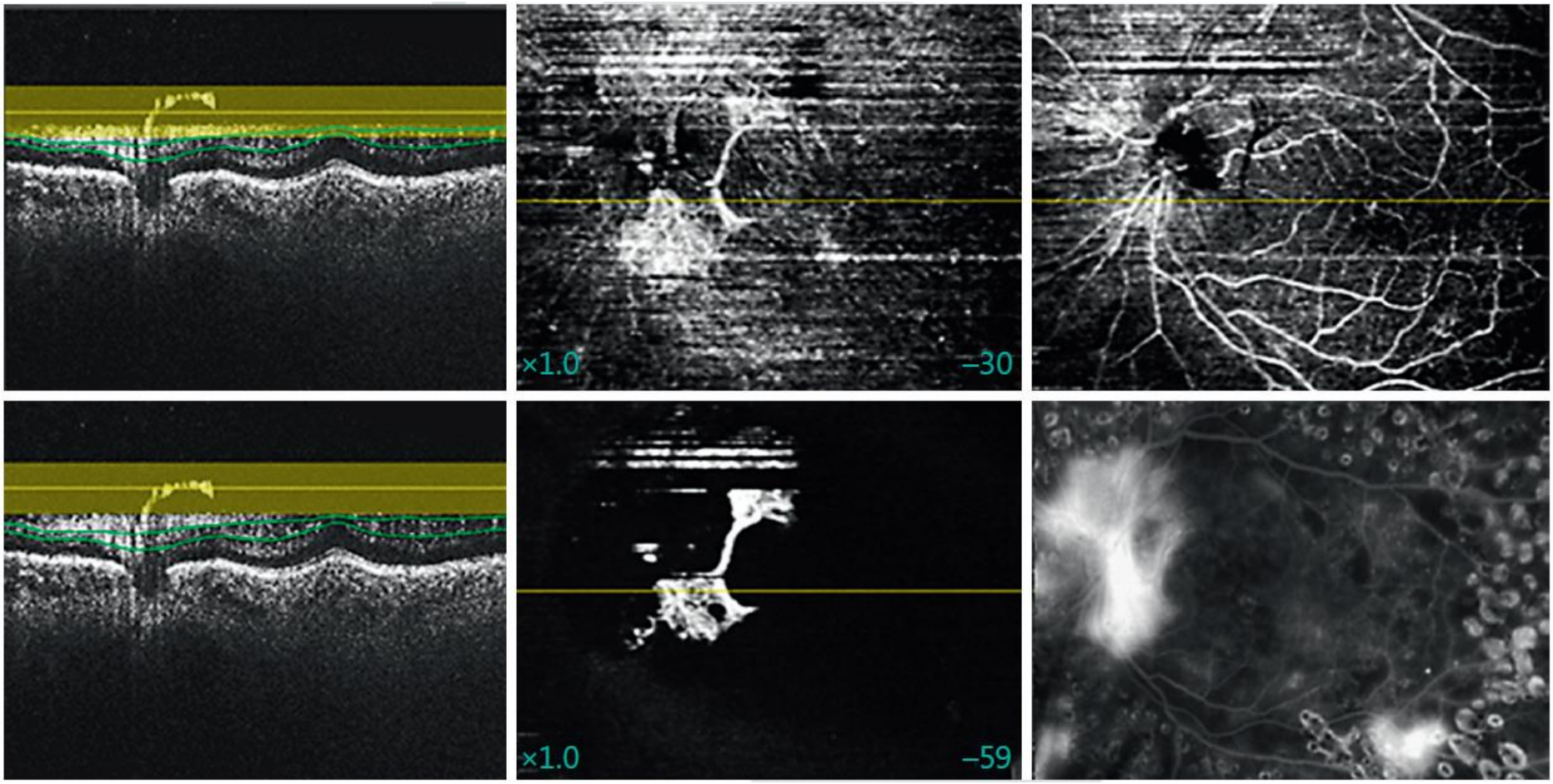
×1.0
–30
×1.0
–59

Figure 2.8: *Examples of vitreoretinal (top row) and outer vitreous (bottom row) segmentations for Topcon's Atlantis. The yellow band on the B-scans (left) indicate the segmentation area after 'flattening' of the internal limiting membrane. Angiograms in the middle are the respective images of the two segmentation protocols. Angiogram at top right is the product of superficial segmentation; green lines on the B-scans. The fluorescein angiogram of this eye is shown at bottom right. Images courtesy of MVR Lab Imaging Database*

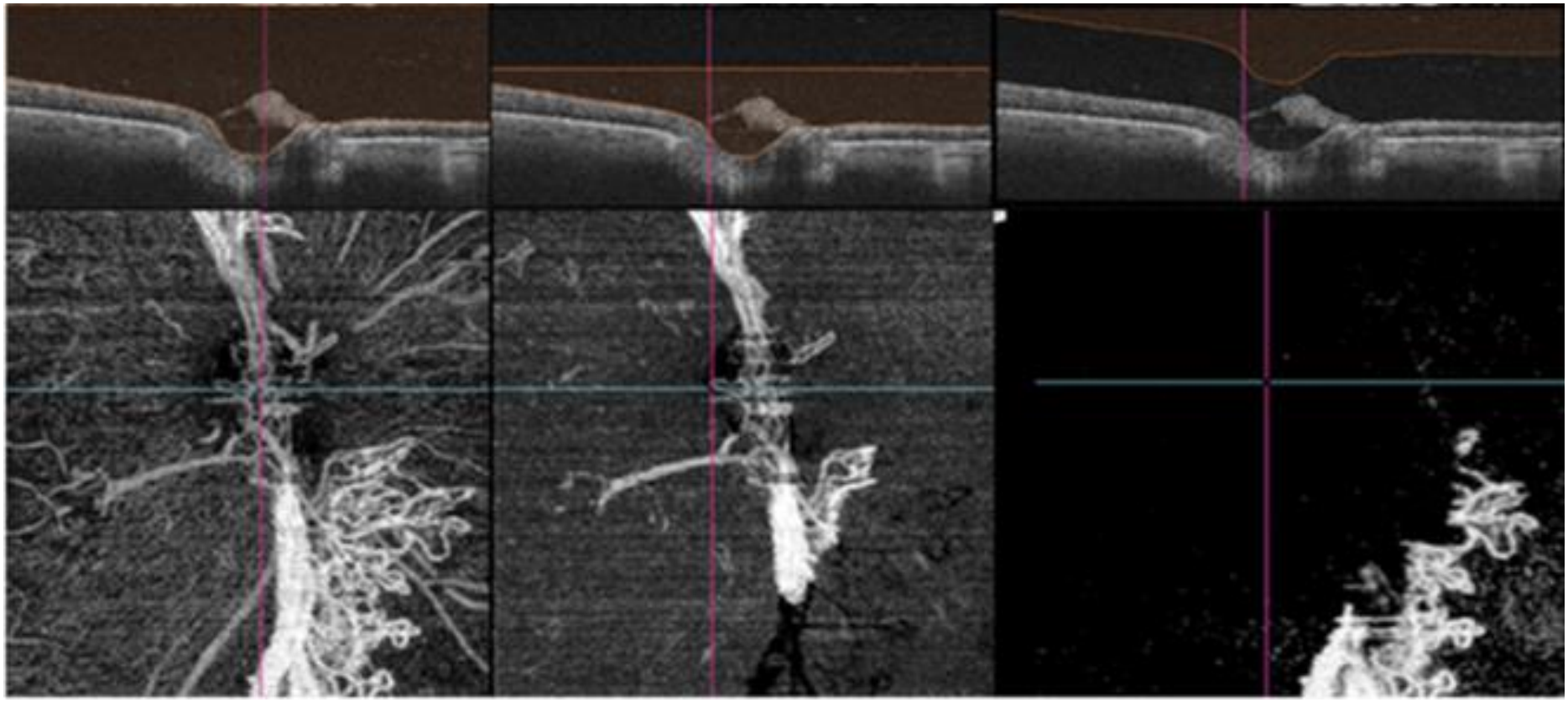

Figure 2.9: *Examples of vitreoretinal (left), outer (middle) and core vitreous segmentations for Topcon's Triton. Top row shows B-scans with orange bands indicating the segmentation zones. Bottom row shows the respective OCTA images. Images courtesy of MVR Lab Imaging Database.*

The segmentation was performed by the operator/researcher (i.e. the author) while the generated OCTA images were reviewed by two clinicians. The evaluation of the vitreous segmentation protocols was performed by estimating inter-observer agreement for the identification of NV features and potential changes (i.e. binary response, yes/no change; applicable in cases with follow-up data). Inter-observer agreement was assessed by calculating Cohen's kappa coefficient and total percentage of agreement.[309] Kappa values range from -1 to 1; the latter indicates complete agreement while Kappa equals 0 when the observed agreement is justified by chance alone. Values higher than 0.80 indicate very good agreement, while those between 0.40 and 0.80 are classified as moderate to good agreement. Total percentage of agreement was simply calculated as the percentage of all identified NV features in which agreement was observed between clinicians.

Study population and equipment

All diabetic patients attending a weekly vitreoretinal and DR clinic (supervised by Prof Stanga) at MREH diagnosed or suspected of having PDR underwent SS-OCTA imaging from June 2015 to January 2016. While both systems can obtain images of superior quality when the scanned area is limited to 3x3 or 6x6mm, the Atlantis system can extend the scanned area to 12x9mm. Raster-pattern retinal scans were obtained through the macula, the optic disc and areas of possible NV in the mid-peripheral retina using scanning patterns of 3x3mm, 6x6mm (for Triton and Atlantis) and 12x9mm (for Atlantis) in all patients. During the acquisition of the OCTA images, the

choroid and the retina were positioned at the lower border of the image plane to produce full depth visualization of potential NV processes in the vitreous cavity.

Eyes with OCTA images and corresponding UWF-FA, performed with an Optos California® (Optos PLC, Dunfermline, Scotland) were included in the study.

2.2.3 RESULTS

Two hundred and twenty-seven (227) consecutive patients with diagnosed or suspected DR had OCTA imaging with both devices were assessed with a view to being enrolled in the study. Corresponding UWF-FA images were found in 67 patients. Twenty-four (24) patients were excluded as either OCTA or UWF-FA images were deemed of inadequate quality; most frequent reason being poor fixation during FA or OCTA. Eighty six eyes from 43 patients were enrolled in this study, 64 of which also had OCTA images from follow-up visits. The mean age of subjects was 52.6 years (±11.0), ranging from 24 to 82. Other descriptive statistics, such as average follow-up time and average number of OCT scans acquired are given in Table 2.1.

Patients	43
Eyes	86
Male:Female Ratio	1.2:1
Mean Age (±SD; Range)	52.6 (±11.0; 24 to 82)
Average Follow-up Time in months (±SD; Range)	4 (±1.5; 2 to 6)
Average # OCT scans per eye (±SD; Range)	6 (±2; 1 to 10)

Table 2.1: *Descriptive information of the study cohort*

Validation of the vitreous segmentation protocols

Scans within the vascular arcades were used to evaluate the above-described vitreous segmentation protocols. Successful segmentation was achieved in all scans. Very good agreement was observed between clinicians when asked to identify NV features and also assess potential changes in a series of images from the 64 eyes with follow-up images. The results of the inter-observer agreement analysis are given in Table 2.2.

	Kappa	TA
Identification of NV features	0.8295	92%
Detection of change in NV features	0.7242	87%

Table 2.2: *Outcome of the inter-observer agreement study for validation of the vitreous segmentation protocols. TA: percentage of Total Agreement*

Evaluation of peripheral NV and ischaemia

All the microvascular lesions observed on UWF-FA within the vascular arcades were also observed on OCTA scans (86/86 eyes). When compared with FA, SS-OCTA allowed for a non-invasive visualization of the microvascular and ischemic alterations with higher definition than conventional FA and with a layer-by-layer analysis of the different retinal plexuses; as shown in Figure 2.10.

Across the 86 examined eyes with OCTA, 13 eyes were identified with signs of diabetic macular oedema (e.g. Figure 2.11), 39 eyes showed signs of posterior pole and mid-peripheral retinal non-perfusion, while 5 and 9 eyes showed evidence of NVD and NVE respectively with 100% inter-reviewer agreement.

Enlarged foveal avascular zone (FAZ) with peripheral ischemic areas was observed in 36 eyes on both UWF-FA and OCTA. Twelve (12) patients had diagnosis of PDR with FA evaluation. Within the central 100° there was good correlation between OCTA and UWF-FA with regards to the capability in detecting PDR. Signs of NVD where observed in 5 eyes with both techniques while OCTA was able to present evidence of NVE (detected with UWF-FA) in 9 over 10 eyes.

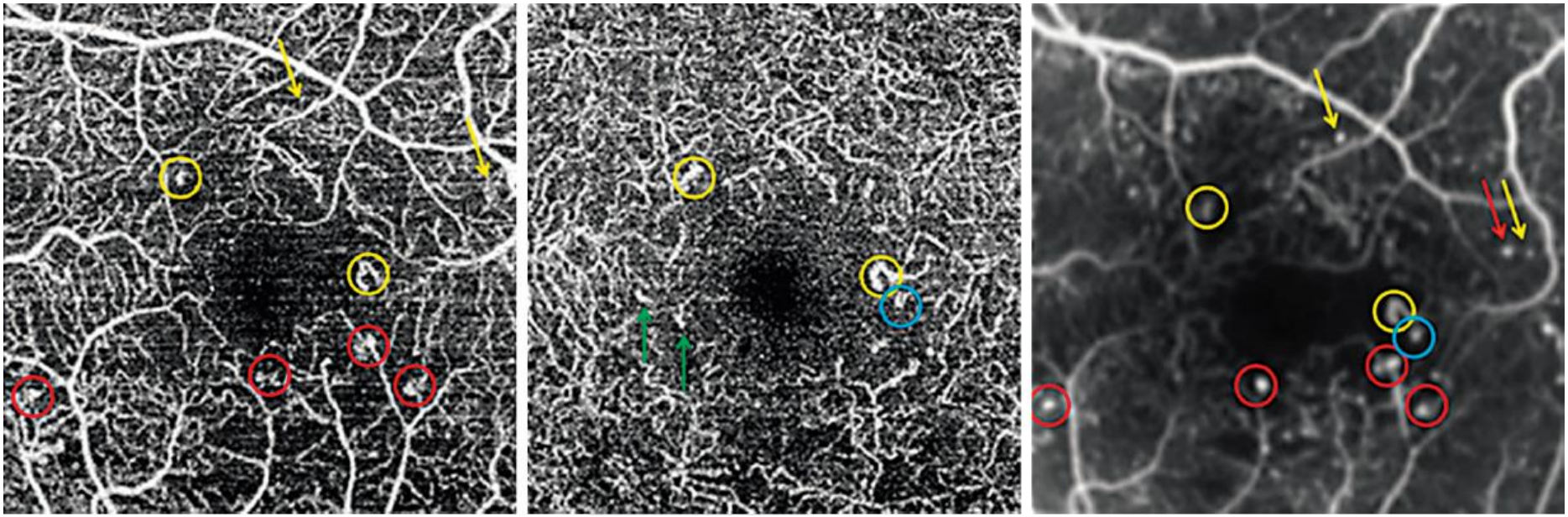

Figure 2.10: *Detailed analysis of 3x3 mm macular OCTA scan of the superficial (left) and deep (center) layers in comparison with a fluorescein angiography (FA) image (right) of a diabetic eye. Red circles indicate microvascular alterations on FA, the origins of which are defined in the superficial vascular layer on OCTA. The blue circles highlight lesions originating in the deep vascular layer. The yellow circles show vascular abnormalities derived from both layers matching those on FA. The arrows point to lesions that are better visualized using one technique over the other (yellow: better visualization with FA; green: better with OCTA). The red arrow highlights a hyperfluorescent spot that cannot be matched with any hyper-reflective alteration on OCTA.*

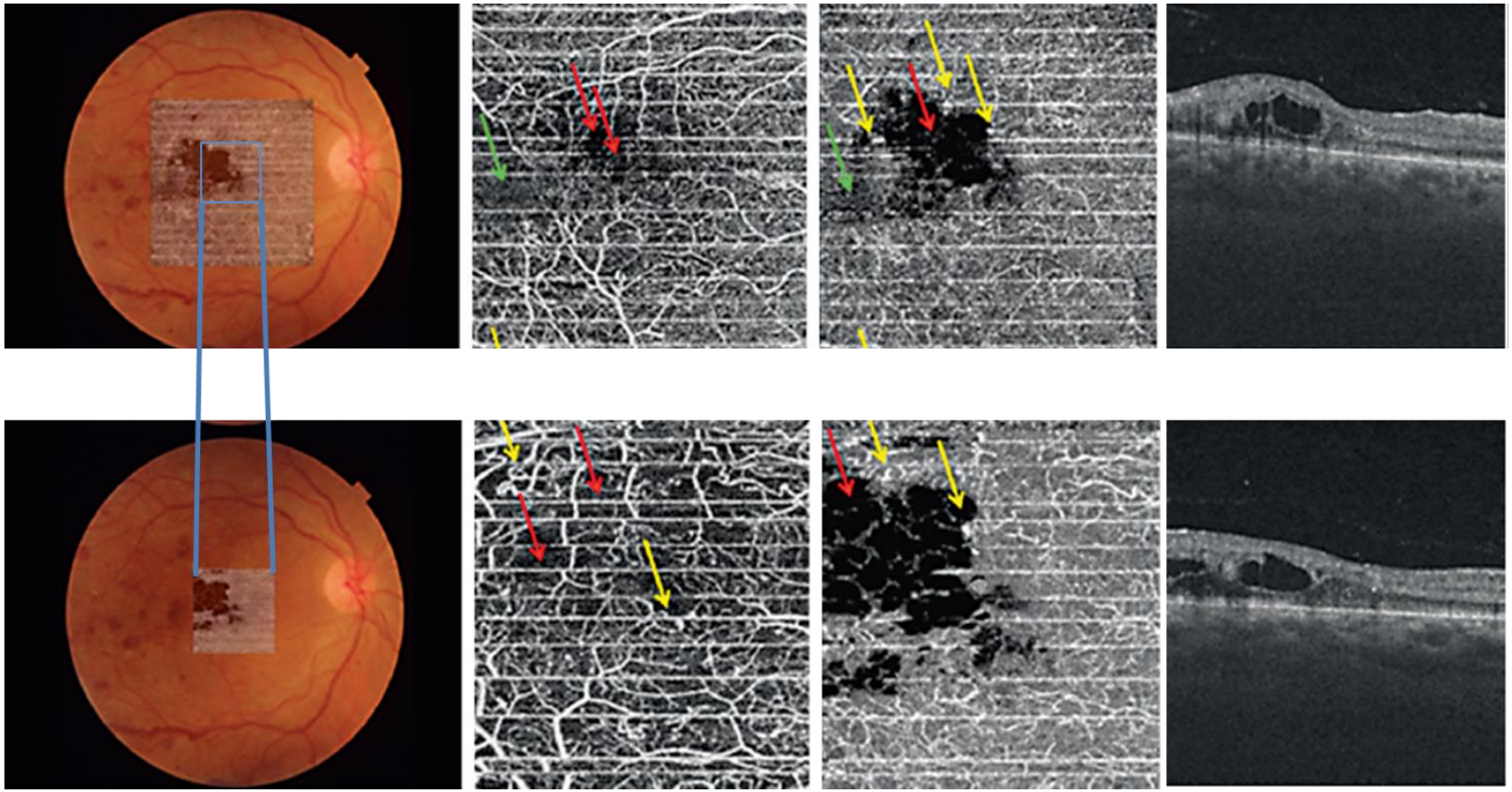

Figure 2.11: *OCTA images (6x6 mm (top row) and 3x3 mm (bottom row)) of a patient with advanced proliferative DR. From left to right: colour fundus images with overlying OCTA image of the superficial vascular network, OCTA images of the superficial and deep layers along with relevant OCT B-scans. The red arrows show hypo-reflective areas due to presence of diabetic macular edema, the yellow arrows point to the associated microvascular alterations and the green arrows indicate areas of associated ischemic alterations of both the superficial and deep layers.*

The OCTA images from scans of the posterior pole and mid-periphery, segmented with the VRS protocol, were put together in a composite image and compared to the UWF-FA image; examples of mid-peripheral VRS and a composite image are given in figures 2.12 and 2.13 respectively. Review and subjective evaluation from the two clinicians reported that imaging of the NVs superiorly and inferiorly of the vascular arcades as well as nasal to the optic disc can be deemed effective. As scans were acquired to more peripheral locations or temporally to the macula, image quality and sensitivity of OCTA would reduce dramatically while approximately 1 in 4 angiograms (more specifically 23%) acquired in the mid-periphery required further adjustment with manual point-to-point segmentation due to decreased capability of the software to segment the outer retinal layers.

All the mid-peripheral OCTA images were acquired without the internal fixation spot that is used routinely for the macular and optic disc imaging. Considering the lack of eye tracking system in both devices, artefacts due to loss of fixation, extreme saccadic movements or blinking during acquisition were common and more frequent in the periphery; as it is evident in most figures in this chapter. The mean time necessary for the acquisition was 15.5 minutes per patient (i.e. both eyes; ranging from 9.5 to 26 min).

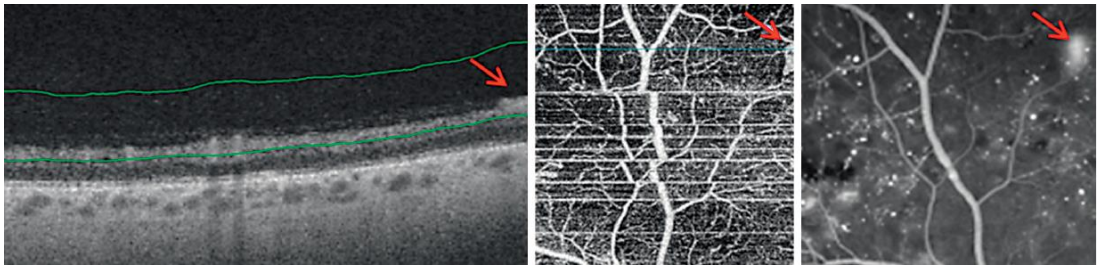

Figure 2.12: *Example of mid-peripheral vitreoretinal segmentation, with the lower segmentation band in the inner plexiform layer/inner nuclear layer boundary and the upper band adjusted at 300 µm inside of the vitreous cavity. The red arrows indicate neovascularization elsewhere in the OCT B-scan (left), OCTA (center) and fluorescein angiography (right) images.*

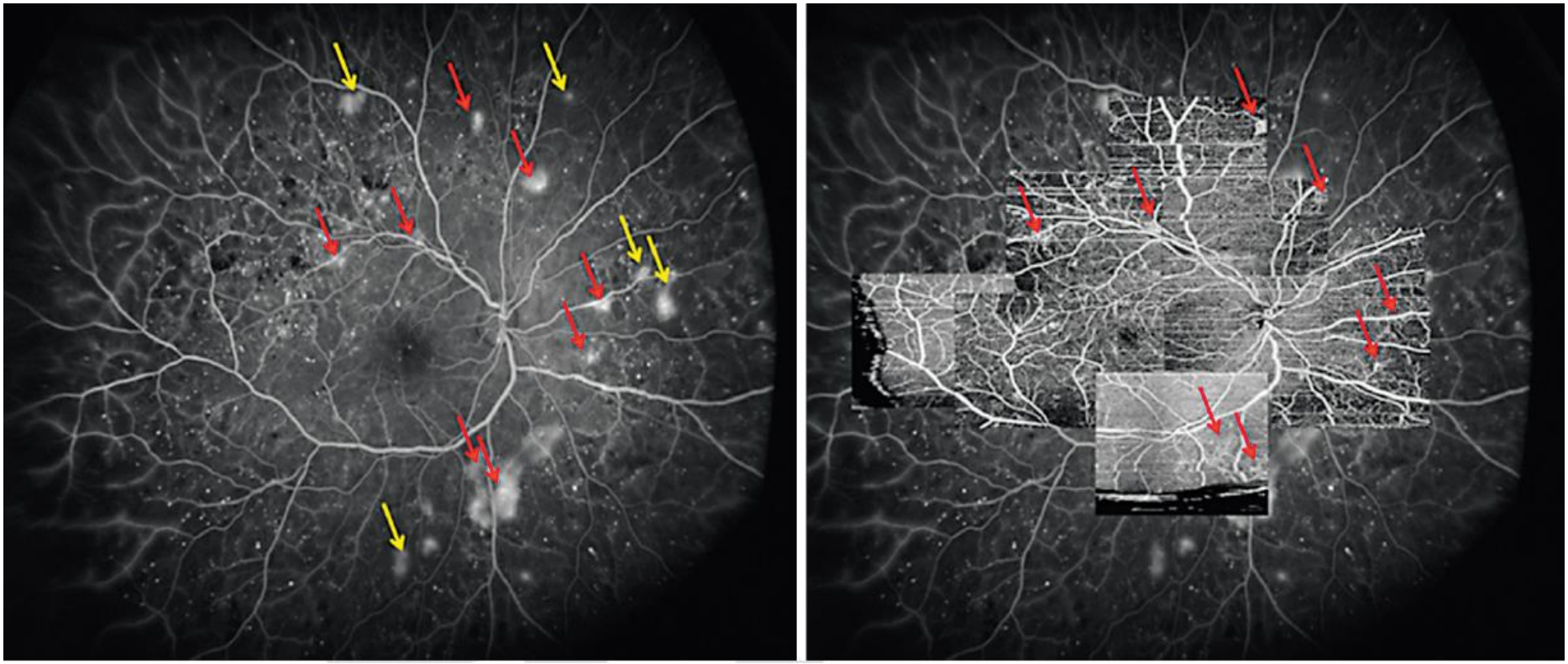

Figure 2.13: *Left - Ultra-wide-field fluorescein angiography image; Right - Topcon's Triton OCTA composite image of the posterior pole and mid-periphery superimposed on the ultra-wide-field fluorescein angiography image. The red arrows indicate the common sites of NV, and the yellow arrows point to the sites of NV that cannot be detected by OCTA in the far periphery.*

2.2.4 DISCUSSION

The reported study utilised swept-source technology to acquire images from the peripheral retina in patients diagnosed/ suspected DR. Its aim was to understand the capabilities (or limitations) of angiography in the mid-periphery with a standardized technique based on SS-OCTA. Subjective review from two clinicians indicated that identification of NVE in the peripheral retina by means of OCTA is possible; highlighting though that significant improvement in the acquisition (and subsequently analysis) of OCT-based angiograms is required.

Swept-source technology has significant benefits when imaging the peripheral retina over other OCT approaches due to lower acquisition time and higher depth penetration, from the vitreous cavity up to the choroid at the limits of the sclera. As previously described, both pieces of equipment utilised in this study had no eye tracking systems. As a result acquired scans from peripheral retina were exposed and heavily affected to microsaccades. Eye tracking systems, now available with every commercial device, offer tremendous advantages as it allows for pausing of the scanning process when a patient blinks (shown as black horizontal stripes on angiograms) and correct image registration and alignment during eye movements (represented as thin horizontal white lines on OCTA images).

Another limitation on peripheral retinal imaging with OCTA is in the width of the scanning pattern. For this study, Atlantis' wide scans (12x9mm) were discarded as they suffered from serious artefacts due to the eye bulb

curvature in the periphery. Such wide scans acquired outside the vascular arcs were deemed inappropriate for clinical purposes as they were characterised by poor resolution and extremely poor automatic segmentation of the retinal layers while there was difficulty in constructing an appropriate composite image. 6x6mm scans acquired with the Triton system, offered higher quality images with fewer artefacts in the periphery.

Segmentation of the vitreous is necessary for the imaging of new vessels located between the surface of the retina and the cortical vitreous. The advent of SS-OCT offers significantly improved visualisation of the anatomy of the cortical vitreous. Features of the swept-source technology, such as longer wavelength and faster scanning speeds compared to SD-OCT, have managed to reduce light scattering by the vitreous and the counteraction of vitreous movement, respectively. The new vitreous segmentation protocols evaluated and proposed here may help OCTA to become an effective and established non-invasive imaging technique that provides three-dimensional information of the morphology and the spatial localization of vascular lesions in DR located in the cortical vitreous affecting the posterior pole and mid-periphery.

The analysis of agreement between observers showed that inter-observer reproducibility can be achieved after utilising the aforementioned protocols. Data on the sensitivity of each protocol are not available as the clinicians would establish the presence (or change) of NV features after reviewing all OCTA images – products of the segmentation processes. They reported though that angiograms from one approach had significant advantages over another.

The VRS protocol allowed optimal visualisation of the anatomic relationships between NV processes and the epiretinal vasculature. In a similar way, the OVS protocol showed high-quality representation of epiretinal neovascular complexes without the background interference of the hyper-reflectivity from the epiretinal capillaries; a feature that was commented to be useful for evaluation of changes in the NV features over time. The third protocol (i.e. CVS) allowed a segmented visualization of NV extending towards the inner vitreous cavity and at different depths, therefore, completing the segmented analysis of vitreoretinal NV. However, the quality of OCTA images along with the sensitivity to detect and monitor NV features reduced dramatically; possibly due to the short ranging distance. In a similar way quality also decreased at the very peripheral locations. Nonetheless, OCTA technology can offer unparalleled capabilities on a layer-by-layer analysis in the choroid, the retina and, as shown, in the cortical vitreous. As a result clinicians and eye care professionals can detect and monitor NV features that were missed or poorly evaluated by conventional slit-lamp examination or FA.

The three-dimensional analysis of the vitreous NV as shown in this study could provide additional information for the pharmacological and surgical management of PDR by allowing, for example, the objective comparative assessment of NV changes after intravitreal treatment with anti-VEGF or retinal laser treatment. These segmentation protocols could assist the preoperative planning of segmentation and delamination techniques during pars plana vitrectomy surgery. Further prospective and larger studies could establish the potential benefits of the proposed new segmentation protocols.

A major limitation in any retinal or vitreous segmentation protocol is, with increasing proximity to the mid-periphery, a reduction in segmentation sensitivity. In this study a quarter of the OCTA images acquired from the peripheral retina demanded further point-by-point adjustment of the reference boundaries to generate more representative angiograms. Manual segmentation is therefore needed to improve the quality of images in the mid-periphery. However, manual segmentation is time consuming leading to delays in clinical decision making. To avoid this targeted peripheral scans could be performed (example in Figure 2.14). The development of automated targeting systems based on automatic recognition of selected areas on ultra-wide-field fundus photography or autofluorescence images could be an alternative way of imaging.

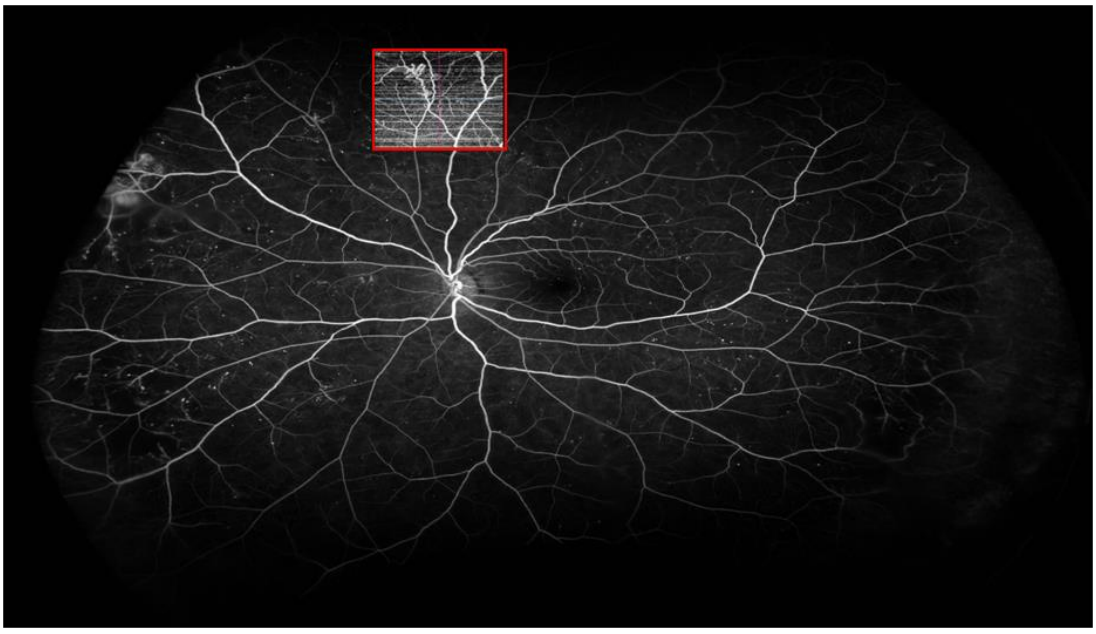

Figure 2.14: *Targeted peripheral OCTA scans guided by ultra-wide-field colour fundus, autofluorescence or fluorescein angiography images could allow for monitoring and a layer-by-layer analysis of new vessels in diabetic retinopathy.*

In consideration of the above observations it is evident that the study of peripheral retina by means of OCTA requires devices that offer good and homogenous quality of signal at all depths of acquisition. This can be achieved with eye tracking systems, high speed of acquisition and powerful image processing algorithms that account for the different types of artefacts in an OCT scan. Further research and technological developments could include the capability to tilt the instrument at different angles in order to better explore the extreme periphery or software that allows automated composite reconstruction. Such software recently become available; however this currently requires significant input from the user to align, rotate or process the OCTA images.

2.2.5 CONCLUSIONS

FA remains the clinical standard technique; OCTA can be considered though a safe non-invasive technique that can allow for routine imaging and monitoring at shorter intervals of NV and ischemic features of the retina in diabetes or other diseases. Moreover, OCTA can be a reliable alternative for patients whose general health does not allow examination by FA as well as reducing the number of FAs performed on patients without contraindications.

This report showed encouraging evidence regarding the reliable study of peripheral retina by means of OCTA with the swept-source technology;

however OCTA scanning of the retinal periphery could be deemed quite cumbersome with the current status of the technology. The shortcomings and limitations presented in this study are likely to be eradicated with new technological advancements; therefore allowing for the examination of the retinal periphery in a non-invasive and highly sensitive way.

2.3 Effectiveness of Bevacizumab Two Days before Vitrectomy for Diabetic Tractional Retinal Detachment - an OCT Angiography Study

Contributions

This small proof-of-concept study was designed by Mr Assad Jalil, vitreoretinal surgeon at MREH. Bevacizumab injections and subsequent vitrectomies were performed by clinical research fellows of the MVR Lab, supervised by Mr Jalil. For this study, and apart from the collection of data, I was responsible for the analysis of the acquired images and their appropriate segmentation to achieve optimal quality. My expertise in the segmentation of OCTA images, an exclusive skill among the investigational team at that time, allowed for the appropriate comparison of OCTA images from the clinicians/investigators for the identification of structural changes and subsequently the evaluation of inter-observer agreement. In addition, I was significantly involved in the preparation of relevant manuscripts and presentations of the study outcomes.

The imaging of an increasing number of patients offered me the chance to improve my skills on image acquisition, analysis (with manual segmentation being essential most of the times) and interpretation for clinical purposes. The following study provided a great opportunity to test the OCTA capabilities on monitoring progression, as well as evaluate its repeatability. I learned and utilised techniques of image registration and alignment to

achieve optimal results. OCTA proved to be successful most of the times in monitoring the regression (or otherwise) of neovascularisation.

Presentations

The outcomes of this study have been presented orally at the British and Eire Association of Vitreoretinal Surgeons in November 2016 and at FLOREtina, April 2017. A manuscript is currently under review by the Retinal Brief Cases and Reports journal.

2.3.1 ABSTRACT

Purpose: To explore the capabilities of SS-OCTA in imaging through vitreous haemorrhages (VH) and demonstrating the effect of intravitreal bevacizumab (IVB) before pars plana vitrectomy on the size and vascularity of the fibro-vascular complex

Methods: Observational case series of three eyes with active diabetic fibro-vascular complex and tractional retinal detachment (TRD) who underwent IVB (1.25mg/0.05ml) two days before proceeding to pars plana vitrectomy. OCTA was carried out prior to IVB, two days after IVB (i.e. on the day of the vitrectomy) and six weeks after pars plana vitrectomy.

Results: Swept-source technology successfully managed to acquire angiograms penetrating the VH. Motion artefacts and automated segmentation errors were evident. OCTA showed a reduction in the size and calibre of the diabetic fibro-vascular complex (i.e. NV) upon imaging on the day of the vitrectomy in all the cases. Consequently, there was less traumatic dissection of the fibro-vascular membranes during pars plana vitrectomy and thus reduced chance of intraoperative and postoperative vitreous cavity bleeding. One case showed mild haemorrhage in the posterior vitreous on the second day post-injection

Conclusion: SS-OCTA proved to be an important tool in monitoring the regression (or otherwise) of NV features even in the presence of VH. IVB is highly effective within two days in reducing the vascularity of diabetic fibro-vascular membranes which is demonstrable on the OCTA. Outcomes could

provide guidance on the timing of bevacizumab before pars plana vitrectomy in the management of diabetic TRD.

2.3.2 INTRODUCTION

Tractional retinal detachment is a leading cause of vision loss in patients with PDR.[310] Pars plana vitrectomy is a successful surgical procedure for the complications of PDR such as TRD.[311] However, intra- and post-operative VH represents a significant complication of the vitrectomy procedure occurring in 20% to 30% of cases.[312-314] It has been hypothesized that VH tends to occur after pars plana vitrectomy for diabetic TRD because of difficulty of haemostasis during surgery, NV stimulated by the sclerotomy site and residual contracting vitreous.[315-319]

Intravitreal bevacizumab (IVB), an inhibitor of VEGF, performed one to twenty days before vitrectomy has been reported to prevent recurrent VH after vitrectomy for PDR by reducing neo-vascular activity.[320]

In this study swept-source-based OCTA was utilised to assess the effectiveness of IVB changes on the active proliferative fibro-vascular network in a series of patients prior to pars plana vitrectomy surgery for diabetic TRD. The primary study objective was to test the capabilities and potential advantages of swept-source technology in cases with signs of NV, potential haemorrhage and irregular retinal layers. This study also provided an opportunity to utilise the vitreous segmentation techniques described in Chapter 2.2.

2.3.3 METHODS

Three diabetic patients with similar characteristics of active PDR with signs of NV, TRD and VH were identified, approached and enrolled in this study during February 2016. One of the participants had early signs of cataract.

Participants were imaged with Topcon's SS-OCT Triton as follows:

- Immediately before IVB 1.25 mg/0.05ml
- On the second morning after the injection and prior to the pars plana vitrectomy procedure
- Six weeks after pars plana vitrectomy once the gas tamponade (if used) had been absorbed

The scanning patterns of the acquired scans were 3x3mm and 6x6mm, positioned primarily over the macular area and over the optic disc. In cases that it were deemed appropriate further scans in targeted areas were obtained.

Topcon ImageNet 6 software was utilised to perform segmentation of the retinal layers. At first, automated segmentation of the superficial and deep retina and the choriocapillaris was performed, with manual point-by-point modifications afterwards when appropriate. The VRS and OVS protocols, as described in Chapter 2.2, were also utilised. No particular quantitative metrics deriving from the OCT-based angiograms were collected; study outcomes were based on the experience (and difficulties encountered) on

utilising SS-OCTA and the ability to detect and monitor NV features as evaluated from two clinicians who independently reviewed the OCTA series of every patient.

2.3.4 RESULTS

OCTA images from all participants were successfully acquired at every time interval demanded by the study protocol. The cataract observed in one of the participants did not dramatically affect the quality of the OCTA images. In all the OCTA images acquired two days after the IVB procedure there was a decrease in the reflectivity and the density of NV features, inter-reviewer agreement 100%; such a decrease shows a regression of the NV process. VH occurred in one patient two days after IVB and was successfully captured by the SS-OCT device. Swept-source technology successfully managed to penetrate the haemorrhage and acquired scans of adequate clinical quality. The patient suffering from VH, however, had significant difficulty in fixating; therefore, the motion artefacts on the generated angiograms were evident. Nonetheless, the generated OCT B-scans and angiograms were deemed of adequate quality and great clinical importance.

After 6 weeks post-operation there were no signs of NV in all three eyes. No VH or postoperative retinal detachment was evident in any OCTA scan. Further manual segmentation and adjustment of the reference planes were

required for all the OCTA series. Concerning the operation of the vitrectomy, no intra-operative complications were observed during the pars plana vitrectomy, while there was no significant bleed from the segmentation and delamination of the fibro-vascular complex during the intervention. Figures 2.15-17 provide images with descriptions from the 3 patients across the study timeline.

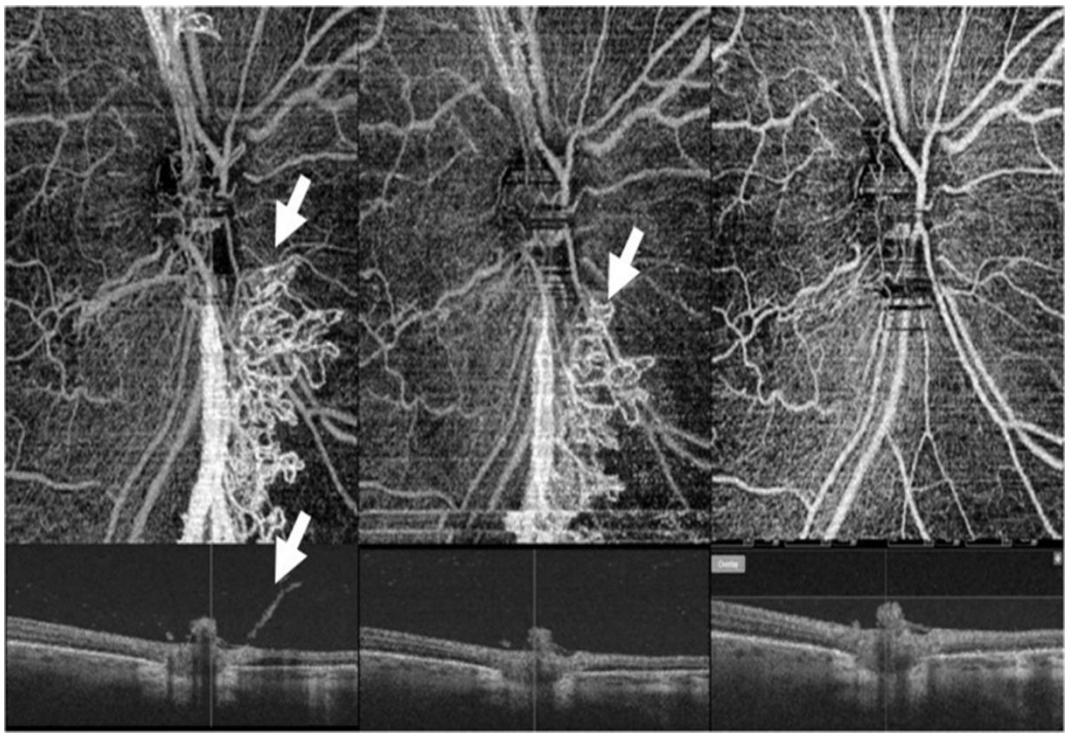

Figure 2.15: *SS-OCT B-Scans (bottom row) and angiograms (top row) over the optic disc of a 45 year-old female. Left to right columns: images before intravitreal* bevacizumab (IVB)*, two days after IVB and 6 weeks after pars plana vitrectomy. White arrow highlights the superior edge of the fibro-vascular membrane (i.e. neovascular feature) before and 2 days after IVB, indicating regression of the neovascularization process. There is no sign of neovascularization 6 weeks post-vitrectomy. Minor artefacts (motion and projection) are also evident in all 3 angiograms.*

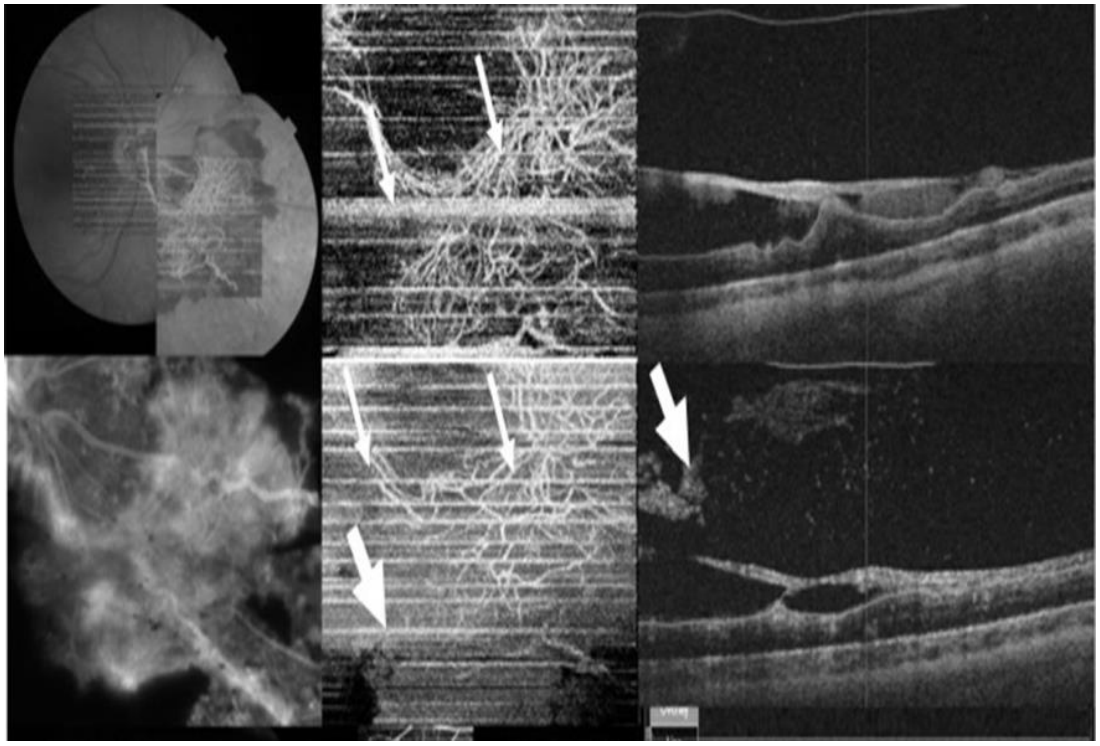

Figure 2.16: *SS-OCT B-scans and angiograms from a 55-year old male. Acquired images before intravitreal* bevacizumab *(IVB; top row) and two days after IVB (bottom row). Small white arrows highlight the reduced size and branching of the vascular complex 2 days after IVB (OCT angiogram at bottom middle). Mild haemorrhage in the posterior vitreous on the second day post-IVB is also evident in the fundus image (bottom left) and highlighted with the big white arrow in both the B-scan and the angiogram. Note the OCTA image at the bottom and the significant amount of motion artefacts (white lines), the effect of the haemorrhage on the quality of the angiogram (but not the B-scan) as well as projection artefacts at the lower corners of the image.*

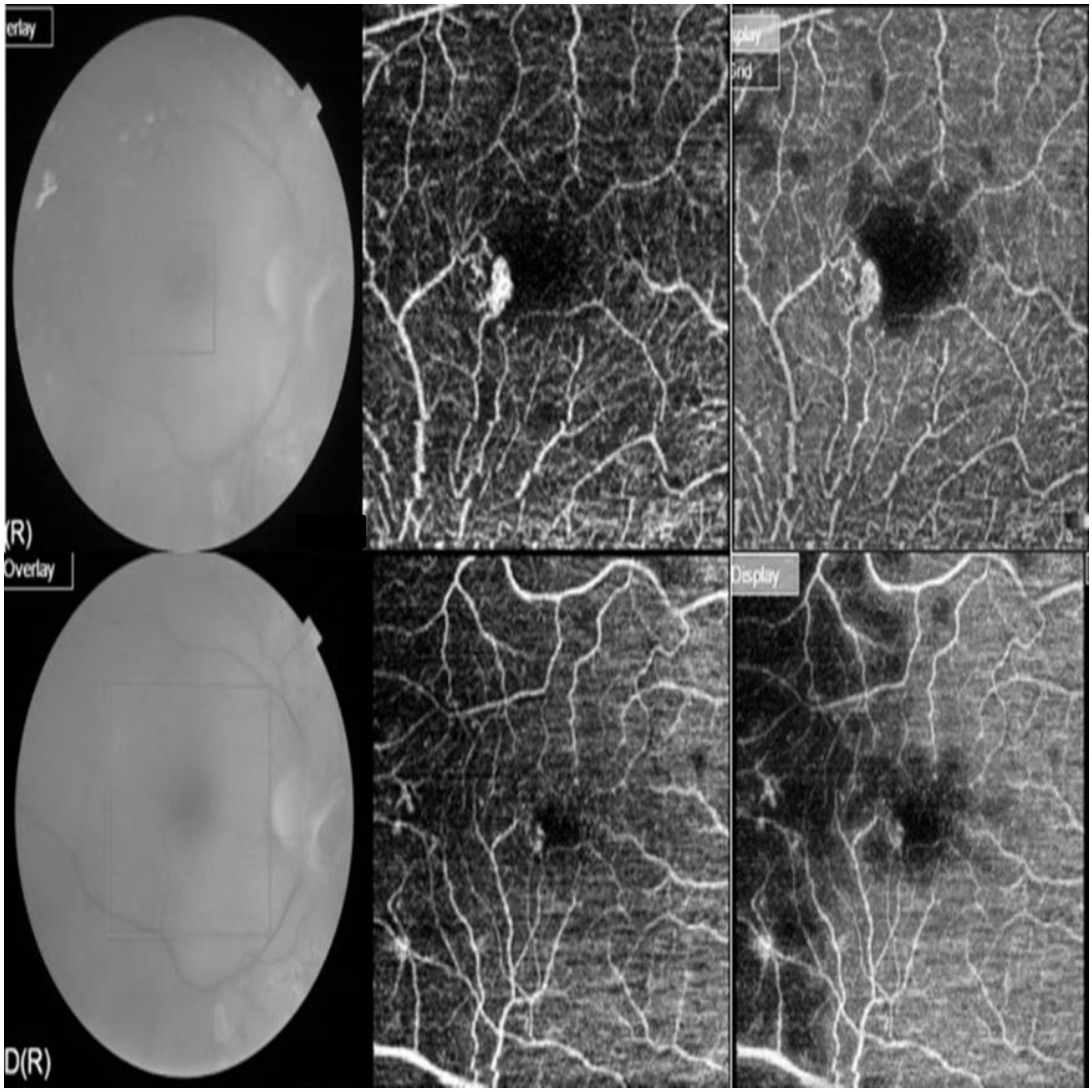

Figure 2.17: *Fundus images (left column), SS-OCT angiograms (middle column) and vascular density maps (right column) of a 30 year-old female with early signs of cataract. Regarding the vascular density maps, prototype software allowed for the representation of retinal vascular density in a greyscale with darker shades of grey indicating sparse vascular complexes while lighter shades representing dense networks. Top row shows images (3x3mm) before the intravitreal injection of bevacizumab while bottom row images (6x6mm) are from two days post-injection. Note in the vascular density maps the effect of bevacizumab were sparse vascular complexes are visualized temporally as well as the decreased size of the active proliferative*

retinal vessel implying the reduced vascularization of the retinal vessel and reduced risk of POVCH. Early cataract did not affect the image quality of the angiograms.

2.3.5 DISCUSSION

This study collected OCTA data from 3 patients diagnosed with DR and signs of TRD. Their scheduled treatment involved the intravitreal injection of an anti-VEGF agent (bevacizumab) two days before a surgical intervention (vitrectomy). SS-OCTA images were acquired before the injection, acting as baseline images, on the day of the pars plana vitrectomy and 6 weeks after treatment.

As described previously, swept-source technology benefits from a longer wavelength and increased scanning speed. Both features proved very useful when imaging participants with non-transparent media; one with early signs of cataract and another with VH. In particular, early cataract did not affect the quality of the angiograms where the vascular layers were clearly seen, Figure 2.17. Haemorrhage in the vitreous, however, reduced the clarity of the images. Figure 2.16 shows the presence of a ‘hazy film’ on the angiograms; the B-scans on the other side were unaffected. This reduction in the clarity of the angiograms, though, did not significantly affect the sensitivity to detect a reduction in the size and density in the neovascular complex, according to

the two clinicians. Future image processing techniques could remove the ‘hazy film’ and enhance the contrast of the angiogram.

The need for an eye tracking system that would reduce or eliminate motion artefacts was evident in this study. Most of the images suffered from the presence of white lines, an indication of a saccadic movement during acquisition. Patients undergoing pars plana vitrectomy are likely to present later with VH, a feature that significantly affects their vision and ability to maintain fixation. Fixation problems were largely the cause of the long imaging sessions (approximately 20 minutes) needed to capture OCTA images of adequate quality from the study participant with VH, see Figure 2.16. Such a long session may not always be clinically feasible. The introduction eye tracking systems in commercially available devices has improved the quality of generated angiograms dramatically; although acquisition of a single (albeit motion artefact free) scan may take up to 10 minutes per eye.

A significant difficulty, observed in the OCTA images of these patients, was with the automated segmentation algorithms. All acquired images (i.e. those not discarded due to artefacts) required further adjustments on the segmentation reference planes to achieve optimal visualisations. The presence of TRD and the relevant retinal irregularities could account for errors in automated segmentations. The modifications in the reference planes took only a short time (~5 minutes), although particular images required a point-by-point fine-tuning of the segmentation. Currently available commercial OCT devices still struggle to correctly identify retinal layers in pathologies, such as macular oedema, retinal detachments etc.[268, 321,

322] Current upgrades to the image processing software, however, have assisted the process of manual segmentation. For example, Heidelberg's Spectralis would need the adjustment of a reference plane at 3-4 points before interpolating the whole plane and positioning it to the right layer while Optovue's OCTA instruments allow for the marking of intraretinal cystoid spaces and the adjustment of the planes above and below that space.

A secondary outcome (or rather observation) of this study was the potential effectiveness of intravitreal injection of bevacizumab two days prior to the operation. Smith and Steel investigated the use of anti-VEGF for prevention of post-operative vitreous cavity haemorrhage for PDR and concluded in their Cochrane review that the use of pre or intra-operative bevacizumab lowers the incidence of early post-operative vitreous cavity haemorrhage with no local or systemic complications of IVB.[320] However, the effect on late post-operative vitreous cavity haemorrhage was uncertain. Different authors have advocated different timelines for IVB use, from one day to three weeks pre-operation, including some who give IVB at the end of the surgical process.[320-323] A long delay from IVB to the day of the intervention also increases the change of progression in pre-existing TRD.[322]

These clinical findings influenced the clinicians' decision to choose a shorter timeframe (two days) to proceed to pars plana vitrectomy after the IVB. This study demonstrated that IVB can be effective at two days pre-operation confirmed with the OCTA findings. It was highly effective in reducing vascularity of diabetic membranes, in turn leading to increased ease of surgical dissection and reducing the chances of post-operative vitreous cavity haemorrhage.

2.3.6 CONCLUSIONS

Swept-source technology-based OCTA was successful in depicting the presence of NV features in cases with non-transparent media. Despite the presence of motion and projection artefacts and automated segmentation errors that required manual fine-tuning, the generated angiograms were able to assist in clinical decisions. Further advancements in both the acquisition of OCT-based angiographic images (e.g. faster scans, eye tracking system etc.) and the processing of OCTA data could enhance the clinical role of OCTA in DR clinics. Future research in the capabilities of the available OCTA technologies could attempt a direct comparison between SS- and SD-OCT and different angiographic algorithms.

The encouraging result on the effectiveness of IVB before the vitrectomy in diabetic TRD from this case series, albeit the small sample, should warrant further research and the design of a randomised controlled trial to confirm the optimum time frame for the use of intravitreal injections of anti-VEGF agents. OCTA has proven to be a valuable tool for such research, although functional assessments, such as visual acuity measurements, should also be included.

2.4 Swept Source Ocular Coherence Tomography Angiography Assessment of the Foveal Avascular Zone in Superficial and Deep Vascular Plexuses: a Potential Prognostic Tool for Proliferative Diabetic Retinopathy

Contributions

My exposure to a vast number of OCTA images and clinical cases allowed for a specialisation in distinguishing between normal and abnormal retinal features and structures, especially in eyes with a diagnosis of diabetic retinopathy. It was very soon that I recognised the FAZ area as a region of interest for this cohort of patients and more particularly as a potential biomarker for progression to the proliferative form of the disease. It was therefore tempting to undertake a study whose focus would be the FAZ area.

This study tests the hypothesis that the surface of the FAZ could act as a surrogate of progression in DR; an idea conceived by Mr Francesco Stringa (Clinical Research Fellow) and myself while evaluating the quality of OCTA images in DR patients. The study was designed by both of us, while Mr Stringa identified potential study participants during his clinics. My contribution also involved the acquisition of OCTA images, data collection, analysis and interpretation. The study outcomes provided further evidence that the combination of the FAZ area in the superficial and deep levels could indicate progression. However, the small number of patients did not allow for strong conclusions.

Presentations

Study outcomes were presented at a poster at ARVO 2017 in Baltimore, MD, USA.

2.4.1 ABSTRACT

Purpose: Segmented SS-OCT angiography (SS-OCTA) imaging of the FAZ and the parafoveal vasculature shows microvascular changes that can be correlated with the severity of DR. This study aims to assess whether alterations in the parafoveal capillary plexuses can be interpreted as a clinical biomarker of disease progression.

Methods: Observational and retrospective study of diabetic patients diagnosed with Non-Proliferative Diabetic Retinopathy (NPDR) and PDR between January and November 2016. DR was classified by two clinicians independently into three groups: mild/moderate NPDR, severe NPDR and PDR. SS-OCTA images with Topcon's Triton were acquired using the 6x6mm fovea-centred cubes scanning protocol. The area was measured using Topcon's IMAGEnet after automated segmentation of the FAZ into superficial vascular (SVP) and deep vascular plexus (DVP). The volume (vFAZ) and the ratio (rFAZ) between FAZ areas in SVP and DVP in each group were calculated.

Results: Imaging results from 59 eyes were included in this study. In all eyes, the FAZ surface area of DVP was larger than that of SVP. Mild/moderate NPDR graded eyes showed the smallest surface area of FAZ in both DVP and SVP ($p<0.01$), whereas PDR eyes showed the largest FAZ area in both plexuses ($p<0.01$). The rFAZ was significantly lower in severe NPDR eyes vs. mild/moderate NPDR and PDR eyes ($p<0.01$).

Conclusion: The surface area of FAZ in both plexuses is correlated with DR severity, increasing with severity of retinopathy. Capillary rarefaction in DVP

compared to that in SVP is more evident in severe NPDR than in the other groups. The enlargement of the FAZ surface area at the DVP level may indicate future enlargement at the superficial level and progression to PDR. Therefore vFAZ (more than rFAZ) could serve as a prognostic tool for the monitoring of DR.

2.4.2 INTRODUCTION

Diabetic retinopathy is, as previously described, a progressive vascular retinal disease and represents the main cause of visual deterioration and blindness in most developed countries.[324, 325] Histological studies have shown that capillary non-perfusion is an important aspect of this vascular disease that is related to progression.[326] In chapter 2.2 a study evaluating peripheral retinal non-perfusion by means of OCTA was thoroughly described.

It has been hypothesized that the FAZ, the region of human retina with the highest density of cone photoreceptors and oxygen consumption, can be more sensitive to hypoxemia than any other part of the retina.[327, 328] The microvascular structure of this area consists of three capillaries networks: the superficial retinal plexus SRP located in the RNFL and two vascular layers located at the inner and outer border of the inner nuclear layer INL, which together form the deep retinal plexus.[329] The photoreceptor layer and the FAZ are supplied by the choriocapillaris.[330] The deep retinal plexus can provide nutrition to the photoreceptor zone (Henle's layer) in cases of systemic hypoxia when the choriocapillaris is unable to meet the demands of the photoreceptors.[331] Previous studies have pointed out that impairment of retinal microvasculature can be present at early stages of DR or even in diabetic patients with no clinical signs of DR, underlying the high sensitivity of parafoveal capillaries to hypoxemia.[326, 332]

Dilated biomicroscopy fundus examination is considered to be the gold standard to screen and assess the progression of DR. FA is more sensitive than dilated biomicroscopy fundus examination and previous FA-based studies have shown various grades of retinal hypo-perfusion in patients with DR.[326, 333] FA limitations have been highlighted elsewhere with those more prominent being the bi-dimensional nature of the generated angiograms, the prolonged assessment times and the potential accompanied risks.

Recent comparative studies have shown that OCTA can provide quantitative changes of the perifoveal capillary plexuses in diabetic patients with and without DR.[334-337] However, the sample size of most of these studies was limited, with study patients not stratified according to different severity levels of the disease, such as non-proliferative and proliferative DR. The relationship between the measured area of FAZ at both plexuses and the progression of DR is still a matter of conjecture. Therefore, the aim of this study was to explore the anatomical differences of the parafoveal capillary plexuses, by utilising SS-OCTA, in patients with DR and assess their potential to act as clinical biomarker of disease progression.

2.4.3 METHODS

This was a retrospective observational study, carried out at the diabetic clinics at MREH, supervised by Prof Stanga. From January to November

2016, patients previously diagnosed with DR and routinely examined at the MREH were identified and invited to participate in this study. The exclusion criteria included the following: neovascular AMD, retinal arterial or vein occlusion, inherited macular disease, intermediate or posterior uveitis and macular scarring. Also eyes were excluded if they had previously been treated with pan-retinal photocoagulation or any type of intraocular surgery (except cataract surgery). OCTA images of eyes with signs of clinically significant macular oedema (CSMO) were not included in the statistical analysis. For the purposes of this study CSMO was defined according to the Early Treatment Diabetic Retinopathy Study (ETDRS) standards as: thickening of the retina at or within 500 μm of the centre of the macula; hard exudates at or within 500 μm of the centre of the macula, if associated with thickening of the adjacent retina; a single or multiple zones of retina thickening 1 disk area or larger, within 1 disk diameter from the centre of the macula.[338]

All eyes had ultra-wide-field colour fundus photography with Optos California® and underwent dilated funduscopy examination as part of the standard care. The results from these assessments were used to identify potential study participants. Enrolled study patients subsequently had both eyes images with Topcon's Triton SS-OCTA device.

The examined eyes were classified, according to the ultra-wide-field colour fundus photography images, into three groups: 1) mild/moderate NPDR - retinal changes, e.g.microaneurysms, but not meeting the definition of severe NPDR; 2) severe NPDR - any of the following: more than 20 intraretinal hemorrhages in each of the four quadrants; definite venous beading in two or

more quadrants; prominent intraretinal microvascular abnormalities in one or more quadrants; no signs of proliferative retinopathy; and 3) PDR - one or more of the following: NV, vitreous or pre-retinal haemorrhage. These criteria are in accordance to the modified ETDRS severity scale.[333] Ultra-wide-field colour fundus photography images were graded by two independent observers whose agreement was found to be 100%.

The acquisition of OCTA images involved 6x6mm cube scans over the foveal area. The generated OCT angiograms were subsequently segmented automatically, and as described in chapter 2.2.

The FAZ was defined as the area of absence of motion contrast inside the central border of the capillary network (example in Figure 2.18). The FAZ surface area from both the superficial and deep vascular layers (SVL and DVL respectively) of every included eye was manually measured. The ratio (SVL/DVL, called rFAZ) between areas for every study eye was calculated. The volume (vFAZ) was estimated in a similar way of assessing the volume of the frustum of a cone. The equation (5) is:

$$V = \frac{\pi h}{3} (R^2 + Rr + r^2) \qquad (5)$$

where *R* is the radius of the lower base (or the DVL in this case), *r* is the radius of the upper base (or the SVL) and *h* is the height between the two bases; see schematic example in Figure 2.19.

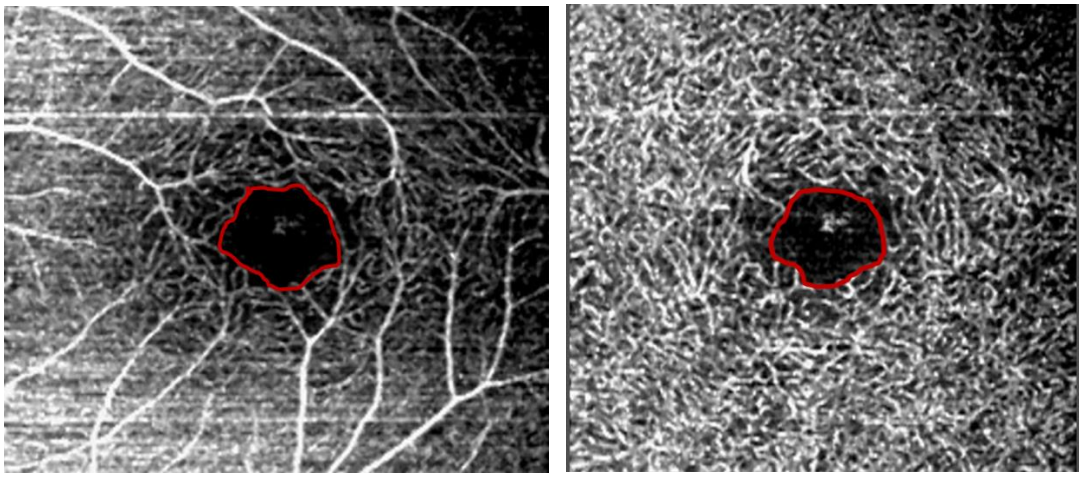

Figure 2.18: *The foveal avascular zone highlighted with a red marker in the superficial (left) and deep (right) capillary plexus. OCTA images courtesy of MVR Lab Imaging Database*

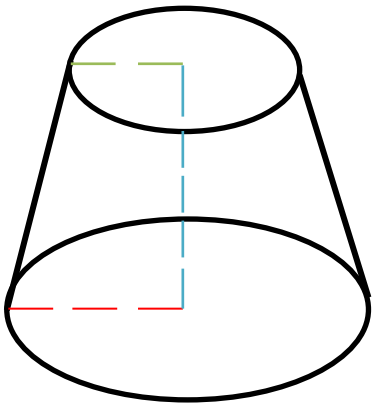

Figure 2.19: *Schematic of the frustum of a cone. Blue dashed line indicate the height (h), red and green dashed lines indicate the radius of the lower (or deep retinal) base (R) and the upper (or superficial retinal) base (r) respectively*

The radii, *R* and *r,* were calculated from the greatest linear dimension of the marked FAZ area (in DVL and SVL respectively). The height *h* was measured in microns from the upper boundary of the superficial retinal layer block (i.e. the internal limiting membrane) to the junction between the outer plexiform and outer nuclear layers; that is the lower boundary of the deep retinal layer compartment. Area and line measurements were performed by utilising the in-built 'measurement' tools of IMAGEnet. The area measurement tool calculates the outlined area in pixels and converts it to microns. A similar conversion from pixels to microns occurs for the line measurement tool. Two independent examiners accomplished the measurements and the mean between their assessments was used to establish 'true' values.

Statistical analysis was performed in SPSS statistical software version 21 (SPSS, Inc., IBM Company, Chicago, IL, USA) and included: descriptive statistics, normality tests for the all the measurements among the 3 groups and comparison of the cohorts with one-way ANOVA with Tukeys post-hoc test for normally distributed data or the Kruskal-Wallis test otherwise.

2.4.4 RESULTS

Eighty eyes were initially identified from the diabetic clinics. Fifteen eyes were excluded because of presence of CSMO or because of previous PRP treatment. Sixty five eyes of 41 patients (mean age: 60.5±13.8 years) were

included in this study. Twenty-three eyes were graded mild/moderate NPDR, 21 severe NPDR and another 21 with PDR.

The median FAZ area in both plexuses was largest in eyes with PDR and smallest in eyes with mild/moderate NPDR. In all groups the median FAZ area of SVL was smaller than the median FAZ area of DVL. The median rFAZ in eyes with severe NPDR was significantly lower than mild/moderate NPDR ($p=0.01$) and PDR ($p<0.001$); indicating that the area of FAZ in the deep plexus enlarges at a faster rate than the superficial layer before progressing to the PDR stage. Full details of the measured FAZ areas in both plexuses are given in Table 2.3. Figure 2.20 illustrates boxplots of the distribution of the rFAZ in the 3 different groups.

	Mild NPDR (n=23)	**Severe NPDR (n=21)**	**PDR (n=21)**
Median FAZ-SVL	263.7†	394.3$^{¥}$	547.1$^{¥\dagger}$
Median FAZ-DVL	400.7*†	775.0*	799.8†
Median height *h*‡	120.0	133.5	143.0
Median rFAZ	0.68*	0.55$^{¥*}$	0.73$^{¥}$
Median vFAZ‡ (x10^{3})	48.27	110.29	167.90

Table 2.3: *Median measurements of the foveal avascular zone (FAZ) in the superficial (SVP) and deep vascular plexus (DVP) for the 3 cohorts of non-proliferative (NPDR) and proliferative diabetic retinopathy (PDR).*

*Calculated ratios (rFAZ = SVP/DVP) and volumes (vFAZ) are also provided. The symbols shown are: *=R1/R2 significance, ¥=R2/R3 significance, †=R1/R3 significance, ‡= significance between all groups*

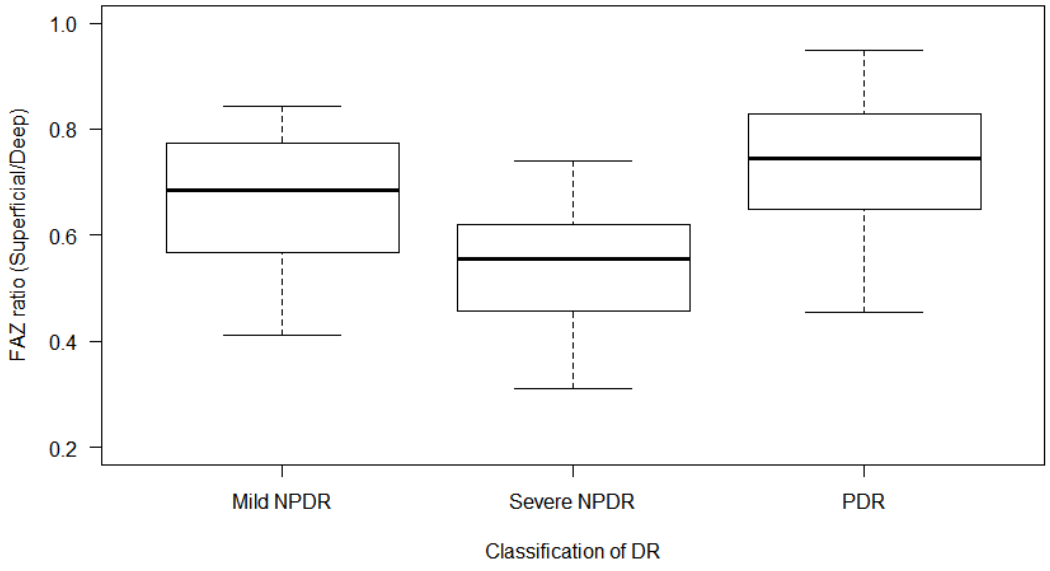

Figure 2.20: *Boxplots of the foveal avascular zone (FAZ) ratio distributions for the 3 groups of non-proliferative (NPDR) and proliferative diabetic retinopathy (PDR).*

The distance between the internal limiting membrane and the inner plexiform/inner nuclear layer boundary was measured to establish the height *h* of the frustum, according to equation 5. The median height *h* was found to be significantly different among the 3 cohorts with an increasing trend. Subsequently, the volume of the FAZ area increased significantly through the

3 groups of DR severity. Figure 2.21 shows distribution boxplots of the vFAZ in the 3 different groups.

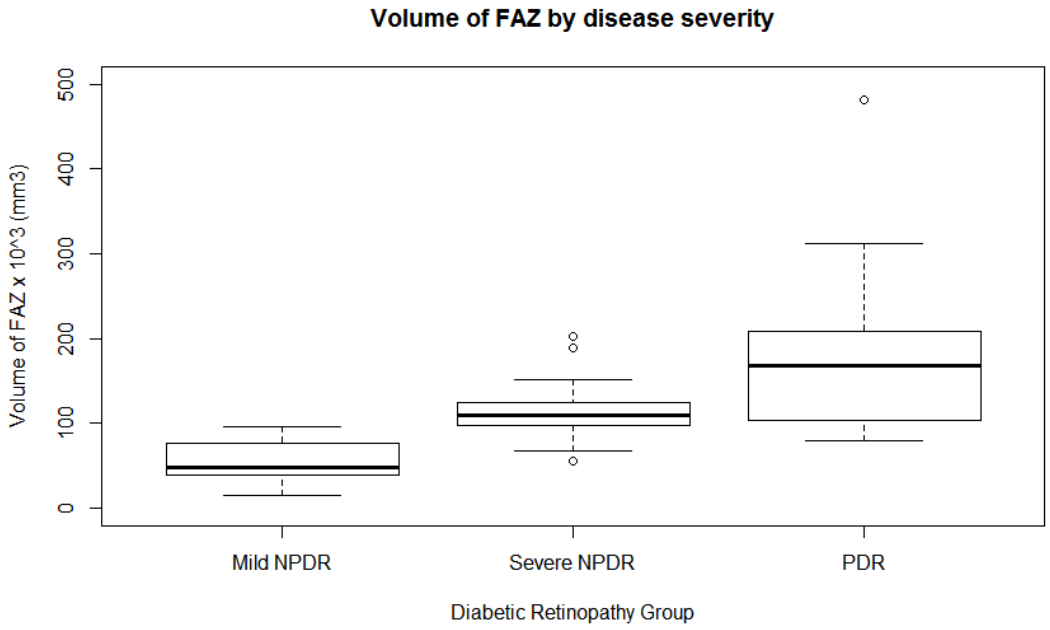

Figure 2.21: *Boxplots of the foveal avascular zone (FAZ) volume distributions for the 3 groups of non-proliferative (NPDR) and proliferative diabetic retinopathy (PDR).*

2.4.5 DISCUSSION

The FAZ is a capillary-free region of the retina encircled by a fine capillary network, that underscores the extraordinary specialization of the fovea for high visual acuity.[293] When a lesion occurs in this site, severe vision loss

can follow and small changes in the regulation of blood supply can cause significant tissue damage. Therefore, given its susceptibility to hypoxemia, it is not surprising to find that the FAZ area is larger in retinal vascular diseases such as DR.[339]

Much of our initial understanding concerning the in vivo topology of the parafoveal microvascular network in the human retina has been attained from studies that utilized FA. These studies showed that not only FAZ area is related to the presence of DR but also to the severity of capillary non-perfusion, and FAZ enlargement can represent an indicator of progression.[340]

Nevertheless, the area of FAZ varies considerably among healthy eyes and factors such as age and sex can be related to its size.[341, 342] These results have been recently corroborated by authors using OCTA technology.[274, 343] Ishibazawa et al. showed that SD-OCTA can clearly visualize the edge of retinal non-perfused areas in DR, whereas it appeared fuzzy with FA. They also found the non-perfused foveal area to be larger in the DVP than SVP.[305]

This study confirms that the area of FAZ in both plexuses was larger in PDR-graded eyes rather than NPDR eyes. Also, eyes graded with mild NPDR showed the smallest FAZ area in both plexuses a finding consistent with previous studies.[336] A detailed review of the data in Table 4 shows an increase of the FAZ area in the deep retinal layers as the severity of NPDR increases. A finding that suggests that the capillaries located at the inner and external border of the INL (i.e. deep retina), which are more distal to the

central retinal artery and have a smaller diameter,[329] could be more sensitive to hypoxemia compared to those located in the nerve fibre layer (i.e. superficial). Therefore, the perifoveal DVP could be more unstable than perifoveal SVP in conditions of altered blood supply.

The ratio of FAZ area, defined as superficial over deep (i.e. SVP/DVP) measurements, was calculated and utilised to confirm the above hypothesis. Indeed, the median rFAZ measured in patients with severe NPDR was significantly lower than the two other groups. In other words, the fraction of capillary rarefaction in both plexuses seemed to be similar at early stages of NPDR and PDR, while in severe NPDR, the difference between the areas of FAZ in both plexuses was more significant, due to a relatively higher amount of non-perfused areas in DVP.

In clinical practice, dilated fundus examination is currently the gold standard to examine DR patients. However, assessing and grading diabetic vascular changes with dilated funduscopy examination is not always easy and some information could be missed during the follow-up. Recent research (including this study report) has shown that OCTA could potentially play an important role in monitoring DR progression. The rFAZ, albeit useful to confirm the notion that deep retinal layers are further affected by hypoxia compared to the superficial layers during progression of NPDR, does not provide a suitable index to monitor deterioration (and potentially conversion to PDR) in a simple linear form.

An alternative approach was investigated where the hypoxic areas between the superficial and the deep layers were treated as a cone frustum. The

distance (or height) between the upper retinal layer of the superficial ‘block’ (i.e. the ILM) and the lower boundary of the deep ‘block (i.e. the INL/IPL junction) was measured in order to estimate the volume of the frustum. The height was found to increase significantly as DR progressed from the early non-proliferative stages through severe non-proliferative to its proliferative form. As a consequence, the median volume showed significant changes and an increasing trend between the 3 disease severity groups.

The reported association between the height and disease severity can be explained the nature of the pathology is taken into consideration. DR is a vascular disease that affects the blood-retina barrier. Because of the increased vascular permeability and breakdown of the blood-retinal barrier, fluid and lipids could leak into the retina and cause it to swell. It is possible that accumulation of the above may cause the reported increase in height (or in other words a diffused retinal thickening) but without qualifying for a diagnosis of CSMO and/or causing any significant vision loss.

As recent research (including this study) has shown, capillary non-perfusion of DVP in patients with severe NPDR may predict further capillary rarefaction in SVP and potentially trigger retinal NV.[336] The ETDRS investigators found that severe NPDR had 15% chance of progression to PDR within 1 year. Also, very severe NPDR (defined by the presence of at least two of the features mentioned in the Methods section) had a 45% chance of progression to PDR within 1 year.[338] Therefore, it has been hypothesized that patients with severe NPDR could be considered for early treatment with PRP.[344] The volume of the FAZ introduced in this chapter could potentially

serve as a biomarker to detect patients with high risk of developing PDR and may be used as a tool to plan early treatment strategies to prevent further retinal damage.

Nonetheless, this study has some limitations that should be taken into consideration. First, the study population was not age- and sex-matched, which are factors that can be correlated with the SA of FAZ and could therefore have affected mean rFAZ and vFAZ measurements. Second, the repeatability of the FAZ areas acquired with the Triton OCTA device utilised in this study has not been established. The repeatability of SS-OCTA between consecutive sessions, however, has been previously studied and it has been found that FAZ measurements are highly repeatable.[345, 346]

In this study, eyes with ophthalmic pathologies that might have affected the retinal vasculature other than DR were excluded and OCTA images of eyes with CSMO were not included in the statistical analysis. The reason behind the latter exclusion criterion is that presence of CSMO could have affected the quantitative measurement because of the mechanical stress by intraretinal cysts on perifoveal capillaries. Intraretinal cysts could also generate shadow effects (i.e. projection artefacts) on retinal layers that could alter measurements of the FAZ area. The latter could be considered another limitation of the current OCTA technology.

2.4.6 CONCLUSIONS

SS-OCTA can be used to perform a non-invasive quantitative assessment of the perifoveal vasculature in patients with DR at different stages. This could prove to be beneficial for the monitoring of progression of the non-proliferative form of the pathology and its potential to convert into the proliferative type.

The impact of structural features, such as macular oedema, that usually accompany DR was not investigated; such eyes were excluded from the analysis. Hence, automated segmentation processes successfully managed to differentiate between superficial and deep retinal layers without any difficulties. This study also introduces a biomarker of progression, such as the vFAZ, that may assist in identifying patients with high risk of developing PDR. Its clinical significance, though, is yet to be determined with a longitudinal prospective study of vFAZ index (and could potentially create a classification system) but also assess the capabilities of SS-OCTA in more complicated cases with presence of retinal irregularities.

2.5 Swept-Source Optical Coherence Tomography Angiography Assessment of Fellow Eyes in Coats' Disease

Contributions

Consultants and clinical research fellows of the MVR Lab are involved in monthly paediatric clinics at MREH where Topcon's Triton SS-OCT was utilised for the purposes of assessing its angiographic capabilities as well as its usability with paediatric patients. It was therefore tempting for me to test the capabilities of the OCTA technology in such a special cohort, such as children with ages ranging from 8 to 15. Would and/or could OCTA provide an efficient alternative to the FFA for children? How much artefacts (of any type) could affect the interpretation of OCTA images? The following two studies attempted to answer these questions. This chapter presents some interesting findings in patients diagnosed with Coats' disease, where fellow eyes of Coats' patients are reported to be carrying quantitative foveal vascular alterations at the superficial layer. This work led to a collaboration between the MVR Lab team and the Department of Ophthalmology in San Raffaele Hospital in Milan, Italy. Due to the low prevalence of the investigated pathology, data from Manchester alone would not be adequate for reaching safe conclusions. My contribution involved imaging of paediatric

patients at the MREH, data analysis[3] and interpretation and preparation of manuscripts and presentations. Given the time that this study was undertaken (i.e. right after the commercial release of swept-source OCTA technology) this is effectively one of the first OCTA studies in children.

Presentations

Initial findings from MREH were presented at ARVO 2016 in Seattle, WA, USA. A manuscript was subsequently reviewed by the Retina journal. Feedback from reviewers recommended a larger sample size to ensure safe conclusions. This led to the collaboration with San Raffaele, Milan, Italy. The findings of this joint project provided stronger evidence to the conclusions made previously. A joint manuscript from both research teams has been re-submitted to the journal Retina, while there was an oral presentation at the Euretina 2017 conference. This chapter will present findings from the most up-to-date joint database, while taking into account previous reviewers' feedback and being modified accordingly for the PhD thesis purposes.

[3] Data were also independently analysed by Mr Francesco Romano from Milan, Italy to ensure correct interpretation and accuracy in the final study outcomes.

2.5.1 ABSTRACT

Purpose: To assess foveal and parafoveal vasculature at SVP), DVP capillary plexuses and choriocapillaris using OCTA in the fellow eyes of patients with Coats' disease.

Methods: Observational and prospective case series. Thirteen patients with unilateral Coats and fourteen healthy age- and sex-matched controls were consecutively recruited at MREH and the Department of Ophthalmology of San Raffaele Hospital. Both groups underwent complete ophthalmologic examination, including OCTA 3x3mm scans. Images were imported into ImageJ software and converted into a binary image; FAZ area was manually outlined and vessel density analyzed in inner (foveal) and outer (parafoveal) areas of SVP, DVP and choriocapillaris.

Results: Fellow eyes disclosed a significant increase in the foveal vessel density of SVP (P = 0.04); in particular, superior and temporal quadrants showed more marked alterations (P = 0.02 and 0.04, respectively). Analysis of FAZ area revealed a significant enlargement in the SVP (P = 0.04). No correlation was found between fellow eyes and the stage of affected eyes.

Conclusions: Fellow eyes of Coats' patients carry quantitative foveal vascular alterations at the SVP. These may represent markers of altered inner blood retinal barrier, due to a bilateral defect in mid-capillary angiogenesis.

2.5.2 INTRODUCTION

Coats' disease is a progressive retinal vascular disorder characterized by development of peripheral retinal telangiectasia, intra- and sub-retinal exudation and frequent exudative retinal detachment.[347-349] This disease preferentially affects young boys (male-to-female ratio ≈ 3:1), in the temporal quadrants and with an age at onset between 8 and 16 years;[350, 351] no ethnic associations have instead been established.[352] Etiology of Coats' disease is currently unknown; nevertheless, the association with several syndromes and genes (e.g. NDP and CRB1) would suggest a genetic component.[353-356] Patients frequently present with a wide range of signs, including loss of visual acuity, strabismus and leukocoria; however, a variable portion can be asymptomatic at diagnosis.[348]

A correct diagnosis is typically achieved by means of fundus FA, ultrasound and computed tomography.[357, 358] In 2001, Shields et al. proposed a five-stage classification, with the purpose of predicting the outcome of the disease and selecting the most appropriate treatment, particularly for more advanced stages.[351]

Despite being generally considered a unilateral disease (80-90%), recent studies have highlighted unexpectedly frequent vascular defects in the fellow eyes of these patients.[359] With regard to this, OCTA might represent the ideal technique to investigate retinal vascular networks and test for the bilateral nature. OCTA features of clinically affected eyes have already been reported in the past;[360, 361] however, no such studies have investigated

foveal microvascular alterations in the fellow eyes of patients with unilateral Coats' disease.

The aim of the present study is therefore to investigate on the microvascular features of the fellow eyes and analyze their relations with the severity of the disease in the affected eye.

2.5.3 METHODS

The study was designed as an observational and prospective clinical series in patients with Coats' disease. Written informed consent was obtained from all the study subjects and the procedures adhered to the tenets of the Declaration of Helsinki.

Patients were consecutively recruited from the paediatric vitreoretinal regional service of MREH (supervised by Prof Stanga and Mr Biswas) and from the Department of Ophthalmology of San Raffaele Hospital in Milan, Italy, from November 2015 to December 2016. Inclusion criteria of the study group encompassed clinical diagnosis of Coats' disease, confirmed by means of intraoperative wide-field digital fundus FA imaging findings (RetCam 3 – Clarity Medical Systems, Inc.), ocular ultrasound scans and computer tomography assessment. Clinical assessment was also meant to rule out history of prematurity, as well as other ocular diseases (e.g. glaucoma and pathologic myopia). Presence of clear media and stable

fixation was considered a necessary condition to allow for reliable SS-OCTA acquisition and analysis. In the event of projection or segmentation artifacts, OCTA scans were repeated; accordingly, a good signal strength was warranted for both patients and controls (Topcon Imaging Quality factor >45). A series of healthy children were considered as a control group. The control group did not reveal any ocular or systemic diseases and was age- and sex-matched with the study group. All subjects, either patient or control, underwent a complete ophthalmological examination, including best corrected visual acuity (BCVA) measurement on EDTRS charts, slit-lamp biomicroscopy, applanation tonometry, dilated fundoscopic examination, SS-OCT and OCTA. BCVA was recorded as Snellen fraction and subsequently converted in the logarithm of the minimum angle of resolution (LogMAR) for statistical purposes.

3x3mm OCTA scans were acquired with the use of Topcon's SS-OCT Triton. Compared to the previous studies described in chapters 2.2 & 2.3, an eye tracking system was introduced resulting in a significant reduction of motion artifacts (more details to follow). The acquired B-scans underwent automated segmentation into SVP, DVP, outer retina and choriocapillaris, as described in Chapter 2.2. Manual segmentation and adjustments to the reference planes were carried out when required.

OCTA 3x3 mm angiograms corresponding to SVP, DVP and choriocapillaris reconstructions were exported from the system as JPEG format and were loaded in National Institutes of Health ImageJ 1.50 (Bethesda, Maryland, USA) software (https://imagej.net/); a program that allowed further processing of OCTA images for the quantification of vessel density. The

adjust auto-threshold tool in ImageJ was set to ‘mean’ in order to highlight the blood vessels in each OCTA scan. Following this threshold each image would have white colored vessels on a black background; Figure 2.21 provides an example.

The FAZ region was manually segmented in SVP and DVP angiograms by two masked reviewers and measured with a method published previously.[362, 363] The region was marked with blue color and excluded when calculating vessel density. A circle of 1.5 mm diameter, positioned on the center of the FAZ, was placed in order to divide each image into an inner (foveal) and an outer (parafoveal) region. These two regions were further divided in four quadrants or sectors: nasal, temporal, superior and inferior. A basic image processing MATLAB script was used to obtain vessel density for SVP, DVP and choriocapillaris by calculating the percentages of white pixels compared to black and blue ones in each sector, both for inner and outer analyses.

Independent samples t-test using Statistical Package for the Social Sciences version 20.0 (SPSS, Chicago, Illinois, USA) was adopted to account for statistical significance between all measures performed. Pearson’s Chi-Square test was used to study the association between the orientation of the main FAZ axis and fellow eyes. Inter-observer reproducibility for the two masked investigators was evaluated with intraclass correlation coefficients (ICC; 95% confidence intervals). Statistical significance was set to $p<0.05$.

2.5.4 RESULTS

Overall, 13 patients were recruited with a diagnosis of unilateral Coats' disease; five of them were classified as stage 2, seven as stage 3 and one as stage 4. The analysis was specifically focused on the fellow eye. Mean age (± standard deviation) was 11.7 ± 4.0 (range, 5-17; median, 13) and BCVA of -0.04 ± 0.09 LogMAR. A single eye was examined in fourteen control subjects to make a reliable comparison; control eyes were randomly selected, seven being right (50%) and 7 left. Mean age was 11.4 ± 3.4 (range, 5-17; median, 13) and BCVA of -0.01 ± 0.05 LogMAR. Further demographic details are given in Table 2.4. No significant difference in age, sex, ethnicity, IOP and visual acuity was evident between patient and control group (p = 0.61, 0.43, 0.32, 0.69 and 0.38, respectively).

Groups	Number	Age		BCVA
		Mean ± SD	Range	
Patients	13	11.7 ± 4.0	5 - 17	-0.04 ± 0.09 LogMAR
Males	11 (85%)			
Females	2 (15%)			
Controls	14	11.4 ± 3.4	5 - 17	-0.01 ± 0.05 LogMAR
Males	11 (79%)			
Females	3 (21%)			

Table 2.4: *Demographic data of the study and control cohorts. SD = Standard Deviation, BCVA = Best Corrected Visual Acuity*

The analyses of vascular abnormalities revealed that the study eyes have an enlarged FAZ in the SVP (0.321 ± 0.117 vs. 0.244 ± 0.068; P = 0.04), whereas FAZ in DVP was similar (0.408 ± 0.118 vs. 0.414 ± 0.100, P = 0.82). Interobserver variability was acceptable for both measurements (ICC=0.945 [0.922-0.968] and 0.931 [0.919-0.943]). In addition, seven fellow eyes (53.8%) disclosed a vertical orientation of the FAZ axis; this finding was more common than in control eyes, where only two subjects (14%) showed a vertical orientation of the FAZ (Chi-squared, 4.25; P = 0.04); example given in Figure 2.22.

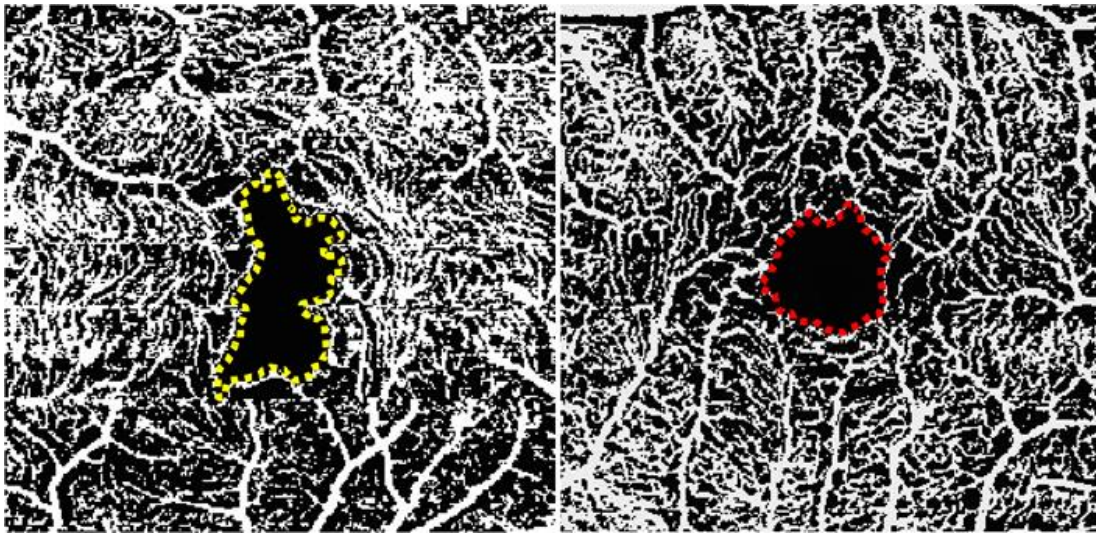

Figure 2.22: *3x3mm binarized OCTA scans showing a distorted and vertically enlarged FAZ in the fellow eye of a patient affected by Coats disease (left, yellow dashed profile). No apparent anomalies can be documented in the FAZ of a normal subject (right, in red)*

Despite the mean vascular density being similar in both SVP and DVP of the study cohort (i.e. fellow eyes of Coats' patients), the specific examination of the foveal area revealed fellow eyes to have a higher vascular density at SVP with respect to control eyes (0.37 ± 0.04 vs. 0.33 ± 0.02; P = 0.01). Figure 2.23 provides a comparison of OCTA images between control and fellow (study) eyes, while figure 2.24 and table 2.5 present full details of the quantitative analysis.

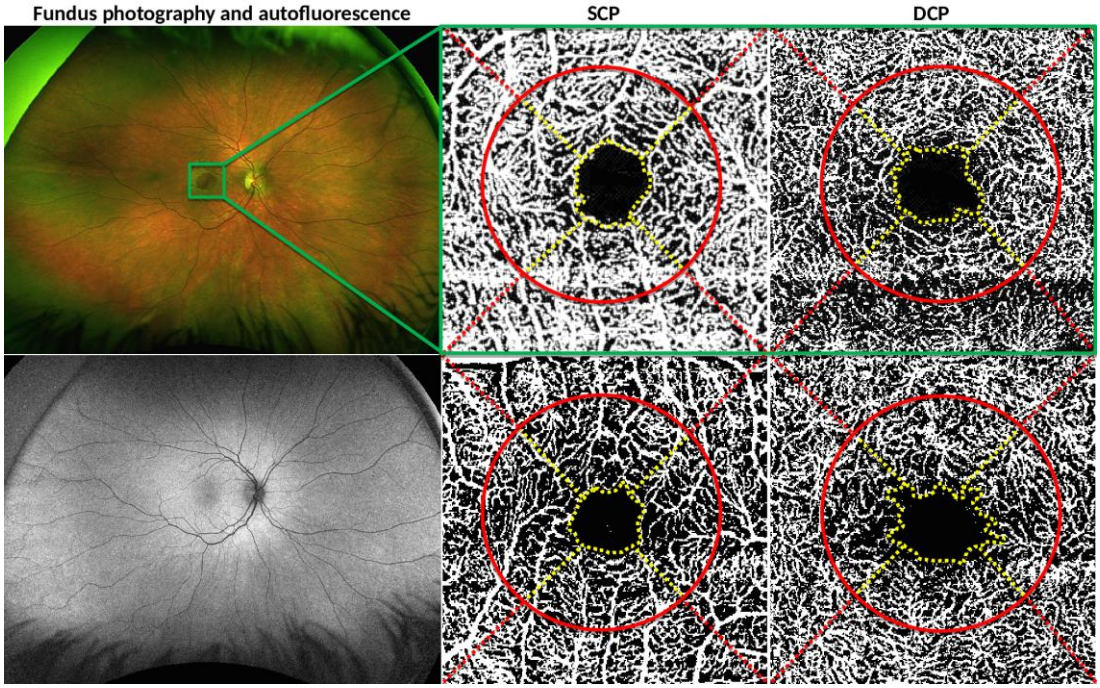

Figure 2.23: *Optos California® ultra-wide-field color fundus photography and blue light fundus autofluorescence of a fellow-study eye (left column) not displaying any clear abnormality. 3x3mm binarized scans of the SVP (center column) and DVP (right column); the divisions in parafoveal/perifoveal regions (red circle) and sectors (dashed lines) are shown. Some vascular congestion can be noticed in the parafoveal region of the SVP, especially when compared with healthy control (bottom center and right). In addition, the FAZ analysis of the SVP reveals a visibly larger area in the fellow eye.*

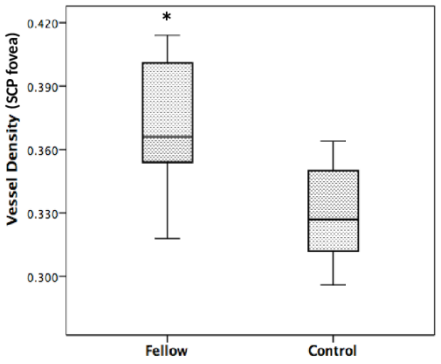
Vessel Density (SCP fovea)
0.420
0.390
0.360
0.330
0.300
*
Fellow
Control

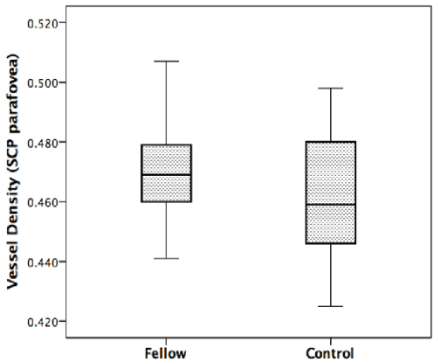
Vessel Density (SCP parafovea)
0.520
0.500
0.480
0.460
0.440
0.420
Fellow
Control

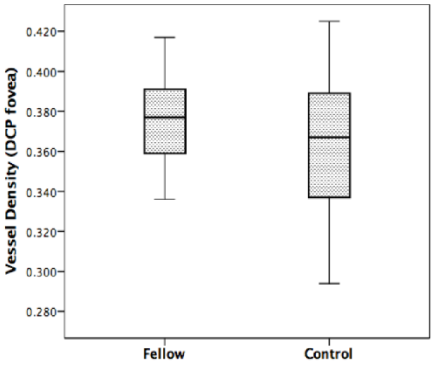
Vessel Density (DCP fovea)
0.420
0.400
0.380
0.360
0.340
0.320
0.300
0.280
Fellow
Control

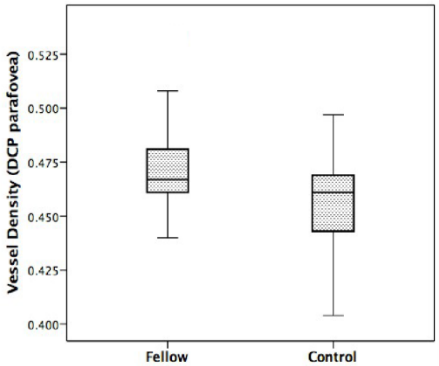
Vessel Density (DCP parafovea)
0.525
0.500
0.475
0.450
0.425
0.400
Fellow
Control

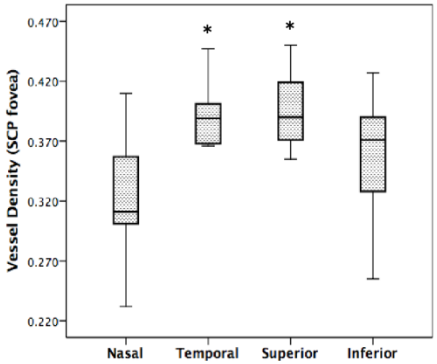
Vessel Density (SCP fovea)
0.470
0.420
0.370
0.320
0.270
0.220
*
*
Nasal
Temporal
Superior
Inferior

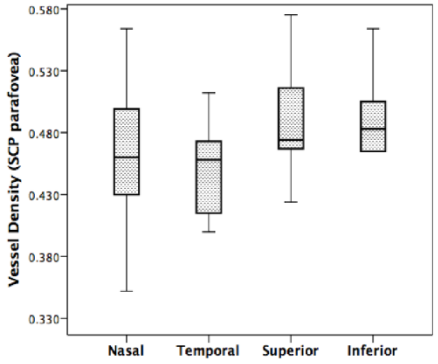
Vessel Density (SCP parafovea)
0.580
0.530
0.480
0.430
0.380
0.330
Nasal
Temporal
Superior
Inferior

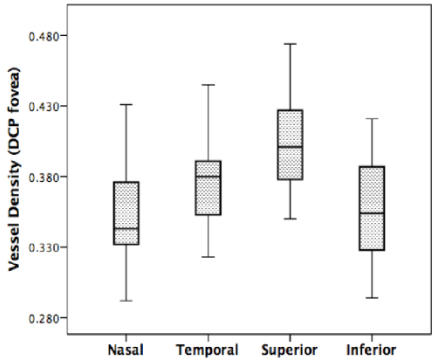
Vessel Density (DCP fovea)
0.480
0.430
0.380
0.330
0.280
Nasal
Temporal
Superior
Inferior

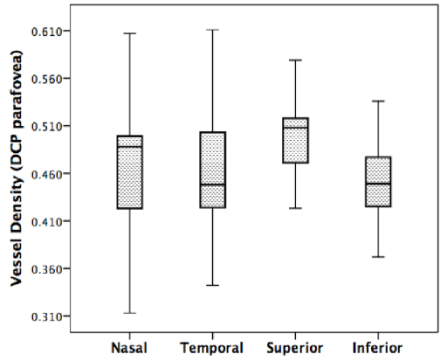
Vessel Density (DCP parafovea)
0.610
0.560
0.510
0.460
0.410
0.360
0.310
Nasal
Temporal
Superior
Inferior

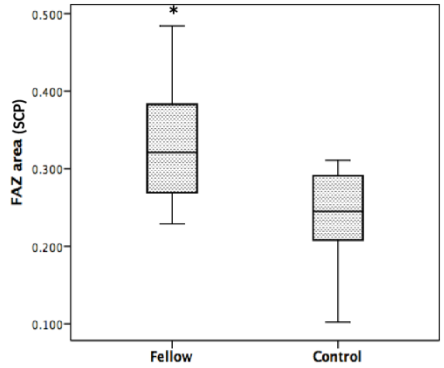
FAZ area (SCP)
0.500
0.400
0.300
0.200
0.100
*
Fellow
Control

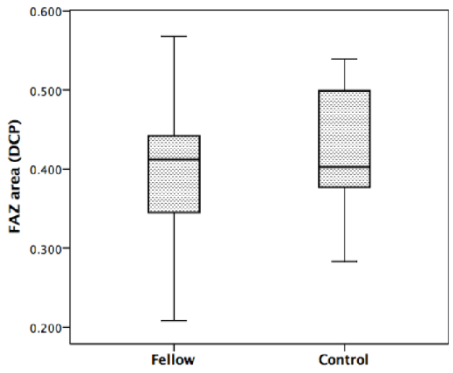
FAZ area (DCP)
0.600
0.500
0.400
0.300
0.200
Fellow
Control

	Fellow eyes	Control eyes	P**
FAZ area (SVP)	0.321 ± 0.120	0.245 ± 0.065	0.04
FAZ area (DVP)	0.405 ± 0.115	0.415 ± 0.082	0.80
SVP parafoveal	0.366 ± 0.042	0.331 ± 0.022	0.01
SVP perifoveal	0.470 ± 0.019	0.461 ± 0.030	0.34
DVP parafoveal	0.375 ± 0.025	0.363 ± 0.037	0.34
DVP perifoveal	0.473 ± 0.025	0.456 ± 0.027	0.10
Choriocapillaris	0.508 ± 0.027	0.497 ± 0.020	0.24

Figure 2.24 & Table 2.5: *Quantitative analysis of fellow and control eyes. FAZ = Foveal Avascular Zone; SVP = Superficial Vascular Plexus; DVP = Deep Capillary Plexus*

The assessment of the SVP vascular density in the different retinal quadrants of the study eyes revealed that the temporal and superior sectors of the foveal region have a more extensive vascular congestion than the nasal sector (0.38 ± 0.05 and 0.39 ± 0.05 vs. 0.32 ± 0.06; P= 0.04 and 0.02, respectively). Three study eyes (23.1%) disclosed signs of mid-peripheral non-perfusion on fundus FA. The analyses of the various sectors for a potential correlation between OCTA vascular alterations in the fellow eye and the stage of the affected eye revealed no statistically valid associations (P = 0.09 to 0.94).

2.5.5 DISCUSSION

Coats' disease was historically considered a unilateral retinal vascular disorder, with only few bilateral exceptions. The investigation of vascular impairment in Coats' disease has therefore been focused on the affected eye, and no in-depth information is currently available in the literature about the condition of the fellow eye. For this reason, this study explicitly focused on the fellow eyes by means of OCTA, which represents an ideal tool to investigate subtle vascular abnormalities in vascular disorders. Despite the unclear role played by genetics in the etiology of the disease, as testified by some controversial results, recently the hypothesis of a genetic contribution has been advanced by the description of an abnormal peripheral vasculature in the majority of the fellow eyes, therefore promoting the idea of a bilateral condition.[353, 359, 364, 365] From this perspective, Coats' disease might be intriguingly considered the result of a bilateral defect in midcapillary angiogenesis, with aneurysmal dilations as secondary abortive features.[366] In another study by Muakassa et al. using OCTA to analyze the FAZ in Coats disease, abnormalities were also reported in 50% of fellow eyes of an older cohort of patients than the study group presented in this chapter.[360] The authors, however, performed only a qualitative analysis of the FAZ, revealing an indistinct profile with anomalous vessels crossing over the central zone.

This report quantitatively demonstrates, by means of OCTA, that the spectrum of vascular impairment of Coats disease is not merely confined to the clinically affected eye. The microvascular changes in the fellow eyes are

presented for the first time demonstrating the bilaterality in this disease. Indeed, these subtle microvascular alterations may represent a sign of altered inner blood retina barrier. Specifically, the most involved plexus was found to be the SVP, disclosing an enlargement of FAZ and vascular congestion in the parafoveal area. The identification of a more frequent FAZ enlargement in the vertical axis might represent an additional marker of vascular alteration in the foveal area, as reported in other retinal vascular diseases.[273] Of particular interest is the finding of a greater involvement of the temporal and superior sectors in the foveal region. This finding can be considered in line with previous observation that a larger vascular impairment is generally found in the same sectors of eyes clinically affected by Coats.[351] Another intriguing feature, frequently seen in more advanced cases, is the predilection for the affected eyes to have a central macular location for chronic exudate, despite the predominant location of vascular telangiectasia in the periphery. These microvascular changes located within the foveal region may be implicated in the pathogenesis of this feature of Coats disease.

Paediatric participants as young as 5 years of age were able to cooperate with the acquisition of OCTA images. All participants from the MREH cohort were imaged successfuly, in a relatively short time although repeated images were often required due to poor quality and motion artefacts[4]. Moreover, automated segmentation techniques successfully managed to identify retinal layers. The absence of structural irregularities in the retinal tissue must have played an important role in the correct segmentation by the ImageNet

[4] No data of this nature are available from the San Raffaele cohort

software. This report confirms the simplicity of the performance and reliability of OCTA examinations in young patients. Non-invasive and non-contact imaging techniques, such as OCTA, are considered essential for the diagnosis, management and monitoring in paediatric clinics.

In the post-image acquisition analysis, the OCTA images were exported to imageJ software and threshold adjustment was used to highlight the signal from the blood vessels prior to the image binarization (i.e. white vessels on black background). Capillary density is technically a numeric value that reflects the amount of blood vessels in a given area. In OCTA, movement of red blood cells within vessels are translated into reflectivity and, hence, blood vessels are seen. In all OCTA devices, there is a limitation, or threshold, of movement that would be interpreted as a "positive" signal. By exporting an image and adjusting the threshold, it is possible that vessels that are not as reflective, would be effectively reduced in intensity, and by manually thresholding, data may be lost. In other words there may be a "wash out" effect on low reflectivity capillaries in the OCTA image.

One way to negate this is to use a standardized, preset, auto thresholding analysis, of which several are available within imageJ. The “mean” threshold utilised in this study is indeed one of the “autothreshold” options available on ImageJ. All the currently available options intrinsically bear pros and cons and represent proposed methods to evaluate angiograms; in other words, evidence of superiority of one method over the other is not present yet. Preseting thresholds and applying to every OCTA image might include some artifacts or lose important signals, as minimum and maximum intensities have broader variabilities in a pediatric population. Consequently, the

adopted scheme (“mean” auto thresholding) can confer some advantages in such young population, as minimum and maximum intensities are independently assessed for each patient and control. To ensure that the product of this process represents the actual OCTA image fairly accurately, a visual inspection of the scans, pre- and post- binarization, was performed by two examiners who agreed on the preservation of a correct vascular profile.

Figure 2.24 provides box-and-whiskers plots to better visualise all the statistical results and to give a sense of the difference between the two groups. Those plots show that there is inadequate separation between the populations in the two samples to provide diagnostic meaning; considering that the diagnostic value is different from the significant difference of means. However, the reported findings are quite suggestive of real microvascular alterations occurring in the fovea of these fellow eyes.

It is noteworthy that this study relied exclusively on OCTA data to reach its conclusions; undoubtedly these findings deserve deeper investigation, coupling other examination modalities (e.g. microperimetry and multifocal electroretinography) in order to accurately characterize the level of the anatomical and functional impairment in patients affected by Coats. Other study limitations are the limited number of patients and the absence of a longitudinal follow-up. Moreover, it should be noted that the majority of these patients (54%) received intravitreal injection of anti-VEGF antibodies in the affected eye, prior to their fellow eyes being imaged with OCTA. Injection of anti-VEGF intravitreally can result in systemic suppression of VEGF; accordingly, a potential effect on the fellow eye retinal microvasculature cannot be ruled out. Study observations regarding the fellow eye may prove

useful to help the diagnosis of Coats in patients with advanced stage in the involved eye. The lack of a statistical correlation between vascular abnormalities on OCTA in the fellow eye and the clinical stage of the affected eye may have been affected by the small sample size. A longitudinal follow-up is currently carried out, as a result of this study, in order to ascertain whether the vascular abnormalities progress over time.

2.5.6 CONCLUSIONS

SS-OCTA was successfully utilized in paediatric clinics to acquire angiograms in a non-invasive manner from the fellow (i.e. non-pathological) eye of a cohort of patients. Image acquisition and processing encountered no difficulties in patients as young as 5 years old; therefore offering a potential alternative to the FA.

Study outcomes report on the microvasculature of the fellow eye in patients with Coats' disease and provide evidence of bilateral involvement. Further studies are warranted to more deeply investigate the severity of involvement of the fellow eye in patients affected by Coats' Disease, including other imaging and psychophysical examinations, and to ensure that unilateral intravitreal anti-VEGF treatment does not affect the retinal capillaries of the fellow, clinically unaffected eye.

2.6 Segmented Swept-Source Optical Coherence Tomography Angiography Assessment of the Perifoveal Vasculature in Patients with X-Linked Juvenile Retinoschisis: A Serial Case Report

Contributions

Further to the investigation of OCTA capabilities in a paediatrics cohort this study reports on some interesting findings in paediatric patients diagnosed with X-linked retinoschisis (XLRS) while attending MREH's monthly paediatric clinics. My contribution included the collection of OCTA data, their analysis and interpretation as well as preparation of posters, draft manuscripts and reports. One of the main outcomes of this investigation (as a whole) was that further development in image analysis, and more particular the removal of artefacts, is required to allow the establishment of OCTA in paediatric clinics.

Presentations

Study outcomes have been presented as a poster at ARVO 2016 in Seattle, WA, USA. A manuscript of this study has been submitted, peer-reviewed and accepted for publication by the International Medical Case Reports journal.

2.6.1 ABSTRACT

Purpose: To explore the capabilities of SS-OCTA and describe perifoveal microvascular changes occurring in XLRS.

Methods: This is a serial case report of three patients. Retrospective data of patients affected by XLRS were collected. Structural OCT and color fundus photography were carried out with Topcon's 3D OCT 2000 as part of standard care. Two patients were imaged on Topcon's prototype Atlantis SS-OCTA and one on Topcon's Triton SS-OCTA. SS-OCTA images were acquired using the 3x3mm fovea-centered cubes scanning protocol. Analysis of both perifoveal superficial vascular plexus (pSVP) and perifoveal deep vascular plexus (pDVP) was performed by two clinicians after automated segmentation.

Results: Four eyes of three males (mean age 14±3.8 years) were analyzed. All eyes showed foveoschisis on color fundus photography images. OCT B-scans of three eyes showed schistic cysts in the RGC layer, INL and outer nuclear layer (ONL); in one eye, cysts were depicted in INL and ONL only. In two eyes, SS-OCTA showed abnormal FAZ shape in the pSVP; while in the other two eyes, FAZ shape was abnormal in both plexuses. In all eyes, retinal vascular abnormalities (ie, microvascular protrusions) were present in pDVP.

Conclusion: SS-OCTA can depict perifoveal microvascular changes in young patients affected by XLRS. In this study, the structural and vascular changes seem to be more evident in the pDVP and may represent a useful biomarker of prognosis.

2.6.2 INTRODUCTION

X-linked juvenile retinoschisis (XLRS; MIM 312700) is an inherited vitreoretinal degenerative disease, affecting, almost exclusively, males early in life.[367] A total of 196 different mutations in the retinoschisin gene (RS1) have been identified to be responsible for XLRS.[368] The RS1 gene encodes a homo-oligomeric complex which binds the surface of photoreceptors and bipolar cells and helps them maintain the structural organization of the synapse. It may also play an important role in the regulation of the fluid balance between the intra- and extracellular space.[369]

Foveal schisis (i.e. intraretinal splitting) is present in 98–100% of patients, and it is ophthalmoscopically seen as a spoke-wheel pattern in the macular region. Vitreous and intraretinal hemorrhages have a prevalence of 30%, while retinal detachment occurs in up to 20% of patients.[370] In young patients affected by XLRS with exudative retinal detachment or vitreous hemorrhage, several retinal vascular abnormalities have been found. These include perivascular sheathing, Coats-like exudative retinopathy and dendritiform vessels in the retinal periphery.[371, 372]

Histopathological reports showed that the foveoschisis mainly occurs at the RNFL and RGC layer.[373, 374] However, studies using TD-OCT systems have shown that foveomacular splitting can occur in other retinal layers as well; more often in deeper layers, rather than exclusively in the RNFL and GCL.[375-378] These results have been corroborated by further evidence

obtained with SD-OCT showing predominant localization of cysts at the INL.[379-381]

FA has shown FAZ enlargement and vascular leakage in patients with XLRS.[382] However, for pediatric patients, general anesthesia may also be required for those undergoing FA. There are insufficient data available to exclude the potentially negative influence of anesthesia on neurodevelopment in children.[383]

The primary purpose of this study was to describe perifoveal microvascular abnormalities using segmented SS-OCTA imaging in young patients affected by XLRS in an attempt to provide novel information on this disease. Study participants were imaged with two different OCTA devices to evaluate their usability and report on their advantages or shortcomings.

2.6.3 METHODS

This was a retrospective observational case series study. All information was routinely collected as part of standard care at the Pediatric-Vitreoretinal Clinic at the MREH between October 2015 and April 2016.

Three patients with XLRS were identified. The following data were collected to confirm XLRS diagnosis: patients' family history, personal medical history, genetic results and details of clinical examination. All eyes were imaged on

Topcon's 3DOCT 2000 which provided structural OCT and color fundus photography images. Two patients were imaged on Topcon's prototype OCT-1 Atlantis, while the other patient was imaged on Topcon's Triton.

The Triton device was effectively an upgrade of the Atlantis by Topcon Corporation, and it was not available at the beginning of this study. One of its advantages is the implementation of the SMART-Track® eye tracking system that results in better image quality and less background noise.[268]

All OCTA images were acquired with 3x3mm scanning cubes with each cube consisting of 320 clusters of B-scans centered on the fovea. OCT angiograms were generated with the automated segmentation as described in chapter 2.2. In brief: the perifoveal superficial vascular plexus (pSVP), from the internal limiting membrane to the boundary between the IPL and the INL; the perifoveal deep vascular plexus (pDVP), from the boundary between IPL and INL to the boundary between the outer plexiform layer and the ONL. Imaging analysis was performed with Topcon's IMAGEnet. Central retinal thickness was automatically calculated using the 3DOCT 2000 device and its mapping software.

All images were independently reviewed by two ophthalmologists. The clinicians were questioned about the absence or presence and location of intraretinal cysts on OCT B-scans. Intraretinal cysts were defined as the occurrence of round or oval hypo-reflective spaces at the level of GCL, INL or ONL on structural OCT images. The examiners were, also, questioned about the absence or presence and location (whether in pSVP or pDVP) of microvascular changes (ie, microvascular protrusions). These were defined

as the presence of expanded and tortuous hyper-reflective capillaries within the pSVP and/or pDVP on OCTA images. Finally, the FAZ shape was judged to be abnormal if interruption of perifoveal capillaries was evident on OCT angiograms.

2.6.4 RESULTS

Four eyes from three patients (mean age 14±3.8 years) with previous diagnosis of XLRS were included. Both reviewers were in agreement in regard to intraretinal cyst location, microvascular changes and FAZ shape abnormalities.

Patient #1

This patient has the RS1 gene mutation c.487 T>C (p.W163R) (Exon 5). In both eyes, fundoscopy examination showed stellate spoke-like maculopathy. BCVA was 6/12 in the right eye and 6/9 in the left. No submacular hemorrhage, exudation or preretinal/subretinal fibrosis was evident in either eye. Structural OCT B-scans showed foveal schistic cysts localized in the GCL, INL (bigger at this level) and ONL. Central retinal thickness was 262 µm in the right eye and 260 µm in the left. SS-OCTA images were acquired with the Atlantis device. No microvascular changes were seen in the pSVPs

in both eyes. However, abnormal microvascular protrusions were identified in both pDVPs. In the right eye, the FAZ shape was judged normal in pSVP and abnormal in pDVP. In the left eye, FAZ shape was abnormal in both plexuses (Figure 2.25).

Patient #2

This patient presented with the RS1 gene mutation c.590 G>A (p.R197H) (Exon 6). Image analysis of the data from the left eye was unsuccessful because of retinal detachment involving the fovea. In the right eye, BCVA was 6/12, and fundoscopy examination showed stellate spoke-like maculopathy with perimacular exudation. Inferior peripheral retinoschisis with bridging vessels between retinal leaflets was also present. Structural OCT B-scans showed high retinal disruption and foveal schistic cysts localized in the GCL, INL (bigger in the INL) and ONL. Right eye's Central retinal thickness was 340 µm. OCTA images were acquired with the Atlantis OCT device. There were no microvascular changes in the pSVP. Vessels with abnormal protrusion and course were identified in pDVP. A single vascular abnormality has been observed at the boundary between the pSVP and pDVP. The FAZ shape was abnormal in both plexuses (Figure 2.26).

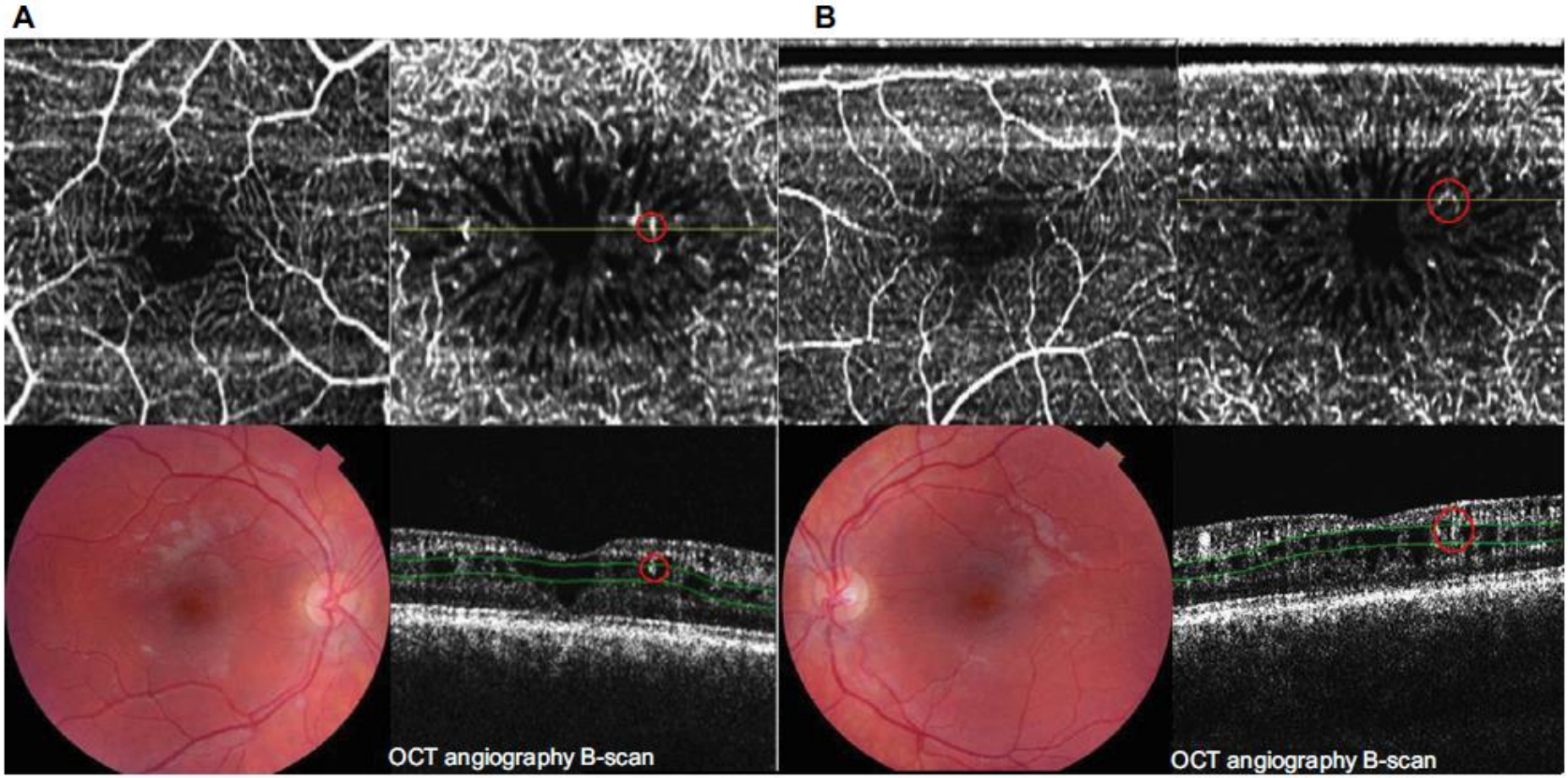

Figure 2.25: *Observations in patient #1. (**A**) Right eye: 3x3 mm fovea-centered OCTA image of pSVP (upper left) shows no perifoveal capillary network interruptions. Hyper-reflective retinal abnormalities (ie, microvascular protrusions in red circle) within*

*enlarged foveal avascular zone in the pDVP (upper right). B-scan image (lower right) shows perifoveal-nasal dilated capillary within a schisis cavity (red circle). (**B**) Left eye: 3x3 mm fovea-centered OCTA image of pSVP (upper left) shows inferior perifoveal capillary network interruption. Hyper-reflective retinal abnormalities (ie, microvascular protrusions in red circle) within enlarged foveal avascular zone in the pDVP (upper right). B-scan image (lower right) shows perifoveal-temporal dilated capillaries within a schisis cavity (red circle). **Abbreviations:** OCTA, optical coherence tomography angiography; pSVP, perifoveal superficial vascular plexus; pDVP, perifoveal deep vascular plexus.*

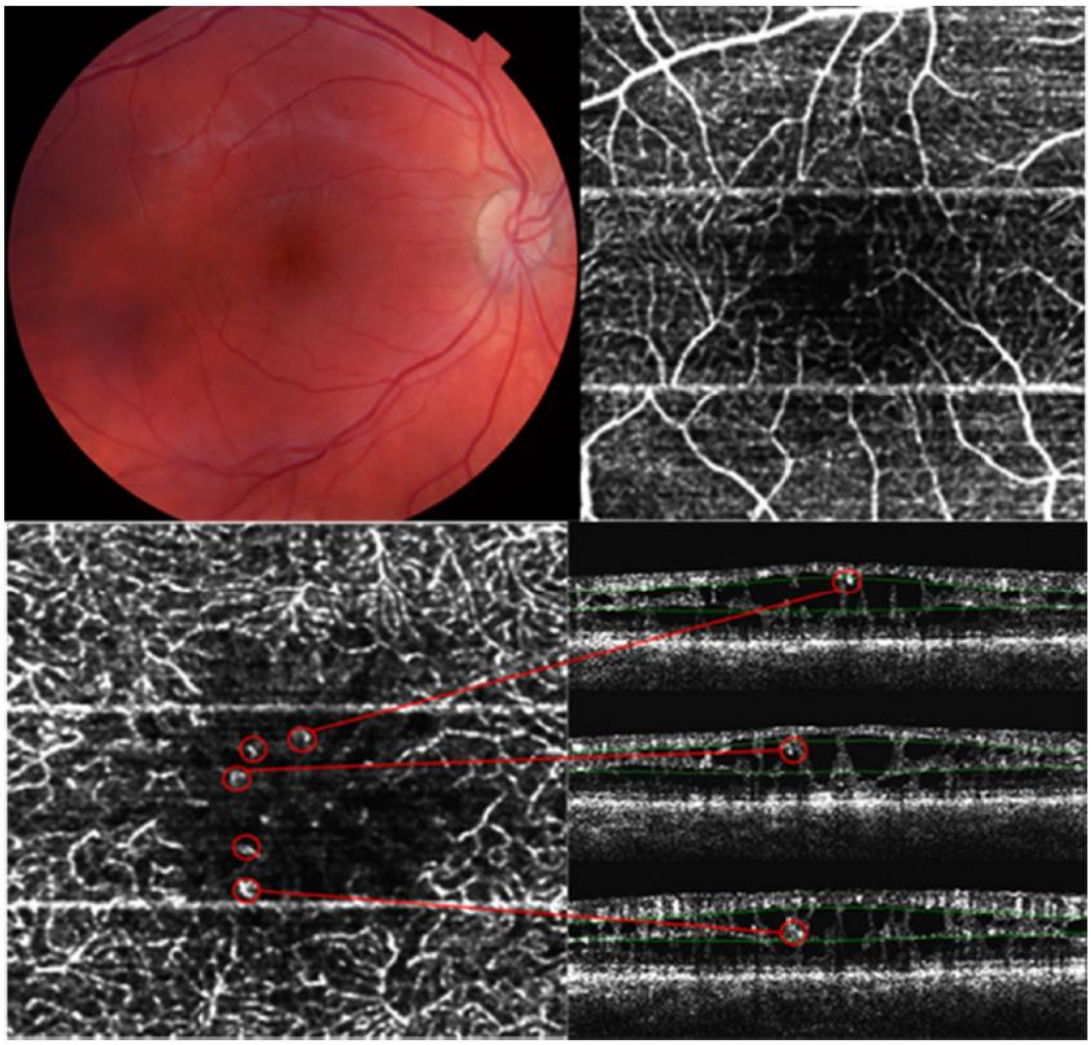

Figure 2.26: *Observations in patient #2. Right eye: Perifoveal superficial vascular plexus in a 3x3mm fovea-centered OCTA image with inferior interruption of the capillary network (upper right). Hyper-reflective retinal abnormalities (ie, microvascular protrusions; red circles) within enlarged foveal avascular zone in the pDVP OCTA and B-scan images (bottom row). Note the vascular retinal abnormality at the boundary between pSVP and pDVP on the upper B-scan image (red circle). Appropriate segmentation is required to better visualize those abnormalities.* ***Abbreviations:*** *OCTA, optical coherence tomography angiography; pDVP, perifoveal deep vascular plexus; pSVP, perifoveal superficial vascular plexus.*

Patient #3

This patient presented with the RS1 gene mutation c.214 G>A (p.E72K) (Exon 4). Imaging analysis of the left eye was not possible because of vitreous hemorrhage. Clinical examination of the right eye showed a BCVA of 6/9 and stellate spoke-like maculopathy with no retinal exudation. Structural OCT B-scans showed intraretinal cysts localized in both INL and ONL, with central retinal thickness of 295 µm. SS-OCTA images were acquired with the Triton device. Microvascular changes were evident in the pDVP only. The FAZ shape was abnormal in both plexuses (Figure 2.27).

2.6.5 DISCUSSION

Despite the well-established clinical appearance of XLRS, the precise mechanism of the schisis cysts formation is still a topic of debate. Identification of RS1 gene and its cell–cell adhesive proprieties between bipolar and photoreceptor cells suggested that the schisis could be generated by loss of adhesion between retinal layers.[369] Joshi et al speculated that the intra-retinal cavities formation could be the result of intra-structural retinal defects combined with vitreous tractional forces.[384] Also, Molday et al pointed out that interactions between mutated RS1 and Na/K^+ ATPase pumps may alter the ionic gradient and tissue balance resulting in extracellular fluid accumulation in intraretinal cysts.[368]

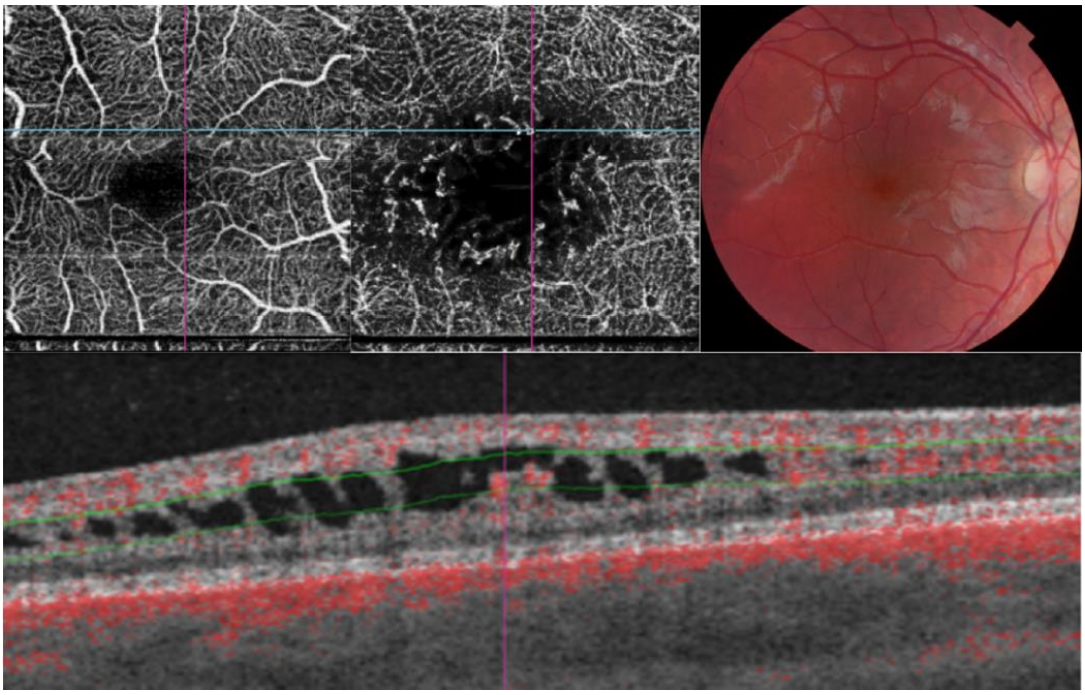

Figure 2.27: *Observations in patient #3. Perifoveal superficial vascular plexus in a 3x3mm fovea-centered OCTA image with supero-nasal interruption of the capillary network (upper left). Hyper-reflective retinal abnormalities (ie, microvascular protrusions) within enlarged foveal avascular zone in the pDVP (upper central). B-scan image (bottom) centered on a dilated capillary shows lack of glial support and protrusion in a schisis cavity in the pDVP. Vascular flow is automatically represented with red color by Triton's processing software.* ***Abbreviations:*** *OCTA, optical coherence tomography angiography; pDVP, perifoveal deep vascular plexus.*

Previous case reports have shown retinal vascular changes such as Coats-like exudative retinopathy, perivascular sheathing and peripheral dendritiform vascular alterations in patients with XLRS complicated by exudative retinal detachment, and vitreous and intraretinal hemorrhage.[372] It has been hypothesized that retinal vessels between the schistic cysts may be more sensitive to mechanical stress because of lack of the glial support. This could lead to alteration of blood – retinal barrier and, consequently, to vitreous hemorrhage and exudative retinal detachment, which are the most frequent sight-threatening complications in XLRS.

This study described, by means of SS-OCTA, retinal structural abnormalities and perifoveal microvascular changes in patients with XLRS. In all eyes, the schisis cavities are more evident in the ONL and INL, mainly in the latter, and this was also reported in previous studies.[379-381] It was the study clinicians' belief that retinal cavities location could be related with the RS1's propriety to lead structural adhesion between bipolar cells and photoreceptors, that is, in between INL (anteriorly) and ONL (posteriorly). Interruption of the superficial perifoveal microvasculature was evident on SS-OCTA images in two out of four eyes, whereas in the pDVP, the interruption was observed in all eyes. FAZ enlargement has also been recently described with FA by Rao et al in seven out of 36 eyes of patients with XLRS.[382] However, the number of eyes with FAZ enlargement in the pDVP might have been higher, because FA is a single-plane imaging modality and a clear visualization of the small retinal vessels beneath the superficial plexus is not always possible.

In all eyes, microvascular abnormalities on pDVP OCTA images were observed. These changes have been described as abnormal protrusions of the microvascular walls and tortuosity of the vessels' course. However, none of them were evident on ophthalmic examination, nor on color fundus photography. SS-OCTA B-scan images showed that these vascular abnormalities were located in pillar-like structures between schisic cavities, with a limited glial support and surrounded by intraretinal fluid (Figure 2.27). Interestingly, no microvascular protrusions were observed in the pSVP. In patient 2, a microvascular protrusion seemed to be placed in between the pSVP and pDVP. A potential reason for the above findings may be that the capillaries located at the inner and external border of the INL, which have a smaller diameter,[329] could be more sensitive to tractional stress compared to those located in the NFL. However, whether these vascular changes were due to a primary weakness of the microvascular walls or secondary to mechanical forces caused by intraretinal fluid accumulation is hard to say. A combination of the two mechanisms might be possible.

Study patients #1 and #2 were imaged with the Atlantis device, while patient #3 had OCTA images acquired with the upgraded Triton device. The latter provided better imaging resolution and a more accurate analysis. The implementation of the eye tracking system significantly reduced motion artefacts (such as the white lines in Figure 2.25 or the black band in Figure 2.26 due to blinking) and it subsequently improved the timing of the imaging session. Apart from benefits in the acquisition though, there were no significant changes in the two image processing procedures (i.e. Atlantis and Triton). Segmentation errors occurred in all cases due to irregular retinal

layers (i.e. the presence of retinoschisis) and manual adjustments were necessary. Moreover, it is noteworthy that imaging of two (later excluded) eyes was unsuccessful due to failure in the analysis of the acquired OCTA images rather than acquisition. One of the excluded eyes was suffering from retinal detachment in the fovea which made the segmentation process very problematic. The extensive vitreous hemorrhage in the other eye also caused significant problems and difficulties resulting in failure of processing the OCT angiograms correctly. Nonetheless, images acquired with the Triton confirmed perifoveal changes observed with the Atlantis in patients #1 and #2.

The above-described perifoveal retinal features (schisis cavities, perifoveal vascular network interruptions and micro-vascular protrusions) seemed to be located more often in the pDVP. Therefore, imaging techniques that provide layer-by-layer analysis, such as OCTA, could have an advantage over single-plane imaging modalities, such as FA. In this study, data were obtained with SS-OCTA, which has a light source centered at 1050 nm and can penetrate tissues to a greater extent with less sensitivity roll-off with depth compared to SD-OCT. This may represent a potential advantage when imaging eyes with edematous retinas such as in XLRS.

2.6.6 CONCLUSIONS

This study reports on the perifoveal vasculature, as depicted by SS-OCTA, in patients with XLRS, a condition characterized by retinal disorganizations, such as retinal and foveal schisis. While findings in this research regarding retinal structure are merely confirming previous knowledge, it is the utilization of a novel technology (i.e. the swept-source approach in OCT) and the description of the vascular features in deeper retinal layers that should be considered as important study outcomes.

The advantages (or otherwise) of OCTA over FA have been established and previously discussed; these are mainly the layer-by-layer analysis (for the identification of abnormalities in deeper layers) and the non-invasive way of acquiring information of the retinal and choroidal vasculature. The latter is an important factor in paediatric clinics. In this study it was shown that swept-source technology features, such as increased scanning speeds and deeper scanning penetration, coupled with an eye tracking technology could provide high-quality visualization of the vasculature even in cases with high retinal irregularities. However, correct segmentation is very important and automated processes seem to usually fail. Manual segmentation and re-assessment of the OCT angiograms are necessary.

Study limitations, such as the small sample size, absence of control group and the fovea-specific scanning pattern should be considered. Nonetheless, OCTA could provide an essential alternative to the invasive FA in paediatric

clinics for the diagnosis, management and monitoring of cases suffering from pathologies with alterations in the eye's vasculature.

2.7 Research Impact and Potential

Current & Future Research

The introduction of OCT technology at the early 1990s and the significant advancements of its technology since then have altered the practice of routine eye care. Another technological breakthrough, that of OCTA, is undoubtedly going to play an important role in the assessment of the eye's vasculature. Current clinical examinations (like fundus FA and ICG), albeit still the clinical standards for evaluation of the retinal and choroidal capillaries respectively, are invasive, time-consuming (e.g. up to 30-40 minutes for an FA examination) and with the involvement of potential risks. Hence, OCTA technology introduced itself as a potential alternative.

As mentioned at the beginning of this section, in 2015 the MVR (research) Lab at the MREH was given the opportunity to trial two devices prior to their commercial release. Both devices were utilising the recently introduced swept-source technology. This section includes research undertaken during the clinical evaluation of those devices. Most of them are characterised by a proof-of-concept or pilot study design and involve relatively small samples; sometimes investigating low-prevalence pathologies also being the reason.

More specifically, chapter 2.2 describes the effectiveness of SS-OCTA to depict alterations not only from the central to the more peripheral regions of the retina (i.e. the X and Y plane) but also through the various depth levels (i.e. the Z plane), from the vitreous to the choroid. It shows the strengths and

drawbacks of the two evaluated devices (i.e. the Triton and the Atlantis; both from Topcon Corp.) when compared to FA angiograms. SS-OCTA seems to be very efficient in visualising alterations of the retina and the choroid, particularly in the central region. Swept-source technology, as described before, benefits from longer (thus more penetrating) wavelength and faster scans compared to SD-OCT. Limitations of the technologies include: 1) automated segmentation errors, especially towards the periphery or in the presence of retinal irregularities, 2) excess motion artefacts, especially in the absence of an eye tracking system and 3) significant reduction of image quality and device usability when imaging peripheral retina. It is noteworthy that evaluation of these devices mostly relied on qualitative data and subjective appraisals from the clinicians (Prof Stanga – vitreoretinal consultant and his fellows) involved.

The following 2 chapters (2.3 and 2.4) report on observations while assessing the suitability and efficiency of SS-OCTA in DR clinics. The study in chapter 2.3 provides proof-of-concept evidence of the potential benefits that intravitreal administration of an anti-VEGF agent prior to vitrectomy for the treatment of cases with PDR. The most appropriate timing for optimal effectiveness of the anti-VEGF administration is yet to be determined with an appropriately designed clinical trial. Findings related to the surface area of the FAZ in patients with difference severity levels and types (i.e. non-proliferative and proliferative) of DR are also reported. It was shown how the size of FAZ changes in the superficial and deep layers across the severity spectrum of the disease and how the calculation of the ‘hypoxic’ volume could potentially be a surrogate for conversion from one type (the

non-proliferative) to another. One of the most important findings of this study was the reported association between disease severity and the increase in the distance between superficial and deep layers; or, in other words, the gradual thickening of the retina but without evident signs of an oedema. This was possibly the first report of such a relationship and further research is required to establish this connection and evaluate its clinical significance.

In a similar way, the last two chapters (2.5 and 2.6) of this section present outcomes of studies while evaluating SS-OCTA in paediatric clinics. The most significant findings are, probably, those in collaboration with the San Raffaele Hospital that show alterations of the foveal vasculature in paediatric patients with a diagnosis of Coats' disease; a pathology that is believed to be unilateral. Alterations in the vasculature of children with an XLRS diagnosis were also described. The particular advantage of OCTA to provide layer-by-layer analysis and its effectiveness in visualising the retinal and choroidal vasculature in a non-invasive way could make OCTA an important tool for the diagnosis and monitoring in paediatric clinics.

The general assessment of SS-OCTA in retinal and paediatric clinics showed that angiograms can be successfully acquired in a fast, patient-friendly way regardless the age of the patient. A factor that seemed to affect the acquisition process was lack of ability to fixate properly, whether that was related to vision loss or other reasons. In such cases the imaging session would last longer until OCTA images of adequate quality were retrieved. The analysis and image processing of the generated angiograms did not always prove to be as efficient as it was expected. Automated segmentation algorithms seemed to fail in cases with extreme retinal irregularities, such as

macular oedemas, schises etc. Manual modification of the reference segmentation planes improved segmentation at the expense of time. The presence of motion and projection artefacts reduced the clinician's capability to identify abnormal features in the eye's vasculature. Motion artefacts are significantly reduced by the introduction of eye tracking systems. Projection artfacts are mostly the result of blocking, scattering or absorption of the laser beam and are a limitation of the technology.

Outcomes of the research described in this section provided information on the usability and efficiency of two SS-OCTA devices (one as a prototype and the other before its commercial release), mainly in collaboration to the manufacturer Topcon Corp. The presented studies were not necessarily designed to evaluate the performance of swept-source technology but rather to provide pilot data for further product improvement. Indeed, since the Triton's commercial release a valuable eye tracking system has been introduced, which significantly reduced the presence of motion artefacts. Moreover, further segmentation tools have been introduced in recent upgrades of the IMAGEnet system; for example, the interpolation of the reference plane after point-by-point alterations.

Non-invasive imaging with OCT technology has expanded our knowledge on ophthalmic pathologies and created more research questions. For example, is Coats' disease a unilateral or bilateral pathology? Could monitoring of the FAZ surface help us identify patients with high risk in progressing to the proliferative type of DR? Further research with larger patient samples and appropriate study designs would, undoubtedly, offer a plethora of information on this newly acquired knowledge on the eye's vascular network.

Section 3

Investigation of a Novel Vision Restoration Therapy by Means of Retinal Implantation

3.1 Preliminary Results of Safety and Efficacy of the Argus® II Retinal Prosthesis System in Age-related Macular Degeneration – First Year Follow-Up

Contributions

One of the major projects at Manchester Vision Regeneration (MVR) Lab was the implantation of the Argus® II Retinal Prosthesis System (Second Sight Medical Products Inc., Sylmar, California, USA) in patients with AMD. This project was designed, sponsored and monitored by Second Sight, with Prof Paulo E Stanga being the Primary Investigator, the lead surgeon and the supervisor of the project. My contribution to this study started in March 2015, that is a couple of months before the first implantation (the patient was already identified), and is on-going. My involvement in this study focuses in 3 primary fields: 1) data collection by performing the required structural and functional testing (a detailed list of the examinations required by protocol can be found later in this section), 2) data analysis, reporting and advising on potential solutions for replacement of existing tests deemed to be inadequate and 3) dissemination of the work by preparing and presenting in various international conferences and preparation of manuscripts for publication.

Given that this study is a registered clinical trial sponsored by a private company, I had no contribution to the study design and the study protocols. However, the continuous data collection and analysis that my role offered allowed for a more spherical review of the study's strengths and drawbacks.

The following chapter includes not only the study outcomes as those were officially reported in scientific conference and meetings (chapter 3.1) but also my personal review (chapter 3.2) discussing flaws of the study design, in particular the wrong choice of tests for functional assessments, and suggestions for improvement in future research attempts. The reader, however, should take into account that this is the very first attempt of retinal implantation in eyes diagnosed with non-exudative AMD. It is therefore an 'uncharted territory' in this research field and some of those study design flaws could only be detected retrospectively. Nonetheless, the plethora of information deriving from this study can direct future research in the right pathways.

Presentations / Publications

Since the time of the first implantation research outcomes from the Argus® II study have been presented at a large number of international meetings and congresses; to name a few: the Association for Research in Vision and Ophthalmology (ARVO 2016 & 2017), the American Academy of Ophthalmology (AAO 2016) and Euretina (2016). My involvement in the preparation of the presentation slides focused on the structural and functional follow-up outcomes. Prof Stanga has been the presenter in the vast majority of times; however, I had the opportunity to present these results at a patient-oriented meeting of the Retinitis Pigmentosa (RP) Society and the honour to defend our poster at ARVO 2016 as a replacement presenter.

Manuscripts related to this work have been drafted by myself and subsequently reviewed and modified by other members of the team, Prof Stanga and Second Sight collaborators. The following chapter involves a modified version (i.e. extensive comments, more detailed figures etc) of the study's core manuscript reporting on the preliminary results for the safety and efficacy of the Argus® II system in 5 patients, one year after their implantation. The manuscript is pending submission.

3.1.1 INTRODUCTION

Almost 1 in 25 people worldwide suffer from severe visual impairment, whether this is low vision or blindness.[1] In approximately 10 to 20% visual impairment is irreversible. As a result, vision regeneration has recently become the focus of some exceptional research in an attempt to restore some of the lost vision; where visual impairment occurred due to retinal or neurological degenerations. Visual prosthesis and gene and cell therapy are currently the main avenue of investigation.[385-393]

Gene therapies utilise the delivery of genes via viral vectors (such as adeno-associated viruses) to either compensate for the malfunctioned disease gene or act as a growth factor to prolong the life and function of photoreceptors.[394] The eye has been identified as an ideal organ for such an approach due to its immune privilege, its compartmentalisation, its accessibility and small size. The main cause of vision loss in genetic disorders such as RP, Stargardt disease and Leber congenital amaurosis has been identified to be the death of retinal cells. However, complex age-related diseases such as AMD or glaucoma also involve cell apoptosis in the retinal region. For these vision-threating conditions, gene-replacement therapies can offer therapeutic intervention at various disease stages.[395] More than 30 clinical trials have obtained approval and they are currently in progress, or have been completed, with promising results therefore prompting further research in this field.[396]

Visual prosthetic technology relies on phosphene production by electrical stimulation. Phosphenes are simply visual perceptions which occur in the absence of a light stimulus or a functioning visual pathway. They appear independently of light stimuli and have been described as sparks of light; usually white but also coloured. In the 1930s, Carl Foerster, a German ophthalmologist, was the first to investigate visual prostheses (also known as 'bionic eyes'), and discovered how direct electrical stimulation of the visual cortex enabled his blind subject to perceive light.[397] Since then 'bionic eyes' have been implanted in a number of locations of the visual pathway and different approaches have been explored, including not only the visual cortex and the ON but also the retina.[393, 398-401] The concept of retinal prosthesis is to elicit neural activity in the remaining retinal neurons by detecting light and converting it into electrical stimuli. Subretinal, epiretinal, and suprachoroidal implants are currently designed to restore functional vision in retinal degenerative diseases.[402-405] Table 3.1 lists the visual prosthetic devices that are currently being trialled or reported upon.

Device	Implant Location	Method of Image Acquisition	No of Stimulating Electrodes	Cause of Vision Loss (trialled)
Dobelle Implant	Visual Cortex	Camera-based	64	Trauma
AV-DONE	Optic Nerve	Camera-based	7	RP
MiViP	Optic Nerve	Camera-based	4	RP
BVA 24	Suprachoroidal	Camera-based	24	RP
STS	Intrascleral	Camera-based	49	RP
Alpha IMS	Subretinal	Optical Sensor	1,500	RP
ASR Microchip	Subretinal	Optical Sensor	5,000	RP
Argus® I	Epiretinal	Camera-based	16	RP
Argus® II	Epiretinal	Camera-based	60	RP, Choroideremia, AMD
Epiret 3	Epiretinal	Camera-based	25	RP
IMI	Epiretinal	Camera-based	49	RP, Usher's syndrome

Table 3.1: *Summary table of the visual prostheses trialed to date*[393]

As seen in Table 3.1, there are two mechanisms that such devices use to convert a visual image into electrical stimulation. Camera-based prostheses

involve a camera which captures the image and sends it to an external vision processing unit (VPU). The processor converts images into electrical waveforms, which are subsequently sent to an implanted array of electrodes. Communication among those parts can be via wired or wireless links; see Figure 3.1 for a schematic example. The main benefit of camera-based prostheses is that the external processor can optimise stimulation parameters according to the captured scene. The quality of the natural visual scene (i.e. levels of luminance, contrast levels etc) need not be high. The main drawback of such an approach is that the camera does not follow eye movements and patients need to understand and familiarise themselves with the need to direct the camera to the object of interest.

Figure 3.1: *Schematics of a camera-based cortical visual prosthesis (left) and an epiretinal prosthesis (right) with an array of electrodes on the retina and an electronic processing unit on the sclera. A picture of an external visual processing unit is shown in the middle. Courtesy of Prof Paulo Stanga and the MVR Lab*

Optical sensor prostheses involve a micro-photodiode array that can convert light into electrical currents without the need for an external camera. They make use of the patient's own optical system and allow for natural eye movements.[406] However, their performance is dependent upon a high quality natural scene and they currently lack a VPU which could potentially optimise stimulation parameters. The Alpha IMS subretinal implant (Retina Implant AG, Reutlingen, Germany) is the only optical-sensor based retinal prosthesis that is currently approved and commercially available.[403]

The investigated retinal implant in this study was the Argus® II Retinal Prosthesis System (Second Sight Medical Products Inc., Sylmar, California, USA); a commercially available device that aims to restore a basic level of vision to patients with profound vision loss from outer retinal dystrophies.[407] The device elicits visual perceptions by means of electrical stimulation of the residual retina.[408] It is an epiretinal device containing 60 electrodes in a 6x10 array. It has initially been trialled on patients with RP with first results reported in 2012 and long-term (up to 3 years) outcomes in 2015.[402, 407] The Argus® II has become the most widely used and most successful retinal prosthesis currently available in terms of regulatory approval. Since obtaining the CE mark in 2011 and FDA approval as a humanitarian device in 2013[409], commercial implantation has begun in many countries worldwide. Use of the device has been predominantly for patients with profound vision loss from RP and to a lesser extent choroideremia.[402, 407, 410-415]

AMD remains one of the leading causes of severe visual impairment and irreversible blindness among the elderly in Western world, such as Australia, Japan, the United States and in Western Europe.[2] During its advanced

stages AMD can be either non-neovascular (dry, atrophic or non-exudative) or neovascular (wet or exudative). Dry AMD is characterised by the presence of drusen and geographic atrophy (GA) at the centre of the macula, while the main characteristic of wet AMD is choroidal NV.[416] Central vision loss is expected while peripheral vision is maintained. Current treatment strategies, such as laser and surgery approaches or anti-angiogenic and targeted molecular therapies, aim to halt the progression of exudative AMD and loss of vision, although improvement in visual acuity (VA) has been reported with anti-VEGF treatment.[417-420] However, there is no approved mean of treatment that restores, partially or fully, functional loss due to AMD.

The main hypothesis of this study (i.e. a Phase 2 type clinical trial) is that the Argus® II System can be safely implanted in patients with atrophic AMD and can elicit electrical stimulation in the retinal neurons located under the area of GA and over the central macula. The outcomes of this study could potentially indicate whether an integrated visual system with an artificial central and peripheral residual vision is a possibility without causing any confusion to the patient. The aim of this report is to describe the surgical outcomes and preliminary (up to 12 months) structural and functional results of 5 patients with a diagnosis of advanced atrophic AMD implanted with the Argus® II System.

3.1.2 METHODS

Trial Design

This is a single arm, non-randomised, controlled feasibility study. Total duration of the study has been set to approximately 4 years: 1 year for recruitment and 3 years for follow-up. Potential candidates were screened to ensure they were eligible for the study until the recruitment target of 5 patients was achieved. The main inclusion criteria were a diagnosis of non-exudative AMD with subfoveal GA and scotoma within the central 20° VF with no other comorbidity that could affect the visual function and VA worse than ETDRS minimum angle of resolution (logMAR) 1.0 in both eyes. Full list of inclusion/exclusion are given in Appendix II.

Counselling of both patients and families has been identified to be a critical component of the selection process which is positively correlated to a positive outcome.[421] Hence, each one of the recruited patients had a thorough consultation with the research team to understand the nature of this study and set realistic expectations. All patients gave their consent and the study adhered to the declaration of Helsinki.

Study procedures to ensure eligibility and to monitor structural and functional changes included medical and ophthalmological evaluation and extensive visits for structural and functional assessment. OCT scans were acquired by using the Topcon Atlantis, a prototype device that the MVR Lab possesses. The scanning protocol included wide OCT scans (i.e. 12x9mm) over the

macular area. The scanning area would effectively include the ONH for a broad structural assessment. In cases where particular regions of interest required an in-depth analysis further scans of better resolution (3x3mm or 6x6mm) would be acquired. Wide-field retinal fundus photographs, fundus autofluorescence and FA images were taken by means of the Optos California. Particular attention was given to the GA area which was measured by two different examiners using the manufacturer's software. The difference between the two examiners was then calculated. Values out of the 95% confidence intervals were assessed by a third examiner and the median was calculated. Other observed retinal features and changes were recorded thoroughly.

With regards to functional assessment at baseline and follow-up visits, the patients' VF was assessed with the HFA, model 740i. The selected testing pattern was the Full-Field 81-point on threshold-related test mode. Other perimetric parameters were standard; stimulus size: Goldmann III and stimulus colour: white. Standard uncorrected ETDRS VA testing was also performed while modified VA tests for extremely low vision subjects (described elsewhere)[402, 422, 423] such as Grating Visual Acuity (GVA), Square Localization (SL) and Direction of Motion (DM) were also performed at baseline, 3, 6 and 12 months post-implant. The three modified VA tests were performed according to protocol standards from previous research studies in RP and choroideremia. In brief, GVA measures the participants' VA with black and white gratings displayed for 5 seconds on a touchscreen monitor. The subjects indicated the perceived orientation in 4-alternative forced-choice way (i.e. horizontal, vertical, diagonal left or right). The spatial

frequency of the gratings followed a staircase pattern based upon the subjects' responses. The scale of measurement is limited between 2.9 and 1.6 logMAR and those whose performance was no better than chance were scored as "acuity worse than 2.9 logMAR". In a similar way, during DM testing a white bar moves across the same touchscreen and the subject indicates the perceived direction of the moving bar by drawing with their finger on the monitor. The difference between the moving bar's angle and the subject's response angle in degrees (or so-called response error) was measured and averaged over 80 trials. In SL testing, the participant has to touch the white square that appeared at random location on the touchscreen monitor. The response error for this test equals to the difference between the subject's response and the centre of the square target in pixels. Measurements are taken and averaged for 40 trials. The significance of differences between mean errors while the system is on or off was evaluated with a 2-tailed *t* test assuming unequal variances. Central visual acuity with a pinhole occluder and microperimetry with the Optos OCT/SLO (i.e. Scanning Laser Ophthalmoscope) were also included in the battery of tests performed prior to implantation.

Two previously validated questionnaires (i.e. NEI-VFQ-25 and Functional Low-Vision Observer Rated Assessment (FLORA))[424, 425] were completed for the assessment of self-reported visual-targeted health status and evaluator-reported functional vision, respectively for baseline and at 12 months post-implant. A brief list of all the procedures at baseline and follow-up visits is given in Appendix II.

Surgery

The eye with the worse vision (per ETDRS VA and microperimetry results) was chosen for this procedure. The study protocol procedure was a pars plana vitrectomy. This allows access to the vitreous cavity through the pars plana region (which is the anatomical border between the iris and the retina) to allow the insertion of the implant. The coil of the implant is inserted at the temporal area of the eye globe underneath the lateral rectus eye muscle. The electronics package is then centred in the superior temporal quadrant. A scleral band is then used to secure the implant superiorly underneath the superior rectus eye muscle and inferiorly underneath the inferior and the medial rectus eye muscles. In the temporal quadrant, the implant is fixed to the eye via sutures passed through suture tabs on the implant.

Following that, a core and peripheral vitrectomy is conducted to remove vitreous to allow safe access to the retinal surface. An epi-retinal membrane or well-adhered posterior hyaloid observed in the area where the surgeon intends to tack the array is carefully peeled away. The array is then inserted through a temporal sclerotomy (approximately 5mm in width). The electrode array is placed onto the retina in the macular region and then tacked using a retinal tack that is supplied with the implant. The extraocular portion of the cable is sutured to the sclera and all sclerotomies are closed with sutures.

Study primary endpoints

The primary endpoints for this study were the number and nature of adverse events (AEs) in the implanted subjects (i.e. safety) and the effect of the Argus® II system on visual function (i.e. efficacy).

AEs were defined as any undesirable medical occurrence, unintended disease or injury or any untoward clinical sign (including an abnormal laboratory finding) in subjects, users or other persons whether or not related to the Argus® II System. Those AEs that were a life-threatening situation, required hospitalization, resulted in death, in a persistent or significant disability or consisted of a congenital abnormality or birth defect were classed as Serious Adverse Events (SAEs). AEs and SAEs are documented throughout the study and included in the data analysis for safety evaluation.

For several performance measures the subjects act as their own control: comparisons are performed between the Argus® II System turned ON and OFF, between implanted eyes and fellow eyes, and between pre-surgery and post-surgery performance. When results are compared with the camera ON and OFF, data from a particular subject at a particular time point is analysed with a two-tailed t-test assuming unequal variances. Where testing is conducted with the implanted and non-implanted eyes separately, comparison is made between subject performances using each eye. Where data are collected for testing conducted prior to surgery and the tests are repeated post-surgery, comparison is made between subject performances at each time point.

3.1.3 RESULTS

The recruitment target of 5 eyes with a diagnosis of atrophic AMD but no other comorbidity that could affect their vision was completed in a period of 10 months. Three female and 2 male patients had the Argus® II System successfully implanted in one eye (i.e. 3 right (OD) and 2 left (OS)) within the recruitment period. The mean age of recruited patients was 75 years (±4.6, range: 70.7–79.9). To date, the follow-up time ranges from 12 to 24 months approximately. Table 3.2 provides detailed descriptive and demographic data for all recruited patients.

ID	Age when implanted	Gender	Implanted eye	Date of implantation
52-201	81	Male	Right (OD)	16/06/2015
52-202	78	Female	Left (OS)	07/10/2015
52-203	69	Female	Right (OD)	03/11/2015
52-204	76	Female	Left (OS)	24/11/2015
52-205	72	Male	Right (OD)	12/04/2016

Table 3.2: *Descriptive and demographics data for all recruited patients.*

The preliminary results presented in this report include structural and functional characteristics at baseline and their development during the course of the first 12 months. The number of subjects assessed at each follow-up visit differs slightly between time points as some visits were missed

due to study deviations. Deviations were collected and reported to the relevant regulatory agencies. Also, note that data from month 6 was only collected from 4 of the participants due to the decease (non-study related cause) of one subject.

Baseline structure and function

Before implantation, the median area of GA was 29.03 mm^2 for the implanted eye (Figure 3.2). Mean retinal, choroidal and RNFL thickness at baseline for four of the five implanted eyes were 219 ± 20.7 µm, 73 ± 44.1 µm and 19 ± 9.8 µm, respectively. Table 3.3 shows detailed baseline structural and functional characteristics for all participants.

At baseline, mean VA measured by means of an ETDRS chart was 1.0 logMAR or worse for all implanted eyes and better than 1.6 logMAR in all implanted eyes when tested at 30cm with the GVA test. Mean error for the SL and DM tests was 39.3 ± 15.1 pixels and 9.9 ± 2.2 degrees, respectively. Microperimetry results showed an absolute scotoma over the macular area (Figure 3.2). It is noteworthy that microperimetric results were significantly hard to obtain while a high number of study deviations were produced during testing. The Optos OCT/SLO proved to be a cumbersome device with extremely high testing times. On average testing duration per eye was 10 minutes with some assessments reaching a total of 15 minutes, without including necessary breaks required by patients. The device's method of testing, and more specifically its poor compensation of eye movements, would lead to the test being idle (i.e. paused) for a long time until the patient

fixates back to the target. Due to the nature of the diagnosed pathology most patients were unable to fixate for long periods while others could not see the fixation target at all. For example, data from the (later) implanted eye from patient 52-202 were not collected, as Figure 3.2 shows. Other study deviations included wrong testing pattern for one patient and mis-location of the testing pattern for another. The median number of defective locations in the VF as evaluated by VF testing with the HFA was 15 (IQR: 25) out of a total of 79 tested locations (approximately 20% of the patients' VF). Available and potentially reliable functional data from both microperimety and conventional perimetry with the HFA were taken into account to assess visual function.

Completion of the FLORA and NEI-VFQ-25 questionnaires showed an overall poor self-perception of vision related function and an overall moderate difficulty in the performance of visual function related tasks (Table 3.3).

Mean score in the NEI-VFQ-25 was 37 on a scale of 0-100 with 100 being the best. FLORA scores range from 4 (impossible) to 1 (easy). Therefore the lower this score (minimum value: 1) the lower the overall difficulty to perform tasks where vision is essential. Mean score was found to be 2.22 ± 0.23.

Surgical results and adverse events

During the implantation surgery there were no complications and surgical results were considered reproducible across the 5 implanted eyes. All 5

implants were placed over the centre of the retina (i.e. macula), where structural and functional defects, that is atrophic retinal areas and central scotomas, were identified and correlated. In 4 of the 5 occasions the atrophic central area was smaller than the implant's size. (Figure 3.3)

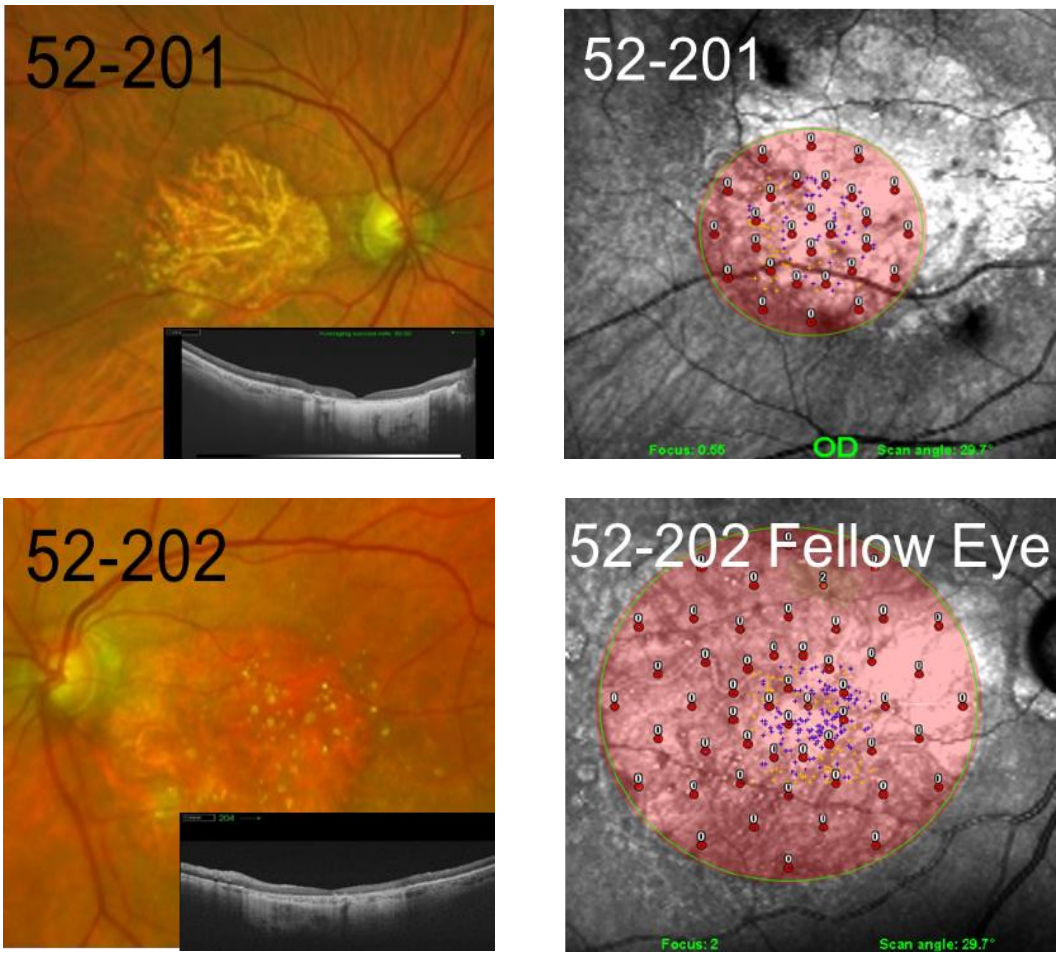

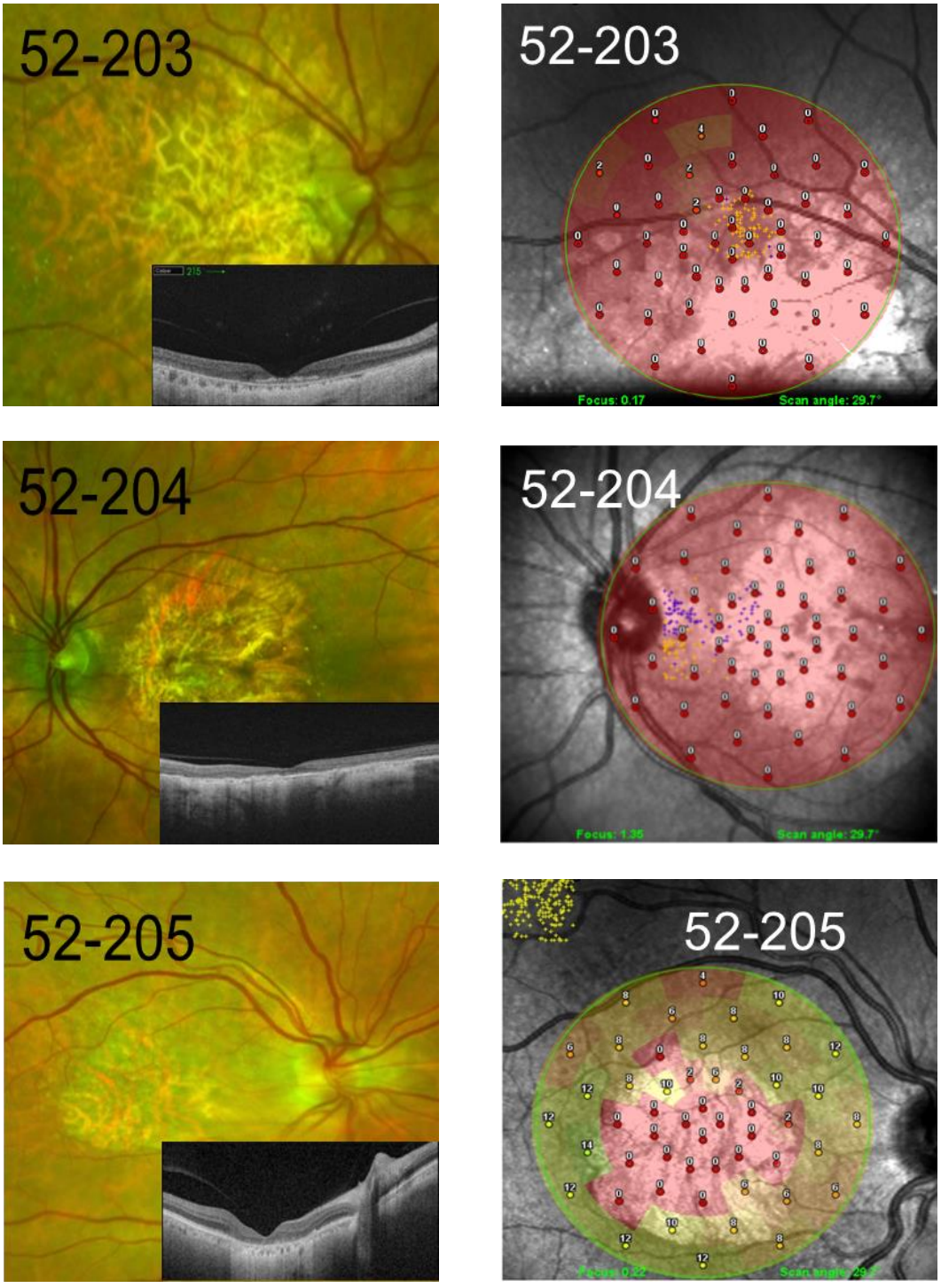

Figure 3.2: *Retinal fundus images and OCT scan sections are shown for the implanted eye of each patient at baseline (left column) along with their visual field results from microperimetry (right column).*

	OCT (implanted-eye)			Ultrasound	Fundus Photography	Visual Acuity – Ultra-low Vision testing			FLORA – all tasks	NEI-VFQ-25	HFA FF-81
ID	**Mean Retinal Thickness (µm)**	**Mean Choroidal Thickness (µm)**	**Mean RNFL Thickness (µm)**	**Axial Length (mm)**	**GA Area (mm^2)**	**GVA (logMAR)**	**SL (pixels)**	**DM (º)**	**Mean score ± SEM**	**Mean score**	**Seen Points**
52-201	198.7 ± 10.4	43.1 ± 30.6	7.2 ± 10.0	22.94	18.55	Better than 1.6	25.2	9.9	1.80 ± 0.23	58	68/79
52-202	214.3 ± 26.7	137.8 ± 36.3	22.0 ± 21.8	22.72	26.63	Better than 1.6	27.9	13.0	2.29 ± 0.53	30	64/81
52-203	216.0 ± 23.8	46.6 ± 15.5	15.0 ± 21.7	23.86	63.40	Better than 1.6	36.1	9.5	2.12 ± 0.29	32	25/81
52-204	-	-	-	21.82	28.47	Better than 1.6	39.1	10.4	2.59 ± 0.33	26	43/81
52-205	248.1 ± 28.2	66.4 ± 10.0	30.1 ± 17.7	23.43	8.13	Better than 1.6	64.5	6.7	2.24 ± 0.29	41	72/81
Mean ± SD	219 ± 20.7	73 ±44.1	19 ± 9.8	22.96 ± 0.89	29.03 ± 20.82	Better than 1.6	39.3 ± 15.1	9.9 ± 2.2	2.21 ± 0.13	37	N/A

Table 3.3: *Individual and mean detailed baseline structural and functional characteristics for all participants. GVA: Grating Visual Acuity; SL: Square Localisation; DM: Direction of Motion*

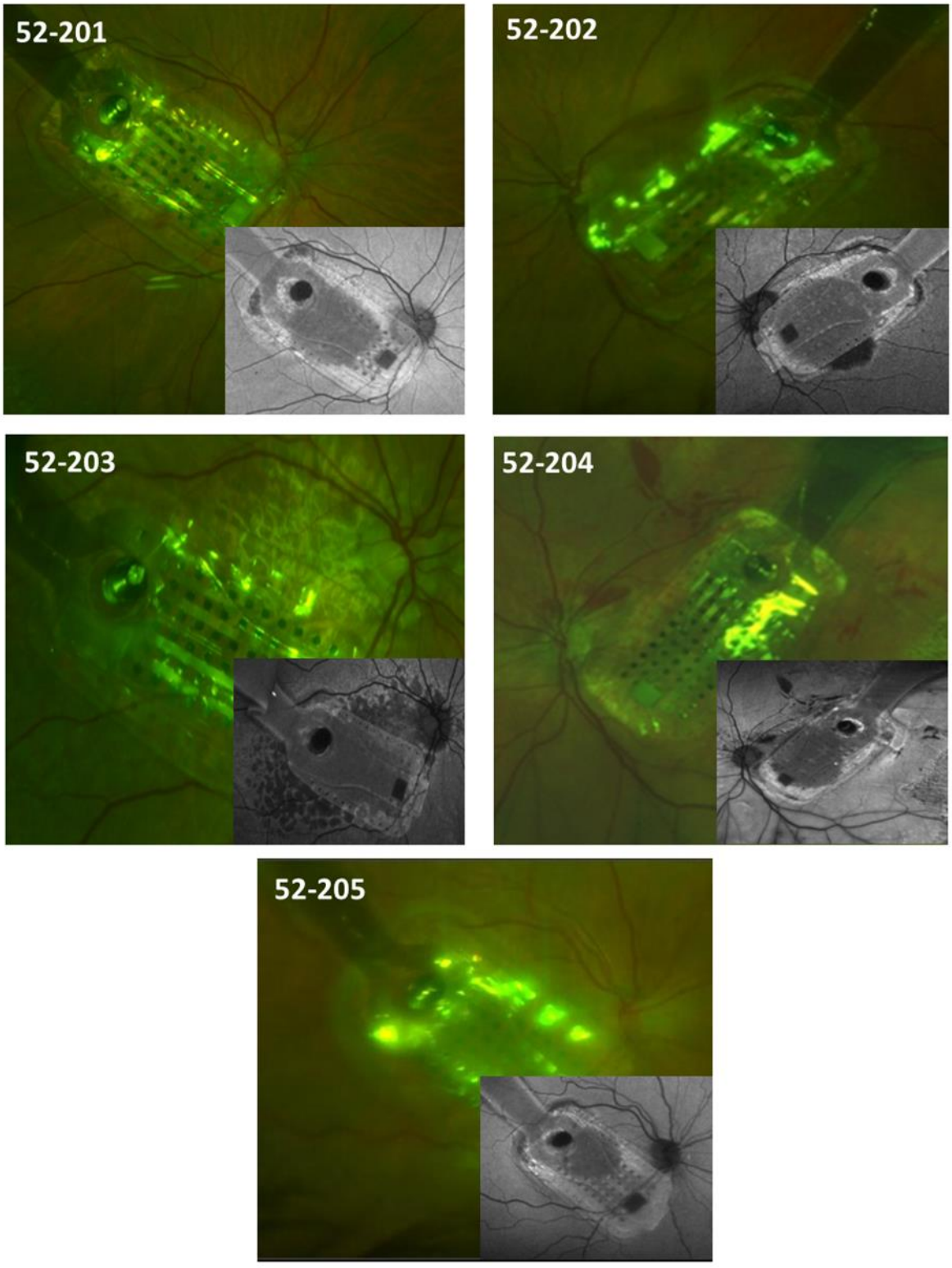

Figure 3.3: *Retinal fundus and autoflorescence images of each patient with the implant over the GA.*

During the 12 months of follow up, 15 AEs were recorded from which 4 of them were classified as SAEs related to the procedure or device. The SAEs were: one localised non-rhegmatogenous retinal detachment (RD) under the cable, two cases of proliferative vitreoretinopathy and one case of hypotony. All SAEs responded to gas injection or pars plana vitrectomy surgery with silicon oil. One patient (52-205) also required retinectomy.

In addition, a scleral patch graft was placed in the subject suffering from hypotony to prevent the leakage around the entry site of the cable. Additionally, non-serious and stable CSMO was evident approximately 1 month after implantation in all patients (Figure 3.4).

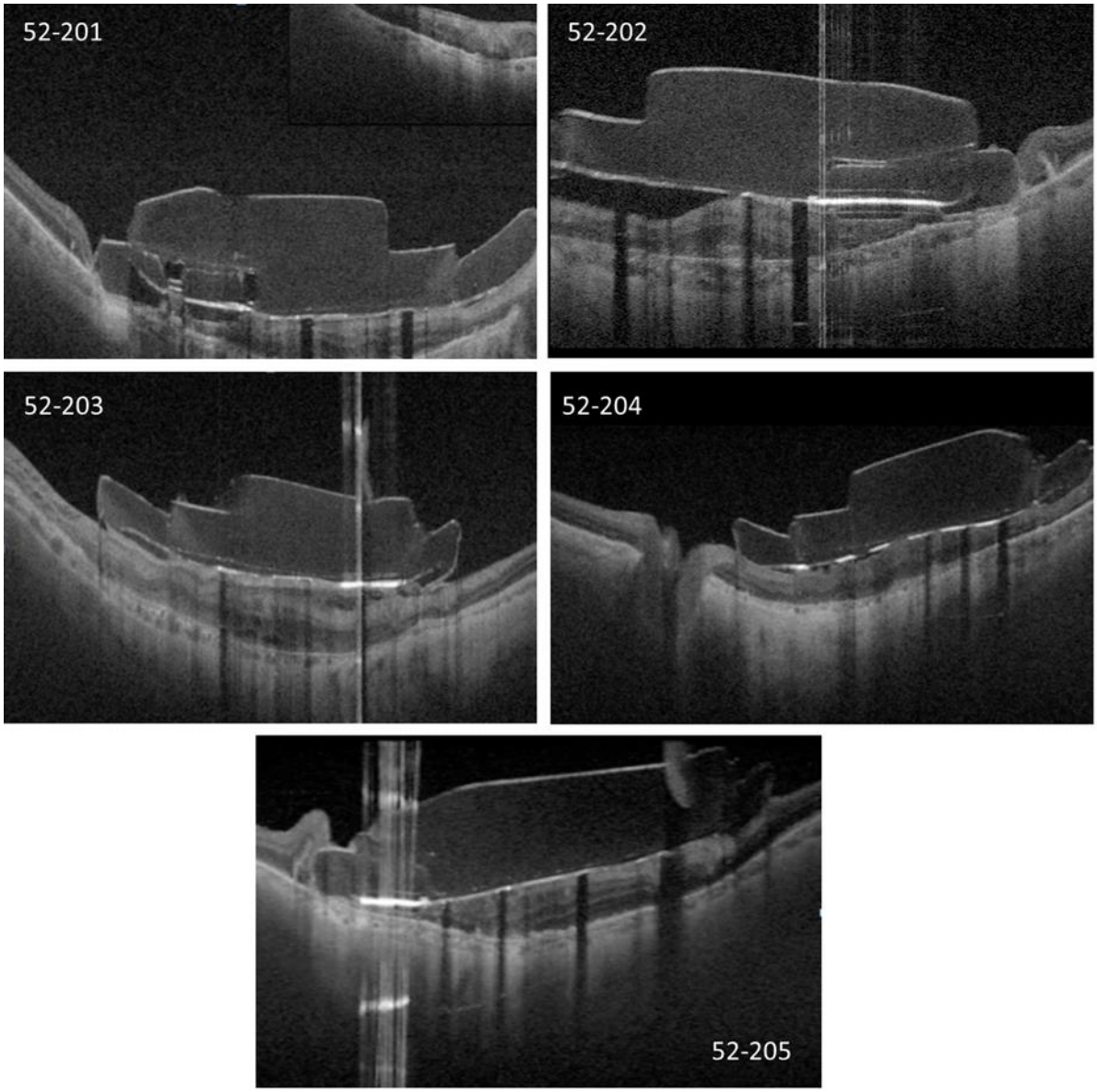

Figure 3.4: *OCT images for every patient showing the post-implant macular oedema.*

Another 5, either AEs or SAEs, were not related to the study process of the implantation of the Argus® II System. The median number of AEs per patient is 3.2. Details of the nature and the total number of AEs for each patient are given in Table 3.4.

Study ID	Total Number of SAEs and AEs, study and non-study related	Total Number of study-related AEs	Total Number of study-related SAEs	Brief description of AEs
52-201	3	1	1	Light Sensitivity **RD** **MO**
52-202	3	2	1	**Inflamation** **Hypotony** **MO**
52-203	2	1	0	**MO** Non ophthalmic AE
52-204	4	1	1	Floaters **PVR** **MO** Lung Cancer
52-205	3	1	1	**PVR** **MO** Pneumonia

Table 3.4: *Individual AEs and SAEs descriptions occurred as part of the study. Device or surgical related AEs and SAEs are written in bold. Non ophthalmic AEs are written in italics. RD: Retinal detachment, MO: Macular Oedema, PVR: Proliferative vitreoretinopathy.*

Follow-up structure and function

Figure 3.5 shows the structural changes over time from both eyes of all patients. For all patients but one (i.e. 52-203), the GA increased after implantation and remained stable during the follow-up. Interpretation of the stable atrophic region in the fellow eye implies that the implant, and possibly its size, played a role in the enlargement of the GA in the implanted eye. Similar results are recorded with VF testing with the HFA Full-Field 81 test.

The number of missed VF locations increased by approximately 35% in implanted eyes which translates in an approximately 50% defective VF for every patient. No significant difference in VF testing with HFA was reported when the system was switched on or off.

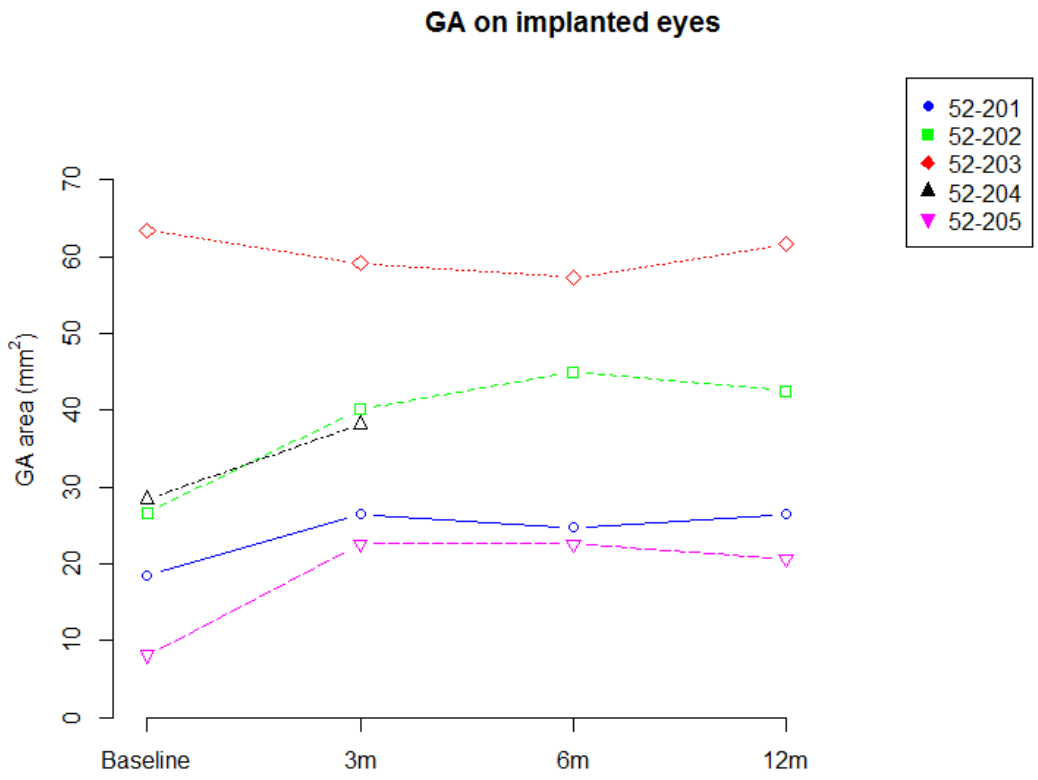

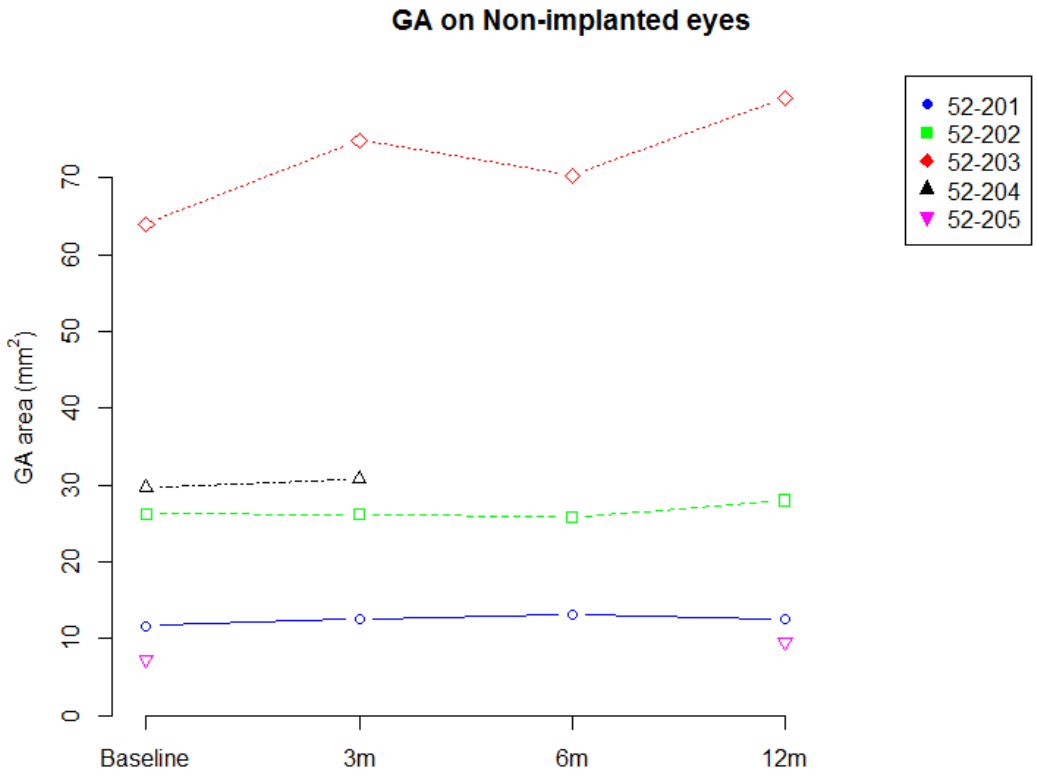

Figure 3.5: *Mean GA area over time from both eyes of all patients*

Figure 3.6 shows the changes in uncorrected VA over time from both eyes of all patients during the first year of follow-up. Monocular VA measured at the implanted eye with the Argus® II system OFF with a standard ETDRS chart was relatively stable over time for 2 out of 3 patients over the first 6 months[5]. The other patient showed significant reduction in the implanted eye 6 months after implantation. By the completion of 12 months 3 patients in total would present with VA measures of counting fingers (patient 201) and perception of hand motion (patients 203 and 205). Uncorrected VA at the fellow eye is reported relatively stable.

[5] Data from patients 204 and 205 were not collected due to then active AEs

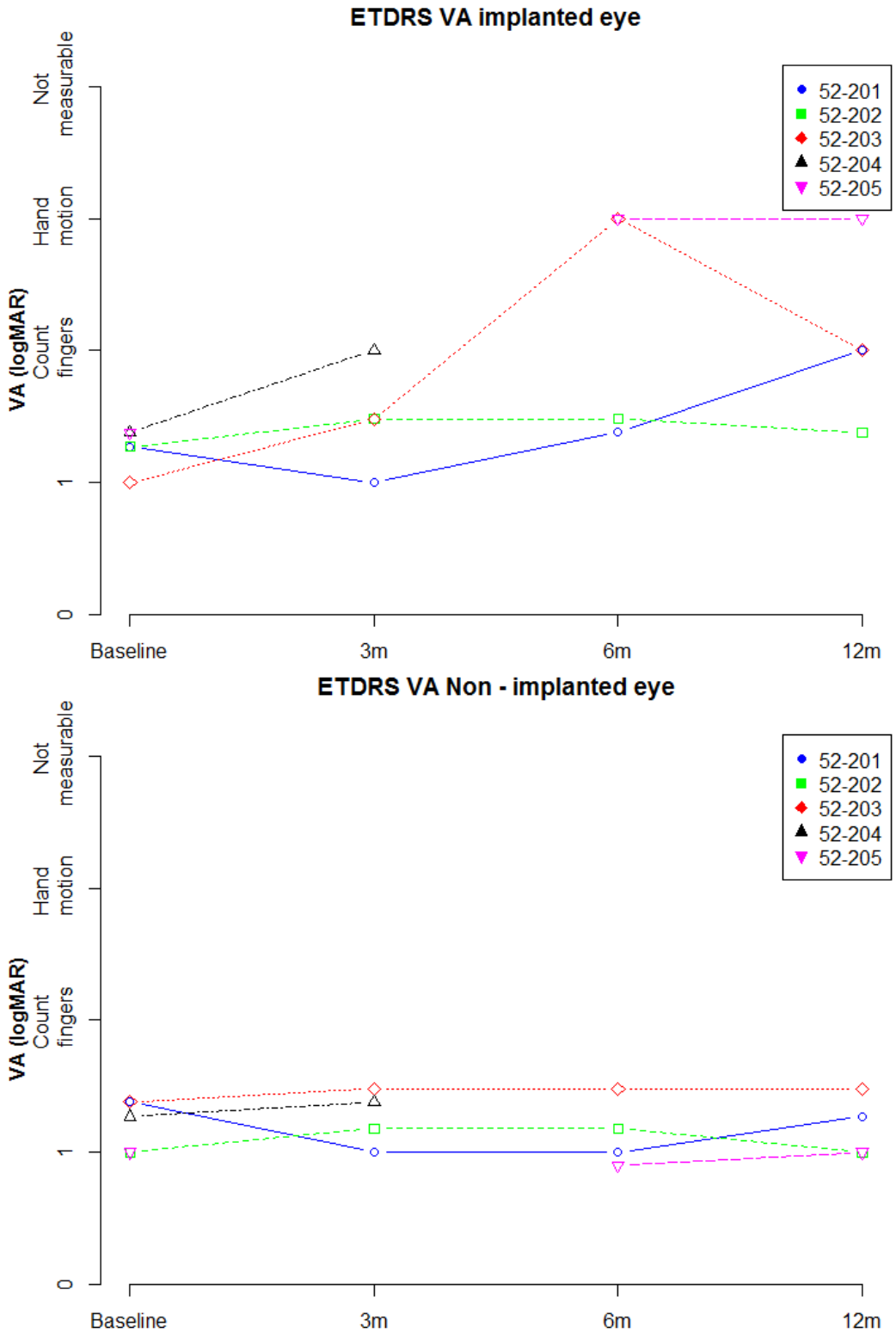

Figure 3.6: *Monocular VA measured by means of an ETDRS chart over time for both eyes of all patients included in the study.*

Visual function testing with the Argus® II system operating, revealed that the implant elicited central visual function over the atrophic area (i.e. the GA area) in all patients; a retinal region with no signs of visual function before implantation. What is more, the presence and nature of AEs did not seem to have an effect on patients perceiving phosphenes, considering that central visual function stimulated by the epiretinal prosthesis system was still recorded after the resolution of the AEs. However, data collected from the above-mentioned functional tests suggest that AEs might have had an impact on the overall performance of the implant.

GVA testing showed no significant change in both eyes and only in one patient at month 3, GVA was significantly better with the system OFF. In the SL test (Figure 3.7 A), 2 of the patients showed a significant improvement in performance with the system ON; one of them at two (6 months and 12 months) follow-up visits and the other patient after 12 months. The rest of follow up visits and patients did not show a significant difference in performance with the system ON and OFF. Both with the system ON and OFF, the mean error was higher over time for all but 1 patient, for whom a statistically significant improvement in performance can be seen over time with the system ON (patient 52-205). Similarly, the same patient showed a systematic statistically significant improvement in performance in the DM test with the system ON over time (Figure 3.7 B). Despite this fact, the trend over time for the rest of the patients is not consistent in the DM test, although patient 202 showed no benefit while operating the system after month 6; a visit that coincides with the onset of an SAE (i.e. hypotony). After 12 months DM was significantly better with the system ON for 2 of the patients.

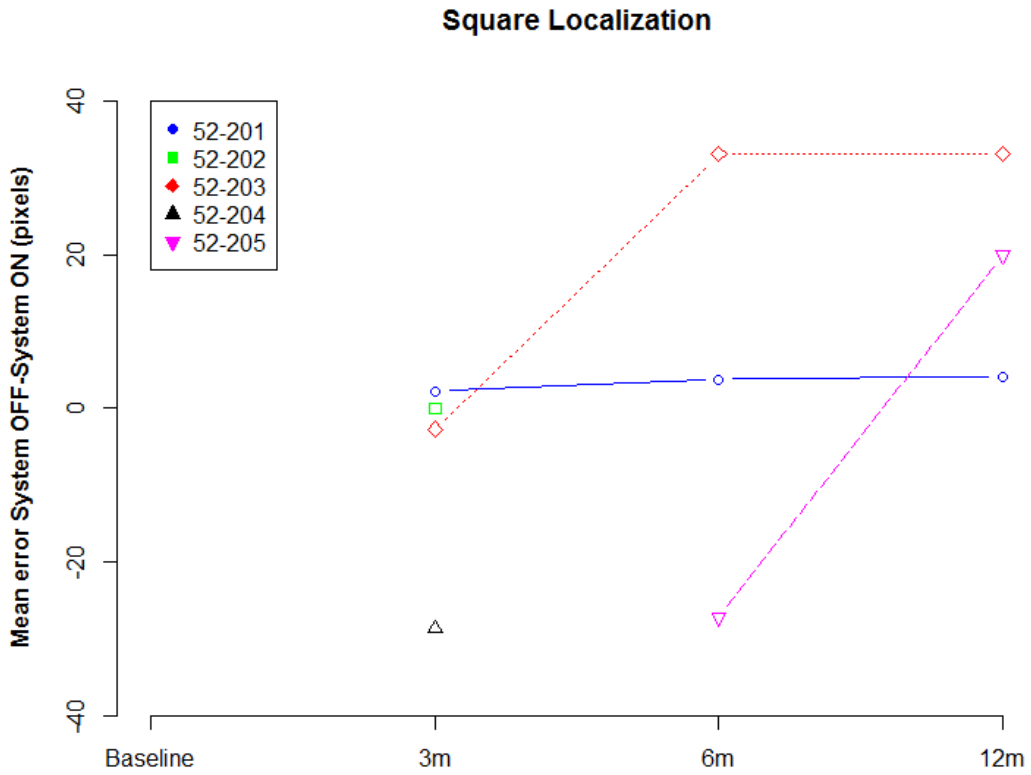

Figure 3.7A: *Individual results of the difference in performance over time (mean error system OFF – mean error system ON; positive values indicate better performance with the system ON) as measured with Square Localisation.*

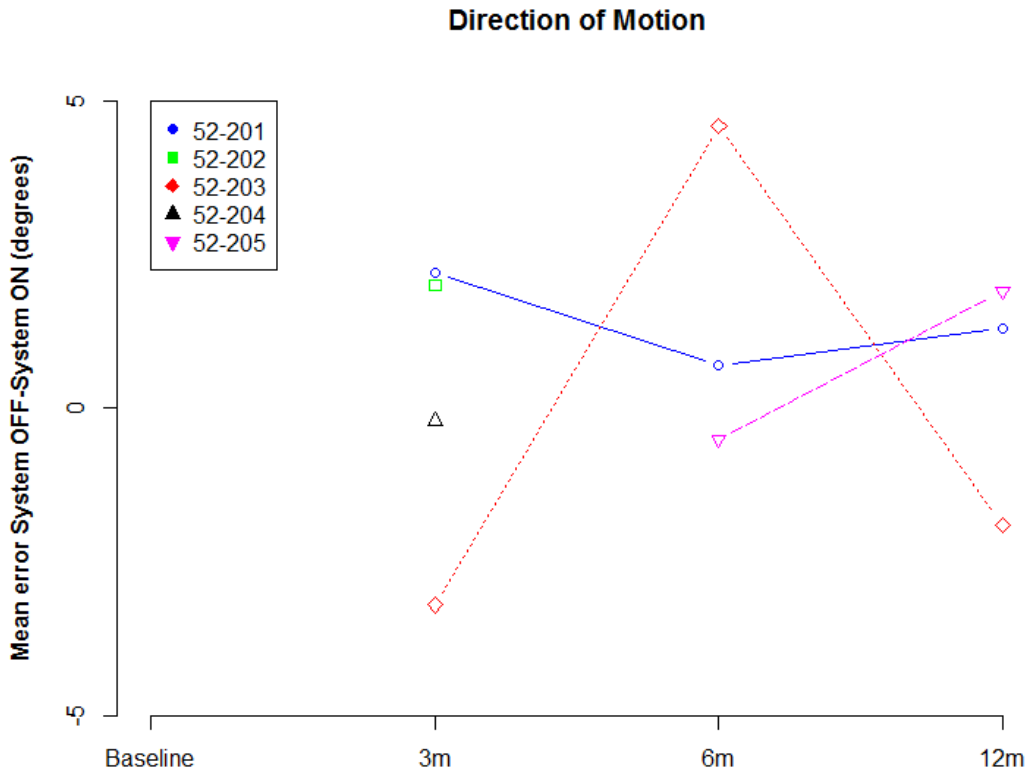

Figure 3.7B: *Individual results of the difference in performance over time (mean error system OFF – mean error system ON; positive values indicate better performance with the system ON) as measured with Direction of Motion (lower graph).*

After one year post-implantation the Argus® II system was found to be marginally beneficial for functional vision in a "real world" environment, according to the FLORA assessment. The impact of the Argus® II system in the subjects' life was rated as mildly positive for 3 of the participants and as positive for one of them. The mean scoring with the system ON and OFF was 2.03 ± 0.17 and 2.61 ± 0.11, respectively; lower scoring indicating better performance in real life tasks. Figure 3.8 shows the percentages of overall

ease of performance for the 4 subjects comparing the system ON and OFF. As shown, all FLORA domains improved with the system ON at one year post-implantation; the visual orientation tasks showed the biggest improvement. However, participants received less benefit when performing daily life tasks. Results from FLORA at the end of year 1 are compared to those at baseline in Figure 3.9. A worsening or increased difficulty of performance over time was found with the system OFF for all the domains. An improvement or easier performance with the system ON was found for all the domains over time, apart from the tasks involving interaction with others. Patients benefited more with the Argus® II System when performing mobility tasks.

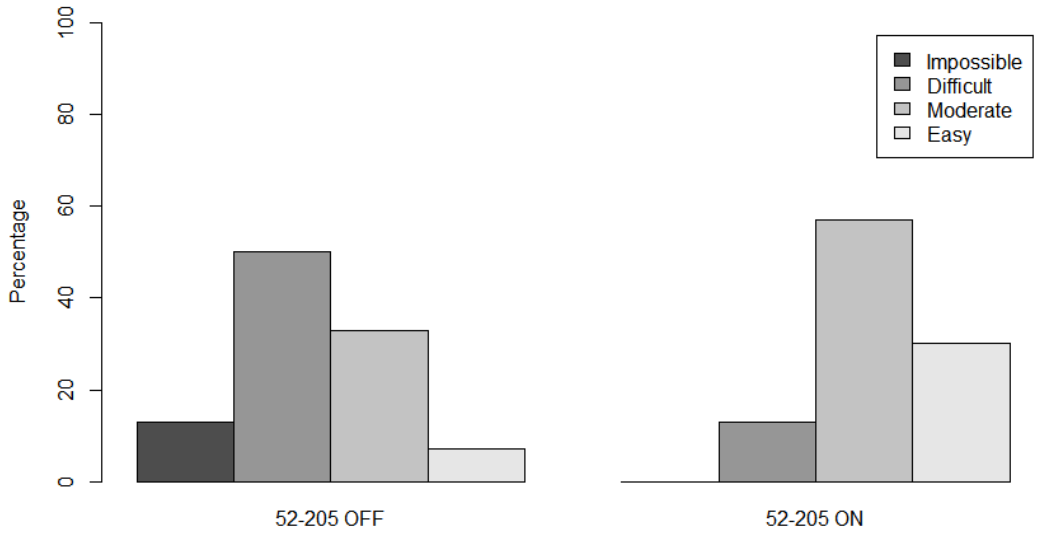

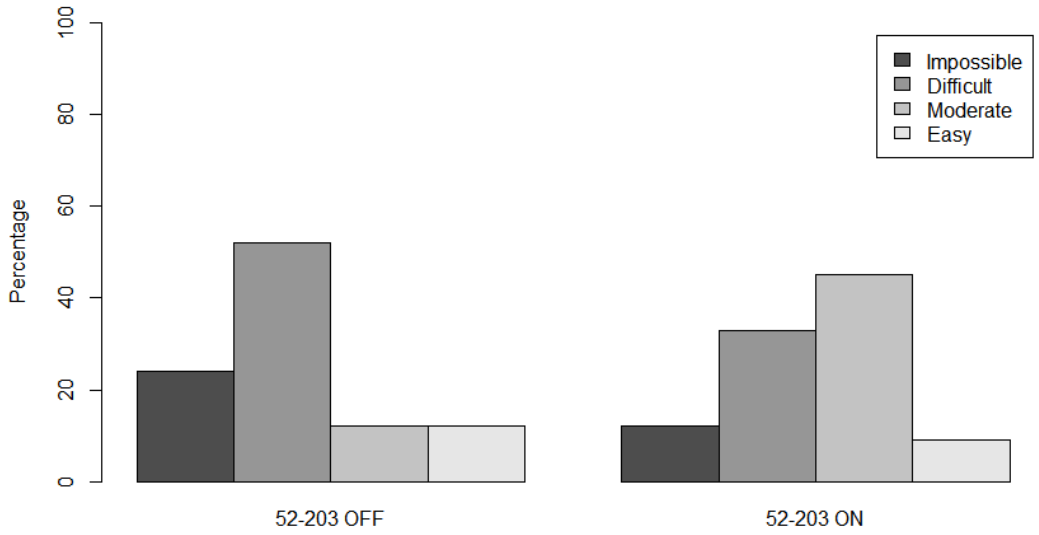
Percentage
0
20
40
60
80
100
Impossible
Difficult
Moderate
Easy
52-203 OFF
52-203 ON

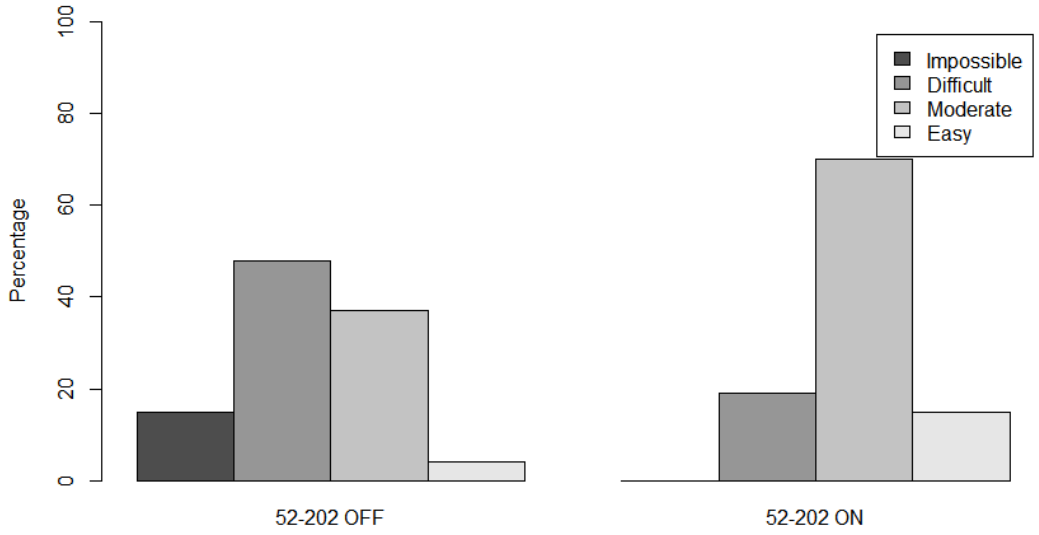
Percentage
0
20
40
60
80
100
Impossible
Difficult
Moderate
Easy
52-202 OFF
52-202 ON

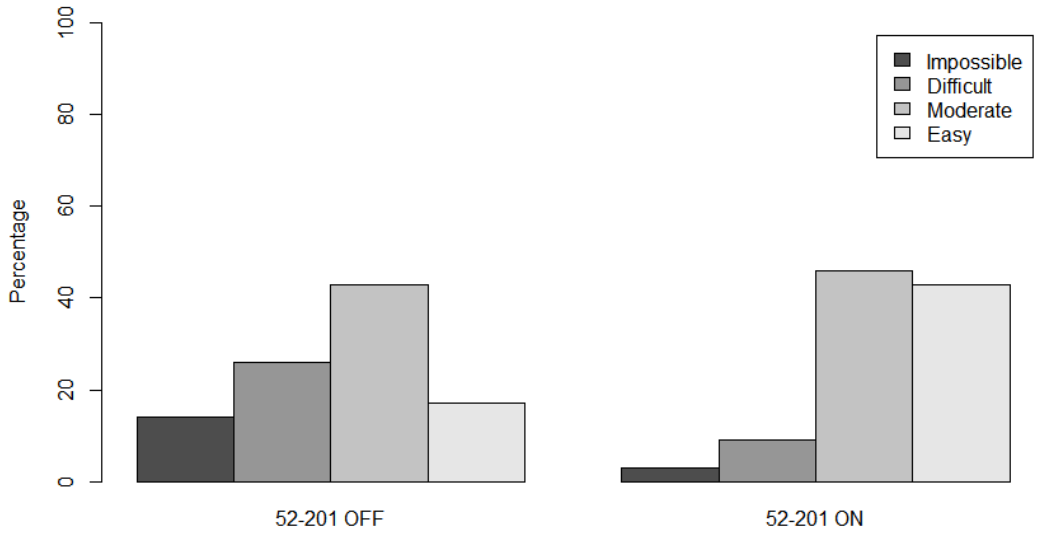

Figure 3.8: *Percentages of overall ease of performance for the 4 participants with the system ON and OFF according to FLORA results.*

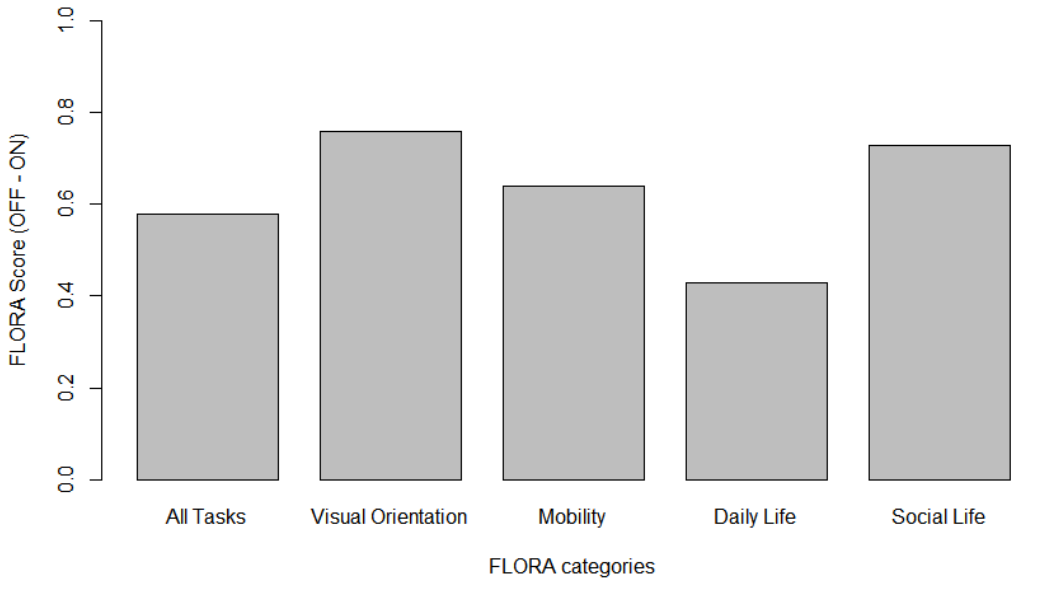

Figure 3.9: *Scoring difference (system OFF minus system ON) for the different tasks and all individuals at 12 months of follow-up according to*

FLORA results. Note that positive values indicate benefits when the system is operating.

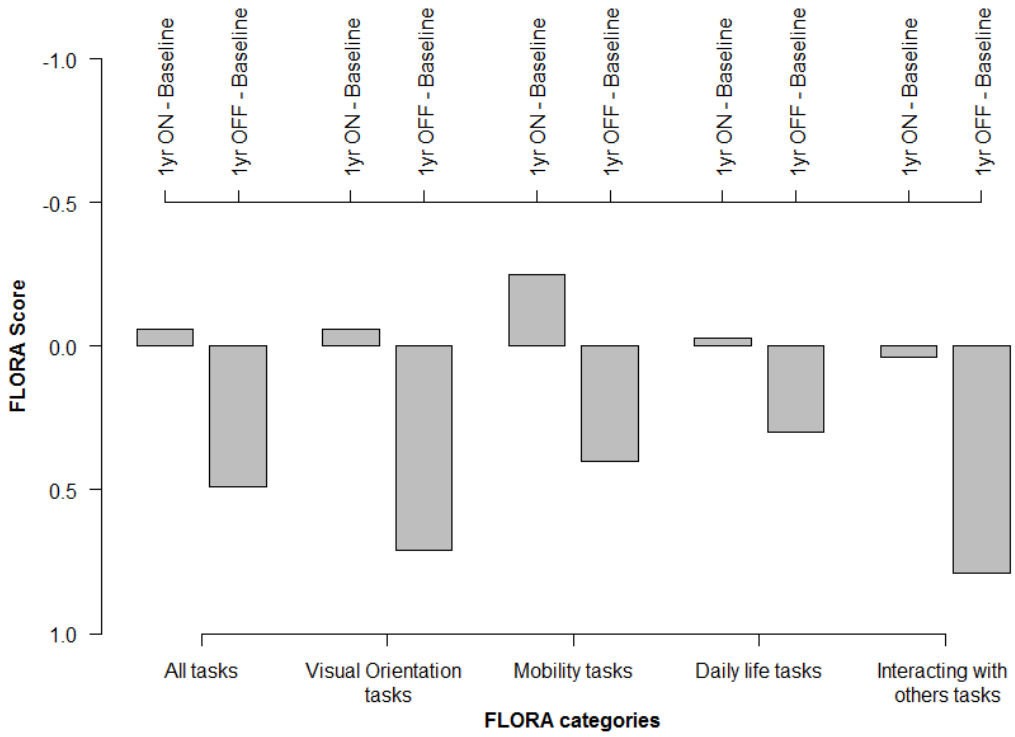

Figure 3.10: *Scoring difference (left bar per category: system ON minus baseline; right bar per category: system OFF minus baseline) for the different tasks for all individuals according to FLORA results. Note that negative values represent an improvement over time while positive scores indicate deterioration after implantation.*

Results from the NEI-VFQ-25 questionnaire are only available for three of the five patients due to study deviations (Table 3.5). The overall mean score for all patients at 12 months was 46, 2 points better than at baseline. When comparing the baseline scores with those at 12 months of follow-up, the

mean number of subscales improved per patient was 5 with the ocular pain, mental health and dependency being the ones showing an improvement for all three patients.

	Overall mean score			No of Subscales	
	Baseline	Month 12	Difference	Improved or stable over time	Worsened over time
All subjects	44	46	2	3	0
52-201	58	53	-5	7	5
52-203	32	39	7	9	3
52-205	41	46	5	9	3

Table 3.5: *Scoring and descriptive results from the NEI-VFQ-25. 100=Best, 0=Worst possible score.*

3.1.4 DISCUSSION

The Argus® II Retinal Prosthesis System was the first to gain CE approval and the only prosthesis to date that has received the FDA approval for commercialization.[409] Since then, over 200 people (mostly diagnosed with RP) have been implanted. Long term safety and performance results have demonstrated that the Argus® II System allows for stable and reliable restoration of some basic visual function in patients with RP.[426] However, this only covers a small percentage of the population suffering severe visual impairment. It is well established that age-related conditions such as AMD,

glaucoma and cataracts are the main causes for severe visual impairment and blindness by the age of 75 years. Approximately 196 million people worldwide will be affected by AMD by 2020 and this figure is projected to reach higher levels due to our increasing elderly population.[427, 428] In consequence, there is an increased economic burden in association with the visual impairment in AMD, and the World Health Organisation has marked this eye pathology as a major public health priority. Approximately 90% of individuals with AMD are suffering from its atrophic type.[429] The atrophic disease progresses more slowly than the neovascular form, but, despite this comforting prospect, there is no approved treatment or cure.

Therefore, the reported study was designed to assess the safety and efficacy (i.e. Phase II clinical trial) of the Argus® II Retinal Prosthesis System in patients with advanced non exudative AMD characterised by enlarged GA areas and central scotomas. The hypothesis is that the Argus® II system may prove to be a potential treatment option for patients of the above cohort, offering artificial vision in the defective central area of their VF while integrating well with their residual peripheral field. Five patients were identified in a period of less than a year and were implanted successfully. According to the protocol and for the assessment of the safety and efficacy of the Argus® II system, various structural and functional measurements were acquired in months 1, 2, 3, 6, 12 (and every 6 months onwards) post-operatively. Adverse events are followed closely with any appointments and tests required as necessary, according to the principal investigator's instructions. The reported results in this manuscript include every available

safety and efficacy assessment up to the first 12 months after implantation. The study is on-going for at least 2 more years.

Safety

Previous studies[402] on the safety of the Argus® II System in implanted patients have found most SAEs to occur towards the early post-operative period (within the first 6-12 months) being conjuntival erosion and hypotony the most prevalent SAEs. Likewise, in our cohort the non-rhegmatogenous RD under the cable occurred at day 1 after implantation, while the two cases of proliferative vitreoretinopathy and the case of hypotony happened after approximately 2 and 8 months post implantation, respectively.

The most common AE (i.e. the presence of cystoid macular oedema) in this study has surprisingly been reported in less than 5% of patients implanted with the Argus II System.[402, 421, 426] It has been suggested that macular oedemas in implanted patients are a result of the deformational forces on the retina, in a similar way that vitreomacular tractions or epiretinal membranes do. The oedema appeared in all patients of this study within a month after implantation and showed no signs of improvement or deterioration along the course of the first 12 months, no treatment or intervention was initiated. It is strongly believed that the reasons behind the presence of this oedema are mechanical; the tack that keeps the implant steady over the retina seems to "press" the system on the tissue, therefore creating retinal folds and an oedematous reaction from the retina. This "asphyxiation" of the tissue under the implant's tack area is evident in the OCT scans and fundus photographs.

Another reason for the presence of cystoid macular oedema may be the abnormal posterior retinal curvature, although the study participants had normal axial lengths and no significant differences. As mentioned before, no treatment was initiated to resolve the oedemas. Such a decision was taken on the basis that the occurred retinal thickening in the macular region may be beneficial in the effective performance of the system by reducing the retina-array distance and improving the array apposition; hence, increasing the sensitivity to electrical stimulations generated by the implant.

Another SAE that appeared in 2 out of 5 patients in this study but has not been previously reported in RP patients implanted with the Argus® II System is proliferative vitreoretinopathy. [402, 421, 426] The periretinal membranes that were observed due to the proliferation of ectopic cells in the vitreous and periretinal area are believed to be secondary to retinal suffering as consequence of excessive tissular compression exerted by the tack used to fixate the implant. The treatment selected for this complication was either gas injection or insertion of silicon oil. All cases responded positively to this intervention. The other two SAEs related to the implant were hypotony and non-rhegmatogenous RD under the cable; for the latter, again mechanical forces between the retinal tack and the macular tissue are considered responsible and was resolved by injecting intraocular gas. Hypotony was the SAE that presented the latest onset after implantation and so it was in previous reports of RP studies in which two cases among 30 patients presented hypotony after 12 months of implantation.[402] This is usually secondary to an open sclerostomy around the cable of the implant. Thus, in this case it was resolved by placing a donor scleral patch graft over the open

entry site. Conjuntival erosion, persisting hypotony or endophthalmitis are events that have previously been reported to happen in the long term.[402] In spite of all the adverse events described in this report having been successfully resolved without compromising the functioning of the Argus® II system, regular follow-ups are warranted to preserve the ocular health of these patients.

Efficacy

The small sample of patients does not allow for a strong statistical interpretation of the structural and functional assessments pre- and post-operatively.

Fundus photography and autofluorescence imaging showed enlargement of the atrophic macular area around the tack that puts the implant in place over the retina for the majority of patients. In the fellow eye the same patients showed no significant changes. The reason of the GA enlargement relies significantly on the compression applied by the implant, while its relatively large size, compared to the aforementioned atrophic areas, could also be a significant factor.

An exemption to these observations was 1 participant (i.e. 52-203) who had the largest atrophic area (~65mm^2) and the worst VFs at baseline. In this case progression of the GA in the implanted eye over time was insignificant. However, the atrophic region of the fellow eye increased by ~15mm^2 suggesting progression of the diagnosed pathology. These observations

could be supportive evidence for a recommendation of a smaller implant or a GA threshold (e.g. >40mm^2) on recruitment in future studies.

Visual function was mainly assessed with the 3 computer-based objective tests developed with the purpose of covering the range of low vision restored by a retinal implant. These same tests have been used before in a cohort of patients diagnosed with RP and implanted with the Argus® II system. While these subjects did not score better than 2.9 logMAR (i.e. performance by pure chance) with the system OFF at any time point, all the AMD patients constantly showed a VA of 1.6 logMAR or better with the system OFF. [402, 426] This is due to the high visual benefit from their peripheral residual vision that those patients with RP lack. Hence, results are not comparable between studies. Another recommendation that could derive from the outcomes of this study is that the design and implementation of these visual function tests should be tailored to the needs of AMD characteristics so more robust conclusions can be drawn regarding the integration of both the natural peripheral vision and the artificial central vision provided by the Argus® II system. From this clinical trial, the variability of results from the visual function tests both with the system ON and OFF and over time prevent any significant conclusions. The GVA results along with those from SL and DM tests supported the impression that conventional testing may not be sufficient for the recording of the system's benefit and life impact and thus, FLORA and the NEI-VFQ-25 questionnaire were used.

When FLORA is performed, patients serve as their own control as results are evaluated both with the Argus® II system ON and OFF. However, it should be pointed out that this is only an evaluator-reported assessment and neither

the evaluator nor the patients were masked to the operational status of the device when completing the tasks. The marginally positive FLORA outcomes could be due to a bias from the evaluator (a low-vision sufferer himself) and his enthusiasm for this new technological advancement. FLORA outcomes at 12 months after implantation from this study are in good agreement with those found in another published multicentre study.[425] The multicentre study comprised 30 patients whose average time of follow up at the time FLORA was administered was 36 months. It was similarly reported that daily life tasks are the ones for which the Argus® II was less effective as they are performed in a familiar, controlled environment. Likewise, the results of this agree with those from Geruschat et al. in that those tasks related to the use of the Argus® II system in conditions of maximum light contrast such as the visual orientation tasks, appeared to benefit most from the usage of the system.[425] In the present study, the completion of tasks involving mobility and interaction with others showed an improvement of performance in favour of the Argus® II system. These are the tasks that involve detection and tracking with the system and enhance patients' independence and social interaction. Regarding visual function assessment with the NEI-VFQ-25 questionnaire, the mean difference in overall score between the results at baseline and at 12 months post implantation was 2 points (range: -5 to 6). A 4 to 6 or 10 points change in NEI-VFQ-25 has previously been found to be clinically meaningful in patients diagnosed of neovascular AMD that corresponds to a 15 letter change in VA.[430, 431] Therefore it appears that a meaningful improvement in subjective visual function was produced over time in two of the patients from this study while a decline in visual function

was perceived by one of the subjects, although overall the improvement could be considered as not meaningful. Again, the presence of bias from the participants cannot be excluded. Improvement was reported for all 3 patients (i.e. those that reached the 12-month milestone and agreed to complete the questionnaire) in the NEI-VFQ-25 scoring in domains like ocular pain or mental health. However, it is highly unlikely that patients feel less ocular pain after they have been through such a long and high-risk eye surgery and additional interventions for resolving SAEs. In a similar way, improvement in patients' mental health is unlikely during the first year post-implantation and those differences may be due to the enthusiasm of the subjects participating in a pioneering research study.

The case of patient (52-205) presenting systematic improvement with the system ON over time merits further discussion. The patient showed meaningful improvement not only in the modified VA tests but also in NEI-VFQ-25, while he achieved the highest difference in score for most of the tasks evaluated with FLORA between the baseline assessment and the assessment at 12 months with the system ON. This patient happens to be the most motivated one, according to reports from the investigational team. Indeed, patient 52-205 is the only patient who attends his follow-up visits while wearing the Argus® II glasses and the system on functional mode. The patient claims to use the system regularly at home and during his social events and interactions. Hence, it is considered that training and visual rehabilitation are crucial after the implantation of the Argus® II system.

Indeed, Ghodasra et al in their position article for the Argus® II system (based on investigators' experience) highlight the importance of the

rehabilitation process after implantation.[421] Rehabilitation aims to enhance quality of life and independence for implanted patients by assisting them to integrate the new visual input they post-operatively acquired with any residual vision they already possess. It is separated into two major components: in-clinic and community rehabilitation, both of which are equally important. In the clinic, patients are shown the parts and functionality of the system, how to use the different settings on the VPU and some basic visual skills; the most important being the substitution of eye movement with the head moving in order to position the camera to the desired target. In the community, rehabilitation focuses on introducing the visual integration into daily living activities while refining already-acquired skills due to the severe visual impairment. In this clinical trial, rehabilitation support was regrettably minimal, considering that processes familiar and effective with the RP patient cohort proved to be unsuccessful with AMD patients whose residual (peripheral) vision was much more adequate.

To sum up, the recruitment of 5 patients with advanced atrophic AMD and their implantation with the Argus® II system has offered a plethora of information over the first 12 months. Invaluable data are still being collected providing an opportunity to assess whether retinal prosthetic devices are a feasible approach for the treatment of non-exudative AMD, one of the most common eye pathologies responsible for severe visual impairment. The Argus® II system has proven to be favourable in patients with RP, and to a lesser extent, choroideremia. However, the current implant design, which has gained regulatory approval and has proven to be beneficial for the above cohort, does not have the same striking effect on patients with atrophic AMD;

although as anticipated Second Sight's 'bionic eye' has elicited visual percepts by electrical stimulation of the atrophic macula of these 5 patients.[432] Recommendations for future research focus mainly on the structure of the evaluated retinal implant. It is believed that different approaches in the design of the retinal implant, mainly the retinal tack that keeps the implant in position, and the image processing settings could benefit potential future research candidates. With this purpose, new ways of testing to accurately evaluate the VF of implanted subjects could be developed as well as new stimulation strategies. These new strategies aim to improve the spatial resolution of the device and may provide real QoL benefits to these patients.

3.2 Research Impact and Potential

Current & Future Research

The benefits, or otherwise, of retinal prostheses in cohorts of patients suffering from severe visual impairment or blindness (such as RP and choroideremia) have been well-documented. A large number of patients implanted with commercially available bionic eyes, and those participating in relevant studies of other similar products, are reporting significant advantages and improvements in their quality of life. Hence, it is tempting to investigate such devices in a larger cohort of patients and with more prevalent pathologies that may present different characteristics than RP and choroideremia.

Such a hypothesis was tested in the above-described commercial study, sponsored by Second Sight and undertaken at MREH. The first implantations of the Argus® II system at patients with non-exudative AMD aimed to primarily assess the safety of the procedure and secondly attempt to answer the research question: “Is integration between central artificial and peripheral residual vision possible?”

The author’s lack of expertise on vitreoretinal procedures does not allow anything more than communicating the reports from other members of the research team on that aspect: implantation procedures are reported to have been complication-free and reproducible while showing successful setting of the implant on the atrophic macular area.

However, study outcomes from structural and functional assessments during the first year of the study along with the recording of AEs of different severity levels suggest that the current study probably required a different approach, rather than the one adopted for previous studies on different pathologies. More specifically, study protocol procedures constructed and followed during evaluation of the system on RP patients were adopted in the investigation of the AMD cohort. It became clear at a very short time that some of those procedures, especially in functional assessment, were inadequate and did not account for the fact that patients from the AMD cohort have significantly higher vision capabilities than those (i.e. RP-diagnosed) trialled in the past. It is noteworthy that the uncorrected VA of AMD patients at baseline was between 1.0-1.5 logMar units while VFs would present central scotomas and fairly adequate peripheral field; significantly different than functional characteristics presented by the RP cohort where VA was at the levels of detection of hand motion or light perception and VFs would barely show any remaining islands of vision.

The modified VA tests (i.e. grating visual acuity, square localisation and direction of motion) were designed and performed according to standards from previous studies; that is for very low vision subjects. As a result of the differences between the two cohorts, the procedures' testing range proved to be very small and unable to record VA measures from the AMD patients and accommodate their needs. What is more, the testing equipment, and more specifically the utilised touch screen monitor, did not seem to conform to phsycophysical testing standards; variations in luminance levels across the

screen and differences in target presentation times (due to lagging) were noticeable without the need of special equipment.

Another important aspect of a study design is the selection and utilisation of appropriate equipment. For the evaluation of the Argus® system on AMD patients a number of applied imaging and diagnostic equipment, albeit being the latest technological developments, could be deemed inappropriate. The particular prototype OCT device used in this study was still under evaluation, therefore lacking features that commercially available devices possess and they are considered essential in standard clinical care. For example, the absence of eye tracking in the aforementioned device made it extremely hard to acquire good quality scans with most of them having a significant number of motion artefacts; shown as black lines in the images. On the other hand, features such as the wide (i.e. 12x9mm) scanning pattern and mostly the implementation of the newly introduced Swept-Source technology, which offers increased penetration through the various retinal layers and the choroid, might have offered an advantage during monitoring; especially after implantation.

The Optos California imaging device is capable for wide-field fundus photographs (up to 200°) that allow assessment of the extreme periphery. While this breakthrough technology can offer a significant advantage in the diagnosis and monitoring of eye pathologies, such as DR or uveitis, it seemed to offer little in this study where the region of interest was the central 40-50° of the retina and more specifically the macular and implanted area. The acquisition of a wide-field picture and its resolution would undoubtedly affect the quality of the image when further focusing (i.e. zooming in) was

required. Lastly, microperimetry (performed with a device by the same company) could be deemed as an unnecessary choice considering that monitoring, and evaluation with the system ON/OFF, was not possible; while confirmation of central scotomas in the VF could be achieved with conventional HFA perimetry.

Nonetheless, this research project is the first to investigate safety and efficacy of a retinal implant in patients with an AMD diagnosis. The study is on-going and further invaluable data are collected on every protocol visit. Essential lessons could and should be learned from current study procedures in order to benefit not only the recruited AMD patients implanted with the bionic eye but also studies that will undoubtedly commence in the near future as further advancements on retinal implant designs (and their relevant components) are introduced.

REFERENCES

1. Pascolini, D. and S.P. Mariotti, *Global estimates of visual impairment: 2010.* Br J Ophthalmol, 2012. **96**(5): p. 614-8.
2. Resnikoff, S., et al., *Global data on visual impairment in the year 2002.* Bulletin of the World Health Organization, 2004. **82**(11): p. 844-851.
3. Thylefors, B., et al., *Global data on blindness.* Bulletin of the World Health Organization, 1995. **73**(1): p. 115-121.
4. Medeiros, F.A., et al., *The Structure and Function Relationship in Glaucoma: Implications for Detection of Progression and Measurement of Rates of Change.* Invest Ophthalmol Vis Sci, 2012.
5. Gordon, M.O., et al., *The Ocular Hypertension Treatment Study: baseline factors that predict the onset of primary open-angle glaucoma.* Arch Ophthalmol, 2002. **120**(6): p. 714-20; discussion 829-30.
6. Leske, M.C., et al., *Factors for glaucoma progression and the effect of treatment: The early manifest glaucoma trial.* Archives of Ophthalmology, 2003. **121**(1): p. 48-56.
7. Gaasterland, D.E., et al., *The Advanced Glaucoma Intervention Study (AGIS): 7. The relationship between control of intraocular pressure and visual field deterioration.* American Journal of Ophthalmology, 2000. **130**(4): p. 429-440.
8. Heijl, A., et al., *Reduction of intraocular pressure and glaucoma progression: results from the Early Manifest Glaucoma Trial.* Arch Ophthalmol, 2002. **120**(10): p. 1268-79.
9. Artes, P.H. and B.C. Chauhan, *Longitudinal changes in the visual field and optic disc in glaucoma.* Progress in Retinal and Eye Research, 2005. **24**(3): p. 333-354.
10. Chauhan, B.C., et al., *Optic disc and visual field changes in a prospective longitudinal study of patients with glaucoma: Comparison of scanning laser tomography with conventional perimetry and optic disc photography.* Archives of Ophthalmology, 2001. **119**(10): p. 1492-1499.
11. Heijl, A., et al., *Natural history of open-angle glaucoma.* Ophthalmology, 2009. **116**(12): p. 2271-6.
12. Saunders, L.J., et al., *What rates of glaucoma progression are clinically significant?* Expert Review of Ophthalmology, 2016. **11**(3): p. 227-234.
13. Jonas, J.B. and A.E. Grundler, *Correlation between mean visual field loss and morphometric optic disk variables in the open-angle glaucomas.* Am J Ophthalmol, 1997. **124**(4): p. 488-97.
14. Boland, M.V. and H.A. Quigley, *Risk factors and open-angle glaucoma: classification and application.* J Glaucoma, 2007. **16**(4): p. 406-18.
15. NHS. *Health checks for the over-65s*. 15/05/2014]; Available from: http://www.nhs.uk/Livewell/Screening/Pages/Checksover65s.aspx.
16. Nickells, R.W., *The cell and molecular biology of glaucoma: mechanisms of retinal ganglion cell death.* Invest Ophthalmol Vis Sci, 2012. **53**(5): p. 2476-81.

17. Kaushik, S., S.S. Pandav, and J. Ram, *Neuroprotection in glaucoma.* J Postgrad Med, 2003. **49**(1): p. 90-5.
18. Quigley, H.A., et al., *Retinal ganglion cell death in experimental glaucoma and after axotomy occurs by apoptosis.* Invest Ophthalmol Vis Sci, 1995. **36**(5): p. 774-86.
19. Spry, P.G.D., Harper, R. A., *Essential Glaucoma Handbook: A Guide to Assessment and Management for Eye Care Professionals*. 2010: Optician.
20. Klein, B.E., et al., *Prevalence of glaucoma. The Beaver Dam Eye Study.* Ophthalmology, 1992. **99**(10): p. 1499-504.
21. Tielsch, J.M., et al., *A population-based evaluation of glaucoma screening: the Baltimore Eye Survey.* Am J Epidemiol, 1991. **134**(10): p. 1102-10.
22. Hendrickx, K.H., et al., *Cumulative incidence of patients with disc hemorrhages in glaucoma and the effect of therapy.* Ophthalmology, 1994. **101**(7): p. 1165-72.
23. Cursiefen, C., et al., *Migraine and tension headache in high-pressure and normal-pressure glaucoma.* Am J Ophthalmol, 2000. **129**(1): p. 102-4.
24. Gass, A., et al., *Inverse correlation between endothelin-1-induced peripheral microvascular vasoconstriction and blood pressure in glaucoma patients.* Graefes Arch Clin Exp Ophthalmol, 1997. **235**(10): p. 634-8.
25. O'Brien, C. and Z. Butt, *Blood flow velocity in the peripheral circulation of glaucoma patients.* Ophthalmologica, 1999. **213**(3): p. 150-3.
26. Wang, J.J., P. Mitchell, and W. Smith, *Is there an association between migraine headache and open-angle glaucoma? Findings from the Blue Mountains Eye Study.* Ophthalmology, 1997. **104**(10): p. 1714-9.
27. Bill, A. and G.O. Sperber, *Control of retinal and choroidal blood flow.* Eye (Lond), 1990. **4 (Pt 2)**: p. 319-25.
28. Chung, H.S., et al., *Peripapillary retinal blood flow in normal tension glaucoma.* Br J Ophthalmol, 1999. **83**(4): p. 466-9.
29. Grunwald, J.E., et al., *Optic nerve blood flow in glaucoma: effect of systemic hypertension.* Am J Ophthalmol, 1999. **127**(5): p. 516-22.
30. Michelson, G., et al., *Visual field defect and perfusion of the juxtapapillary retina and the neuroretinal rim area in primary open-angle glaucoma.* Graefes Arch Clin Exp Ophthalmol, 1998. **236**(2): p. 80-5.
31. Bonomi, L., et al., *Vascular risk factors for primary open angle glaucoma: the Egna-Neumarkt Study.* Ophthalmology, 2000. **107**(7): p. 1287-93.
32. Harris, A., et al., *A comparative study of betaxolol and dorzolamide effect on ocular circulation in normal-tension glaucoma patients.* Ophthalmology, 2000. **107**(3): p. 430-4.
33. Nomura, H., et al., *Age-related changes in intraocular pressure in a large Japanese population: a cross-sectional and longitudinal study.* Ophthalmology, 1999. **106**(10): p. 2016-22.
34. Foster, P.J., et al., *The definition and classification of glaucoma in prevalence surveys.* Br J Ophthalmol, 2002. **86**(2): p. 238-42.

35. Quigley, H.A. and A.T. Broman, *The number of people with glaucoma worldwide in 2010 and 2020.* Br J Ophthalmol, 2006. **90**(3): p. 262-7.
36. Franks, W. and D. Taylor, *Congenital glaucoma--a preventable cause of blindness.* Arch Dis Child, 1989. **64**(5): p. 649-50.
37. Cook, C. and P. Foster, *Epidemiology of glaucoma: what's new?* Can J Ophthalmol, 2012. **47**(3): p. 223-6.
38. Anderson, D.R., J.C. Jin, and M.M. Wright, *The physiologic characteristics of relative pupillary block.* Am J Ophthalmol, 1991. **111**(3): p. 344-50.
39. Jin, J.C. and D.R. Anderson, *The effect of iridotomy on iris contour.* Am J Ophthalmol, 1990. **110**(3): p. 260-3.
40. Tiedeman, J.S., *A physical analysis of the factors that determine the contour of the iris.* Am J Ophthalmol, 1991. **111**(3): p. 338-43.
41. Tham, Y.C., et al., *Global prevalence of glaucoma and projections of glaucoma burden through 2040: a systematic review and meta-analysis.* Ophthalmology, 2014. **121**(11): p. 2081-90.
42. *NICE Guidelines - Glaucoma: Diagnosis and Management of Chronic Open Angle Glaucoma and Ocular Hypertension (CG85)*, in *CG85*, NICE, Editor. 2009, National Institute for Health and Clinical Excellence: London.
43. Graham, S., *Defining the structure/function relationship in glaucoma.* Clin Experiment Ophthalmol, 2012. **40**(4): p. 337-8.
44. Kerrigan-Baumrind, L.A., et al., *Number of ganglion cells in glaucoma eyes compared with threshold visual field tests in the same persons.* Invest Ophthalmol Vis Sci, 2000. **41**(3): p. 741-8.
45. Quigley, H.A., E.M. Addicks, and W.R. Green, *Optic nerve damage in human glaucoma. III. Quantitative correlation of nerve fiber loss and visual field defect in glaucoma, ischemic neuropathy, papilledema, and toxic neuropathy.* Arch Ophthalmol, 1982. **100**(1): p. 135-46.
46. Quigley, H.A., G.R. Dunkelberger, and W.R. Green, *Retinal ganglion cell atrophy correlated with automated perimetry in human eyes with glaucoma.* Am J Ophthalmol, 1989. **107**(5): p. 453-64.
47. Harwerth, R.S., et al., *Visual field defects and neural losses from experimental glaucoma.* Prog Retin Eye Res, 2002. **21**(1): p. 91-125.
48. Harwerth, R.S., et al., *Neural losses correlated with visual losses in clinical perimetry.* Invest Ophthalmol Vis Sci, 2004. **45**(9): p. 3152-60.
49. Artes, P.H. and B.C. Chauhan, *Longitudinal changes in the visual field and optic disc in glaucoma.* Prog Retin Eye Res, 2005. **24**(3): p. 333-54.
50. Anderson, R.S., *The psychophysics of glaucoma: improving the structure/function relationship.* Prog Retin Eye Res, 2006. **25**(1): p. 79-97.
51. Curcio, C.A. and K.A. Allen, *Topography of ganglion cells in human retina.* J Comp Neurol, 1990. **300**(1): p. 5-25.
52. Gonzalez-Hernandez, M., et al., *Structure-function relationship depends on glaucoma severity.* Br J Ophthalmol, 2009. **93**(9): p. 1195-9.
53. Huang, D., et al., *Optical coherence tomography.* Science, 1991. **254**(5035): p. 1178-1181.

54. Vessani, R.M., et al., *Comparison of quantitative imaging devices and subjective optic nerve head assessment by general ophthalmologists to differentiate normal from glaucomatous eyes.* J Glaucoma, 2009. **18**(3): p. 253-61.
55. Sehi, M., et al., *Diagnostic ability of Fourier-domain vs time-domain optical coherence tomography for glaucoma detection.* Am J Ophthalmol, 2009. **148**(4): p. 597-605.
56. Hougaard, J.L., A. Heijl, and B. Bengtsson, *Glaucoma detection by Stratus OCT.* J Glaucoma, 2007. **16**(3): p. 302-6.
57. Sihota, R., et al., *Diagnostic capability of optical coherence tomography in evaluating the degree of glaucomatous retinal nerve fiber damage.* Invest Ophthalmol Vis Sci, 2006. **47**(5): p. 2006-10.
58. Jeoung, J.W., et al., *Diagnostic ability of optical coherence tomography with a normative database to detect localized retinal nerve fiber layer defects.* Ophthalmology, 2005. **112**(12): p. 2157-63.
59. Jeoung, J.W. and K.H. Park, *Comparison of Cirrus OCT and Stratus OCT on the ability to detect localized retinal nerve fiber layer defects in preperimetric glaucoma.* Invest Ophthalmol Vis Sci, 2010. **51**(2): p. 938-45.
60. Vizzeri, G., et al., *Agreement between spectral-domain and time-domain OCT for measuring RNFL thickness.* Br J Ophthalmol, 2009. **93**(6): p. 775-81.
61. Knight, O.J., et al., *Comparison of retinal nerve fiber layer measurements using time domain and spectral domain optical coherent tomography.* Ophthalmology, 2009. **116**(7): p. 1271-7.
62. Chang, R.T., et al., *Sensitivity and specificity of time-domain versus spectral-domain optical coherence tomography in diagnosing early to moderate glaucoma.* Ophthalmology, 2009. **116**(12): p. 2294-9.
63. Moreno-Montanes, J., et al., *Cirrus high-definition optical coherence tomography compared with Stratus optical coherence tomography in glaucoma diagnosis.* Invest Ophthalmol Vis Sci, 2010. **51**(1): p. 335-43.
64. Reus, N.J., M. de Graaf, and H.G. Lemij, *Accuracy of GDx VCC, HRT I, and clinical assessment of stereoscopic optic nerve head photographs for diagnosing glaucoma.* Br J Ophthalmol, 2007. **91**(3): p. 313-8.
65. Deleon-Ortega, J.E., et al., *Discrimination between glaucomatous and nonglaucomatous eyes using quantitative imaging devices and subjective optic nerve head assessment.* Invest Ophthalmol Vis Sci, 2006. **47**(8): p. 3374-80.
66. Wollstein, G., D.F. Garway-Heath, and R.A. Hitchings, *Identification of early glaucoma cases with the scanning laser ophthalmoscope.* Ophthalmology, 1998. **105**(8): p. 1557-63.
67. Swindale, N.V., et al., *Automated analysis of normal and glaucomatous optic nerve head topography images.* Invest Ophthalmol Vis Sci, 2000. **41**(7): p. 1730-42.
68. Andersson, S., A. Heijl, and B. Bengtsson, *Optic disc classification by the Heidelberg Retina Tomograph and by physicians with varying experience of glaucoma.* Eye, 2011. **25**(11): p. 1401-1407.

69. Medeiros, F.A., et al., *Influence of Disease Severity and Optic Disc Size on the Diagnostic Performance of Imaging Instruments in Glaucoma.* Investigative Ophthalmology & Visual Science, 2006. **47**(3): p. 1008-1015.
70. Leske, M.C., et al., *Distribution of intraocular pressure: The Barbados Eye Study.* Archives of Ophthalmology, 1997. **115**(8): p. 1051-1057.
71. Saccà, S.C., et al., *Fluctuations of intraocular pressure during the day in open-angle glaucoma, normal-tension glaucoma and normal subjects.* Ophthalmologica, 1998. **212**(2): p. 115-119.
72. *Terminology and Guidelines for Glaucoma*. 3rd ed. 2008: European Glaucoma Society.
73. Vass, C., et al., *Medical interventions for primary open angle glaucoma and ocular hypertension.* Cochrane Database of Systematic Reviews, 2007(4): p. CD003167.
74. *The effectiveness of intraocular pressure reduction in the treatment of normal-tension glaucoma. Collaborative Normal-Tension Glaucoma Study Group.* Am J Ophthalmol, 1998. **126**(4): p. 498-505.
75. Kass, M.A., et al., *The Ocular Hypertension Treatment Study: a randomized trial determines that topical ocular hypotensive medication delays or prevents the onset of primary open-angle glaucoma.* Arch Ophthalmol, 2002. **120**(6): p. 701-13; discussion 829-30.
76. Gaasterland, D.E., et al., *The Advanced Glaucoma Intervention Study (AGIS): 7. The relationship between control of intraocular pressure and visual field deterioration.* American Journal of Ophthalmology, 2000. **130**(4): p. 429-440.
77. Garway-Heath, D.F., et al., *The United Kingdom glaucoma treatment study: A multicenter, randomized, placebo-controlled clinical trial: Design and methodology.* Ophthalmology, 2013. **120**(1): p. 68-76.
78. Anderson, D.R., Patella VM, *Automated Static Perimetry*. 2nd Edition ed. 1998, St Louis: Mosby.
79. Sample, P.A., et al., *Imaging and perimetry society standards and guidelines.* Optometry and Vision Science, 2011. **88**(1): p. 4-7.
80. Hart, W.M., Jr. and R.M. Burde, *Three-dimensional topography of the central visual field. Sparing of foveal sensitivity in macular disease.* Ophthalmology, 1983. **90**(8): p. 1028-38.
81. von Graefe, A., *Über die Untersuchung des Gesichtsfeldes bei amblyopischen Affectionen.* Archive für Ophthalmologie, 1856. **vol. 2**(no. 2): p. pp. 258-298.
82. Scherk, S., *Ein neuer Apparat zur Messung des Gesichtsfeldes.* Klin Monatsbl Augenheilkd, 1872. **vol. 10**: p. pp. 151-163.
83. Harrington, D.O. and M. Flocks, *The multiple-pattern method of visual field examination; a five-year evaluation of its effectiveness as a visual field screening technique.* AMA Arch Ophthalmol, 1959. **61**(5): p. 755-65.
84. Heijl, A., *Studies on computerized perimetry.* Acta Ophthalmol Suppl, 1977. **132**: p. 1-42.
85. Heijl, A. and C.E. Krakau, *An automatic static perimeter, design and pilot study.* Acta Ophthalmol (Copenh), 1975. **53**(3): p. 293-310.

86. Spahr, J., *Optimization of the presentation pattern in automated static perimetry.* Vision Res, 1975. **15**(11): p. 1275-81.
87. Fechner, G.T., *Elemente der Psychophysik*. 1860, Leipzig: Breitkopf und Härtel.
88. Artes, P.H., *Developments in Suprathreshold Perimetry*. 2001, University of Manchester.
89. Green, D.M.S., J.A., *Signal Detection Theory and Psychophysics*. 1966, New York: John Wiley & Sons Inc.
90. Heijl, A., A. Lindgren, and G. Lindgren, *Test-retest variability in glaucomatous visual fields.* Am J Ophthalmol, 1989. **108**(2): p. 130-5.
91. Holmin, C. and C.E. Krakau, *Variability of glaucomatous visual field defects in computerized perimetry.* Albrecht Von Graefes Arch Klin Exp Ophthalmol, 1979. **210**(4): p. 235-50.
92. Weber, J. and S. Rau, *The properties of perimetric thresholds in normal and glaucomatous eyes.* Ger J Ophthalmol, 1992. **1**(2): p. 79-85.
93. Henson DB, C.S., Artes PH., *The relationship between sensitivity and variability in normal and glaucomatous visual fields.* Wall M eds. Perimetry Update 1997/1999.: Kugler Amsterdam.
94. Henson, D.B., et al., *Response variability in the visual field: comparison of optic neuritis, glaucoma, ocular hypertension, and normal eyes.* Invest Ophthalmol Vis Sci, 2000. **41**(2): p. 417-21.
95. Chauhan, B.C. and C.A. Johnson, *Test-retest variability of frequency-doubling perimetry and conventional perimetry in glaucoma patients and normal subjects.* Invest Ophthalmol Vis Sci, 1999. **40**(3): p. 648-56.
96. Henson, D.B., *Visual Fields*. 2000: Butterworth-Heinemann.
97. Martinez, G.A., P.A. Sample, and R.N. Weinreb, *Comparison of high-pass resolution perimetry and standard automated perimetry in glaucoma.* American Journal of Ophthalmology, 1995. **119**(2): p. 195-201.
98. Martin, L., et al., *Concordance of high-pass resolution perimetry and frequency-doubling technology perimetry results in glaucoma: No support for selective Ganglion cell damage.* Journal of Glaucoma, 2003. **12**(1): p. 40-44.
99. Khoury, J.M., et al., *Comparison of 24-2 and 30-2 perimetry in glaucomatous and nonglaucomatous optic neuropathies.* Journal of Neuro-Ophthalmology, 1999. **19**(2): p. 100-108.
100. Traynis, I., et al., *Prevalence and nature of early glaucomatous defects in the central 10° of the visual field.* JAMA Ophthalmology, 2014. **132**(3): p. 291-297.
101. Henson, D.B. and B.C. Chauhan, *Informational content of visual field location in glaucoma.* Documenta Ophthalmologica, 1985. **59**(4): p. 341-352.
102. Henson, D.B., S.M. Dix, and A.C. Oborne, *Evaluation of the friedmann visual field analyser mark II. Part 1. Results from a normal population.* British Journal of Ophthalmology, 1984. **68**(7): p. 458-462.
103. Wang, Y. and D.B. Henson, *Diagnostic performance of visual field test using subsets of the 24-2 test pattern for early glaucomatous field*

loss. Investigative Ophthalmology and Visual Science, 2013. **54**(1): p. 756-761.
104. Barlow, H.B., *Temporal and spatial summation in human vision at different background intensities.* The Journal of Physiology, 1958. **141**(2): p. 337-350.
105. Wilson, M.E., *Invariant features of spatial summation with changing locus in the visual field.* The Journal of Physiology, 1970. **207**(3): p. 611-622.
106. Redmond, T., et al., *The effect of age on the area of complete spatial summation for chromatic and achromatic stimuli.* Investigative Ophthalmology and Visual Science, 2010. **51**(12): p. 6533-6539.
107. Redmond, T., et al., *Sensitivity loss in early glaucoma can be mapped to an enlargement of the area of complete spatial summation.* Investigative Ophthalmology and Visual Science, 2010. **51**(12): p. 6540-6548.
108. Wall, M., K.E. Kutzko, and B.C. Chauhan, *Variability in patients with glaucomatous visual field damage is reduced using size V stimuli.* Invest Ophthalmol Vis Sci, 1997. **38**(2): p. 426-35.
109. Wall, M., et al., *Size threshold perimetry performs as well as conventional automated perimetry with stimulus sizes III, V, and VI for glaucomatous loss.* Invest Ophthalmol Vis Sci, 2013. **54**(6): p. 3975-83.
110. Pennebaker, G.E., et al., *The effect of stimulus duration upon the components of fluctuation in static automated perimetry.* Eye (Lond), 1992. **6 (Pt 4)**: p. 353-5.
111. Mulholland, P., *Temporal Summation with Age and in Glaucoma*, in *Faculty of Life and Health Sciences*. 2014, University of Ulster.
112. Urban, F.M., *The method of constant stimuli and its generalizations.* Psychological Review, 1910. **17**(4): p. 229-259.
113. Cornsweet, T.N., *The Staircase-Method in Psychophysics.* The American Journal of Psychology, 1962. **75**(3): p. 485-491.
114. Taylor, M.M. and C.D. Creelman, *PEST: Efficient Estimates on Probability Functions.* The Journal of the Acoustical Society of America, 1967. **41**(4A): p. 782-787.
115. Wetherill, G.B. and H. Levitt, *SEQUENTIAL ESTIMATION OF POINTS ON A PSYCHOMETRIC FUNCTION.* Br J Math Stat Psychol, 1965. **18**: p. 1-10.
116. Bebie, H., F. Fankhauser, and J. Spahr, *Static perimetry: strategies.* Acta Ophthalmol (Copenh), 1976. **54**(3): p. 325-38.
117. Flanagan, J.G., et al., *Evaluation of FASTPAC: a new strategy for threshold estimation with the Humphrey Field Analyser.* Graefes Arch Clin Exp Ophthalmol, 1993. **231**(8): p. 465-9.
118. Gillies, B., M. Rivers, and A.M. Brooks, *Comparison of Fastpak with full-threshold 24-2 glaucoma field tests.* Ophthalmic Surg Lasers, 1996. **27**(9): p. 758-62.
119. Watson, A.B. and D.G. Pelli, *Quest: A Bayesian adaptive psychometric method.* Perception & Psychophysics, 1983. **33**(2): p. 113-120.
120. King-Smith, P.E., et al., *Efficient and unbiased modifications of the QUEST threshold method: theory, simulations, experimental*

evaluation and practical implementation. Vision Res, 1994. **34**(7): p. 885-912.
121. Bengtsson, B., et al., *A new generation of algorithms for computerized threshold perimetry, SITA.* Acta Ophthalmol Scand, 1997. **75**(4): p. 368-75.
122. Bengtsson, B., A. Heijl, and J. Olsson, *Evaluation of a new threshold visual field strategy, SITA, in normal subjects. Swedish Interactive Thresholding Algorithm.* Acta Ophthalmol Scand, 1998. **76**(2): p. 165-9.
123. Artes, P.H., et al., *Properties of perimetric threshold estimates from Full Threshold, SITA Standard, and SITA Fast strategies.* Invest Ophthalmol Vis Sci, 2002. **43**(8): p. 2654-9.
124. Turpin, A., et al., *Performance of efficient test procedures for frequency-doubling technology perimetry in normal and glaucomatous eyes.* Investigative Ophthalmology and Visual Science, 2002. **43**(3): p. 709-715.
125. Turpin, A., et al., *Development of efficient threshold strategies for frequency doubling technology perimetry using computer simulation.* Investigative Ophthalmology and Visual Science, 2002. **43**(2): p. 322-331.
126. Artes, P.H., et al., *Multisampling suprathreshold perimetry: A comparison with conventional suprathreshold and full-threshold strategies by computer simulation.* Investigative Ophthalmology and Visual Science, 2003. **44**(6): p. 2582-2587.
127. Miranda, M.A. and D.B. Henson, *Perimetric sensitivity and response variability in glaucoma with single-stimulus automated perimetry and multiple-stimulus perimetry with verbal feedback.* Acta Ophthalmol, 2008. **86**(2): p. 202-6.
128. Wall, M., et al., *Long- and short-term variability of automated perimetry results in patients with optic neuritis and healthy subjects.* Archives of Ophthalmology, 1998. **116**(1): p. 53-61.
129. Wall, M., et al., *The psychometric function and reaction times of automated perimetry in normal and abnormal areas of the visual field in patients with glaucoma.* Investigative Ophthalmology and Visual Science, 1996. **37**(5): p. 878-885.
130. Wall, M., et al., *The repeatability of mean defect with size III and size V standard automated perimetry.* Investigative Ophthalmology and Visual Science, 2013. **54**(2): p. 1345-1351.
131. Wood, J.M., et al., *Serial examination of the normal visual field using Octopus automated projection perimetry. Evidence for a learning effect.* Acta Ophthalmol (Copenh), 1987. **65**(3): p. 326-33.
132. Heijl, A. and S.M. Drance, *Changes in differential threshold in patients with glaucoma during prolonged perimetry.* British Journal of Ophthalmology, 1983. **67**(8): p. 512-516.
133. Flammer, J., et al., *Quantification of glaucomatous visual field defects with automated perimetry.* Investigative Ophthalmology and Visual Science, 1985. **26**(2): p. 176-181.
134. Sample, P.A., C.F. Bosworth, and R.N. Weinreb, *The loss of visual function in glaucoma.* Seminars in Ophthalmology, 2000. **15**(4): p. 182-193.

135. Lalkhen, A.G. and A. McCluskey, *Clinical tests: sensitivity and specificity.* Continuing Education in Anaesthesia, Critical Care & Pain, 2008. **8**(6): p. 221-223.
136. Bland, J.M., *An Introduction to Medical Statistics*. 2000: OUP Oxford.
137. Gilbert, R., et al., *Evidence-Based Case Review: Assessing diagnostic and screening tests: Part 1. Concepts.* Western Journal of Medicine, 2001. **174**(6): p. 405.
138. National Screening Committee, U. *First Report of the National Screening Committee*. 1998 15/05/2014]; Available from: http://aogm.org.mo/assets/Uploads/aogm/Guidelines/NHS/National-Screening-Committee-UK-1998.pdf.
139. Altman, D.G., *Practical Statistics for Medical Research*. 1990: Taylor & Francis.
140. Saunders, L.J., et al., *Examining visual field loss in patients in glaucoma clinics during their predicted remaining lifetime.* Invest Ophthalmol Vis Sci, 2014. **55**(1): p. 102-9.
141. Deva, N.C., et al., *Risk factors for first presentation of glaucoma with significant visual field loss.* Clin Experiment Ophthalmol, 2008. **36**(3): p. 217-21.
142. Fraser, S., et al., *Deprivation and late presentation of glaucoma: case-control study.* BMJ, 2001. **322**(7287): p. 639-43.
143. Rudnicka, A.R., et al., *Variations in primary open-angle glaucoma prevalence by age, gender, and race: a Bayesian meta-analysis.* Invest Ophthalmol Vis Sci, 2006. **47**(10): p. 4254-61.
144. Reidy, A., et al., *Prevalence of serious eye disease and visual impairment in a north London population: population based, cross sectional study.* Bmj, 1998. **316**(7145): p. 1643-6.
145. King, A.J., R.E. Stead, and A.P. Rotchford, *Treating patients presenting with advanced glaucoma--should we reconsider current practice?* Br J Ophthalmol, 2011. **95**(9): p. 1185-92.
146. Henson, D.B. and R. Thampy, *Preventing blindness from glaucoma.* Bmj, 2005. **331**(7509): p. 120-1.
147. Sinclair, A., A. Hinds, and R. Sanders, *Ten years of glaucoma blindness in Fife 1990-99 and the implications for ophthalmology, optometry and rehabilitation services.* Ophthalmic & physiological optics : the journal of the British College of Ophthalmic Opticians (Optometrists), 2004. **24**(4): p. 313-318.
148. Prior, M., et al., *Why do people present late with advanced glaucoma? A qualitative interview study.* British Journal of Ophthalmology, 2013. **97**(12): p. 1574-1578.
149. Wilson, J.M.G., Jungner, G., *Principles And Practice Of Screening For Disease* 1968: World Health Organization.
150. Traverso, C.E., et al., *Direct costs of glaucoma and severity of the disease: A multinational long term study of resource utilisation in Europe.* British Journal of Ophthalmology, 2005. **89**(10): p. 1245-1249.
151. RNIB, *Future sight loss UK 1: Economic impact of partial sight and blindness in the UK adult population*.

152. Burr, J., et al., *Is it worthwhile to conduct a randomized controlled trial of glaucoma screening in the united kingdom?* Journal of Health Services Research and Policy, 2014. **19**(1): p. 42-51.
153. Hernández, R., et al., *Screening for open angle glaucoma: Systematic review of cost-effectiveness studies.* Journal of Glaucoma, 2008. **17**(3): p. 159-168.
154. Burr, J.M., et al., *The clinical effectiveness and cost-effectiveness of screening for open angle glaucoma: A systematic review and economic evaluation.* Health Technology Assessment, 2007. **11**(41): p. iii-170.
155. Celler, B., et al., *Impact of At-Home Telemonitoring on Health Services Expenditure and Hospital Admissions in Patients With Chronic Conditions: Before and After Control Intervention Analysis.* JMIR Medical Informatics, 2017. **5**(3): p. e29.
156. McBain, H., M. Shipley, and S. Newman, *The impact of self-monitoring in chronic illness on healthcare utilisation: a systematic review of reviews.* BMC Health Services Research, 2015. **15**: p. 565.
157. Panagioti, M., et al., *Self-management support interventions to reduce health care utilisation without compromising outcomes: a systematic review and meta-analysis.* BMC Health Serv Res, 2014. **14**: p. 356.
158. Kitsiou, S., G. Pare, and M. Jaana, *Effects of home telemonitoring interventions on patients with chronic heart failure: an overview of systematic reviews.* J Med Internet Res, 2015. **17**(3): p. e63.
159. Bowling, B., S.D.M. Chen, and J.F. Salmon, *Outcomes of referrals by community optometrists to a hospital glaucoma service.* British Journal of Ophthalmology, 2005. **89**(9): p. 1102-1104.
160. De Moraes Cv, J.V.J.L.J.M. and et al., *RIsk factors for visual field progression in treated glaucoma.* Archives of Ophthalmology, 2010. **129**(5): p. 562-568.
161. Oie, S., K. Ishida, and T. Yamamoto, *Impact of intraocular pressure reduction on visual field progression in normal-tension glaucoma followed up over 15 years.* Jpn J Ophthalmol, 2017. **61**(4): p. 314-323.
162. Jin, S.W. and S.Y. Noh, *Long-Term Clinical Course of Normal-Tension Glaucoma: 20 Years of Experience.* J Ophthalmol, 2017. **2017**: p. 2651645.
163. De Moraes, C.G., et al., *Visual field progression outcomes in glaucoma subtypes.* Acta Ophthalmol, 2013. **91**(3): p. 288-93.
164. Verma, S., et al., *Visual Field Progression in Patients with Primary Angle-Closure Glaucoma Using Pointwise Linear Regression Analysis.* Ophthalmology, 2017. **124**(7): p. 1065-1071.
165. Boodhna, T., L.J. Saunders, and D.P. Crabb, *Are rates of vision loss in patients in English glaucoma clinics slowing down over time? Trends from a decade of data.* Eye (Lond), 2015. **29**(12): p. 1639.
166. Chauhan, B.C., et al., *Rates of glaucomatous visual field change in a large clinical population.* Investigative Ophthalmology and Visual Science, 2014. **55**(7): p. 4135-4143.
167. Fujino, Y., et al., *Evaluation of Glaucoma Progression in Large-Scale Clinical Data: The Japanese Archive of Multicentral Databases in Glaucoma (JAMDIG).* Invest Ophthalmol Vis Sci, 2016. **57**(4): p. 2012-20.

168. Musch, D.C., et al., *Intraocular pressure control and long-term visual field loss in the Collaborative Initial Glaucoma Treatment Study.* Ophthalmology, 2011. **118**(9): p. 1766-73.
169. De Moraes, C.G.V., et al., *Glaucoma with early visual field loss affecting both hemifields and the risk of disease progression.* Archives of Ophthalmology, 2009. **127**(9): p. 1129-1134.
170. Henson, D.B. and S. Shambhu, *Relative risk of progressive glaucomatous visual field loss in patients enrolled and not enrolled in a prospective longitudinal study.* Arch Ophthalmol, 2006. **124**(10): p. 1405-8.
171. Brusini, P. and S. Filacorda, *Enhanced Glaucoma Staging System (GSS 2) for classifying functional damage in glaucoma.* J Glaucoma, 2006. **15**(1): p. 40-6.
172. Ross, S., *Peirce's Criterion for the Elimination of Suspect Experimental Data.* Journal of Engineering Technology, Fall 2003. **vol 20**(no. 2).
173. Anderson, A.J., *Comparison of Three Parametric Models for Glaucomatous Visual Field Progression Rate Distributions.* Transl Vis Sci Technol, 2015. **4**(4): p. 2.
174. Van Gestel, A., et al., *The relationship between visual field loss in glaucoma and health-related quality-of-life.* Eye, 2010. **24**(12): p. 1759-1769.
175. Saunders, L.J., R.A. Russell, and D.P. Crabb, *Practical landmarks for visual field disability in glaucoma.* British Journal of Ophthalmology, 2012. **96**(9): p. 1185-1189.
176. Chauhan, B.C., et al., *Practical recommendations for measuring rates of visual field change in glaucoma.* Br J Ophthalmol, 2008. **92**(4): p. 569-73.
177. Pleet, A., et al., *Risk Factors Associated with Progression to Blindness from Primary Open-Angle Glaucoma in an African-American Population.* Ophthalmic Epidemiol, 2016: p. 1-9.
178. Actis, A.G., et al., *Risk Factors for Primary Open Angle Glaucoma (POAG) Progression: A Study Ruled in Torino.* Open Ophthalmol J, 2016. **10**: p. 129-39.
179. Naito, T., et al., *Relationship between progression of visual field defect and intraocular pressure in primary open-angle glaucoma.* Clin Ophthalmol, 2015. **9**: p. 1373-8.
180. Baril, C., et al., *Rates of glaucomatous visual field change after trabeculectomy.* Br J Ophthalmol, 2017. **101**(7): p. 874-878.
181. Garway-Heath, D.F., et al., *Latanoprost for open-angle glaucoma (UKGTS): A randomised, multicentre, placebo-controlled trial.* Lancet, 2015. **385**(9975): p. 1295-304.
182. Forchheimer, I., et al., *Baseline mean deviation and rates of visual field change in treated glaucoma patients.* Eye (Lond), 2011. **25**(5): p. 626-32.
183. Heijl, A., et al., *Rates of visual field progression in clinical glaucoma care.* Acta Ophthalmologica, 2013. **91**(5): p. 406-412.
184. Leske, M.C., et al., *Predictors of Long-term Progression in the Early Manifest Glaucoma Trial.* Ophthalmology, 2007. **114**(11): p. 1965-1972.

185. Grant, W.M. and J.F. Burke, Jr., *Why do some people go blind from glaucoma?* Ophthalmology, 1982. **89**(9): p. 991-8.
186. Appelboom, G., et al., *Smart wearable body sensors for patient self-assessment and monitoring.* Archives of Public Health, 2014. **72**(1).
187. Abril, E.P., *Tracking Myself: Assessing the Contribution of Mobile Technologies for Self-Trackers of Weight, Diet, or Exercise.* Journal of Health Communication, 2016. **21**(6): p. 638-646.
188. Yu, H.Q., et al. *Design and implementation of an automatic visual acuity test software*. in *Proceedings - 2016 International Conference on Information System and Artificial Intelligence, ISAI 2016*. 2016.
189. Rodríguez-Vallejo, M., et al., *Visual acuity and contrast sensitivity screening with a new iPad application.* Displays, 2016. **44**: p. 15-20.
190. Phung, L., et al., *Reproducibility and comparison of visual acuity obtained with Sightbook mobile application to near card and Snellen chart.* Retina, 2016. **36**(5): p. 1009-1020.
191. Kosikowski, R., et al. *Senses - What u see? Vision screening system dedicated for iOS based devices development and screening results*. in *SIGMAP 2011 - Proceedings of the International Conference on Signal Processing and Multimedia Applications*. 2011.
192. Bodduluri, L., M.Y. Boon, and S.J. Dain, *Evaluation of tablet computers for visual function assessment.* Behavior Research Methods, 2016: p. 1-11.
193. Aslam, T.M., et al., *An assessment of a modern touch-screen tablet computer with reference to core physical characteristics necessary for clinical vision testing.* Journal of the Royal Society Interface, 2013. **10**(84).
194. Sauro, J., *A Practical Guide to the System Usability Scale: Background, Benchmarks & Best Practices*. 2011: CreateSpace Independent Publishing Platform.
195. Olsen, A.S., et al., *Glaucoma detection with damato multifixation campimetry online.* Eye (Lond), 2016. **30**(5): p. 731-9.
196. B. Damato and C. Groenewald, *Multifixation campimetry on line: a perimeter for the detection of visual field loss using the internet.* Br J Ophthalmol, 2003. **87**(10): p. 1296-8.
197. Ianchulev, T., et al., *Peristat: A computer-based perimetry self-test for cost-effective population screening of glaucoma.* Current Eye Research, 2005. **30**(1): p. 1-6.
198. Brooke, J., *SUS-A quick and dirty usability scale.* Usability evaluation in industry, 1996. **189**(194): p. 4-7.
199. Sauro, J. and J.R. Lewis, *Chapter 2 - Quantifying user research*, in *Quantifying the User Experience (Second Edition)*. 2016, Morgan Kaufmann: Boston. p. 9-18.
200. Nielsen, J., *Iterative User-Interface Design.* Computer, 1993. **26**(11): p. 32-41.
201. International Organization for Standardization. (1998) 9241-11, I., *Ergonomic requirements for office work with visual display terminals (VDTs) -- Part 11: Guidance on usability. Retrieved from: https://www.iso.org/standard/16883.html*
202. Miranda, M.A. and D.B. Henson, *Perimetric sensitivity and response variability in glaucoma with single-stimulus automated perimetry and*

multiple-stimulus perimetry with verbal feedback. Acta ophthalmologica, 2008. **86**(2): p. 202-206.
203. Tahir, H.J., et al., *Optimisation and assessment of three modern touch screen tablet computers for clinical vision testing.* PLoS ONE, 2014. **9**(4).
204. Aslam, T.M., et al., *Development and testing of an automated computer tablet-based method for self-testing of high and low contrast near visual acuity in ophthalmic patients.* Graefe's Archive for Clinical and Experimental Ophthalmology, 2016. **254**(5): p. 891-899.
205. Chauhan, B.C., et al., *Practical recommendations for measuring rates of visual field change in glaucoma.* British Journal of Ophthalmology, 2008. **92**(4): p. 569-573.
206. Glen, F.C., H. Baker, and D.P. Crabb, *A qualitative investigation into patients' views on visual field testing for glaucoma monitoring.* BMJ Open, 2014. **4**(1).
207. Eck, D.J., *Programming: Introduction to Programming Using JAVA*. 2009: CreateSpace. 700.
208. Wang, Y. and D.B. Henson, *Diagnostic performance of visual field test using subsets of the 24-2 test pattern for early glaucomatous field loss.* Invest Ophthalmol Vis Sci, 2013. **54**(1): p. 756-61.
209. Artes, P.H., et al., *Multisampling suprathreshold perimetry: a comparison with conventional suprathreshold and full-threshold strategies by computer simulation.* Invest Ophthalmol Vis Sci, 2003. **44**(6): p. 2582-7.
210. Wall, M., et al., *SITA standard in optic neuropathies and hemianopias: a comparison with full threshold testing.* Invest Ophthalmol Vis Sci, 2001. **42**(2): p. 528-37.
211. Budenz, D.L., et al., *Sensitivity and specificity of the Swedish interactive threshold algorithm for glaucomatous visual field defects.* Ophthalmology, 2002. **109**(6): p. 1052-8.
212. Vingrys, A.J., et al., *Validation of a Tablet as a Tangent Perimeter.* Translational Vision Science & Technology, 2016. **5**(4): p. 3.
213. Nelson, P., et al., *Quality of life in glaucoma and its relationship with visual function.* J Glaucoma, 2003. **12**(2): p. 139-50.
214. Bengtsson, B. and A. Heijl, *Evaluation of a new perimetric threshold strategy, SITA, in patients with manifest and suspect glaucoma.* Acta Ophthalmol Scand, 1998. **76**(3): p. 268-72.
215. Bengtsson, B. and A. Heijl, *SITA Fast, a new rapid perimetric threshold test. Description of methods and evaluation in patients with manifest and suspect glaucoma.* Acta Ophthalmol Scand, 1998. **76**(4): p. 431-7.
216. Aslam, T.M., et al., *A novel paediatric game-based visual-fields assessor.* Br J Ophthalmol, 2011. **95**(7): p. 921-4.
217. Murray, I.C., et al., *Feasibility of saccadic vector optokinetic perimetry: a method of automated static perimetry for children using eye tracking.* Ophthalmology, 2009. **116**(10): p. 2017-26.
218. Kong, Y.X., et al., *A Comparison of Perimetric Results from a Tablet Perimeter and Humphrey Field Analyzer in Glaucoma Patients.* Transl Vis Sci Technol, 2016. **5**(6): p. 2.

219. Gardiner, S.K., C.A. Johnson, and P.G. Spry, *Normal age-related sensitivity loss for a variety of visual functions throughout the visual field.* Optom Vis Sci, 2006. **83**(7): p. 438-43.
220. Russell, R.A., et al., *The Relationship between Variability and Sensitivity in Large-Scale Longitudinal Visual Field DataVF Variability and Sensitivity.* Investigative Ophthalmology & Visual Science, 2012. **53**(10): p. 5985-5990.
221. Turpin, A., P.H. Artes, and A.M. McKendrick, *The Open Perimetry Interface: an enabling tool for clinical visual psychophysics.* J Vis, 2012. **12**(11).
222. Chong, L.X., A. Turpin, and A.M. McKendrick, *Assessing the GOANNA Visual Field Algorithm Using Artificial Scotoma Generation on Human Observers.* Transl Vis Sci Technol, 2016. **5**(5): p. 1.
223. Autzen, T. and K. Work, *The effect of learning and age on short-term fluctuation and mean sensitivity of automated static perimetry.* Acta Ophthalmol (Copenh), 1990. **68**(3): p. 327-30.
224. Castro, D.P., J. Kawase, and L.A. Melo, Jr., *Learning effect of standard automated perimetry in healthy individuals.* Arq Bras Oftalmol, 2008. **71**(4): p. 523-8.
225. Wild, J.M., et al., *The influence of the learning effect on automated perimetry in patients with suspected glaucoma.* Acta Ophthalmol (Copenh), 1989. **67**(5): p. 537-45.
226. Kutzko, K.E., C.F. Brito, and M. Wall, *Effect of instructions on conventional automated perimetry.* Investigative Ophthalmology and Visual Science, 2000. **41**(7): p. 2006-2013.
227. Waisbourd, M., et al., *The Philadelphia Glaucoma Detection and Treatment Project: Detection Rates and Initial Management.* Ophthalmology, 2016. **123**(8): p. 1667-74.
228. Moyer, V.A., *Screening for glaucoma: U.S. Preventive Services Task Force Recommendation Statement.* Ann Intern Med, 2013. **159**(1539-3704 (Electronic)): p. 484-9.
229. Hernandez, R., et al., *Screening for open angle glaucoma: systematic review of cost-effectiveness studies.* J Glaucoma, 2008. **17**(3): p. 159-68.
230. Wu, Z., et al., *Measurement of Retinal Sensitivity on Tablet Devices in Age-Related Macular Degeneration.* Transl Vis Sci Technol, 2015. **4**(3): p. 13.
231. Matsumoto, C., et al., *Visual Field Testing with Head-Mounted Perimeter 'imo'.* PLoS One, 2016. **11**(8): p. e0161974.
232. Turpin, A., D.J. Lawson, and A.M. McKendrick, *PsyPad: a platform for visual psychophysics on the iPad.* J Vis, 2014. **14**(3): p. 16.
233. Lowry, E.A., et al., *Comparison of Peristat Online Perimetry with the Humphrey Perimetry in a Clinic-Based Setting.* Transl Vis Sci Technol, 2016. **5**(4): p. 4.
234. Jones, S.R., S. Carley, and M. Harrison, *An introduction to power and sample size estimation.* Emerg Med J, 2003. **20**(5): p. 453-8.
235. Gilbert, R., et al., *Assessing diagnostic and screening tests: Part 1. Concepts.* Western Journal of Medicine, 2001. **174**(6): p. 405-409.

236. Monsalve, B., et al., *Diagnostic ability of Humphrey perimetry, Octopus perimetry, and optical coherence tomography for glaucomatous optic neuropathy.* Eye, 2017. **31**(3): p. 443-451.
237. Bowd, C., et al., *Detecting Early Glaucoma by Assessment of Retinal Nerve Fiber Layer Thickness and Visual Function.* Investigative Ophthalmology & Visual Science, 2001. **42**(9): p. 1993-2003.
238. Schweitzer, C., et al., *Diagnostic Performance of Peripapillary Retinal Nerve Fiber Layer Thickness for Detection of Glaucoma in an Elderly Population: The ALIENOR StudyDiagnostic Performance of OCT for Glaucoma Detection.* Investigative Ophthalmology & Visual Science, 2016. **57**(14): p. 5882-5891.
239. Lee, S.-Y., et al., *Asymmetry Analysis of Macular Inner Retinal Layers for Glaucoma Diagnosis: Swept-Source Optical Coherence Tomography Study.* PLoS ONE, 2016. **11**(10): p. e0164866.
240. Guedes, V., et al., *Optical coherence tomography measurement of macular and nerve fiber layer thickness in normal and glaucomatous human eyes.* Ophthalmology, 2003. **110**(1): p. 177-189.
241. The, A.H.S.R.G., et al., *Effectiveness of Different Monitoring Modalities in the Detection of Neovascular Age-Related: Macular Degeneration: The HOME Study. Report Number 3.* Retina (Philadelphia, Pa.), 2016. **36**(8): p. 1542-1547.
242. Henson, D.B. and T. Emuh, *Monitoring Vigilance during Perimetry by Using Pupillography.* Investigative Ophthalmology & Visual Science, 2010. **51**(7): p. 3540-3543.
243. Crabb, D.P. and D.F. Garway-Heath, *Intervals between visual field tests when monitoring the glaucomatous patient: wait-and-see approach.* Invest Ophthalmol Vis Sci, 2012. **53**(6): p. 2770-6.
244. Anderson, A.J., et al., *Can Home Monitoring Allow Earlier Detection of Rapid Visual Field Progression in Glaucoma?* Ophthalmology, 2017.
245. Fujimoto, J.G., et al., *Optical Coherence Tomography: An Emerging Technology for Biomedical Imaging and Optical Biopsy.* Neoplasia (New York, N.Y.), 2000. **2**(1-2): p. 9-25.
246. Kashani, A.H., et al., *Optical coherence tomography angiography: A comprehensive review of current methods and clinical applications.* Progress in Retinal and Eye Research, 2017.
247. Marschall, S., et al., *Optical coherence tomography-current technology and applications in clinical and biomedical research.* Analytical and Bioanalytical Chemistry, 2011. **400**(9): p. 2699-2720.
248. Nassif, N., et al., *In vivo human retinal imaging by ultrahigh-speed spectral domain optical coherence tomography.* Optics Letters, 2004. **29**(5): p. 480-482.
249. Wojtkowski, M., et al., *In vivo human retinal imaging by Fourier domain optical coherence tomography.* Journal of Biomedical Optics, 2002. **7**(3): p. 457-463.
250. Drexler, W. and J.G. Fujimoto, *State-of-the-art retinal optical coherence tomography.* Progress in Retinal and Eye Research, 2008. **27**(1): p. 45-88.
251. Yaqoob, Z., J. Wu, and C. Yang, *Spectral domain optical coherence tomography: a better OCT imaging strategy.* BioTechniques, 2005. **39**(6 Suppl): p. S6-13.

252. van Velthoven, M.E.J., et al., *Recent developments in optical coherence tomography for imaging the retina.* Progress in Retinal and Eye Research, 2007. **26**(1): p. 57-77.
253. Flammer, J., et al., *The impact of ocular blood flow in glaucoma.* Progress in Retinal and Eye Research, 2002. **21**(4): p. 359-393.
254. Patel, V., et al., *Retinal blood flow in diabetic retinopathy.* British Medical Journal, 1992. **305**(6855): p. 678.
255. Friedman, E., *A hemodynamic model of the pathogenesis of age-related macular degeneration.* American journal of ophthalmology, 1997. **124**(5): p. 677-682.
256. Gass, J.D.M., *Stereoscopic atlas of macular diseases: diagnosis and treatment*. 1987, St. Louis: Mosby. 2 v. (xiii, 801, 26 p.
257. Yannuzzi, L.A., et al., *Fluorescein angiography complication survey.* Ophthalmology, 1986. **93**(5): p. 611-7.
258. Hope-Ross, M., et al., *Adverse reactions due to indocyanine green.* Ophthalmology, 1994. **101**(3): p. 529-33.
259. Cheung, N., et al., *Diabetic retinopathy and the risk of coronary heart disease: the Atherosclerosis Risk in Communities Study.* Diabetes Care, 2007. **30**(7): p. 1742-6.
260. Kwiterovich, K.A., et al., *Frequency of adverse systemic reactions after fluorescein angiography. Results of a prospective study.* Ophthalmology, 1991. **98**(7): p. 1139-42.
261. Wang, R.K., et al., *Three dimensional optical angiography.* Optics Express, 2007. **15**(7): p. 4083-4097.
262. Chen, C.L. and R.K. Wang, *Optical coherence tomography based angiography [invited].* Biomedical Optics Express, 2017. **8**(2): p. 1056-1082.
263. Wang, R.K., *Optical Microangiography: A Label Free 3D Imaging Technology to Visualize and Quantify Blood Circulations within Tissue Beds in vivo.* IEEE J Sel Top Quantum Electron, 2010. **16**(3): p. 545-554.
264. Tokayer, J., et al., *Blood flow velocity quantification using split-spectrum amplitude-decorrelation angiography with optical coherence tomography.* Biomed Opt Express, 2013. **4**(10): p. 1909-24.
265. Huang, Y., et al., *Swept-source OCT angiography of the retinal vasculature using intensity differentiation-based optical microangiography algorithms.* Ophthalmic Surg Lasers Imaging Retina, 2014. **45**(5): p. 382-9.
266. Fingler, J., et al., *Volumetric microvascular imaging of human retina using optical coherence tomography with a novel motion contrast technique.* Opt Express, 2009. **17**(24): p. 22190-200.
267. Zhang, A., et al., *Methods and algorithms for optical coherence tomography-based angiography: a review and comparison.* J Biomed Opt, 2015. **20**(10): p. 100901.
268. Stanga, P.E., et al., *Swept-Source Optical Coherence Tomography Angio (Topcon Corp, Japan): Technology Review.* Dev Ophthalmol, 2016. **56**: p. 13-7.
269. Spaide, R.F., J.G. Fujimoto, and N.K. Waheed, *Image Artifacts In Optical Coherence Tomography Angiography.* Retina, 2015. **35**(11): p. 2163-80.

270. Jia, Y., et al., *Quantitative optical coherence tomography angiography of vascular abnormalities in the living human eye.* Proc Natl Acad Sci U S A, 2015. **112**(18): p. E2395-402.
271. Liu, L., et al., *Automated choroidal neovascularization detection algorithm for optical coherence tomography angiography.* Biomed Opt Express, 2015. **6**(9): p. 3564-76.
272. Zhang, A., Q. Zhang, and R.K. Wang, *Minimizing projection artifacts for accurate presentation of choroidal neovascularization in OCT micro-angiography.* Biomed Opt Express, 2015. **6**(10): p. 4130-43.
273. Freiberg, F.J., et al., *Optical coherence tomography angiography of the foveal avascular zone in diabetic retinopathy.* Graefes Arch Clin Exp Ophthalmol, 2016. **254**(6): p. 1051-8.
274. Di, G., et al., *A morphological study of the foveal avascular zone in patients with diabetes mellitus using optical coherence tomography angiography.* Graefes Arch Clin Exp Ophthalmol, 2016. **254**(5): p. 873-9.
275. Danis, R.P., et al., *Association of fluorescein angiographic features with visual acuity and with optical coherence tomographic and stereoscopic color fundus photographic features of diabetic macular edema in a randomized clinical trial.* Retina, 2010. **30**(10): p. 1627-37.
276. Giani, A., et al., *Spectral-domain optical coherence tomography as an indicator of fluorescein angiography leakage from choroidal neovascularization.* Invest Ophthalmol Vis Sci, 2011. **52**(8): p. 5579-86.
277. Campochiaro, P.A., et al., *Neutralization of vascular endothelial growth factor slows progression of retinal nonperfusion in patients with diabetic macular edema.* Ophthalmology, 2014. **121**(9): p. 1783-9.
278. Sophie, R., et al., *Long-term outcomes in ranibizumab-treated patients with retinal vein occlusion; the role of progression of retinal nonperfusion.* Am J Ophthalmol, 2013. **156**(4): p. 693-705.
279. An, L., M. Johnstone, and R.K. Wang, *Optical microangiography provides correlation between microstructure and microvasculature of optic nerve head in human subjects.* J Biomed Opt, 2012. **17**(11): p. 116018.
280. Wang, X., et al., *Correlation between optic disc perfusion and glaucomatous severity in patients with open-angle glaucoma: an optical coherence tomography angiography study.* Graefes Arch Clin Exp Ophthalmol, 2015. **253**(9): p. 1557-64.
281. Leveque, P.M., et al., *Optic Disc Vascularization in Glaucoma: Value of Spectral-Domain Optical Coherence Tomography Angiography.* J Ophthalmol, 2016. **2016**: p. 6956717.
282. Bojikian, K.D., et al., *Optic Disc Perfusion in Primary Open Angle and Normal Tension Glaucoma Eyes Using Optical Coherence Tomography-Based Microangiography.* PLoS One, 2016. **11**(5): p. e0154691.
283. Rao, H.L., et al., *Diagnostic ability of peripapillary vessel density measurements of optical coherence tomography angiography in primary open-angle and angle-closure glaucoma.* Br J Ophthalmol, 2017. **101**(8): p. 1066-1070.

284. Levison, A.L., et al., *Choroidal neovascularisation on optical coherence tomography angiography in punctate inner choroidopathy and multifocal choroiditis.* Br J Ophthalmol, 2017. **101**(5): p. 616-622.
285. Kim, A.Y., et al., *Quantifying Retinal Microvascular Changes in Uveitis Using Spectral-Domain Optical Coherence Tomography Angiography.* American Journal of Ophthalmology, 2016. **171**: p. 101-112.
286. Yau, J.W.Y., et al., *Global prevalence and major risk factors of diabetic retinopathy.* Diabetes Care, 2012. **35**(3): p. 556-564.
287. Wild, S., et al., *Global Prevalence of Diabetes: Estimates for the year 2000 and projections for 2030.* Diabetes Care, 2004. **27**(5): p. 1047-1053.
288. Antonetti, D.A., R. Klein, and T.W. Gardner, *Diabetic retinopathy.* New England Journal of Medicine, 2012. **366**(13): p. 1227-1239.
289. Buabbud, J.C., M.M. Al-latayfeh, and J.K. Sun, *Optical coherence tomography imaging for diabetic retinopathy and macular edema.* Curr Diab Rep, 2010. **10**(4): p. 264-9.
290. Norton, E.W. and F. Gutman, *Diabetic retinopathy studied by fluorescein angiography.* Trans Am Ophthalmol Soc, 1965. **63**: p. 108-28.
291. Gass, J.D., *A fluorescein angiographic study of macular dysfunction secondary to retinal vascular disease. IV. Diabetic retinal angiopathy.* Arch Ophthalmol, 1968. **80**(5): p. 583-91.
292. Johnson, R.N., et al., *Fluorescein Angiography: Basic Principles and Interpretation*, in *Retina Fifth Edition*. 2012. p. 2-50.e1.
293. Bresnick, G.H., et al., *Abnormalities of the foveal avascular zone in diabetic retinopathy.* Arch Ophthalmol, 1984. **102**(9): p. 1286-93.
294. Wessel, M.M., et al., *Ultra-wide-field angiography improves the detection and classification of diabetic retinopathy.* Retina, 2012. **32**(4): p. 785-91.
295. Muqit, M.M.K., et al., *Optos-guided pattern scan laser (Pascal)-targeted retinal photocoagulation in proliferative diabetic retinopathy.* Acta Ophthalmologica, 2013. **91**(3): p. 251-258.
296. Muqit, M.M. and P.E. Stanga, *Fourier-domain optical coherence tomography evaluation of retinal and optic nerve head neovascularisation in proliferative diabetic retinopathy.* Br J Ophthalmol, 2014. **98**(1): p. 65-72.
297. Vaz-Pereira, S., et al., *Optical Coherence Tomography Features Of Active And Inactive Retinal Neovascularization In Proliferative Diabetic Retinopathy.* Retina, 2015.
298. Silva, P.S., et al., *Peripheral lesions identified by mydriatic ultrawide field imaging: distribution and potential impact on diabetic retinopathy severity.* Ophthalmology, 2013. **120**(12): p. 2587-95.
299. Stanga, P.E., et al., *In vivo imaging of cortical vitreous using 1050-nm swept-source deep range imaging optical coherence tomography.* Am J Ophthalmol, 2014. **157**(2): p. 397-404 e2.
300. Itakura, H., et al., *En face imaging of posterior precortical vitreous pockets using swept-source optical coherence tomography.* Invest Ophthalmol Vis Sci, 2015. **56**(5): p. 2898-900.
301. Muqit, M.M. and P.E. Stanga, *Swept-source optical coherence tomography imaging of the cortical vitreous and the vitreoretinal*

interface in proliferative diabetic retinopathy: assessment of vitreoschisis, neovascularisation and the internal limiting membrane. Br J Ophthalmol, 2014. **98**(7): p. 994-7.
302. Ghadiali, Q., et al., *An Assessment of Vitreous Degeneration in Eyes with Vitreomacular Traction and Macular Holes.* J Ophthalmol, 2017. **2017**: p. 6834692.
303. Schaal, K.B., et al., *The premacular bursa's shape revealed in vivo by swept-source optical coherence tomography.* Ophthalmology, 2014. **121**(5): p. 1020-1028.
304. Pang, C.E., K.B. Schaal, and M. Engelbert, *Association of prevascular vitreous fissures and cisterns with vitreous degeneration as assessed by swept source optical coherence tomography.* Retina, 2015. **35**(9): p. 1875-1882.
305. Ishibazawa, A., et al., *Optical Coherence Tomography Angiography in Diabetic Retinopathy: A Prospective Pilot Study.* Am J Ophthalmol, 2015. **160**(1): p. 35-44 e1.
306. Stanga, P.E., et al., *New Findings in Diabetic Maculopathy and Proliferative Disease by Swept-Source Optical Coherence Tomography Angiography.* Dev Ophthalmol, 2016. **56**: p. 113-21.
307. de Carlo, T.E., et al., *A review of optical coherence tomography angiography (OCTA).* International Journal of Retina and Vitreous, 2015. **1**(1): p. 1-15.
308. Campbell, J.P., et al., *Detailed Vascular Anatomy of the Human Retina by Projection-Resolved Optical Coherence Tomography Angiography.* Sci Rep, 2017. **7**: p. 42201.
309. Cohen, J., *A Coefficient of Agreement for Nominal Scales.* Educational and Psychological Measurement, 1960. **20**(1): p. 37-46.
310. Rice, T.A., R.G. Michels, and E.F. Rice, *Vitrectomy for diabetic traction retinal detachment involving the macula.* Am J Ophthalmol, 1983. **95**(1): p. 22-33.
311. Ho, T., W.E. Smiddy, and H.W. Flynn, Jr., *Vitrectomy in the management of diabetic eye disease.* Surv Ophthalmol, 1992. **37**(3): p. 190-202.
312. Blankenship, G.W., *Management of vitreous cavity hemorrhage following pars plana vitrectomy for diabetic retinopathy.* Ophthalmology, 1986. **93**(1): p. 39-44.
313. West, J.F. and Z.J. Gregor, *Fibrovascular ingrowth and recurrent haemorrhage following diabetic vitrectomy.* Br J Ophthalmol, 2000. **84**(8): p. 822-5.
314. Yorston, D., et al., *Predictive clinical features and outcomes of vitrectomy for proliferative diabetic retinopathy.* Br J Ophthalmol, 2008. **92**(3): p. 365-8.
315. Novak, M.A., et al., *Vitreous hemorrhage after vitrectomy for diabetic retinopathy.* Ophthalmology, 1984. **91**(12): p. 1485-9.
316. Branisteanu, D.C., A. Bilha, and A. Moraru, *Vitrectomy surgery of diabetic retinopathy complications.* Rom J Ophthalmol, 2016. **60**(1): p. 31-6.
317. Berinstein, D.M., B.R. Garretson, and G.A. Williams, *Ultrasound biomicroscopy in a case of anterior hyaloidal fibrovascular proliferation.* Ophthalmic Surg Lasers, 2000. **31**(1): p. 69-70.

318. Lewis, H., G.W. Abrams, and R.Y. Foos, *Clinicopathologic findings in anterior hyaloidal fibrovascular proliferation after diabetic vitrectomy.* Am J Ophthalmol, 1987. **104**(6): p. 614-8.
319. Campo, R.V. and J.O. Sipperley, *Anterior hyaloidal fibrovascular proliferation after diabetic vitrectomy.* Am J Ophthalmol, 1988. **105**(4): p. 432-4.
320. Smith, J.M. and D.H. Steel, *Anti-vascular endothelial growth factor for prevention of postoperative vitreous cavity haemorrhage after vitrectomy for proliferative diabetic retinopathy.* Cochrane Database Syst Rev, 2015(8): p. Cd008214.
321. Al-Kharashi, A., et al., *The adjunctive use of pre-operative intravitreal bevacizumab in the setting of proliferative diabetic retinopathy.* Saudi Journal of Ophthalmology, 2016. **30**(4): p. 217-220.
322. Ghasemi Falavarjani, K., et al., *Optical Coherence Tomography Angiography Analysis of the Foveal Avascular Zone and Macular Vessel Density After Anti-VEGF Therapy in Eyes With Diabetic Macular Edema and Retinal Vein OcclusionOCTA After Intravitreal Injection.* Investigative Ophthalmology & Visual Science, 2017. **58**(1): p. 30-34.
323. Sultan, Z., et al., *Role of bevacizumab in the prevention of early postoperative haemorrhage after 25-gauge microincision vitrectomy surgery.* Pakistan Journal of Medical Sciences, 2016. **32**(5): p. 1184-1187.
324. Klein, R., et al., *The Wisconsin Epidemiologic Study of Diabetic Retinopathy XXII. The Twenty-Five-Year Progression of Retinopathy in Persons with Type 1 Diabetes.* Ophthalmology, 2008. **115**(11): p. 1859-1868.
325. Stefánsson, E., et al., *Screening and prevention of diabetic blindness.* Acta Ophthalmologica Scandinavica, 2000. **78**(4): p. 374-385.
326. Durham, J.T. and I.M. Herman, *Microvascular modifications in diabetic retinopathy.* Curr Diab Rep, 2011. **11**(4): p. 253-64.
327. Jonas, J.B., U. Schneider, and G.O. Naumann, *Count and density of human retinal photoreceptors.* Graefes Arch Clin Exp Ophthalmol, 1992. **230**(6): p. 505-10.
328. Yu, D.Y., S.J. Cringle, and E.N. Su, *Intraretinal oxygen distribution in the monkey retina and the response to systemic hyperoxia.* Invest Ophthalmol Vis Sci, 2005. **46**(12): p. 4728-33.
329. Snodderly, D.M. and R.S. Weinhaus, *Retinal vasculature of the fovea of the squirrel monkey, Saimiri sciureus: three-dimensional architecture, visual screening, and relationships to the neuronal layers.* J Comp Neurol, 1990. **297**(1): p. 145-63.
330. Linsenmeier, R.A. and R.D. Braun, *Oxygen distribution and consumption in the cat retina during normoxia and hypoxemia.* J Gen Physiol, 1992. **99**(2): p. 177-97.
331. Yi, J., et al., *Visible light optical coherence tomography measures retinal oxygen metabolic response to systemic oxygenation.* Light, science & applications, 2015. **4**(9): p. e334.
332. Nagaoka, T., et al., *Impaired Retinal Circulation in Patients with Type 2 Diabetes Mellitus: Retinal Laser Doppler Velocimetry Study.*

Investigative Ophthalmology & Visual Science, 2010. **51**(12): p. 6729-6734.
333. Wilkinson, C.P., et al., *Proposed international clinical diabetic retinopathy and diabetic macular edema disease severity scales.* Ophthalmology, 2003. **110**(9): p. 1677-82.
334. Chalam, K.V. and K. Sambhav, *Optical Coherence Tomography Angiography in Retinal Diseases.* Journal of Ophthalmic & Vision Research, 2016. **11**(1): p. 84-92.
335. de Carlo, T.E., et al., *Detection Of Microvascular Changes In Eyes Of Patients With Diabetes But Not Clinical Diabetic Retinopathy Using Optical Coherence Tomography Angiography.* Retina, 2015. **35**(11): p. 2364-70.
336. Al-Sheikh, M., et al., *Swept-Source OCT Angiography Imaging of the Foveal Avascular Zone and Macular Capillary Network Density in Diabetic Retinopathy.* Investigative Ophthalmology & Visual Science, 2016. **57**(8): p. 3907-3913.
337. Balaratnasingam, C., et al., *Visual Acuity Is Correlated with the Area of the Foveal Avascular Zone in Diabetic Retinopathy and Retinal Vein Occlusion.* Ophthalmology, 2016. **123**(11): p. 2352-2367.
338. *Photocoagulation for diabetic macular edema. Early Treatment Diabetic Retinopathy Study report number 1. Early Treatment Diabetic Retinopathy Study research group.* Arch Ophthalmol, 1985. **103**(12): p. 1796-806.
339. Mansour, A.M., et al., *Foveal avascular zone in diabetes mellitus.* Retina, 1993. **13**(2): p. 125-8.
340. Laatikainen, L. and J. Larinkari, *Capillary-free area of the fovea with advancing age.* Invest Ophthalmol Vis Sci, 1977. **16**(12): p. 1154-7.
341. Zheng, Y., et al., *Automated segmentation of foveal avascular zone in fundus fluorescein angiography.* Invest Ophthalmol Vis Sci, 2010. **51**(7): p. 3653-9.
342. Tam, J., J.A. Martin, and A. Roorda, *Noninvasive visualization and analysis of parafoveal capillaries in humans.* Invest Ophthalmol Vis Sci, 2010. **51**(3): p. 1691-8.
343. Iafe, N.A., et al., *Retinal Capillary Density and Foveal Avascular Zone Area Are Age-Dependent: Quantitative Analysis Using Optical Coherence Tomography Angiography.* Invest Ophthalmol Vis Sci, 2016. **57**(13): p. 5780-5787.
344. *Early photocoagulation for diabetic retinopathy. ETDRS report number 9. Early Treatment Diabetic Retinopathy Study Research Group.* Ophthalmology, 1991. **98**(5 Suppl): p. 766-85.
345. Al-Sheikh, M., et al., *Impact of image quality on OCT angiography based quantitative measurements.* Int J Retina Vitreous, 2017. **3**: p. 13.
346. Mastropasqua, R., et al., *Reproducibility and repeatability of foveal avascular zone area measurements using swept-source optical coherence tomography angiography in healthy subjects.* Eur J Ophthalmol, 2017. **27**(3): p. 336-341.
347. Jones, J.H., et al., *Coats' disease.* International Ophthalmology Clinics, 2001. **41**(4): p. 189-198.

348. Shields, J.A., et al., *Clinical variations and complications of Coats disease in 150 cases: The 2000 Sanford Gifford Memorial Lecture.* American Journal of Ophthalmology, 2001. **131**(5): p. 561-571.
349. Coats, G., *Forms of retinal diseases with massive exudation.* Roy Lond Ophthal Hosp Rep, 1908. **17**: p. 440-525.
350. Egerer, I., W. Tasman, and T.L. Tomer, *Coats disease.* Archives of Ophthalmology, 1974. **92**(2): p. 109-112.
351. Shields, J.A., et al., *Classification and management of Coats disease: the 2000 Proctor Lecture.* Am J Ophthalmol, 2001. **131**(5): p. 572-83.
352. Rubin, M.P. and S. Mukai, *Coats' disease.* Int Ophthalmol Clin, 2008. **48**(2): p. 149-58.
353. Black, G.C., et al., *Coats' disease of the retina (unilateral retinal telangiectasis) caused by somatic mutation in the NDP gene: a role for norrin in retinal angiogenesis.* Hum Mol Genet, 1999. **8**(11): p. 2031-5.
354. Cremers, F.P., et al., *The expanding roles of ABCA4 and CRB1 in inherited blindness.* Novartis Found Symp, 2004. **255**: p. 68-79; discussion 79-84, 177-8.
355. Cameron, J.D., M. Yanoff, and W.C. Frayer, *Coats' disease and turner's syndrome.* Am J Ophthalmol, 1974. **78**(5): p. 852-4.
356. Fitzsimons, R.B., E.B. Gurwin, and A.C. Bird, *Retinal vascular abnormalities in facioscapulohumeral muscular dystrophy. A general association with genetic and therapeutic implications.* Brain, 1987. **110 (Pt 3)**: p. 631-48.
357. Edward, D.P., et al., *Coats' disease and persistent hyperplastic primary vitreous. Role of MR imaging and CT.* Radiol Clin North Am, 1998. **36**(6): p. 1119-31, x.
358. Atta, H.R. and N.J. Watson, *Echographic diagnosis of advanced Coats' disease.* Eye (Lond), 1992. **6 (Pt 1)**: p. 80-5.
359. Blair, M.P., et al., *Peripheral retinal nonperfusion in fellow eyes in coats disease.* Retina, 2013. **33**(8): p. 1694-9.
360. Muakkassa, N.W., et al., *Optical Coherence Tomography Angiography Findings in Coats' Disease.* Ophthalmic Surg Lasers Imaging Retina, 2016. **47**(7): p. 632-5.
361. Stanga, P.E., et al., *Swept-Source Optical Coherence Tomography Angiography of Paediatric Macular Diseases.* Dev Ophthalmol, 2016. **56**: p. 166-73.
362. Joshi, K.M., et al., *Optical Coherence Tomography Angiography in Adult-Onset Foveomacular Vitelliform Dystrophy.* Retina, 2018. **38**(3): p. 600-605.
363. Battaglia Parodi, M., et al., *Quantitative Analysis of Optical Coherence Tomography Angiography in Adult-Onset Foveomacular Vitelliform Dystrophy.* Retina, 2018. **38**(2): p. 237-244.
364. Robitaille, J.M., et al., *The role of Frizzled-4 mutations in familial exudative vitreoretinopathy and Coats disease.* Br J Ophthalmol, 2011. **95**(4): p. 574-9.
365. Dickinson, J.L., et al., *Mutations in the NDP gene: contribution to Norrie disease, familial exudative vitreoretinopathy and retinopathy of prematurity.* Clin Exp Ophthalmol, 2006. **34**(7): p. 682-8.

366. Grosso, A., et al., *Pearls and pitfalls in diagnosis and management of coats disease.* Retina, 2015. **35**(4): p. 614-23.
367. Ide, C.H. and R.J. Wilson, *Juvenile retinoschisis.* The British Journal of Ophthalmology, 1973. **57**(8): p. 560-562.
368. Molday, R.S., U. Kellner, and B.H.F. Weber, *X-linked juvenile retinoschisis: Clinical diagnosis, genetic analysis, and molecular mechanisms.* Progress in Retinal and Eye Research, 2012. **31**(3): p. 195-212.
369. Wu, W.W., et al., *RS1, a discoidin domain-containing retinal cell adhesion protein associated with X-linked retinoschisis, exists as a novel disulfide-linked octamer.* J Biol Chem, 2005. **280**(11): p. 10721-30.
370. Sikkink, S.K., et al., *X-linked retinoschisis: an update.* J Med Genet, 2007. **44**(4): p. 225-32.
371. Fong, D.S., et al., *Exudative retinal detachment in X-linked retinoschisis.* Ophthalmic Surg Lasers, 1998. **29**(4): p. 332-5.
372. Greven, C.M., R.J. Moreno, and W. Tasman, *Unusual manifestations of X-linked retinoschisis.* Trans Am Ophthalmol Soc, 1990. **88**: p. 211-25; discussion 226-8.
373. Yanoff, M., E. Kertesz Rahn, and L.E. Zimmerman, *Histopathology of juvenile retinoschisis.* Arch Ophthalmol, 1968. **79**(1): p. 49-53.
374. Condon, G.P., et al., *Congenital hereditary (juvenile X-linked) retinoschisis. Histopathologic and ultrastructural findings in three eyes.* Arch Ophthalmol, 1986. **104**(4): p. 576-83.
375. Azzolini, C., et al., *OCT images and surgery of juvenile Macular retinoschisis.* Eur J Ophthalmol, 1997. **7**(2): p. 196-200.
376. Yu, J., et al., *Foveomacular schisis in juvenile X-linked retinoschisis: an optical coherence tomography study.* Am J Ophthalmol, 2010. **149**(6): p. 973-978.e2.
377. Brucker, A.J., et al., *Optical coherence tomography of X-linked retinoschisis.* Retina, 2004. **24**(1): p. 151-2.
378. Azzolini, C., et al., *Clinical analysis of macular edema with new software for SD-OCT imaging.* Eur J Ophthalmol, 2013. **23**(6): p. 899-904.
379. Apushkin, M.A., G.A. Fishman, and M.J. Janowicz, *Correlation of optical coherence tomography findings with visual acuity and macular lesions in patients with X-linked retinoschisis.* Ophthalmology, 2005. **112**(3): p. 495-501.
380. Gregori, N.Z., et al., *Macular spectral-domain optical coherence tomography in patients with X linked retinoschisis.* Br J Ophthalmol, 2009. **93**(3): p. 373-8.
381. Biswas, S., et al., *Nidek MP-1 microperimetry and Fourier domain optical coherence tomography (FD-OCT) in X linked retinoschisis.* Br J Ophthalmol, 2010. **94**(7): p. 949-50.
382. Rao, P., et al., *Wide-Field Imaging Of Nonexudative And Exudative Congenital X-Linked Retinoschisis.* Retina, 2016. **36**(6): p. 1093-100.
383. Lee, J.H., et al., *Neurodevelopmental implications of the general anesthesia in neonate and infants.* Exp Neurol, 2015. **272**: p. 50-60.
384. Joshi, M.M., et al., *Intraschisis cavity fluid composition in congenital X-linked retinoschisis.* Retina, 2006. **26**(7 Suppl): p. S57-60.

385. Acland, G.M., et al., *Gene therapy restores vision in a canine model of childhood blindness.* Nature Genetics, 2001. **28**(1): p. 92-95.
386. Bainbridge, J.W.B., et al., *Effect of gene therapy on visual function in Leber's congenital amaurosis.* New England Journal of Medicine, 2008. **358**(21): p. 2231-2239.
387. Hauswirth, W.W., et al., *Treatment of Leber congenital amaurosis due to RPE65 mutations by ocular subretinal injection of adeno-associated virus gene vector: Short-term results of a phase I trial.* Human Gene Therapy, 2008. **19**(10): p. 979-990.
388. Jacobson, S.G., et al., *Gene therapy for leber congenital amaurosis caused by RPE65 mutations: Safety and efficacy in 15 children and adults followed up to 3 years.* Archives of Ophthalmology, 2012. **130**(1): p. 9-24.
389. Simonelli, F., et al., *Gene therapy for leber's congenital amaurosis is safe and effective through 1.5 years after vector administration.* Molecular Therapy, 2010. **18**(3): p. 643-650.
390. MacLaren, R.E., et al., *Retinal gene therapy in patients with choroideremia: Initial fi ndings from a phase 1/2 clinical trial.* The Lancet, 2014. **383**(9923): p. 1129-1137.
391. Maguire, A.M., et al., *Safety and efficacy of gene transfer for Leber's congenital amaurosis.* New England Journal of Medicine, 2008. **358**(21): p. 2240-2248.
392. Damle, S., Y.H. Lo, and W.R. Freeman, *High Visual Acuity Retinal Prosthesis: Understanding Limitations and Advancements Toward Functional Prosthetic Vision.* Retina, 2017. **37**(8): p. 1423-1427.
393. Brandli, A., et al., *Progress in the clinical development and utilization of vision prostheses: An update.* Eye and Brain, 2016. **8**: p. 15-25.
394. Fine, I., C.L. Cepko, and M.S. Landy, *Vision research special issue: Sight restoration: Prosthetics, optogenetics and gene therapy.* Vision Res, 2015. **111**(Pt B): p. 115-23.
395. Solinís, M.Á., et al., *Treatment of ocular disorders by gene therapy.* European Journal of Pharmaceutics and Biopharmaceutics, 2015. **95**: p. 331-342.
396. Dalkara, D., et al., *Let There Be Light: Gene and Cell Therapy for Blindness.* Human Gene Therapy, 2016. **27**(2): p. 134-147.
397. Foerster, O., *Beitraege zur Pathophysiologie der Sehbahn und der Sehsphaere [Contributions to the pathophysiology of the visual pathway and the visual sphere].* J Psychol Neurol, 1929. **39**: p. 435-463.
398. Dobelle, W.H., *Artificial vision for the blind by connecting a television camera to the visual cortex.* ASAIO Journal, 2000. **46**(1): p. 3-9.
399. Brelén, M.E., et al., *Creating a meaningful visual perception in blind volunteers by optic nerve stimulation.* Journal of Neural Engineering, 2005. **2**(1): p. S22-S28.
400. Delbeke, J., et al., *The microsystems based visual prosthesis for optic nerve stimulation.* Artificial Organs, 2002. **26**(3): p. 232-234.
401. Veraart, C., et al., *Pattern Recognition with the Optic Nerve Visual Prosthesis.* Artificial Organs, 2003. **27**(11): p. 996-1004.

402. Ho, A.C., et al., *Long-Term Results from an Epiretinal Prosthesis to Restore Sight to the Blind.* Ophthalmology, 2015. **122**(8): p. 1547-1554.
403. Kitiratschky, V.B.D., et al., *Safety evaluation of "retina implant alpha IMS"—a prospective clinical trial.* Graefe's Archive for Clinical and Experimental Ophthalmology, 2015. **253**(3): p. 381-387.
404. Ayton, L.N., et al., *First-in-human trial of a novel suprachoroidal retinal prosthesis.* PLoS One, 2014. **9**(12): p. e115239.
405. Chuang, A.T., C.E. Margo, and P.B. Greenberg, *Retinal implants: a systematic review.* British Journal of Ophthalmology, 2014. **98**(7): p. 852.
406. Peachey, N.S., *Subretinal implantation of semiconductor-based photodiodes: Progress and challenges.* Journal of Rehabilitation Research and Development, 1999. **36**(4): p. 371-376.
407. Humayun, M.S., et al., *Interim results from the international trial of second sight's visual prosthesis.* Ophthalmology, 2012. **119**(4): p. 779-788.
408. Zhou, D.D., J.D. Dorn, and R.J. Greenberg. *The Argus® II retinal prosthesis system: An overview*. in *Electronic Proceedings of the 2013 IEEE International Conference on Multimedia and Expo Workshops, ICMEW 2013*. 2013.
409. FDA. *Humanitarian Device Exemption (HDE)*. [cited 2017 3 July]; Available from: https://www.accessdata.fda.gov/scripts/cdrh/cfdocs/cfhde/hde.cfm?id=H110002.
410. Ahuja, A.K., et al., *Blind subjects implanted with the Argus II retinal prosthesis are able to improve performance in a spatial-motor task.* British Journal of Ophthalmology, 2011. **95**(4): p. 539-543.
411. Da Cruz, L., et al., *The Argus II epiretinal prosthesis system allows letter and word reading and long-term function in patients with profound vision loss.* British Journal of Ophthalmology, 2013. **97**(5): p. 632-636.
412. Dorn, J.D., et al., *The detection of motion by blind subjects with the epiretinal 60-electrode (Argus II) retinal prosthesis.* JAMA Ophthalmology, 2013. **131**(2): p. 183-189.
413. Humayun, M.S., et al. *Preliminary 6 month results from the argus™ II epiretinal prosthesis feasibility study*. in *Proceedings of the 31st Annual International Conference of the IEEE Engineering in Medicine and Biology Society: Engineering the Future of Biomedicine, EMBC 2009*. 2009.
414. Rizzo, S., et al., *The Argus II retinal prosthesis: 12-month outcomes from a single-study center.* American Journal of Ophthalmology, 2014. **157**(6): p. 1282-1290.
415. Stronks, H.C. and G. Dagnelie, *The functional performance of the Argus II retinal prosthesis.* Expert Review of Medical Devices, 2014. **11**(1): p. 23-30.
416. Jager, R.D., W.F. Mieler, and J.W. Miller, *Age-Related Macular Degeneration.* New England Journal of Medicine, 2008. **358**(24): p. 2606-2617.

417. Jager, R.D., W.F. Mieler, and J.W. Miller, *Age-related macular degeneration.* New England Journal of Medicine, 2008. **358**(24): p. 2606-2617+2544.
418. Rosenfeld, P.J., et al., *Ranibizumab for neovascular age-related macular degeneration.* New England Journal of Medicine, 2006. **355**(14): p. 1419-1431.
419. Spaide, R.F., et al., *Intravitreal bevacizumab treatment of choroidal neovascularization secondary to age-related macular degeneration.* Retina, 2006. **26**(4): p. 383-390.
420. Algvere, P.V., et al., *A prospective study on intravitreal bevacizumab (Avastin) for neovascular age-related macular degeneration of different durations.* Acta Ophthalmol, 2008. **86**(5): p. 482-9.
421. Ghodasra, D.H., et al., *Worldwide Argus II implantation: recommendations to optimize patient outcomes.* BMC Ophthalmol, 2016. **16**: p. 52.
422. Ahuja, A.K., et al., *Blind subjects implanted with the Argus II retinal prosthesis are able to improve performance in a spatial-motor task.* Br J Ophthalmol, 2011. **95**(4): p. 539-43.
423. Dorn, J.D., et al., *The Detection of Motion by Blind Subjects With the Epiretinal 60-Electrode (Argus II) Retinal Prosthesis.* JAMA Ophthalmol, 2013. **131**(2): p. 183-9.
424. Geruschat, D.R., et al., *FLORA: Phase I development of a functional vision assessment for prosthetic vision users.* Clin Exp Optom, 2015. **98**(4): p. 342-7.
425. Geruschat, D.R., et al., *An analysis of observer-rated functional vision in patients implanted with the Argus II Retinal Prosthesis System at three years.* Clin Exp Optom, 2016. **99**(3): p. 227-32.
426. da Cruz, L., et al., *Five-Year Safety and Performance Results from the Argus II Retinal Prosthesis System Clinical Trial.* Ophthalmology, 2016. **123**(10): p. 2248-54.
427. United Nations, D.o.E.a.S.A., Population Division (2015), *World Population Ageing 2015.* (ST/ESA/SER.A/390).
428. Wong, W.L., et al., *Global prevalence of age-related macular degeneration and disease burden projection for 2020 and 2040: a systematic review and meta-analysis.* Lancet Glob Health, 2014. **2**(2): p. e106-16.
429. Ferris, F.L., 3rd, S.L. Fine, and L. Hyman, *Age-related macular degeneration and blindness due to neovascular maculopathy.* Arch Ophthalmol, 1984. **102**(11): p. 1640-2.
430. Miskala, P.H., N.M. Bressler, and C.L. Meinert, *Relative contributions of reduced vision and general health to NEI-VFQ scores in patients with neovascular age-related macular degeneration.* Arch Ophthalmol, 2004. **122**(5): p. 758-66.
431. Suner, I.J., et al., *Responsiveness of NEI VFQ-25 to changes in visual acuity in neovascular AMD: validation studies from two phase 3 clinical trials.* Invest Ophthalmol Vis Sci, 2009. **50**(8): p. 3629-35.
432. Humayun, M.S., et al., *Visual perception elicited by electrical stimulation of retina in blind humans.* Arch Ophthalmol, 1996. **114**(1): p. 40-6.

List of Publications and Presentations

Publications

- Stanga PE, Tsamis E, Papayannis A, et al. Swept-Source Optical Coherence Tomography Angio (Topcon Corp, Japan): Technology Review. Developments in ophthalmology 2016;56:13-7.

- Stanga PE, Papayannis A, Tsamis E, et al. New Findings in Diabetic Maculopathy and Proliferative Disease by Swept-Source Optical Coherence Tomography Angiography. Developments in ophthalmology 2016;56:113-21.

- Stanga PE, Papayannis A, Tsamis E, et al. Swept-Source Optical Coherence Tomography Angiography of Paediatric Macular Diseases. Developments in ophthalmology 2016;56:166-73.

- Stringa F, Tsamis E, Papayannis A, et al. Segmented Swept Source Optical Coherence Tomography Angiography Assessment Of The Perifoveal Vasculature In Patients With X-Linked Juvenile Retinoschisis: A Serial Case Report. Int Med Case Rep J. 2017 Oct 11;10:329-335.

- Stanga PE, Romano F, Chwiejczak K, Tsamis E, et al. Swept-Source Optical Coherence Tomography Angiography Assessment Of Fellow Eyes In Coats Disease. Retina. 2017 Dec 15.

- Papayannis A, Tsamis E, et al. Ultra-Wide Field Swept-Source Optical Coherence Tomography Angiography (Uwf Ss Oct-A) In Diabetic

Retinopathy. European Journal Of Ophthalmology; Volume: 26; Issue: 4; Pages: E94-E94Stanga PE, Papayannis A, Tsamis E, et al. Vitreous Segmentation Of Ocular Coherence Tomography Angiography Of The Posterior Pole And Mid-Periphery In Diabetic Retinopathy. European Journal Of Ophthalmology; Volume: 26; Issue: 4; Pages: E104-E104

- Tsamis E, Chwiejczak K, et al. Ultra Wide-Field Fundus Fluorescein Angiography-Guided Pascal Laser Targeted Retinal Photocoagulation As A First Treatment Option For The Management Of Proliferative And Exudative Vascular Retinal Disorders. European Journal Of Ophthalmology; Volume: 26; Issue: 4; Pages: E106-E106

- Stanga PE, Stringa F, Ch'ng S. Chwiejczak K, Papayannis A, Tsamis E. Wet Age-Related Macular Degeneration. Edited by: Bandello F, Querques G, Loewenstein A. Medical Retina: Update 2017. Book Series: ESASO Course Series; Volume: 9; Pages: 1-13

Presentations

- Tsamis, Emmanouil; Fenerty, Cecilia; Harper, Robert; et al. Performance Evaluation of a Novel Computer-Based Self-Administered Visual Field Screening Test for Glaucoma. Conference: Annual Meeting of the Association-for-Research-in-Vision-and-Ophthalmology (ARVO) Location: Seattle, WA Date: May 01-05, 2016

- Tsamis, Emmanouil; Fenerty, Cecilia; Harper, Robert; et al. Performance Evaluation of a Novel Computer-Based Self-Administered Visual Field Screening Test for Glaucoma. Conference: Imaging and Perimetry Society (IPS); Location: Udine, Italy, Date: September 2016

- Tsamis, Emmanouil; Henson David B. A Novel Simulation Tool for the Evaluation of Perimetric Algorithms: Benefits of Using Prior Data at Test Onset. Conference: Annual Meeting of the Association-for-Research-in-Vision-and-Ophthalmology (ARVO) Location: Orlando, FL, Date: May, 2014 [Poster[

- Tsamis, Emmanouil; Henson David B. Usability Evaluation Of A New Computer-Based Self-Administered Visual Field Test For Glaucoma Screening. Conference: UK and Eire Glaucoma Society (UKEGS) meeting. Location: Leicester, UK, Date: November, 2015 [Poster]

- Tsamis, Emmanouil; Development And Evaluation Of A Self-Administered/Assisted Visual Field Screening Tool For Glaucoma. Conference: Manchester Optometry Meeting (MOM). Location: Manchester, UK, Date: May, 2016Tsamis, Emmanouil; The Role Of Self-Testing In The Evaluation Of The Visual Field. Conference: Manchester Optometry Meeting (MOM). Location: Manchester, UK, Date: May, 2017

- Stanga PE, Tsamis E, et al. Preliminary Results of Safety and Efficacy of the Argus® II Retinal Prosthesis System in Age-related Macular Degeneration – First Year Follow-Up. Conference: Annual Meeting of

the Association-for-Research-in-Vision-and-Ophthalmology (ARVO) Location: Seattle, WA Date: May 01-05, 2016 [Poster; Presenter replacing Prof Stanga]

Appendix I

Supplementary Material 1: *This is a sample of the questionnaire given to patients during the usability evaluation of the currently available online visual field tests. Note that part of the questionnaire follows the System Usability Scale questionnaire principles.*

Patient questionnaire on the usability of online visual field tests

Thank you for participating in this study. You will be given instructions on visiting 5 web pages where you can test your visual field, the part of your surroundings that can be seen at any time. Your data are anonymous and confidential. Your answers will help us determine those features that make an online self-test easy for use by patients.

First we would like to ask a few questions about you and your previous experience with computers and visual field testing.

How old are you? _____

What is your gender? □ Male □ Female

Have you ever had a visual field test before? □ Yes □ No

If yes, how many visual field tests you had in the past?
□ 1 □ 2 □ 3 □ 4 □ 5 or more

Please, select the scenario that best describes you:

□ I have never used a computer
□ I rarely use a personal computer and I am not comfortable using one yet
□ I have used a personal computer and I can find my way around it
□ I use a personal computer and I am comfortable using one
□ I am very comfortable with personal computers and I use one almost daily

Have you ever used email? □ Yes □ No

Do you have a computer at home? □ Yes □ No

Do you feel comfortable using the Internet? □ Yes □ No

(Name of Test 1)

Open your web browser and type www.nameoftest.website. Read the welcome message and click on 'Enter' next to 'First Time Visitors'. After reading the instructions complete at least one visual field test and then complete this questionnaire

I liked using Test 1 as a tool for checking my visual field function	1	2	3	4	5
	Totally Disagree				Totally Agree

I found Test 1 unnecessary complex	1	2	3	4	5
	Totally Disagree				Totally Agree

I thought Test 1 was easy to use	1	2	3	4	5
	Totally Disagree				Totally Agree

I think I would need the support of a technical person (e.g. a relative/friend that uses computers more often) to be able to use Test 1	1	2	3	4	5
	Totally Disagree				Totally Agree

I found the content and navigation in Test 1 was well integrated	1	2	3	4	5
	Totally Disagree				Totally Agree

I thought there was too much inconsistency between the design and navigation of Test 1	1	2	3	4	5
	Totally Disagree				Totally Agree

I would imagine that most	1	2	3	4	5

patients asked to use Test 1 would learn to do so very quickly	Totally Disagree				Totally Agree

I found Test 1 very cumbersome to use / inefficient	1	2	3	4	5
	Totally Disagree				Totally Agree

I would be very confident using Test 1	1	2	3	4	5
	Totally Disagree				Totally Agree

I would need to learn a lot of things about using computers before I could get going with Test 1	1	2	3	4	5
	Totally Disagree				Totally Agree

Write any comments or notes in the box provided below:

(The same format is repeated 4 more times for the other tests being evaluated at this study. Note that the order of appearance in each questionnaire is different and randomly chosen. At the last page, there are open-comment boxes for participants to comment on the positive and negative features of the all the tests that they have been tested.)

General Questions

Please, name up to 3 positive features that you liked in any of these tests; for example about the graphical design of the website/test or any task that you performed easily and enjoyed

E.g I found it easier when I had to click the fixation point before the stimulus presentation – Visual Field Online test

Please, name up to 3 negative features that made any of these tests difficult to perform; for example about the delivery of instructions or any task that you found it very complex

E.g I did not understand what exactly I was asked to do – Visual Field Online Test

Would you recommend any of these online tests? (tick any that apply):

□ Damato Multifixation Campimeter
□ Vuscope
□ NovaVision
□ EyesCream
□ Peristat
□ I would recommend any of them
□ I would **not** recommend any of them

Supplementary Material 2: *The database of the simulated cases; 10 examples per GSS2 stage. A greyscale representation is given along with the sensitivity values for every location of the 24-2 distribution. Red circles highlight the 20 locations that were implemented in the new test*

GSS2 Stage 1

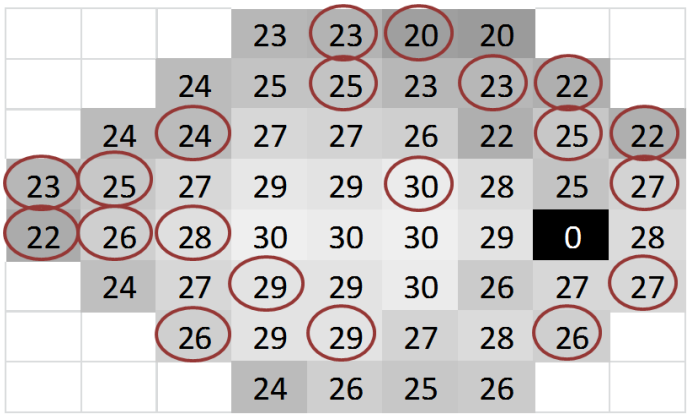

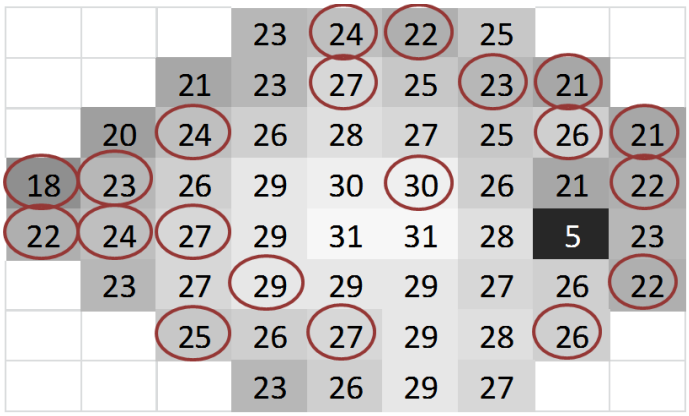

			22	22	19	18		
		24	25	24	22	22	21	
	24	28	27	28	27	26	24	20
22	26	29	29	30	29	28	15	26
23	28	29	29	30	31	30	8	26
	25	28	27	28	28	27	28	27
		27	25	27	29	29	28	
			28	27	28	27		

			19	21	21	18		
		22	24	24	24	24	22	
	23	25	26	26	26	26	26	25
23	26	27	28	29	28	28	22	27
23	27	28	29	28	29	27	0	28
	25	28	28	28	28	28	27	27
		25	28	27	27	28	27	
			24	26	27	26		

			21	21	22	21		
		24	24	21	24	24	24	
	20	24	25	26	27	26	23	25
18	23	25	27	29	28	27	23	26
23	25	26	28	28	29	28	0	26
	25	29	29	28	28	29	28	27
		26	29	27	27	29	28	
			26	24	27	26		

			21	22	20	18		
		25	27	25	25	24	21	
	24	27	29	28	26	26	24	17
23	26	28	29	29	29	29	21	24
21	25	28	29	29	29	27	0	23
	24	27	29	28	27	27	28	24
		25	27	28	25	27	25	
			21	26	26	25		

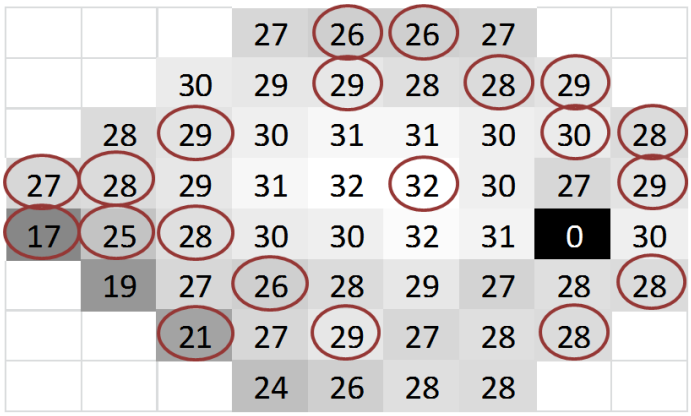
27 26 26 27
30 29 29 28 28 29
28 29 30 31 31 30 30 28
27 28 29 31 32 32 30 27 29
17 25 28 30 30 32 31 0 30
19 27 26 28 29 27 28 28
21 27 29 27 28 28
24 26 28 28

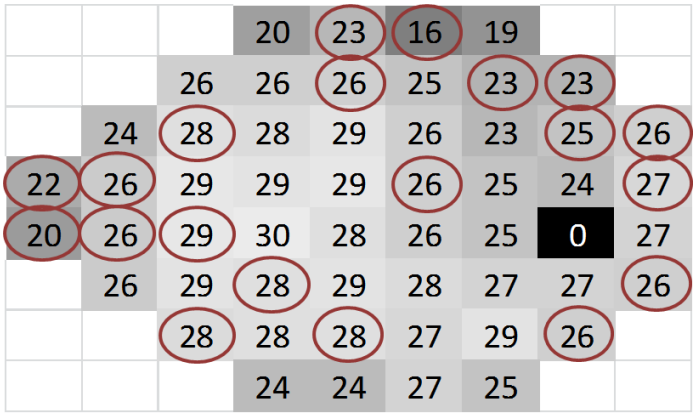
20 23 16 19
26 26 26 25 23 23
24 28 28 29 26 23 25 26
22 26 29 29 29 26 25 24 27
20 26 29 30 28 26 25 0 27
26 29 28 29 28 27 27 26
28 28 28 27 29 26
24 24 27 25

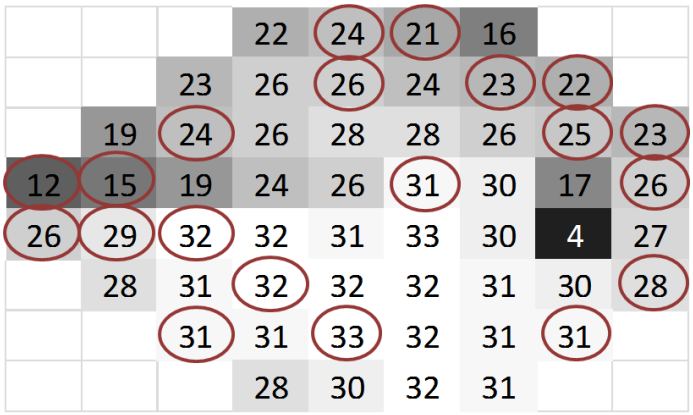
22 24 21 16
23 26 26 24 23 22
19 24 26 28 28 26 25 23
12 15 19 24 26 31 30 17 26
26 29 32 32 31 33 30 4 27
28 31 32 32 32 31 30 28
31 31 33 32 31 31
28 30 32 31

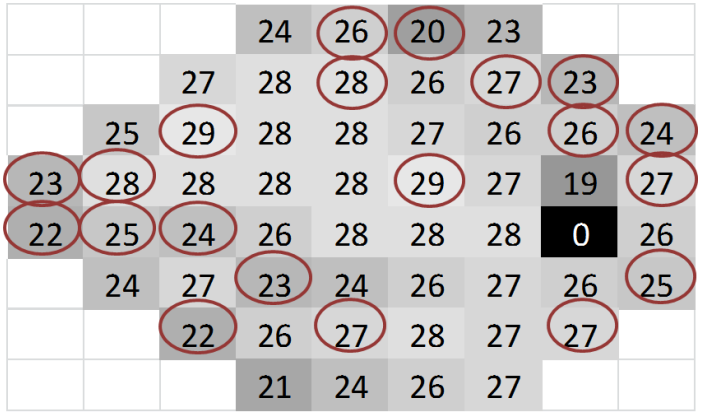
24 26 20 23
27 28 28 26 27 23
25 29 28 28 27 26 26 24
23 28 28 28 28 29 27 19 27
22 25 24 26 28 28 28 0 26
24 27 23 24 26 27 26 25
22 26 27 28 27 27
21 24 26 27

GSS2 Stage 2

			7	6	11	18		
		21	23	23	23	23	25	
	18	25	26	26	26	27	26	26
15	20	27	29	29	29	28	26	27
16	25	31	30	30	31	31	0	31
	27	29	31	30	31	32	27	26
		29	28	29	30	29	29	
			26	28	26	25		

			20	24	24	24		
		20	25	25	25	26	27	
	12	26	26	27	28	27	27	28
13	21	25	27	26	28	26	28	29
14	22	24	26	28	27	24	28	28
	25	25	26	28	29	28	30	28
		29	26	29	30	29	31	
			27	28	29	28		

			29	28	26	25		
		27	27	28	27	28	25	
	27	27	29	27	27	27	27	28
27	28	27	28	28	28	28	24	27
26	26	27	28	28	29	26	12	23
	26	27	28	27	26	25	25	25
		23	25	26	24	24	24	
			24	25	24	26		

			16	18	18	15		
		19	22	22	22	23	18	
	19	25	25	25	26	24	23	18
17	21	25	27	29	28	23	20	22
5	12	25	28	29	29	26	0	24
	12	18	25	26	28	25	24	23
		12	20	24	25	27	23	
			16	19	21	18		

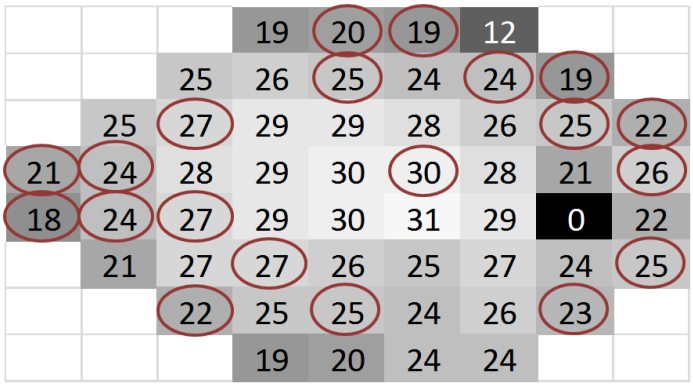
19 20 19 12
25 26 25 24 24 19
25 27 29 29 28 26 25 22
21 24 28 29 30 30 28 21 26
18 24 27 29 30 31 29 0 22
21 27 27 26 25 27 24 25
22 25 25 24 26 23
19 20 24 24

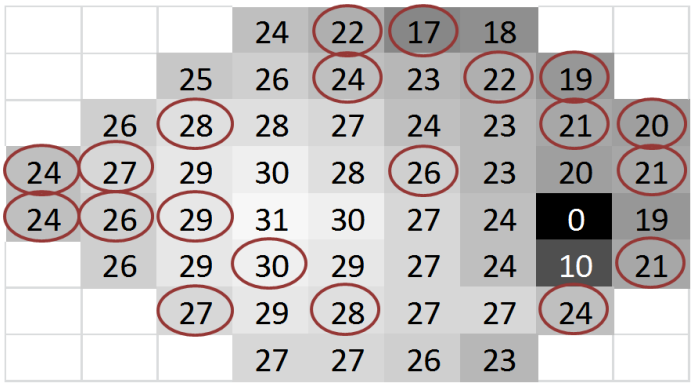
24 22 17 18
25 26 24 23 22 19
26 28 28 27 24 23 21 20
24 27 29 30 28 26 23 20 21
24 26 29 31 30 27 24 0 19
26 29 30 29 27 24 10 21
27 29 28 27 27 24
27 27 26 23

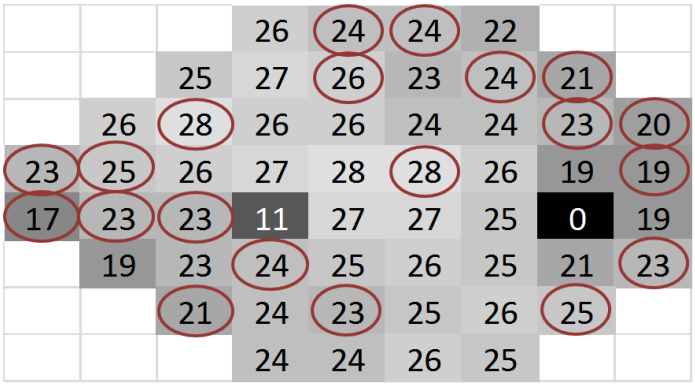
26 24 24 22
25 27 26 23 24 21
26 28 26 26 24 24 23 20
23 25 26 27 28 28 26 19 19
17 23 23 11 27 27 25 0 19
19 23 24 25 26 25 21 23
21 24 23 25 26 25
24 24 26 25

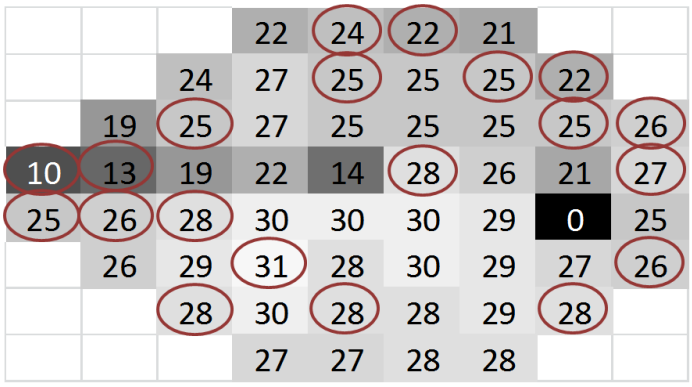
22 24 22 21
24 27 25 25 25 22
19 25 27 25 25 25 25 26
10 13 19 22 14 28 26 21 27
25 26 28 30 30 30 29 0 25
26 29 31 28 30 29 27 26
28 30 28 28 29 28
27 27 28 28

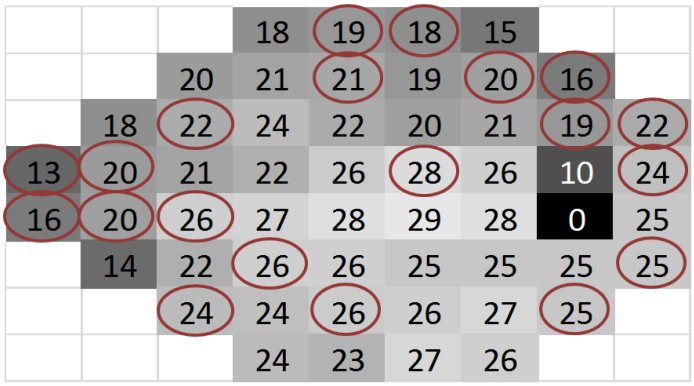
18 19 18 15
20 21 21 19 20 16
18 22 24 22 20 21 19 22
13 20 21 22 26 28 26 10 24
16 20 26 27 28 29 28 0 25
14 22 26 26 25 25 25 25
24 24 26 26 27 25
24 23 27 26

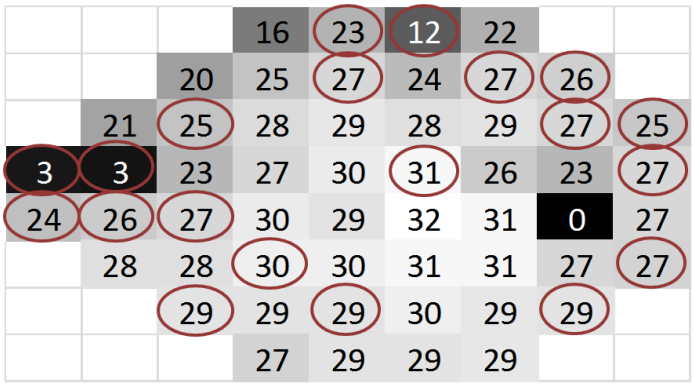
16 23 12 22
20 25 27 24 27 26
21 25 28 29 28 29 27 25
3 3 23 27 30 31 26 23 27
24 26 27 30 29 32 31 0 27
28 28 30 30 31 31 27 27
29 29 29 30 29 29
27 29 29 29

GSS2 Stage 3

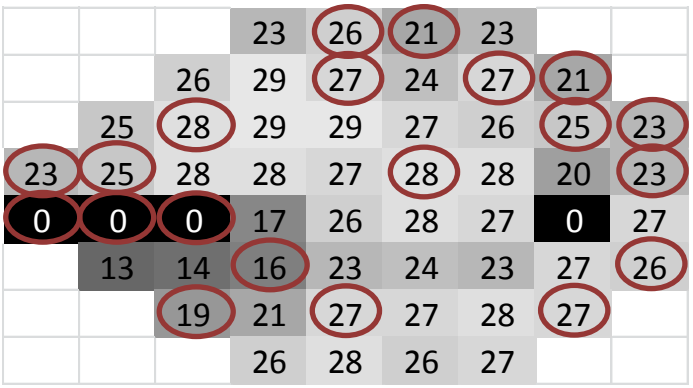
23 26 21 23
26 29 27 24 27 21
25 28 29 29 27 26 25 23
23 25 28 28 27 28 28 20 23
0 0 0 17 26 28 27 0 27
13 14 16 23 24 23 27 26
19 21 27 27 28 27
26 28 26 27

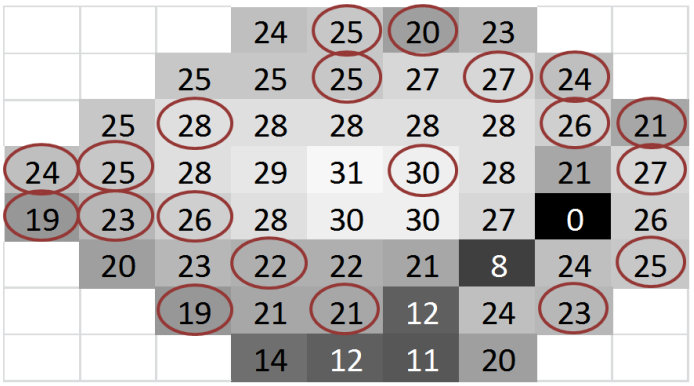
24 25 20 23
25 25 25 27 27 24
25 28 28 28 28 28 26 21
24 25 28 29 31 30 28 21 27
19 23 26 28 30 30 27 0 26
20 23 22 22 21 8 24 25
19 21 21 12 24 23
14 12 11 20

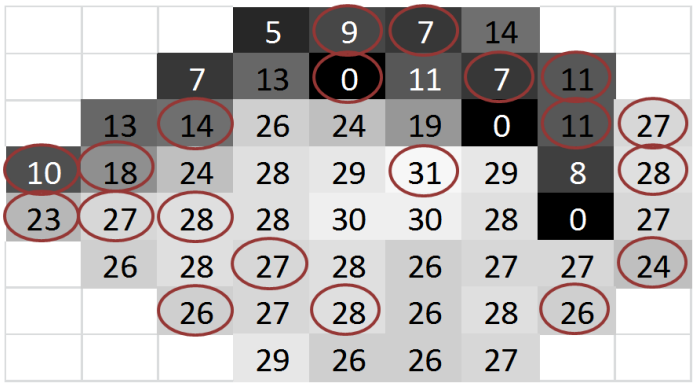
5 9 7 14
7 13 0 11 7 11
13 14 26 24 19 0 11 27
10 18 24 28 29 31 29 8 28
23 27 28 28 30 30 28 0 27
26 28 27 28 26 27 27 24
26 27 28 26 28 26
29 26 26 27

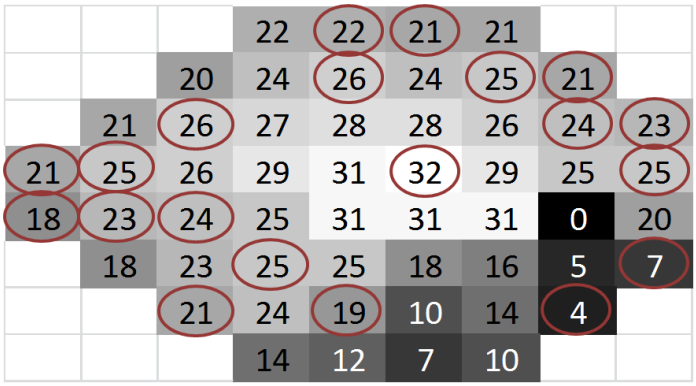
22 22 21 21
20 24 26 24 25 21
21 26 27 28 28 26 24 23
21 25 26 29 31 32 29 25 25
18 23 24 25 31 31 31 0 20
18 23 25 25 18 16 5 7
21 24 19 10 14 4
14 12 7 10

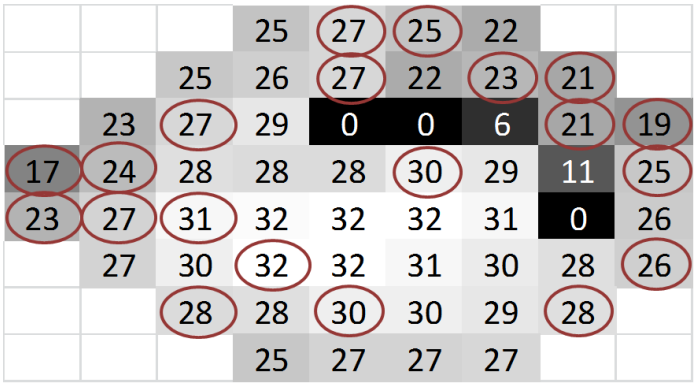
25 27 25 22
25 26 27 22 23 21
23 27 29 0 0 6 21 19
17 24 28 28 28 30 29 11 25
23 27 31 32 32 32 31 0 26
27 30 32 32 31 30 28 26
28 28 30 30 29 28
25 27 27 27

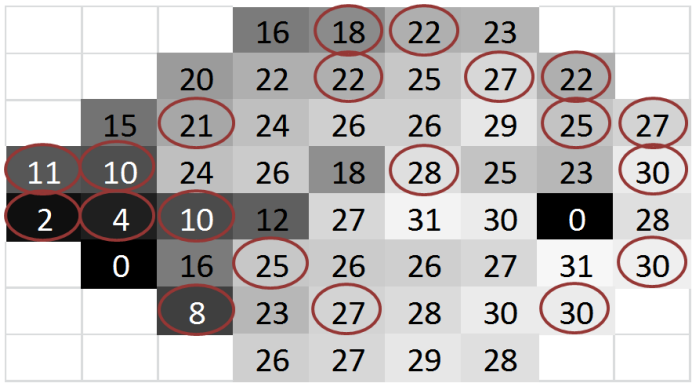
16 18 22 23
20 22 22 25 27 22
15 21 24 26 26 29 25 27
11 10 24 26 18 28 25 23 30
2 4 10 12 27 31 30 0 28
0 16 25 26 26 27 31 30
8 23 27 28 30 30
26 27 29 28

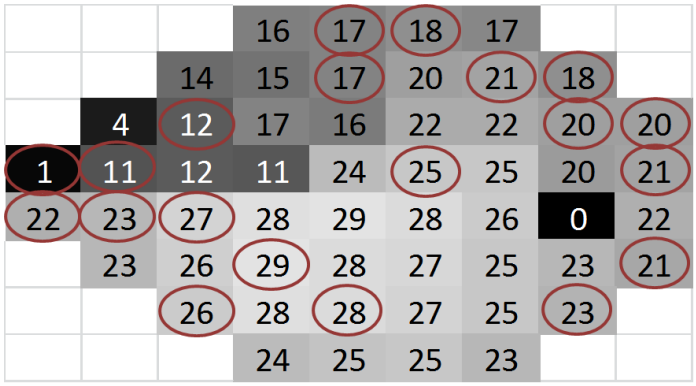
16 17 18 17
14 15 17 20 21 18
4 12 17 16 22 22 20 20
1 11 12 11 24 25 25 20 21
22 23 27 28 29 28 26 0 22
23 26 29 28 27 25 23 21
26 28 28 27 25 23
24 25 25 23

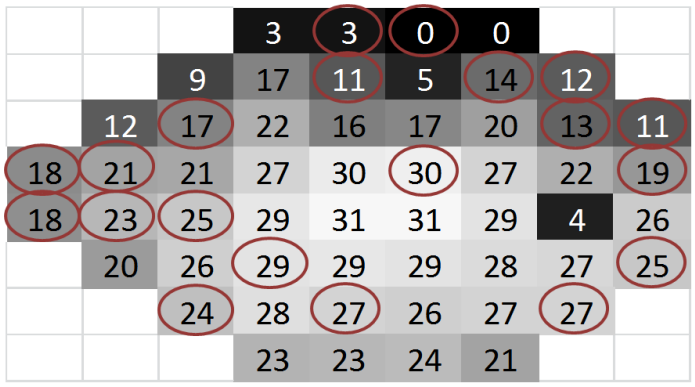
3 3 0 0
9 17 11 5 14 12
12 17 22 16 17 20 13 11
18 21 21 27 30 30 27 22 19
18 23 25 29 31 31 29 4 26
20 26 29 29 29 28 27 25
24 28 27 26 27 27
23 23 24 21

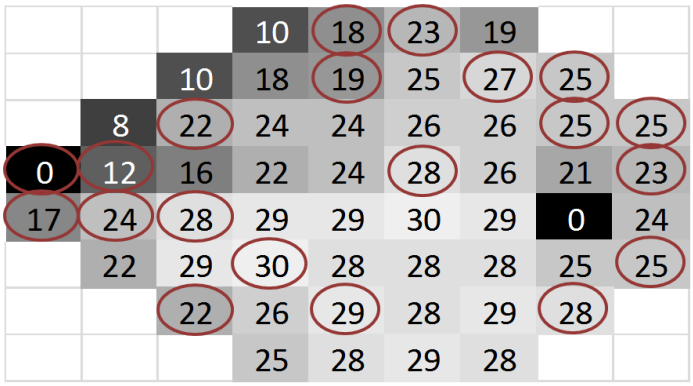
10 18 23 19
10 18 19 25 27 25
8 22 24 24 26 26 25 25
0 12 16 22 24 28 26 21 23
17 24 28 29 29 30 29 0 24
22 29 30 28 28 28 25 25
22 26 29 28 29 28
25 28 29 28

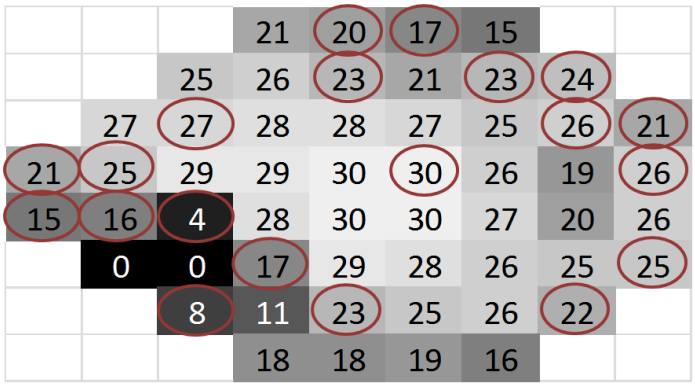
21 20 17 15
25 26 23 21 23 24
27 27 28 28 27 25 26 21
21 25 29 29 30 30 26 19 26
15 16 4 28 30 30 27 20 26
0 0 17 29 28 26 25 25
8 11 23 25 26 22
18 18 19 16

Appendix II

Inclusion	Exclusion

• Give consent
• Age between 25 and 85
• Non-exudative AMD diagnosis
• Severely sight impaired:
  ○ VA 1.0 logMAR or worse measured by ETDRS
  ○ Hand motion or worse central vision in eye to be implanted measured with pinhole occlude
  ○ GA and central escotoma in central 20º measured by FA and microperipetry, respectively
• Pseudophakic or aphakic both with a clear capsule
• Motivated and competent to use the Argus II System
• Not suffer from non-oftalmic serious or non-curable conditions
	• Ocular conditions that prevent Argus II system to work or be successfully implanted
	• Evidence of active CNV
	• Ocular conditions that hamper inner ocular structures visualization
	• Implantable Miniature Telescope in either eye
	• Pre-disposition to eye rubbing
	• Condition that prevents understanding or communication of informed consent, study demands and testing protocols
	• Pregnant or wishing to become during the study
	• Participating in another investigational study
	• Intolerance to any of the drugs associated with the implantation surgery
	• Conditions likely to limit life to less than 1 year from inclusion

Supplementary Material 4: *Full List of Inclusion and Exclusion Criteria*

Evaluation or Test	Baseline	Implant (Day 0)	Day 1 post-op	1 Wk	2 Wk	1 Mo	2 Mo	3 Mo	4 Mo	6 Mo	12, 18, 24, 30, 36 Mo
Visit Window (d=days)	**< 60 days pre-implant**		**+ 1 d**	**- 1 d / + 2 d**	**± 2 d**	**± 5d**	**± 10d**	**± 10 d**	**± 15d**	**± 15d**	**± 30d**
Informed Consent	X										
Medical Evaluation & Eye Exam	X		X	X	X	X	X	X	X	X	X
Ultrasound A-scan (Axial length measurement) and ultrasound B-scan	X										
Retinal Fundus Photography	X			X		X	X	X	X	X	X
Fundus Autofluorescence	X					X		X		X	X
Fluorescein Angiography	X					X		X		X	X[1]
Optical Coherence Tomography	X					X		X		X	X
Microperimetry (SLO, MP-1, or MP-3)	X									X	X[1]
Humphrey Visual Field	X									X	X[1]
Visual Acuity Tests	X							X		X	X[1]
NEI VFQ-25	X										X[1]
FLORA	X										X[2]
Implant Surgery		X									

[1] Months 12, 24 and 36 only

[2] Months 12 and 36 only

Supplementary Material 5: *Brief list of all the procedures for every given follow-up visit.*